




Effects of hydropower operation and oligotrophication on internal processes in Lake Brienz

D. Finger

Effects of hydropower operation and oligotrophication on internal processes in Lake Brienz

David Christian Finger

Diss. ETH No. 16827

Diss. ETH No. 16827

EFFECTS OF HYDROPOWER OPERATION AND OLIGOTROPHICATION ON INTERNAL PROCESSES IN LAKE BRIENZ

A dissertation submitted to the
SWISS FEDERAL INSTITUTE OF TECHNOLOGY ZÜRICH
for the degree of
DOCTOR OF SCIENCES

presented by
David Christian Finger
Dipl. Umwelt-Natw. ETH
born August 22nd , 1974
citizen of Klagenfurt, Austria

accepted on the recommendation of
Prof. Dr. Alfred Wüest (Eawag), examiner
Prof. Dr. Peter Reichert (Eawag), co-examiner
Prof. Dr. Bernhard Wehrli (ETH), co-examiner
Prof. Dr. Peter Huggenberger (University of Basel), co-examiner
2006

En mémoire de Marianne Irminger

(1918 - 2004)

"Understanding the hydrodynamics of lakes, rivers and coastal waters is central for addressing the consequences of human activities and climate change in these systems. The future challenge of environmental science lies in implementing this knowledge in order to preserve the beauty of nature."

Sally MacIntyre,
during the PPNW workshop in Lancaster, 6 September 2005
Marine Science Institute and
Institute for Computational Earth Systems Science
University of California, Santa Barbara

TABLE OF CONTENTS

ABSTRACT

Since the 1980's, local fishermen have been complaining about the declining fishing yield in Lake Brienz. A preliminary review indicated that the local whitefish (*Coregonus fatioi*) are suffering from undernourishment due to low phytoplankton and zooplankton densities. Two main hypotheses were put forth to explain the low level of biomass and fish food production: (1) during the last 30 years constructions of sewage treatment plants in the catchment have drastically reduced the phosphorus input into the lake. As phosphorus is the limiting nutrient, algae growth must have decreased accordingly. (2) Increasing hydropower production has lead to a continuous supply of suspended glacial particles which are transported with the melt water to the lake. The suspended particles reduce the light penetration, thus limiting algae growth to the top few meters of the lake.

Based on extensive measurements and numerical model calculations the present Ph.D. thesis assesses and quantifies the effects of the above mentioned anthropogenic interferences on primary production in Lake Brienz. In a first step the suspended particle budget, under consideration of two particle size classes, was established for both present conditions and hypothetical conditions without upstream hydropower dams (no-dam conditions). Subsequently the effects of suspended solids on the light regime of the lake were assessed by direct observations of beam and in situ light attenuation. Based on in situ C-assimilation rates, light attenuation, and the established suspended particle budgets, gross primary production was assessed for present conditions and estimated for hypothetical no-dam conditions. In the last step, the assembled information of the previous steps was implemented in a numerical, biogeochemical lake model predicting plankton densities both for present and no-dam conditions. The calibrated model was used to perform predictions for various hypothetical scenarios with increased phosphorus input and altered surface turbidity. By comparing the different scenarios with each other, the causes for the biological changes observed in Lake Brienz were identified.

In summary, damming drastically diminishes particle fluxes which leads to lower particle supply during summer, but higher loads in winter due to hydropower production. As a consequence, light attenuation is now half during summer and almost double in winter compared to no-dam conditions. This result is consistent with pre-dam measurements of

Secchi depths in the early 1920's. Under current light conditions gross production is extremely low (~66 gC m^{-2} yr^{-1}) in comparison with other oligotrophic lakes not affected by surface turbidity (e.g. production in neighboring downstream Lake Thun is estimated to be 45% higher). Under a hypothetical light situation without dams gross production in Lake Brienz would be about 36% lower in summer but up to 17% higher in winter.

Enhanced nutrients supply increases the nutritious value of algae, thus stimulating zooplankton growth. Phytoplankton growth, however, hardly changes as the top-down control by zooplankton is enhanced. Annually integrated productivity is only slightly influenced by damming induced changes in water turbidity, since algae growth is strongly limited by phosphorus availability. However, in winter and spring the hydropower production leads to increased turbidity, therefore the spring production peak is delayed. Due to higher algae growth in summer phosphate is continuously consumed, thus preventing a second production peak in fall.

In summary, oligotrophication was identified as the main cause for declining zooplankton densities during the last 30 years. However, with ongoing oligotrophication the effects of light limitation become more important. While the results of the model calculations suggest that oligotrophication is the primary cause for declining fish yields, they also suggest that the effects of oligotrophication are amplified by damming induced changes in turbidity.

ZUSAMMENFASSUNG

Seit den 1980er Jahren klagen lokale Fischer über rückläufige Fischerträge im Brienzersee. Frühere Studien sind zum Schluss gekommen, dass die Felchenpopulationen im Brienzersee (*Coregonus fatioi*) an Unterernährung leiden, weil Zooplankton und Phytoplankton in nur sehr geringen Mengen vorkommen. Für das geringe Vorkommen des Planktons kommen zwei Hypothesen in Frage: (1) Im Laufe der letzten 30 Jahren hat der Bau von Kläranlagen im Einzugsgebiet den Phosphoreintrag drastisch reduziert. In der Folge muss sich die Primärproduktion entsprechend verringert haben. (2) Intensive Wasserkraftnutzung im Einzugsgebiet führt zu einem kontinuierlichen Schwebstoffeintrag in den See, wodurch sich die Lichtdurchflutung verringert und die Primärproduktion sich somit auf die obersten Meter des Sees beschränkt.

Anhand von umfangreichen Messungen und Modellrechnungen werden in der vorliegenden Doktorarbeit die Auswirkungen der Veränderungen im Einzugsgebiet des Sees auf dessen Primärproduktion analysiert und quantifiziert. In einem ersten Schritt wurden die Schwebstofffrachten in den Zuflüssen des Sees erfasst. Anhand von Modellrechnungen wurde die Schwebstoffdynamik für eine hypothetische Situation ohne Stauseen abgeschätzt. Im zweiten Schritt wurde der Einfluss der Inhaltsstoffe auf die Lichtabschwächung im Brienzersee untersucht und der bioverfügbare Phosphorinhalt im See bestimmt. In einem dritten Schritt wurde die Primärproduktion im See quantifiziert und deren Sensitivität auf Veränderungen in der Schwebstoffdynamik analysiert.

Im letzten Schritt wurden die gewonnenen Erkenntnisse in einem numerischen biogeochemischen Seen-Modell zusammengebaut. Anhand des kalibrierten Modells wurden hypothetische Szenarien für eine veränderte Trübung und erhöhten Phosphoreintrag gerechnet.

Generell verringern die Stauseen den natürlichen Schwebstofftransport. Während im Sommer heute deutlich weniger Schwebstoffe in den See eingetragen werden, ist die Winterfracht fast ausschliesslich auf den Wasserablass der Kraftwerke zurückzuführen. Modellrechnungen und Zeitreihen von Secchi-Tiefen zeigen übereinstimmend, dass im Vergleich zu früher (vor dem Bau der Stauseen) die Lichtabschwächung heute im Sommer um die Hälfte verringert und im Winter fast doppelt so hoch ist. Diese starke

Lichtabschwächung führt zu einer äusserst niedrigen Algenproduktion von ~66 gC m^{-2} yr^{-1}. Zum Beispiel wurde für den benachbarten Thunersee, der von Gletschertrübung jedoch nicht betroffen ist, eine etwa 45% höhere Produktion geschätzt. Im Brienzersee führt der Betrieb der Wasserkraftwerke zu einer ~36% höheren Produktion im Sommer (aufgrund geringer Trübung) und einer um 17% niedrigeren Produktion im Winter (erhöhte Trübung). Eine Erhöhung des Phosphat-Eintrages erhöht den Nährwert der Algenbiomasse und führt folglich zu höheren Zooplanktondichten. Phytoplankton ist jedoch einem erhöhten Frassdruck ausgesetzt und weist deshalb keine höheren Dichten auf. Die veränderte Trübe durch den Kraftwerksbetrieb hat keine signifikanten Auswirkungen auf die integrierte Jahresproduktion. Die erhöhte Wintertrübe verzögert jedoch die Frühjahrsproduktion um fast zwei Monate. Im Hochsommer ist die Produktion hingegen durch die geringere Trübung begünstigt. Dadurch wird während des ganzen Sommers Phosphat aufgebraucht und eine zweite Produktionsspitze im Herbst wird folglich verhindert.

Zusammenfassend wurde der Rückgang des Phosphoreintrages durch Kläranlagen als Hauptursache für die rückläufigen Zooplanktondichten und somit für die abnehmenden Fischerträge identifiziert. Die Modellrechnungen zeigen jedoch, dass mit zunehmender Oligotrophierung die durch den Kraftwerksbetrieb erzeugte Wintertrübe sich zunehmend negativ auf die Algenproduktion auswirkt.

CHAPTER 1

INTRODUCTION

1.1 Background

Professional and hobby fishing have experienced a long tradition in many Bernese lakes. The three most important natural lakes are Bielersee, Thunersee and Lake Brienz. Lake Brienz is situated most upstream and has been less affected by anthropogenic impacts, such as untreated sewage, chemical pollution, or agricultural fertilization. While during the late 1970's annual yields of professional fishing reached typically up to 15 kg ha^{-1}, yields dropped to less than 1 kg ha^{-1} in 1999 (GSA, 2003) (Figure 1.1). Simultaneously, the Office of Water Protection and Waste Management of Canton Bern (GSA) observed that Daphnia (primarily *Daphnia hyalina*), the main food source of the local whitefish (*Coregonus fatioi*), had also disappeared in 1999. A preliminary review concluded that the whitefish were suffering from undernourishment (Müller, 2003), however, no conclusions regarding the causes for the food shortage could be drawn.

Professional fishermen argue that the collapse in 1999 was just an amplification of the persistent decline of fishing yield noticed since the late 1970's. Their main concern is that surface turbidity in Lake Brienz has been continuously increasing, reducing penetration depth of sun light, and jeopardizing the entire ecosystem. Due to its glaciated catchments, Lake Brienz has always been turbid due to allochthonous particle input caused by glacier melting in the summer (see section 1.2). Nevertheless, since the 1930's hydropower activities have been continuously intensified, leading to a temporal shift of water discharge from summer to winter. The potential link between hydro power activities and surface turbidity has been investigated several times (Naturaqua, 1993; Schudel and Ochsenbein, 1995; Siegenthaler et al., 1996) without answering the concerns of local fishermen satisfactorily.

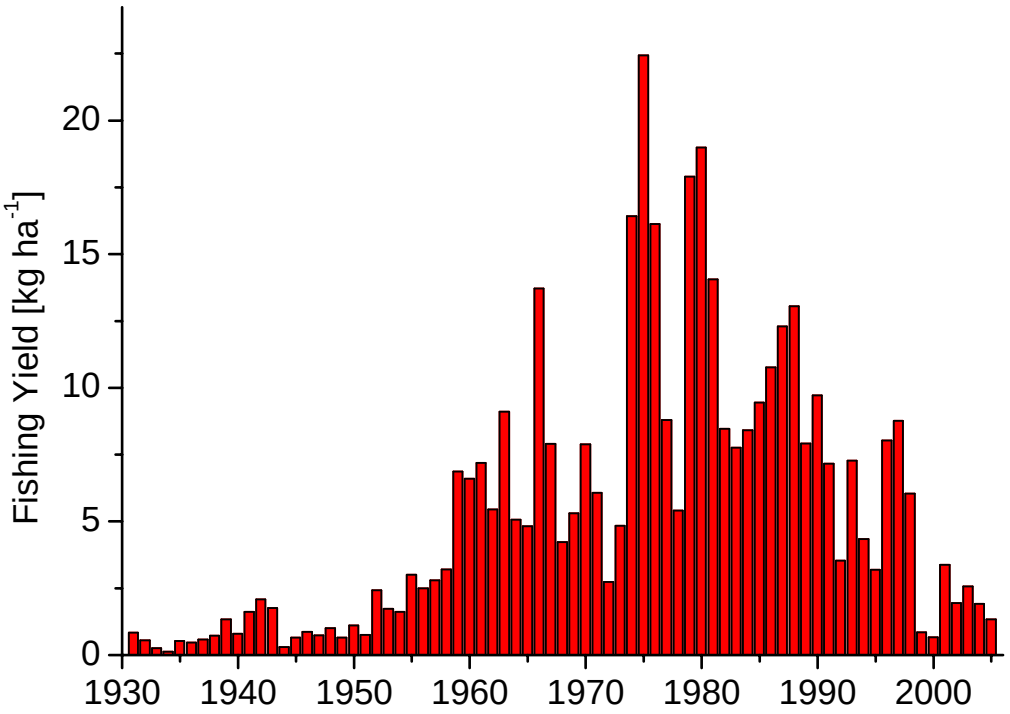

Figure 1.1: Professional fishing yield in Lake Brienz

The present Ph.D. thesis assesses the effects of catchment alterations on internal processes in Lake Brienz using a system analytical approach. The goal of the thesis is to give satisfactory explanations for the long-term changes observed in biotic indicators of Lake Brienz.

1.2 Unique characteristics of Lake Brienz

Lake Brienz is situated about 20 km south west of the geographical center of Switzerland in the foothills of the *Bernese Oberland*. With a volume of 5.17 km^3 and a surface area of 29.8 km^2 it is a typical representative of peri-alpine lakes in Switzerland. Fluvial and glacial forces eroded a 260 m deep and simple basin out of Mesozoic rocks (Sturm and Matter, 1978), making Lake Brienz, together with Lago Maggiore, the lake with the greatest average depth (173 m) in Switzerland. In the north and south of the lake steep mountain ranges reach up to 2300 m asl leaving almost no space for shallow littoral zones.

The rest of the 1134 km^2 large alpine catchment area (average altitude of the catchment: 1950 m asl) is drained by the two major inflows, Aare and Lütschine, which enter the lake at its eastern and western longitudinal end, respectively. The alpine water shed is composed to 56% by unproductive area, 21% forests, 21% agricultural areas and only about 2% of the area is attributed to housing areas (BFS Geostat data). The extensive land use leads to an exceptionally low nutrients input to Lake Brienz.

With 2 m yr^{-1} the average precipitation lies about 40% above the national average, which is typical for high mountain regions. Over 80% of the precipitation flows into Lake Brienz, while the rest evaporates. This water input to Lake Brienz (1.815 km^3 yr^{-1}) leads to an average water residence time of less than 2.7 years. Intensive deep water intrusions (Chapter 2) and convective mixing in winter renew the deep water on a time scale of a few years only. Consequently, unlike many other Swiss Lakes, oxygen concentration most of the time remains above 8 mg L^{-1} in the entire basin.

1.3 Allochthonous particle input to Lake Brienz

Erosion rates vary in the European Alps between 0.1 and 0.65 mm yr^{-1} (Hinderer, 2001). This leads to mineral particle loads of several thousand tons per year in many Alpine streams which flow into lowland lakes (Table 1.1).

Table 1.1: Comparison of allochthonous particle input in Swiss Lakes

River	Suspended load[1] (kt yr^{-1})	Area[2] (km^2)	Lake	Volume (Mio m^3)	Input per Volume[3] (kg m^{-3} yr^{-1})	Mean depth	Reference
Rhein	~3200	6119	Lake Constance	48000	~67	89	(LHG-BWG, 2005)
Rhone	~2700	5220	Lake Geneva	89900	~30	154	(LHG-BWG, 2005)
Reuss	~105	832	Lake Lucerne	11800	~9	103	(LHG-BWG, 2005)
Ticino	~190	1611	Lago Maggiore	37100	~5	173	(LHG-BWG, 2005)
Lütschine	~174	379	Lake Brienz	5170	~58	173	(Finger et al., 2006)
Aare	~128	554					(LHG-BWG, 2005)
Aare[4]	~9		Lake Thun	6500		135	(Finger et al., 2006)

[1] Mean estimated load close to river entrance into downstream lake between 1994 and 2003 in 1000 metric tons.

[2] Catchment area close to river entrance into the lake.

[3] Allochthonous particle input per lake volume; note: only the load in the major inflows listed to the left is considered.

[4] Aare downstream of Lake Brienz at entrance to Lake Thun.

In comparison to its volume, Lake Brienz is subject to one of the highest allochthonous particle inputs in Switzerland (Table 1.1); this is due to the glaciers in the watershed, which cover about one fifth of the entire catchment (LHG-BWG, 2005). These glaciers grind rock into small particles and release them with the melt water to downstream rivers. While gravel and sand settle in the headwaters, smaller particles (e.g. colloids) remain suspended for weeks to months and are transported to downstream Lake Brienz. Especially during hot periods (intense glacier melting) or during heavy precipitation (increased erosion) suspended particle concentration in Aare and Lütschine can reach several g L^{-1}. This input of allochthonous mineral particles into Lake Brienz renders the lake grey-greenish every summer. During winter, when water discharge reaches a minimum (temperatures are usually below freezing point), allochthonous particle input is low and the lake color turns to a clear blue again.

1.4 Impacts: Re-oligotrophication and hydropower operations

Two major anthropogenic impacts affecting Lake Brienz can be identified: (1) Until 1970 untreated sewage from adjacent communities has been introduced into Aare and Lütschine. Starting in 1970, sewage treatment plants have been constructed for all major communities. As a direct consequence, phosphate loads have been decreasing since 1970, today reaching a level similar to the natural input at the beginning of the 20th century. (2)

Several hydropower dams have been constructed in the headwater of River Aare shifting discharge from summer to winter.

1.4.1 Eutrophication and re-oligotrophication

In the very sparsely populated (< 29 habitants per km^2 (BUWAL, 1994)) water shed of Lake Brienz, the construction of sewer systems has increased the P load in the first half of the twentieth century by directing domestic effluents waste directly into the lake. Subsequently, the bio-available phosphate input increased up to ~30 tP yr^{-1}, about four times the natural input. Since the early 1980's, sewage treatment plants (STP) with Fe-induced P Precipitation have successfully reduced P loads to the original status (Müller et al., 2007a). Further optimization of sewage treatment and the ban of P-containing detergents have reduced present P-loads to ~8 tP yr^{-1}, a level comparable to natural inputs.

1.4.2 Upstream hydropower operations

At the beginning of the 1930's the *Kraftwerke Oberhasli AG* (KWO) constructed the first hydropower dams (Gelmersee and Grimselsee) in the headwaters of River Aare. Until the 1950's further hydropower dams (Räterichsbodensee and Oberaarsee) amounted up to a total operational storage volume of 197 Mio m^3. Between Oberaarsee (highest reservoir at 2303 m asl) and Innertkirchen (outlet of turbinated water at 622 m asl) the stored water is turbinated at 9 different altitudes with up to 26 turbines resulting in an annual energy production of ~ 2250 GWh.

The huge storage volume of the hydropower reservoirs has a drastic effect on the discharge patter in the downstream Aare. Nowadays, hydropower operation shifts ~14% of the annual Aare discharge from summer to winter. This temporal water retention subsequently affects the dynamics of suspended sediment loads in Aare. The increased discharge in winter leads to a continuous suspended particle supply to Lake Brienz (Figure 1.2), while under natural conditions (without hydropower dams) almost no particles are discharged into the lake. This suggests that during the last century hydropower operations have altered the surface turbidity dynamics in Lake Brienz. Reduced light availability within the lake might hamper primary production, therby jeopardizing the entire ecosystem of Lake Brienz.

Figure 1.2: Confluence of residual flow of Aare (right stream) and outlet of hydropower installations (left stream). During winter season, intense hydropower production leads to continuous supply of turbid glacial water to the naturally clear run off in Aare.

1.4.3 Global climate change

Increasing air temperatures trigger glacier melting which leads to a gradual retreat of the ice fields. Glacier surveys in the catchment of Grimselsee, performed by *Flotron AG,* indicate that Ober- and Unteraar Glacier have retreated more than 1.5 km over the past 80 years clearing an area of 3.5 km^2 (KWO, 1999). Due to glacier melting total annual water discharges in the two inflows have been continuously increasing, particularly during recent decades. Increasing discharge usually imply higher suspended particle loads. Long-term river monitoring since the 1970's, however, does not reveal any significant trends in riverine particle loads during the last dacades.

1.5 Objectives and outline

In order to understand the alleged changes of the Lake Brienz ecosystem, the lake and its catchments have to be considered as one system with various dependencies. The potential external influences directly affecting the discharge and riverine particle and nutrient transport have been identified in a preliminary review study (GSA, 2003). In Figure 1.3 the dependencies between the physical, nutritional and the external influences are summarized in a schematic way.

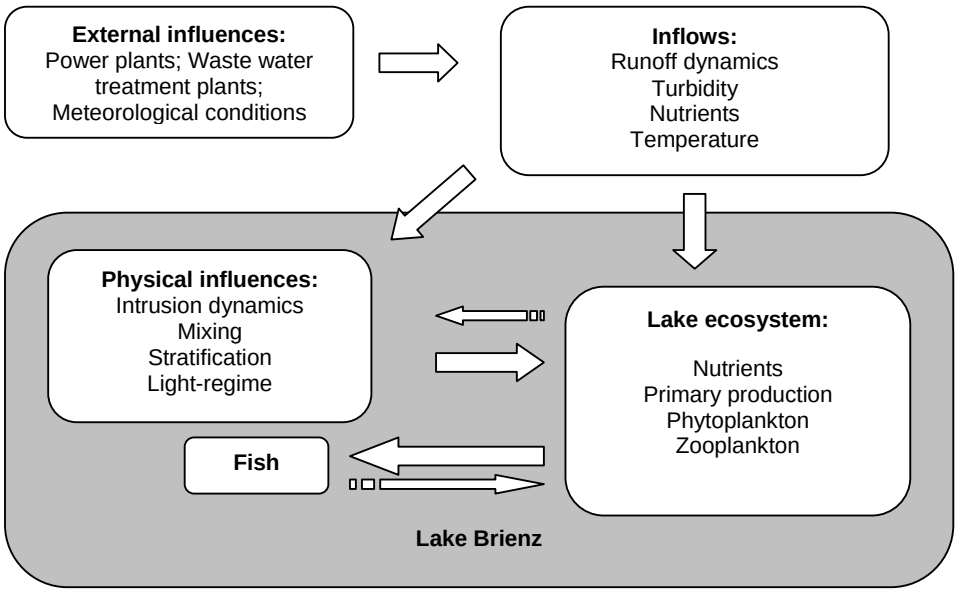

Figure 1.3: Overview of the interrelations form a system analytical approach

Hydropower operations affect the natural runoff in River Aare, sewage treatment plants have reduced the nutrients supply to rivers and meteorological conditions cause natural fluctuations of discharge and erosion rates. The impacts on the inflows directly affect the nutrient cycle (nutrient supply to the Lake comes primarily from the rivers) and the physical boundary conditions of the biogeochemical cycle in Lake Brienz (stratification, river intrusion depth impact on distribution of nutrients; light attenuation limits primary production). Based on a system analytical approach conclusions can be drawn concerning the biotic conditions which impact the fish populations.

The goals of the present Ph.D. thesis are to quantify the effect of the external anthropogenic influences on the primary production in the surface layers of Lake Brienz. The

thesis is organized in four individual investigations which together allow an assessment of those two anthropogenic impacts on Lake Brienz.

1.5.1 *Chapter 2: Effects of upstream hydropower operation on riverine particle transport and turbidity in downstream lakes*

In a first step, the size-dependent particle budgets of the surface layer of Lake Brienz have been determined for the year 1997 to 2004 and compared to a hypothetical no-dam scenario based on numerical simulations. For this purpose current tributary particle loads, as well as lake-internal sedimentation and turbidity dynamics were assessed with in-situ measurements. The analysis of measurements and numerical simulations constitute the basis of the physical boundary conditions for primary production today and previous to hydro power operations.

1.5.2 *Chapter 3: Effects of upstream hydropower operations and re-oligotrophication on the light regime of a turbid peri-alpine lake*

To assess the causes of light attenuation in-situ irradiance was compared to optical active substances in the photic layer of Lake Brienz. Based on the particle budget of a hypothetical situation without hydropower operations (presented in Chapter 2) and on historical Secchi recordings, light attenuation was predicted for a pre-dam situation. Human perception of lake turbidity is primarily dependent on the reflection of light. For this reasons the reflectance of light was assessed for the present situation and for a potential situation during a higher trophic status.

1.5.3 *Chapter 4: Effects of upstream hydropower operations on primary production in downstream lakes*

To assess the effects of surface turbidity on gross primary production ^{14}C assimilation was determined on a monthly basis between December 2003 and May 2005. Based on the experimental data a numerical model was established in order to predict production under changing light conditions. Using this numerical model and the results of chapters 2 and 3, primary production under no-dam light conditions could be predicted.

1.5.4 Chapter 5: Effects of oligotrophication and upstream hydropower operations on plankton biomass in peri alpine lakes

In the last chapter the effects of reduced nutrients supply and altered surface turbidity on plankton biomass production are compared. Using the assembled information on the effects of damming on surface turbidity (Chapter 2), suspended solids on light attenuation (Chapter 3), and present rates of algae production (Chapter 4), a numerical, biogeochemical lake model was developed. The calibrated model was used to perform predictions for various hypothetical scenarios, with increased nutritional input and altered surface turbidity. By comparing the different scenarios with each other, the causes for the biological changes observed in Lake Brienz were identified.

The thesis concludes with a synthesis of all results, giving a scientific explanation for the observed changes in biotic observations in Lake Brienz. Furthermore, it evaluates the potential impacts due to hydropower operations on biotic indicators in Lake Brienz.

CHAPTER 2

EFFECTS OF UPSTREAM HYDROPOWER OPERATION ON RIVERINE PARTICLE TRANSPORT AND TURBIDITY IN DOWNSTREAM LAKES

David Finger, Martin Schmid and Alfred Wüest

Printed in Water Resources Research, 2006,
42: W08429, doi: 10.1029/2005WR004751

Abstract

Retention in upstream storage dams results in modified riverine water and particle discharge patterns. Particularly, suspended solids input and intrusion dynamics in downstream lakes are affected by dam operations. In a case-study, size-dependent particle budgets for peri-alpine Lake Brienz (Switzerland), downstream of major hydropower installations, were determined for a recent eight-year period (1997 - 2004) and compared to hypothetical no-dam scenarios based on numerical simulations. For this purpose current tributary particle loads, as well as lake-internal sedimentation and turbidity dynamics were assessed with in situ measurements. The analysis shows that hydropower damming drastically diminishes particle fluxes and minimizes (short-term) peak discharges. Reductions of high-flow events substantially cut the number of deep intrusions increasing particle supply to the lake surface layer. Furthermore these hydropower operations shift particle inputs from summer to winter. As a consequence, such peri-alpine lakes become more turbid during winter and less turbid during summer, influencing the seasonal light regime and subsequently the dynamics of phytoplankton growth.

2.1 Introduction

Growing demands for freshwater, irrigation and hydropower in the recent decades have called for increasing water storage in dams, reservoirs and artificial lakes throughout the world (McCully, 1996; Vörösmarty et al., 1997). The downstream ecological and social impacts are subject to ongoing investigations (Rosenberg et al., 1995; Rosenberg et al., 1997; WCD, 2000). Important biological implications range from interference with fish migration and biodiversity (Hart and Poff, 2002), to changes in downstream vegetation (Nilsson et al., 1997), and damaging river ecosystems (Ward and Stanford, 1995; Hart et al., 2002). Some consequences of altered discharge in rivers are subtle and interfere with the biogeochemical cycle and hence only become evident at long time scales (Friedl and Wüest, 2002). Notably, damming might interfere physico-biogeochemically by causing: (1) water temperature changes resulting from hydropower operations (Preece and Jones, 2002; Meier et al., 2003; Bartholow et al., 2005), (2) nutrient retention (Humborg et al., 2000; Friedl et al., 2004) and (3) hydrological pattern changes and reductions in suspended particle loads (Vörösmarty et al., 2003; Teodoru and Wehrli, 2005; McGinnis et al., 2006).

Ablation rates in the European Alps range from 0.1 to 0.65 mm yr^{-1} (Hinderer, 2001), leading to a total particle transport of about 50 Mt yr^{-1} (Veit, 2002). Especially large loads are

observed in rivers with glacial catchments (e.g. Massa: ~265 kt yr^{-1} (500 m^3 yr^{-1} km^{-2}); Dixence: ~177 kt yr^{-1} (650 m^3 yr^{-1} km^{-2}); Drance: ~1,555 kt yr^{-1} (850 m^3 yr^{-1} km^{-2}) (Bezinge, 1987)). Accordingly particle retention in large alpine reservoirs is tremendous and can locally lead to siltation problems (Fan and Morris, 1992; Schleiss and Oehy, 2002). As a direct consequence, the suspended particle load downstream of hydropower dams is significantly reduced and its daily and seasonal dynamics are governed by hydropower operations (Loizeau and Dominik, 2000). Typically Alpine rivers in Europe flow into peri-alpine lakes, which act as deposition tanks for upstream sediment erosion.

Both the particulate matter inputs and the river intrusion dynamics into such lakes can be strongly modified. The intrusion depth is mainly determined by river water density, which is a function of temperature (T), salinity (S) and suspended particle concentrations (CR; in the following suspended particle concentrations are denoted as CR for river water and CL for lake water; Table 2.1). Hence, if CR exceeds a certain value, river water plunges within the lake, resulting in CR-driven turbidity currents. Such phenomena were observed for the first time by Forel (1885) in Lake Geneva and have been reinvestigated recently (Lambert and Giovanoli, 1988; Loizeau and Dominik, 2000). These riverine deep water renewal processes are of major importance for oxygen supply to many hypolimnia (Lambert et al., 1976; Lambert et al., 1984; Wüest et al., 1988). Recent studies indicate that intense hydropower operations can reduce the frequency of such CR-driven turbidity currents and consequently lower the oxygen supply to the deep water layers of downstream lakes (Loizeau and Dominik, 2000).

Furthermore, changes in the intrusion dynamics affect the vertical distribution of suspended matter and therefore the light regime in downstream lakes. Frequent turbid intrusions into the epilimnion can alter the optical properties and thereby increase the vertical attenuation of light (Kirk, 2003). As a direct impact, the primary production of algae is diminished (Jewson and Taylor, 1978; Field and Effler, 1988; Duarte, 1995), which can trigger negative effects on the zooplankton population and eventually on the entire food chain. A bottom-up reduction of biological activity might jeopardize plankton and fish growth and finally hamper fishing yields.

Motivated by the ongoing discussion on such effects of hydropower production (Hart and Poff, 2002), our study assesses the boundary conditions under which the light regime in those downstream lakes is affected to become relevant for the biological production and the subsequent internal biological cycling. Details of the mechanisms affecting primary production are presented in a companion study (Finger et al., 2007a).

Lake Brienz and its major tributary, River Aare, situated next to the highest Alps of Switzerland, are chosen for this study, as their setting (Figure 2.1 and section 2.2) is representative for many lakes affected by surface turbidity in the European Alps (Lambert et al., 1976), the Rocky Mountains (Gilbert and Shaw, 1981; Weirich, 1986) and the Alps of New Zealand (Schallenberg et al., 1999). Simultaneous to intensified hydropower activities in the Aare catchment, a continuous decline of fishing yields (especially of the local whitefish, *Coregonus fatioi*) during the last few years (GSA, 2003; Müller, 2003) was observed, raising concerns of a potential link to the hydropower operation (Naturaqua, 1993). Following a drastic collapse (of over 90%) of the fishing yield in 1999, a scientific survey, investigating the causes, was established (GSA, 2003).

In the present study, the effects of hydropower operation on downstream riverine particle transport and lake intrusions are assessed by establishing the recent particle budget (1997 to 2004) for Lake Brienz and comparing it to the hypothetical no-dam scenario, based on numerical simulations. CR samples and continuous discharge recordings in the major inflows were used to estimate the suspended particle loads entering the lake. The vertical turbidity dynamics in the lake were assessed by light transmission profiles, which were related to CL, allowing a comparison of suspended particles with load estimations in the rivers. During 2003 and 2004 in situ sedimentation, measured with traps, was compared to suspended particle input and long-term sedimentation, estimated from cores. Finally, to analyze the impacts of hydropower activities, flow conditions and particle transport without upstream water retention were simulated. The study concludes by assessing the impacts on the particle distribution and surface turbidity in the downstream lake.

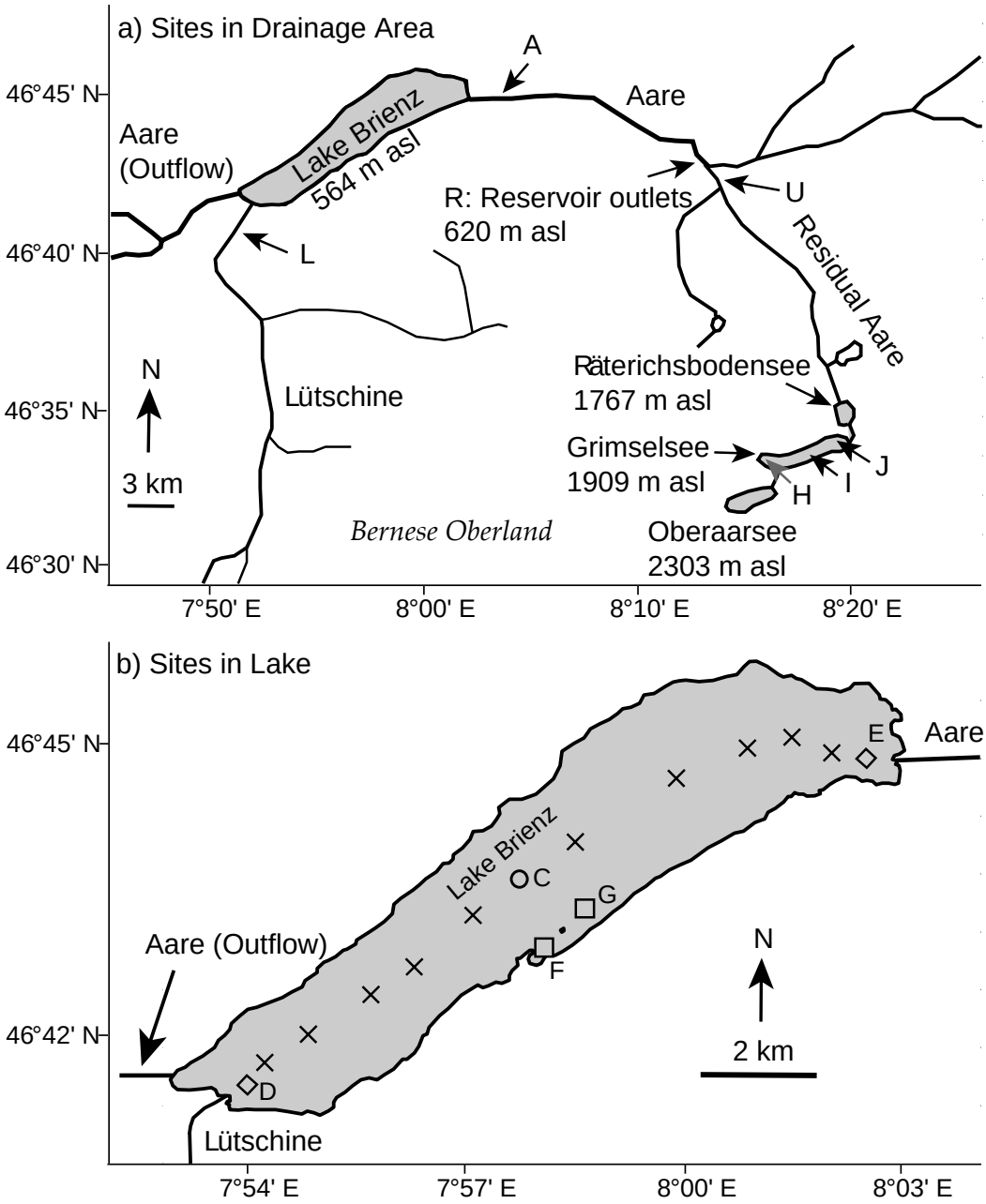

Figure 2.1: Map of study site: a) Overview of Lake Brienz and the three major reservoirs; sampling sites at Aare (A), Lütschine (L), outflow, in the residual Aare (U), at reservoir outlets (R) and in Grimselsee (H, I, and J) are located at the arrowheads; b) Sampling sites within the lake: circle (C) marks the deepest location with CTD profiling and sediment traps mooring; diamonds (D and E) represent the two thermistor strings in front of Aare and Lütschine; crosses visualize CTD stations for 2003 and 2004; squares (F and G) illustrate the locations of sediment coring.

Table 2.1: Overview of the sampling program

Monitoring of tributaries and water sampling					
Location[(a)]	**Sampling dates**	**Parameters**[(b)]	**Unit**	**Number of samples**	**Performed by**
Grimselsee, Oberaarsee[(c)]	9 October 2002 12 March 2003 8 October 2003	CR_{Gr}; CR_{Oa}	g m^{-3}	~30 per sampling	Authors
Reservoir outlets at location (R)[(d)]	10 February 2003-9 February 2004	CR_{res}; Q	g m^{-3}; m^3 s^{-1}	468	Authors/ KWO
Aare upstream of reservoir outlets at location (U)	10 February 2003-9 February 2004	$CR_{residual}$	g m^{-3}	259	Authors/ KWO
Aare at location (A) [(e,f,g)]	1974 – 2004	CR_A; T_A; Q_A; $S_A(\kappa_{25})$	g m^{-3}; °C; m^3 s^{-1}; µS cm^{-1}	4161	LHG-BWG
Lütschine at location (L) [(e,f,g)]	1974 – 2004	CR_L; T_L; Q_L; $S_L(\kappa_{25})$	g m^{-3}; °C; m^3 s^{-1}; µS cm^{-1}	4514	LHG-BWG
Lake Brienz at location (C)[(h)]	February 2003-December 2004	CL	g m^{-3}	~11 per profile	Authors
CTD-profiling in Lake Brienz					
Location CTD-profiles[(a)]	**Sampling period**	**Frequency**	**Parameters**[(b)]	**Number of profiles/ samples**	**Performed by**
Longitudinal transects[(i)]	February 2003-December 2004	bimonthly/ monthly	T, $S(\kappa_{25})$, $Tr_{in\text{-}situ}$, pH, O_2	266	Authors
Profile at deepest location (C) [(k)]	January 1997-December 2004	monthly	T, $S(\kappa_{25})$, $Tr_{in\text{-}situ}$, pH, O_2, D	96	GSA
Continuous measurements with moorings at location (C)					
Moorings[(a)]	**Sampling period**	**Parameters**	**Unit**	**Frequency**	**Performed by**
Z traps (50 and 255 m depth)	March 2003-January 2005	sedimentation-rate	g m^{-2} d^{-1}	bimonthly/ monthly	Authors
S traps (50 and 255 m depth)	April 2004-January 2005	sedimentation-rate	g m^{-2} d^{-1}	every 4 days	Authors
Two thermistor strings (in front of Aare and Lütschine inflows)	December 2003-January 2005	T at 11 depths	°C	resolution: 20 min	Authors

(Footnotes are on next page)

Table 2.1: Overview of the sampling program (continued)

Sediment cores				
Location[(a)]	**Sampling date**	**Depth**	**Label**	**Performed by**
F	23 October 2003	22	BR 03- 01 C	Authors
G	6 May 2004	212	BR 04-03 D	Authors

[(a)] Locations are marked in Figure 2.1.

[(b)] CR: suspended particle concentrations in rivers and reservoirs with subscript index indicating sampling location (L: Lütschine; A: Aare; Gr: Grimselsee; Oa: Oberaarsee; res: reservoirs outlets; residual: residual Aare); CL: suspended particle concentrations in Lake Brienz; T: temperature; S(κ_{25}): salinity based on temperature-corrected electrical conductivity determined with the algorithms by Wüest et al. (1996); $Tr_{in\text{-}situ}$: in situ light transmission (%); O_2: dissolved Oxygen (g m^{-3}).

[(c)] On 8 October 2003 additional sediment samples were collected at location H, I and J using a grab corer.

[(d)] The reservoir system comprises two distinct outlets; both sampled daily resulting in 468 samples within one year. KWO discharge is recorded with 15 min resolution.

[(e)] Although Q is monitored since 1905 in Aare and 1908 in Lütschine digitized high resolution records exist only since 1974; CR sampling started in 1964; κ_{25} has been sampled between 1991 and 1996 on a monthly basis.

[(f)] T and Q is monitored with 10 min resolution.

[(g)] Data publicly available: http://www.bwg.admin.ch/service/hydrolog/e/.

[(h)] Water samples were collected simultaneously to CTD profiling from following depths (m): 0, 5, 10, 20, 40, 60, 100, 150, 200, 250 and 255.

[(i)] Dates of sampling in 2003: 25 February; 25 March; 13 May; 19 June; 22 August; 21 October; 19 December; in 2004: 19 January; 03 March; 30 March; 04 May; 09 June; 01 July; 14 July; 27 July; 25 August; 21 September; 14 October; 24 November; 21 December.

[(k)] D: Secchi depth recordings performed twice a week by GSA.

2.2 Study Site

Lake Brienz is situated in the front ranges of the Swiss Alps at an altitude of 564 m asl (Table 2.2). With a volume of 5.17 km^3, a surface area of 29.8 km^2, and a maximum depth of 260 m, it is a typical representative of the peri-alpine lakes in Switzerland. In the north and south the lake is surrounded by steep slopes of minor drainage area of less than 200 km^2. The rest of the 1127 km^2 large catchment is drained by the two major inflows, Aare and Lütschine (Table 2.3), which enter the lake respectively at its eastern and western longitudinal ends. While Aare drains a primarily crystalline watershed, Lütschine's catchment is mainly of sedimentary geology (Sturm, 1976). As shown below, both rivers together transport on average 302 kt yr^{-1} (1997 - 2004) of suspended particles into the lake. A significant part of the suspended loads have their origin at the glaciers of the *Bernese Oberland*, which cover ~19% of the drainage area (LHG-BWG, 2005). These inorganic glacial particles dominate lake-internal sedimentation (Sturm and Matter, 1978). Due to the alpine watershed (low agricultural activities and low population of 29 habitants per km^2 (BUWAL, 1994)) the nutrient input to the lake is extremely low, rendering it exceptionally oligotrophic (Müller et al., 2006).

Unlike Lütschine (Figure 2.1), whose hydrologic regime has remained natural, the flow of Aare is affected by seven reservoirs (total operable storage volume: 0.197 km^3) and six hydropower units, administrated by the *Kraftwerke Oberhasli AG* (KWO). The system is designed to generate a nominal power of up to 1060 MW during hydro-peaking operations with an annual production of 2000 GWh yr^{-1} (KWO, unpublished data, 2003). About 68% of the runoff from the Aare drainage area is collected in the reservoir system (at altitudes between 862 and 2,365 m asl) and returned into Aare at an altitude of 620 m asl (Figure 2.1). The effects on the runoff dynamics in the Aare downstream of the reservoir outlets are distinct: compared to pre-damming, the average runoff has decreased by 18% from June to August and increased by a factor 2.5 from December to March. Recent seismic surveys in the three major reservoirs, Grimselsee (operation since 1932), Räterichsbodensee (since 1950) and Oberaarsee (since 1953) revealed that the sediment trapping amounts to 232 kt yr^{-1} (Anselmetti et al., 2007).

Table 2.2: Characteristics of Lake Brienz

PROPERTY	UNIT	QUANTITY	REFERENCE
Surface area	km^2	29.8	(BUWAL, 1994)
Volume	km^3	5.17	(BUWAL, 1994)
Volume of surface layer [(a)] (depth < 50 m)	km^3	1.40[(a)]	
Volume of deep layer [(a)] (depth > 50 m)	km^3	3.77[(a)]	
Maximum depth	m	260	(BUWAL, 1994)
Location of deepest point		46° 43' 13.6" N 7° 57' 14.4" E	
Average depth	m	173	
Altitude of the lake level	m asl	564	
Average water residence time	yr	2.69	
Catchment population	Inhabitants	26,600	(BUWAL, 1994)
Average CL in surface layer	g m^{-3}	2.7[(b)]	
Average ortho-phosphate concentration	µg P L^{-1}	0.9	(Finger et al., 2007a)

[(a)] Obtained by integrating cross sectional areas using 1:25,000 Swiss Topo map.

[(b)] Average content of suspended particles in surface layer (section 2.4.4) divided by the volume of the surface layer.

Table 2.3: Characteristics of Aare and Lütschine (major tributaries)

PROPERTY	UNIT	AARE	LÜTSCHINE	REFERENCE
Catchment area	km^2	554	379	(LHG-BWG, 2005)
Average altitude of catchment	m asl	2150	2050	(LHG-BWG, 2005)
Glaciation of catchment area	%	21	17	(LHG-BWG, 2005)
Average discharge (1997-2004)	$m^3 s^{-1}$	37.9	19.7	(LHG-BWG, 2005)
Average water temperatures (1997-2004)	°C	5.9	5.7	(LHG-BWG, 2005)
Average salinity (1991-2004)	$g kg^{-1}$	0.069[(a)]	0.189[(a)]	
Average CR (1997-2004)	$g m^{-3}$	76[(b)]	130[(b)]	(LHG-BWG, 2005)
90%- quantile of suspended particle concentrations	$g m^{-3}$	162	293	
Average suspended particle load (1997-2004)	$kt yr^{-1}$	128[(c)]	174[(c)]	
Particle retention in reservoirs	$kt yr^{-1}$	232	no reservoirs	(Anselmetti, 2007)

[(a)] Average salinity was calculated based on electrical conductivity using the algorithms by Wüest et al. (1996).

[(b)] Load-averaged CR between 1997 and 2004 (108 g m^{-3} in Aare and 280 g m^{-3} in Lütschine) is larger than the average of randomly measured CRs given above.

[(c)] Loads estimated with the adaptive rating-curve as described in section 2.3.2; according to LHG average annual loads estimated with the duration-curve method (Grasso, 2003) amount to 119 kt yr^{-1} in the Aare and 160 kt yr^{-1} in the Lütschine.

2.3 Material and Methods

In order to assess the suspended particle budget of the lake, a sampling and measurement program was established in the area, as a basis of our system analytical approach. In the following we present the sampling program, data collected by other institutions, techniques used to interpret the data and the modeling approach. Table 2.1 reviews the measurements available for this study.

2.3.1 Monitoring and Sampling of In- and Outflows

In order to estimate the suspended particle load originating from the reservoir, daily water samples were collected at the two hydropower outlets, as well as in the upstream residual flow of the Aare (at locations R and U, respectively in Figure 2.1) between 10 February 2003 and 9 February 2004. Altogether 727 samples were collected by KWO employees during work days (Table 2.1). Additionally, on three occasions samples from Grimselsee and Oberaarsee were collected for consistency checks. Furthermore, on 8 October 2003 sediment samples were collected in Grimselsee at locations H, I and J in order to determine particle size distributions of the reservoir sediment.

The collected samples were stored in a dark environment at 4 °C, until analysis for suspended particle concentrations (CR). CR was determined by filtering, using Whatman glass microfiber filters GF/F, and weighing the filter residue. The filters were pre-annealed for 1 – 3 hrs at 450 °C and dried at 50 °C for several days after filtering (APHA, 1998). Water discharge from the hydropower facilities is routinely recorded by KWO. Furthermore particle size distributions were analyzed in all samples using static light scattering measured with a Beckman Coulter LS 230 instrument (Zimmermann, 1996).

As part of the national river monitoring, the Swiss Hydrological Survey (LHG-BWG) operates hydrological stations just upstream of the lake entrance of both rivers (locations A and L in Figure 2.1) and at the outlet of the lake (Figure 2.1). Monitoring includes continuous discharge (Q), water temperature (T), as well as CR sampling twice a week and monthly salinity (electrical conductivity) readings (Table 2.1). All hydrological data is published in annual reports (LHG-BWG, 2005).

2.3.2 *Riverine Suspended Particle Loads*

In the rivers the suspended particle transport (mass per time) is given, at a point in time t, by the discharge Q(t) times concentration CR(t). As data sets are never continuously available, a certain interpolation is always necessary to estimate the load over a time range τ, given by

$$L(t, t+\tau) = \int_{t}^{t+\tau} Q(t) \cdot CR(t) \cdot dt \qquad [g] \qquad (2.1)$$

At the hydropower outlets of the reservoir system CR_{res} varied only gradually and therefore a daily time step for integration is entirely appropriate. In the two rivers, however, Q and CR fluctuations are of much higher frequencies and amplitude. Hence, the appropriate estimation of loads requires more detailed interpolation for CR to ensure resolving its variance (Bodo and Unny, 1983; Richards and Holloway, 1987).

Various estimation techniques have been developed to meet these challenges, such as stratification techniques (Richards and Holloway, 1987; Thomas and Lewis, 1995), duration curves (Grasso, 2003) and rating-curves procedures (Cohn et al., 1989; Crawford, 1991). Details of these techniques are summarized in reviews (Preston et al., 1989; Cohn, 1995).

Often, Q is quasi-continuously available, whereas CR data are scarce. With the rating-curve technique, the CR(t) interpolation is approximated by empirically relating CR to Q and by quantifying CR(t) = CR(Q(t)). In the present study we use the approach proposed by Walling (1977)

$$CR(t) = a \cdot Q(t)^b \qquad [\text{g m}^{-3}] \qquad (2.2)$$

for the construction of rating-curves, with Q in $m^3 s^{-1}$, CR in g m^{-3}, and a and b dimensionless coefficients. To optimize the predictions for CR three runoff regimes in each river were defined: (1) for low flow, (2) intermediate discharge and (3) high water events. Thus, the rating-curve is composed of six rating-curve parameters and two threshold discharges, which were determined with the least square method (Table 2.4). Nevertheless, CR samples from Aare and Lütschine at a given Q are subjected to a scatter of over two orders of magnitude (Figure 2.2).

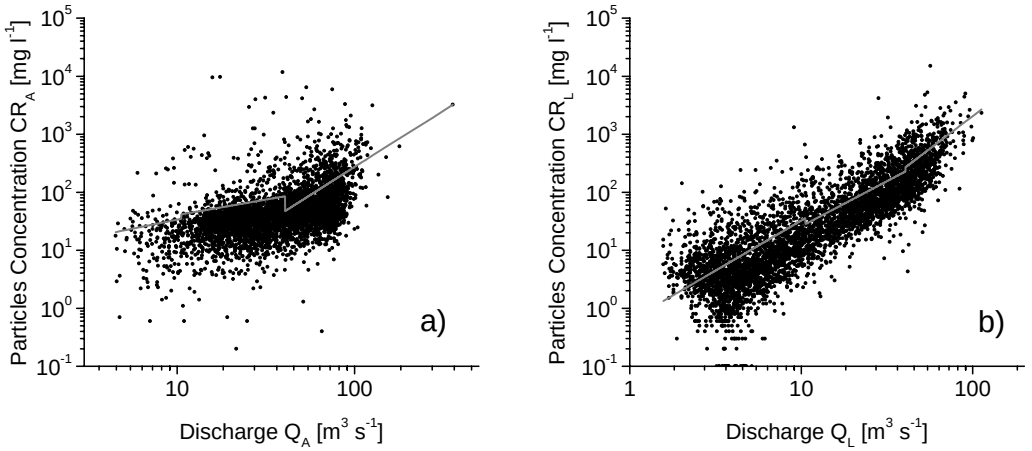

Figure 2.2: Scatter plots of instant discharge (Q) versus suspended particle concentrations (CR) in the Aare (a) and Lütschine (b) with the corresponding rating curves (solid line).

Hence, to determine CR(t) with a high temporal resolution we used the rating-curve, but only to interpolate between CR samples. We adjusted the rating-curve to all the measured CR values (approximately every 3 to 4 days) by adding the difference (ΔCR) between measured CR and rating-curve CR. In between CR samples we interpolated ΔCR(t). The load over a certain time range is given by replacing CR(t) in equation (2.1) with the adapted CR(t):

$$CR\big(Q(t)\big) = aQ(t)^b + \Delta CR(t) \qquad [\text{g m}^{-3}] \qquad (2.3)$$

$$\Delta CR(t) = \Delta CR_{prev} + \left(t - t_{prev}\right)\left(\frac{\Delta CR_{next} - \Delta CR_{prev}}{t_{next} - t_{prev}}\right) \qquad [\text{g m}^{-3}] \qquad (2.4)$$

where the indices (prev and next) indicate most recent CR measurements before and after time t. Negative CR(t)-values were set equal to zero. While this mathematical approach cannot precisely predict loads during specific flood peaks it allows a statistically adequate

estimation of long-term load-patterns as demonstrated below. In the following, this method will be referred to as the adaptive rating-curve technique (ARC).

Table 2.4: Numeric values of fitted parameters

Equation	Equation number	Parameter	Unit	Value
Rating-curves Aare[(a)] $CR_A(t) = a \cdot Q_A(t)^b$	2.2	Q_{crit1}	$m^3 s^{-1}$	10.5
		Q_{crit2}	$m^3 s^{-1}$	40.5
		a_1		8.054
		b_1		0.621
		a_2		11.774
		b_2		0.535
		a_3		0.035
		b_3		40.534
Rating-curves Lütschine and hypothetical no-dam Aare[(a)] $CR_L(t) = a \cdot Q_L(t)^b$	2.2 and 2.14	Q_{crit1}	$m^3 s^{-1}$	10.5
		Q_{crit2}	$m^3 s^{-1}$	40.5
		a_1		0.612
		b_1		1.725
		a_2		0.717
		b_2		1.557
		a_3		0.065
		b_3		2.251
Calibration curve for CL $CL = \frac{-\ln\left(\frac{Tr_{in-situ} + k_1}{k_2}\right)}{0.1 \cdot \varepsilon}$	2.5	k_1		-0.156 ± 0.015
		k_2		0.825 ± 0.010
		ε	$m^2 g^{-1}$	1.022 ± 0.062
Entrainment of Aare intrusion $\alpha(t) = \alpha_0 + r_{Aare} \cdot \Delta\rho(t)$	2.7	$\alpha_{\Delta\rho<0}$[(b,c)]		0.842
		α_0[(c)]		0.925[(d)]
		r_{Aare}		-0.65 ± 0.05[(e)]
Entrainment of Lütschine intrusion $\alpha(t) = \alpha_0 + r_{Luet} \cdot \Delta\rho(t)$	2.7	$\alpha_{\Delta\rho<0}$[(b,c)]		0.842
		A_0[(c)]		0.925[(d)]
		r_{Luet}		-0.45 ± 0.05[(e)]
Scaling factor	2.14	f		0.9231

[(a)] For $Q(t) < Q_{crit1}$ coefficients sub indexed with 1 apply, for $Q_{crit1} < Q(t) < Q_{crit2}$ coefficients sub indexed with 2 apply and for $Q(t) > Q_{crit2}$ coefficients sub indexed with 3 apply; sub index of Q differentiates between A: Aare and L: Lütschine; fitting to least-square-difference was performed in linear space.

[(b)] to account for cabbeling, α was set equal to $\alpha_{\Delta\rho<0}$ if $\Delta\rho(t) < 0$.

[(c)] α_0 and $\alpha_{\Delta\rho<0}$ were assumed equal for Aare and Lütschine as accuracy is too small to determine a difference.

[(d)] Errors on α_0 were neglected, because intrusion depths for $\Delta\rho(t) = 0$ are evidently close to the lake surface.

[(e)] Error of r lies below 0.05 as smaller variations do not effect simulation significantly.

To reduce computing time in simulations presented below and still adequately account for the short-term precipitation events, Q recordings were subsampled on a 0.1 d fixed-grid before CR(Q(t)) interpolation. This temporal resolution was retained for all further simulations and calculations.

By definition the rating-curve predicts a typical CR value for a given Q. The predictability of CR depends on the variability of the measured CRs at identical Qs. In Aare and Lütschine CR values vary by two orders of magnitude for the same Q leading to an irreducible uncertainty in the load estimations. To determine their accuracy, we performed Monte Carlo simulations by randomly choosing measured CR values for the corresponding Q's, similar to Moosmann et al. (2005). The Q-CR data pairs for each of the two rivers were sorted in ascending order and Q-bins containing 10 Q-CR data pairs were established (resulting in 452 Q-bins for Lütschine and 417 Q-bins for Aare) allocating 10 possible CRs to a given Q. During Monte Carlo simulations for a specific time period twice weekly CRs were randomly picked from the corresponding Q-bins and applied to the ARC-technique. The standard deviation of 1000 Monte Carlo runs was used as an upper limit for the uncertainty of the adaptive rating-curve estimates. 1000 Monte Carlo simulations proved to represent the variance adequately as ten subsets of 100 simulations each depict similar standard deviations (less than 1% difference).

2.3.3 *Particle Distributions in Downstream Lake Brienz*

On 19 occasions between February 2003 and December 2004, 266 CTD profiles were collected along the thalweg of Lake Brienz (Figure 2.1) using a SBE-19 profiler (Seabird Electronics). The device was equipped – in addition to the conductivity, temperature and depth probe – with a pH and a dissolved oxygen sensor, as well as a 10 cm Sea Tech transmissometer (660 nm light source). Routinely performed transmission gauging revealed a linear temporal drift of 0.33% per month, which was corrected accordingly.

Simultaneously to CTD profiling at the deepest location (Figure 2.1) eleven water samples at different depths were collected. Niskin bottles were attached 1 m above the CTD allowing concurrent sampling. Suspended particle concentrations (CL) were determined by the same procedure as for river samples. Since suspended matter in natural water consists of specific mixtures of different sizes and types of particles, calibration is required to determine CL based on in situ light transmission (Baker and Lavelle, 1984; Gordon et al., 1984; Hofmann and Dominik, 1995). Light attenuation at 660 nm can unambiguously be related to particle concentrations assuming that the particle mixture is homogeneous and the attenuation

by the water is constant (Boss et al., 2001). The background of the calibration curve used relies on the Beer–Lambert Law which applies to anisotropic light (Commoner and Lipkin, 1949). In situ light transmission ($Tr_{in\text{-}situ}$) was linearly corrected in order to adjust for instrument specific properties. Combining the Beer-Lambert Law with the linear correction, the relation between CL and $Tr_{in\text{-}situ}$ is given by

$$CL = \frac{-\ln\left(\frac{Tr_{in-situ} + k_1}{k_2}\right)}{0.1 \cdot \varepsilon} \qquad [g\ m^{-3}] \qquad (2.5)$$

Coefficients k_1, k_2 and ε were determined by least square fitting ($R^2 = 0.97$) equation (2.5) to measured CL and $Tr_{in\text{-}situ}$ (Table 2.4) and the factor 0.1 is the used light path length of 0.1 m. Using equation (2.5) all $Tr_{in\text{-}situ}$ profiles were converted into CL profiles and the suspended particle masses were obtained by integrating CL over cross sectional areas using a 1:25,000 Swiss Topographic map. Profile integrals at the lake center deviated by less than 15% from transect integrals across the lake.

Monthly $Tr_{in\text{-}situ}$ profiles, using an identical Sea Tech transmissometer have been performed by the Office of Water Protection and Waste Management of the Canton of Bern (GSA) since 1997. Comparison of $Tr_{in\text{-}situ}$ profiles between the two sensors showed consistent results, allowing a reconstruction of the vertical particle distribution back to 1997.

2.3.4 Sediment Traps, Cores and Thermistor Moorings

About 500 m north of the deepest point, two pairs of plastic cylinder traps (Z traps), each with an effective sampling area of 66 cm^2 and aspect ratio (height: diameter) of nine were deployed at 50 and 255 m depth. After the first deployment on 25 March 2003, traps were exchanged approximately every two months until 7 January 2005 (Table 2.1). To determine the variance of sedimentation rates, two sequencing traps (S traps) were installed next to the Z-traps (2 April 2004 to 7 January 2005). Each S trap consisted of a funnel (effective area 500 cm^2; aspect ratio 4) above a carousel of 12 sample-bottles (200 cm^3 each), rotating at predefined intervals of a few days. Trap material was freeze-dried and local sedimentation rates were calculated. The sediment was further analyzed for phosphorus and organic carbon in companion studies (Müller et al., 2007; Wüest et al., 2007).

Two sediment cores were obtained from location F (22 m depth) and G (212 m depth), respectively (Table 2.1; Figure 2.1). The cores were dated by ^{210}Pb (decay curve) and ^{137}Cs (1963 bomb fallout and 1986 Chernobyl catastrophe) measured in freeze-dried slices using a Ge-Li borehole detector (Hakanson and Jansson, 1983). As shown below, sedimentation at

location F includes primarily matter from summer (referring to months between April and October) because of its shallow depth, whereas location G is subjected to sedimentation throughout the year (due to its great depth). Both locations exclude slope slides and intense turbidity currents, as they usually follow the thalweg of the lake.

Starting on 19 December 2003 until 18 February 2005, two thermistor moorings, equipped each with eleven 8-bit Vemco Minilog sensors, were deployed about 450 m in front of Lütschine and 700 m in front of Aare (location D and E in Figure 2.1). Using temperature as a tracer, the intrusion dynamics of the two rivers could be observed throughout 2004.

2.3.5 Estimation of Riverine Intrusion Depth

Vertical distributions of dissolved and suspended matter in lakes of short residence times depend primarily on the river intrusion depths. The intrusion depth is reached once the density of the river intrusion (mixture of river and surrounding lake water) matches the density of the surrounding lake water. We used the following procedure - based on the time series of temperature, electrical conductivity and suspended particles in the rivers - to determine the intrusion depth of Aare and Lütschine.

The density of freshwater is a function of temperature (T) and salinity (S) (Chen and Millero, 1986; Millero, 2000) as well as suspended particles C (here CL or CR):

$$\rho_{T,S,C} = \rho_{T,S} + \left(1 - \frac{\rho_{T,S}}{\rho_C}\right) \cdot C = \rho_{T,S} + 0.62 \cdot C \qquad (2.6)$$

Freshwater salinity S [g kg^{-1}] was determined from ionic compositions and temperature-corrected (25 ^{o}C) conductivity (κ_{25}) readings according the procedure by Wüest et al. (1996). The term $\rho_{T,S}$ is the density for T and S using the algorithms by Chen and Millero (1986). Here, C, $\rho_{T,S}$ and $\rho_{T,S,C}$ are all given in kg m^{-3}. According to Sturm (1976), sediments are composed of minerals with $\rho_C \sim 2650$ kg m^{-3}. Fluctuations of ρ_C due to changing particle composition are minor and can be neglected for our purposes.

Based on monthly CTD-profiles from the lake center, time series of T(z), S(z) and CL(z) - and subsequently $\rho_{T,S,C}$ profiles using equation (2.6) - were determined by temporal interpolation with 0.1 d resolution. Identical time series were determined based on T, S, and CR from both inflows.

During the process of plunging, the advancing intrusion entrains surrounding lake water. Often the entrainment is parameterized by an overall Richardson number, based on local density excess and intrusion thickness as well as angle of incline (Turner, 1986). Neglecting

thickness variations, the proportion of entrained lake water is governed by the initial density difference $\Delta\rho$ between river and ambient lake water. Hence, in the present study the entrainment factor (α; proportion of lake water in the river intrusion at its final equilibrium level) was determined by the following empirical approach:

$$\alpha(t) = \alpha_0 + r \cdot \Delta\rho(t) \tag{2.7}$$

where $\Delta\rho(t)$ denotes the difference between river density and mean density of the upper 10 m water column of the open water and r represents an empirical coefficient. Accordingly, time series of $\alpha(t)$ were determined by distinguishing the following cases:

(1) $\Delta\rho(t) \sim 0$: The entrainment factor α_0, valid for river intrusions close to the lake surface, was determined by:

$$\alpha_0 = \frac{P^i_{Intrusion} - P^i_{River}}{P^i_{Lake} - P^i_{River}} \tag{2.8}$$

where P^i represents the transient tracer i recorded during CTD profiling (superscript index i standing for T, S and C). The value of $P^i_{Intrusion}$ reflects the peak of the tracer in the river intrusion, representing the center (highest concentration of river water) of the intruding plume. P^i_{Lake} was calculated by averaging the tracer values in the water column above the intruding plume, representing typical lake water above the plume. P^i_{River} reflects the average tracer content in the river during the five preceding days (as the river intrusions contain those characteristics). Equation 2.8 was always applied to all three tracers, assuring proper identification of river intrusions (e.g. temperature failed being a useful tracer during summer as the temperature stratification overruled the river signal).

(2) $\Delta\rho(t) < 0$: During winter (referring to months between November and March) low T renders $\Delta\rho$ occasionally negative. Nonlinearity of the equation of state triggers cabbeling instability (see section 2.4.3) making the approach of equation (2.7) unsuitable. Therefore a constant $\alpha_{\Delta\rho<0}$ was determined with equation (2.8) for situations when $\Delta\rho(t) < 0$ (Table 2.4).

(3) $\Delta\rho(t) > 0$: During deep river intrusions in summer (with $\Delta\rho >> 0$), α is difficult to determine and even harder to predict. Therefore we calibrated the parameterization given in equation (2.7), by adjusting r, so that predicted deep river intrusions matched the observed plunging in the temperature data from the thermistor strings in front of the river inlet (Table 2.4). Knowing $\alpha(t)$, the characteristics in the river intrusions are given by:

$$P^i_{Intrusion}(t) = \alpha(t) \cdot P^i_{Lake}(t) + \big(1 - \alpha(t)\big) \cdot P^i_{River}(t) \tag{2.9}$$

As intrusion depth and river intrusions characteristics are dependent on each other, the depth has to be determined as an iterative process performed until convergence. The load of suspended solids entering Lake Brienz can hence be split up into a part entering into the upper layer (top 50 m; equivalent with the maximal depth of the thermocline) relevant for productivity and a part entering the deep water (below 50 m depth) irrelevant for productivity.

2.3.6 One-Box Model of the Upper Layer of Lake Brienz

As only particles near the surface are relevant for light attenuation (and subsequently for productivity) focus is laid on the particle budget of the upper layer. By considering (1) particle input, (2) sedimentation and (3) outflow we used a one-box model to asses the particle balance of the top 50 m of Lake Brienz.

The size of suspended particles from both rivers ranges from infinitely small to several 100 µm, leading to settling rates of zero to several mm s^{-1} (Stoke's law). Calculations for the measured size distributions in Lake Brienz specify that 80% of light attenuation is caused by particles smaller than 4 µm in diameter (Jaun, 2005). Hence, to account for slow sedimentation and high light attenuation we distinguished between fine (< 4 µm) and coarse particles (> 4 µm).

Based on particle size distributions measured in the two rivers and at the reservoir outlets, the fraction of fine matter in the suspended load entering above 50 m depth can be determined using equation (2.10) listed in Table 2.5. Basically the loads entering the upper layer from Lütschine ($F_{Luet}(t)$), from the reservoir outlets ($F_{res}(t)$) and from the residual Aare ($F_{Aare}(t) - F_{res}(t)$) are proportionally split up into a load of coarse particles ($I^{coarse}(t)$) and a load of fine matter ($I^{fine}(t)$) according to the measured fine fraction in the corresponding water samples (X_{River}: fine fraction in Lütschine and residual Aare; X_{res}^{h}: fine fraction in reservoir outlets during high particle discharge; and X_{res}^{l}: fine fraction in reservoir outlets during low particle discharge – see Table 2.5 for details). Considering particle input, defined in equation (2.10), and particle flushing through the outflow ($Q_{out}(t)$), the content of coarse particles (M_{upper}^{coarse}) and fine matter (M_{upper}^{fine}) can be simulated with a one box approach (equation (2.11) in Table 2.5).

Table 2.5: Equations for the surface layer one box-model

Coarse particles (I^{coarse}) and fine matter (I^{fine}) input into the upper layer	**Terms**	**Unit**
	$F_{Luet}(t)$	[t d^{-1}]
$I_{Luet}^{coarse}(t) = (1 - X_{River})F_{Luet}(t)$	$F_{Aare}(t)$	[t d^{-1}]
$I_{Luet}^{fine}(t) = X_{River}F_{Luet}(t)$	$F_{res}(t)$	[t d^{-1}]
$I_{Aare}^{coarse}(t) = (1 - X_{res})F_{res}(t) + (1 - X_{River})(F_{Aare}(t) - F_{res}(t))$	$X_{res}^{l} = 0.82$ [(b)]	[-]
$I_{Aare}^{fine}(t) = X_{res}F_{res}(t) + (X_{River}(F_{Aare}(t) - F_{res}(t)))$	$X_{res}^{h} = 0.56$ [(b)]	[-]
Equation (2.10) [(a)]	$X_{River} = 0.27$	[-]
	$F_{res}^{crit} = 100$	[t d^{-1}]
Content of coarse particles (M_{upper}^{coarse}) and fine matter (M_{upper}^{fine}) in the upper layer		
	$M_{upper}^{coarse}(t)$	[t]
$\frac{dM_{upper}^{coarse}(t)}{dt} = I_{Aare}^{coarse}(t) + I_{Luet}^{coarse}(t) - \sigma_{coarse}M_{upper}^{coarse}(t) - \frac{M_{upper}^{coarse}(t)}{V_{upper}}Q_{out}(t)$	$M_{upper}^{fine}(t)$	[t]
	$\sigma_{coarse} = 0.22$	[d^{-1}]
$\frac{dM_{upper}^{fine}(t)}{dt} = I_{Aare}^{fine}(t) + I_{Luet}^{fine}(t) - \sigma_{fine}M_{upper}^{fine}(t) - \frac{M_{upper}^{fine}(t)}{V_{upper}}Q_{out}(t)$	$\sigma_{fine}^{s} = 0.01$	[d^{-1}]
	$\sigma_{fine}^{w} = 0.05$	
Equation (2.11) [(c,d)]	$Q_{out}(t)$	[m^3 d^{-1}]
Hypothetical no-dam situation: coarse particles ($I_{Aare(no-dam)}^{coarse}$) and fine matter ($I_{Aare(no-dam)}^{fine}$) input into the upper layer		
$I_{Aare(no-dam)}^{coarse}(t) = (1 - X_{res})q_{res}F_{Aare(no-dam)}(t)$	$q_{res} = 0.108$	
$+ (1 - X_{river})q_{River}F_{Aare(no-dam)}(t) + (1 - X_{Gr})q_{Gr}F_{Aare(no-dam)}(t)$	$q_{River} = 0.247$	
$I_{Aare(no-dam)}^{fine}(t) = X_{res}q_{res}F_{Aare(no-dam)}(t)$	$q_{Gr} = 0.644$	
$+ X_{River}q_{River}F_{Aare(no-dam)}(t) + X_{Gr}q_{Gr}F_{Aare(no-dam)}(t)$	$X_{Gr} = 0.03$	
Equation (2.12) [(e)]		

[(a)] F_{Luet} , F_{Aare} and F_{res} : particle input from Lütschine, Aare and reservoir outlets into the upper layer respectively, where $F_{Aare}(t) - F_{res}(t)$ results in the particle load from the residual Aare into upper layer; X_{River} : fraction of fine matters in Lütschine and residual Aare loads; X_{res} : fraction of fine matters in reservoir outlets loads; Note: during January and February F_{Luet} and F_{Aare} are set equal to the volume distributed particle input (F= (volume of upper layer / volume of lake) * particle load in the river), in order to account for convective mixing during winter.

[(b)] X_{res}^{h} : fine fraction observed during periods when $F_{res}(t) < F_{res}^{crit}$; X_{res}^{l} : fine fraction observed during periods when $F_{res}(t) > F_{res}^{crit}$.

[(c)] σ_{coarse} and σ_{fine} : sedimentation constants for coarse particles and fine matter, respectively; V_{upper} : volume of the upper layer; Q_{out} : discharge at the outflow of the lake.

[(d)] σ_{fine} differs during winter (taking the value of σ_{fine}^{w} between November and March) and summer (taking the value of σ_{fine}^{s} between April and October) because average particle size during winter is significantly smaller than during summer.

(e) $F_{Aare(no-dam)}$: hypothetical Aare load entering the upper layer under no-dam conditions, where q_{res} = present outlets load / no-dam load = 39 kt yr^{-1}/ 360 kt yr^{-1}, q_{river} = (present Aare load – present outlets load) / no-dam load = (128 kt yr^{-1}- 39 kt yr^{-1})/ 360 kt yr^{-1}, q_{Gr} = particles presently trapped in the reservoirs/ no-dam load = 232 kt yr^{-1}/ 360 kt yr^{-1} and X_{Gr} denotes fraction of fine matters trapped in reservoirs.

As stated in equation (2.11) residence times of fine matter and coarse particles in the upper layer depend directly on sedimentation constants (σ) for the two particle classes. Particle size distributions of fine matter during summer reveal larger diameters than during winter. Accordingly we introduced different sedimentation constants (Table 2.5) for fine matter during summer (σ^{s}_{fine}) and winter (σ^{w}_{fine}). σ^{w}_{fine} was determined by fitting predicted to measured particle content during winter, when they consisted of fine matter. Subsequently σ^{s}_{fine} and the sedimentation constant for coarse particles (σ_{coarse}) was determined by fitting maximal predicted to maximal measured particle content (usually in August), when they were of rather larger sizes.

2.3.7 Modeling the Natural Hydrology of River Aare

In order to assess the potential effects of upstream water storage on the lake surface turbidity, suspended loads, discharge dynamics and temperature for the hypothetical no-dam scenario must be reconstructed, since the only available pre-dam data are daily discharges between 1908 and 1932. The Aare no-dam runoff, was simulated with hourly resolution in a companion study (Sägesser and Weingartner, 2005). The natural Aare discharge was simulated using a regression model, based on the instant discharge of Lütschine and precipitation in the Aare catchment.

The water temperature is altered by the retention as well: since water is stored at an altitude of 1909 m asl (Figure 2.1) and flows via pipes down to an altitude of 620 m asl, the warming in summer is reduced (transformation of potential to electrical energy; no heat exchange with atmosphere), while winter temperatures are slightly higher due to heat conservation in the reservoirs. To account for these alterations, the water temperature for the hypothetical no-dam situation (T_{sim}) was simulated using a linear regression model relying on the instant water temperature of the Lütschine (Moosmann, 2005).

Regarding the suspended particles in Lake Brienz, the most important hydrological effects of hydropower operation are the alterations in Aare of (1) the integrated particle load and (2) its seasonal structure. The dynamics of CR_A was reconstructed for a no-dam situation using the rating-curves from Lütschine and the no-dam Aare discharge (Q_{sim}) as simulated by

Sägesser and Weingartner (2005). For this purpose Q_{sim} was scaled to annual Lütschine discharge according to:

$$Q_{scaled}(t) = \left(\frac{Q_{Luet}^{annual}}{Q_{sim}^{annual}} \right) Q_{sim}(t) \quad (2.13)$$

where $Q_{Luet}^{annual} / Q_{sim}^{annual}$ denotes the annually variable ratio of Lütschine to Aare discharge. $Q_{scaled}(t)$ serves only as input parameter to determine CR_A in the no-dam Aare with the rating-curve of Lütschine given by:

$$CR_{sim}\left(Q_{scaled}(t)\right) = f \cdot a \cdot \left(Q_{scaled}(t)\right)^b \quad (2.14)$$

where a and b take the values determined for the Lütschine rating-curves (Table 2.4). The no-dam load ($F_{Aare(no-dam)}(t)$) can hence be calculated by integrating the product $Q_{sim}(t) \cdot CR_{sim}(t)$ as stated in equation (2.1). The scaling factor f permits to match average no-dam loads to the sum of current average loads and retention in the reservoirs (128 kt yr^{-1} + 232 kt yr^{-1} = 360 kt yr^{-1}; Table 2.3). As f takes a value of 0.92 the correction is rather small, indicating that the assumption behind the reconstruction of pre-dam loads is reasonably adequate. This approach relies on the assumption that ablation rates are the same now as they were prior to damming. The assumption appears reasonable as the watershed of Aare is steep (altitude difference of ~3600 m for 20 km of water flow) and the river largely channeled leaving little space for floodplains (potential particle sink and sources) or land use changes.

Based on the simulations of the pre-dam scenario ($Q_{sim}; T_{sim}; CR_{sim}$) the turbidity dynamics in Lake Brienz can be assessed for no-dam conditions. For this purpose particle input from Aare was divided into three parts: (1) fraction transported in the residual flow (q_{River} = (present Aare load – present outlets load) / no-dam load); (2) fraction discharged presently from the reservoir outlets (q_{res} = present outlets load / no-dam load); (3) fraction presently trapped in the reservoirs (q_{Gr} = particles presently trapped in the reservoirs / no-dam load) (see footnotes of Table 2.5). Adding up the three fractions (equation (2.12) in Table 2.5) and considering the ratios of fine matter in each fraction, the particle content in the lake can be estimated using the one box approach. The fraction of fine matter in the sediments currently trapped in the reservoirs (X_{Gr}) depicts the volume-average determined from sediment samples taken at three locations in the Grimselsee (Figure 2.1).

2.4 Observations and Results

2.4.1 Estimation of Riverine Suspended Particle Load

For the assessment of particle balances in Lake Brienz it is essential to determine the reliability of the estimation techniques introduced in section 2.3. The results of the rating-curve (RC) and the adaptive rating-curve method (ARC) as well as averages of Monte Carlo simulations (MC) are illustrated in Figure 2.3. While RC- and MC-estimations are based on long-term data, ARC-estimations include also integral-specific information. The latter estimations are period-specific loads, while the former represent typical loads for the considered discharge conditions.

For the years 1974 until 2004 all three techniques provide consistent annual averages of suspended particle loads with less than 5% maximal differences for both Aare (RC: 134 kt yr^{-1} ARC: 129 kt yr^{-1}; MC: 131 kt yr^{-1}) and Lütschine (RC: 191 kt yr^{-1}; ARC: 183 kt yr^{-1}; MC: 192 kt yr^{-1}). The annual particle input is furthermore in good accordance with sedimentation close to the lake center observed in (1) sediment traps at 50 m (3.3 kg m^{-2} yr^{-1} in 2003) and 255 m depth (10.7 kg m^{-2} yr^{-1} in 2003) and (2) ^{137}Cs dating of sediment cores from location F (22 m depth) and G (212 m depth) which reveal sedimentation rates of 0.33 cm yr^{-1} (4.6 kg m^{-2} yr^{-1}; considering measured porosity of 46.9%) and 0.64 cm yr^{-1} (8.7 kg m^{-2} yr^{-1}; 48.2% porosity), respectively. Integration of these sedimentation rates over depth and the corresponding cross sectional areas gives an annual sediment flux of 230 kt yr^{-1}, implying that over 76% of the particle input reaches the center of the lake.

Individual episodes depict important differences between ARC and RC/MC estimations, especially during extraordinary hydrological conditions. For instance, increased loads in Aare due to reservoir sediment flushing (preventing siltation), as performed in 1991 (Figure 2.3), can only adequately be reproduced by the ARC method, as CR_A is dominated by sediment release and hence independent from Q_A. But also the heat wave during summer 2003 (Schär et al., 2004) led to intense erosion underneath glaciers, altering the relation between Q and CR. Hence, the rating-curve for both rivers are biased since (1) CR_{res} at the reservoir outlets is independent of hydropower discharge and (2) erosion rates underneath the glaciers and in the lower valley relate differently to momentary runoff.

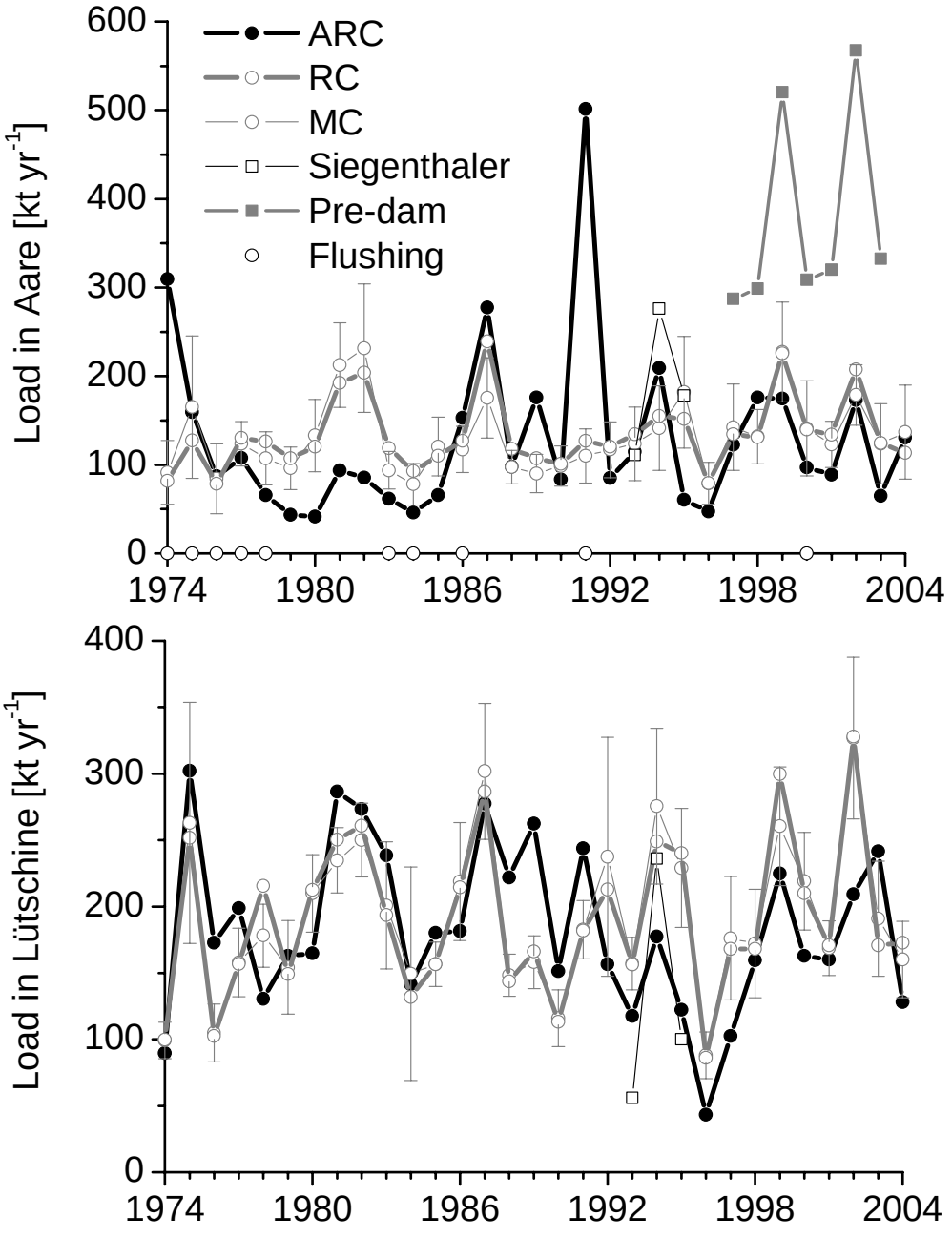

Figure 2.3: Estimations of the annual particle load in Aare (A in Figure 2.1) and Lütschine (L in Figure 2.1): ARC = adaptive rating curve; RC = rating curve; MC = mean of Monte Carlo simulation runs with error bars indicating standard deviations; Siegenthaler = integration of daily products of CR times Q; Pre-dam = estimated annual loads of Aare before construction of the reservoirs; Flushing = years with flushing for reservoirs maintenance.

The low loads in Aare estimated with ARC between 1978 and 1985 are also remarkable. In fact during this period average measured CR lies 47% (48 g m^{-3}) below the average of all measured CR since 1964 (90 g m^{-3}) while no significant drop is observed in the corresponding Q. Therefore, we conclude that RC and MC overestimate the load during this period while ARC appears most representative, although not knowing the reason for the lower CRs.

Considering these aspects we conclude that the ARC technique is the best possible approach to estimate continuous particle concentrations in the rivers for the following reasons: (1) It relies on episode-specific data pairs as well as on long-term relation between CR and Q expressed in the rating-curve; (2) the effects of the mentioned bias of a CR(Q(t)) function are minimized by adjusting CR at every instant of a measured CR value. Finally, we had access to a Q-CR dataset of one-day resolution, collected between 1993 and 1995 in both rivers (Siegenthaler et al., 1996) (Figure 2.3). In Lütschine, the square differences to the measured concentrations are 17% lower for ARC predictions compared to RC predictions.

However, two water samples per week can still not represent short-term precipitation events and some uncertainty in the estimation remains inevitable. The standard deviations of 1000 Monte Carlo simulations for one specific year provide the statistical error of ARC-estimations. On average (between 1997 and 2004) the standard deviations constitute 29% of the mean annual load of the Monte Carlo runs for Aare and 19% for Lütschine. As ARC-estimations relay on episode-specific data pairs we consider these inaccuracies for ARC as upper limits. Nevertheless, as mentioned above, long-term averages (1974-2004) have uncertainties of less then 3%.

In the following we refer to ARC to discuss suspended particle input to the lake. Furthermore, we limit the particle balance to the period of CTD monitoring (1997 to 2004).

2.4.2 Dynamics of Suspended Particle Input to Lake Brienz

Seismic measurements indicate that 232 kt yr^{-1} of coarse particles settle out in the upstream reservoirs (Anselmetti et al., 2007), while the fine-grained matter remains suspended. In fact, concentrations of suspended particles in Grimselsee (Figure 2.1) remain for most of the time below 60 g m^{-3} (measured averages: 57 g m^{-3} (October 2002), 35 g m^{-3} (March 2003), and 56 g m^{-3} (October 2003)). However, occasional peak input events lead to short-term (days to weeks) elevated concentrations of several hundred g m^{-3} (Bühler et al., 2004).

The consistency of particles concentrations from the daily water samples and the continuous discharge record allows direct load integration (section 2.3.2). From 10 February

2003 to 9 February 2004 the suspended particle load at the hydropower outlets accounts for 40.2 kt yr^{-1}, compared to 69 kt yr^{-1} estimated in the downstream Aare during the same time period (Table 2.6). As particle concentrations vary only gradually in the reservoirs, their annual suspended matter outflow is assumed being proportional to the water discharges – disregarding maintenance flushing. Accordingly the average annual load between 1997 and 2003 amounts up to 39 kt yr^{-1} and the inter-annual variation is less than 10%.

Table 2.6: Summary of discharges and suspended particle loads

		Discharge [km^3 yr^{-1}]			**Suspended particle load [kt yr^{-1}]**		
		Sampling period [a]	**Average[b]**	**Extremes**	**Sampling period[a]**	**Average[b]**	**Extremes**
Reservoir-Outlets		0.826[c]	0.807[c]	0.750/0.905	40.2	39.3[d]	37/44
Aare (Location A)	yr[e]	1.129	1.195	1.087/1.404	69	128	65/176
	w[f]		0.050		1.5	2.7	
	s[g]		0.135		8.8	16.4	
Contributed from the reservoirs		73%	68%		58%	31%	
Lütschine (Location L)	yr[e]	0.598	0.620	0.576/0.700	242	174	103/242
	w[f]		0.015		0.2	0.6	
	s[g]		0.078		34.4	24.4	
Outflow from lake			1.973[h]	1.684/2.273		6[i]	5/10

[a] CR sampling at the reservoir outlets between 10 February 2003 and 9 February 2004.

[b] Averages over eight years (1997 – 2004).

[c] KWO, unpublished data, 2004; as dataset of 2002 is incomplete average values do not consider the year 2002.

[d] Average load at the outlets assuming linear proportionality of load and annual discharge and based on measured load between February 2003 and February 2004.

[e] yr denotes annual values.

[f] w denotes monthly values during winter (November – March) (kt mo^{-1} and km^3 mo^{-1} respectively).

[g] s denotes monthly values during summer (April – October) (kt mo^{-1} and km^3 mo^{-1} respectively).

[h] Difference between inflows and outflow are explained by net precipitation (mean precipitation (1174 mm) –mean evaporation (851 mm)) of 0.01 km^3 yr^{-1} and 0.148 km^3 input from minor inflows. Precipitation date publicly available at: http://www.meteoschweiz.ch/web/en/services/data_portal/online_data_acquisition.html.

[i] Integrated monthly loads based on mean discharge and CL at 5 m depth in the center of the lake.

The volume-averaged particle size at the reservoir outlets of ~3.4 µm is relatively small compared to samples from Aare (~4.9 µm) and Lütschine (~8.0 µm). Accordingly, the sinking velocity of ~0.008 mm s^{-1} (Stoke's law) is very small and particles remain suspended until they reach the lake entrance. Therefore, the reservoir outlet loads at location R will be contained in the loads estimated in Aare at location A. As summarized in Table 2.6 during the sampling period the reservoir outlets accounted for 73% of the water discharge and 58% of

the suspended particle load in Aare. For the eight years of 1997 to 2004 this partitioning is somewhat different: ~68% of the Aare flow but only 31% of the suspended particles can be attributed to the reservoir outlet. These differences are primarily due to extraordinary warm and dry weather during summer 2003 as discussed in section 2.4.4.

While monthly loads in Lütschine drop below 0.6 kt mo^{-1} during winter, the Aare provides still 2.7 kt mo^{-1}. The elevated load in Aare during winter is caused by hydropower-related water discharge from the reservoirs.

During the productive summer both rivers transport several times more particles than during winter (Summer loads: Aare: 16.4 kt mo^{-1}; Lütschine: 24.4 kt mo^{-1}). The load at the reservoir outlets accounted for only 4.8 kt mo^{-1} during summer in 2003. Therefore, ~70% of the load at the lake entrance originates from the inter-catchments below the reservoirs.

In summary, Lütschine discharges particles primarily during summer (natural hydrology), while Aare's load is spread more evenly throughout the year (hydropower operation). Furthermore, although Aare discharges 89% more water than Lütschine, the mean load is 26% lower because of the particle retention in the upstream reservoirs (~232 kt yr^{-1}). The distinctly different particle load dynamics of the two rivers affect the depths at which suspended matter enters into the lake.

2.4.3 Intrusion Depths of Aare and Lütschine

Intrusion depths of Aare and Lütschine were observed in Lake Brienz by CTD-profiles and thermistor strings close to the river entrances (section 2.3.3). With these observations, the river intrusion model was calibrated, as described in section 2.3.5. Subsequently simulations were performed over a time period of eight years (1997 – 2004) and the distinct intrusion dynamics of Aare and Lütschine were assessed.

River Aare is characterized by average S_A of ~0.069 g kg^{-1}, load-averaged CR_A of 108 g m^{-3} and average T_A of 5.9 °C (Table 2.3). For most of the time, these water properties lead to intrusions into the thermocline (Figure 2.4). After heavy precipitation, CR_A increases to several hundreds to thousands g m^{-3}, increasing the river water density and river intrusion depths. During winter, T_A drops usually below the temperature of maximum density (T_{md} = 4 °C), causing cabbeling instability (Carmack et al., 1979; Shimaraev et al., 1993). The cold river front mixes with warmer lake water leading to temperatures close to T_{md} resulting in density-driven intrusions into the deep water.

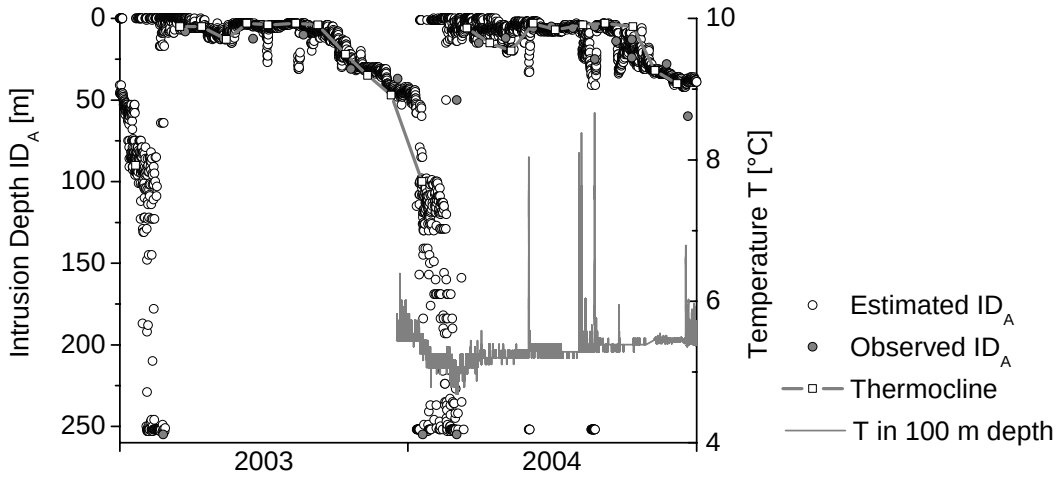

Figure 2.4: Devolution of intrusion dynamics of Aare into Lake Brienz. Circles denote simulated intrusion depth ID_A, filled circles represent intrusion depth observed in CTD profiles, squares symbolize depth of thermocline (largest density gradient) and the solid line illustrates the temperature signal of the deepest logger of the Aare entrance (E in Figure 2.1).

River Lütschine is characterized by average S_L of ~ 0.189 g kg^{-1}, load-averaged CR_L of 280 g m^{-3} and average T_L of 5.7 °C (Table 2.3). In comparison to Aare, the higher S_L and CR_L averages in Lütschine relate to density increases of ~105 g m^{-3} and ~107 g m^{-3}, respectively, enhancing deep water intrusions to some extent. Like Aare, Lütschine water plunges during winter by cabbeling to greater depths and intrudes into the thermocline during summer (Figure 2.5). However, high discharge events occur more frequently in the non-dammed Lütschine, initiating plunging to great depth.

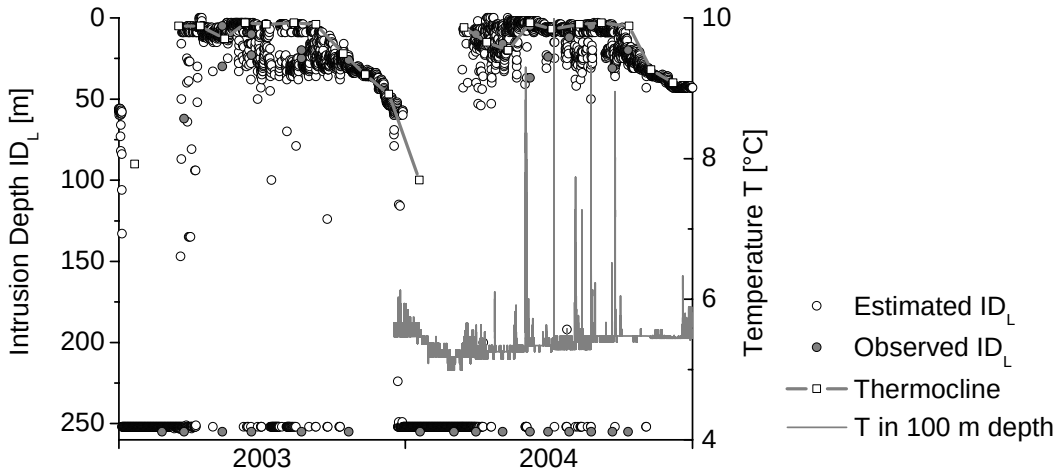

Figure 2.5: Devolution of intrusion dynamics of Lütschine water into Lake Brienz. Circles denote simulated intrusion depth ID_L, filled circles represent intrusion depth observed in CTD profiles, squares symbolize depth of thermocline (largest density gradient) and the solid line illustrates the temperature signal of the deepest logger of Lütschine entrance (D in Figure 2.1).

Based on simulations for the years 1997 to 2004, Aare water intruded on average ~1280 hrs yr^{-1} (± 80 hrs; considering 10% inaccuracy in CR and up to 11% inaccuracy in empirical coefficient r; Table 2.4) below 50 m depth (~15% of the total time). Similar simulations for Lütschine indicate about 2.3 times more frequent plunging for ~3030 ± 90 hrs yr^{-1} below 50 m depth (~35% of total time). Consequently the corresponding particle input into the upper layer (< 50 m depth) from Aare F_{Aare} lies at 93 kt yr^{-1} and from Lütschine F_{Luet} at 65 kt yr^{-1} (Figure 2.6). These results are supported by the measurements of the vertical distribution of suspended particles in the lake, described in section 2.4.4.

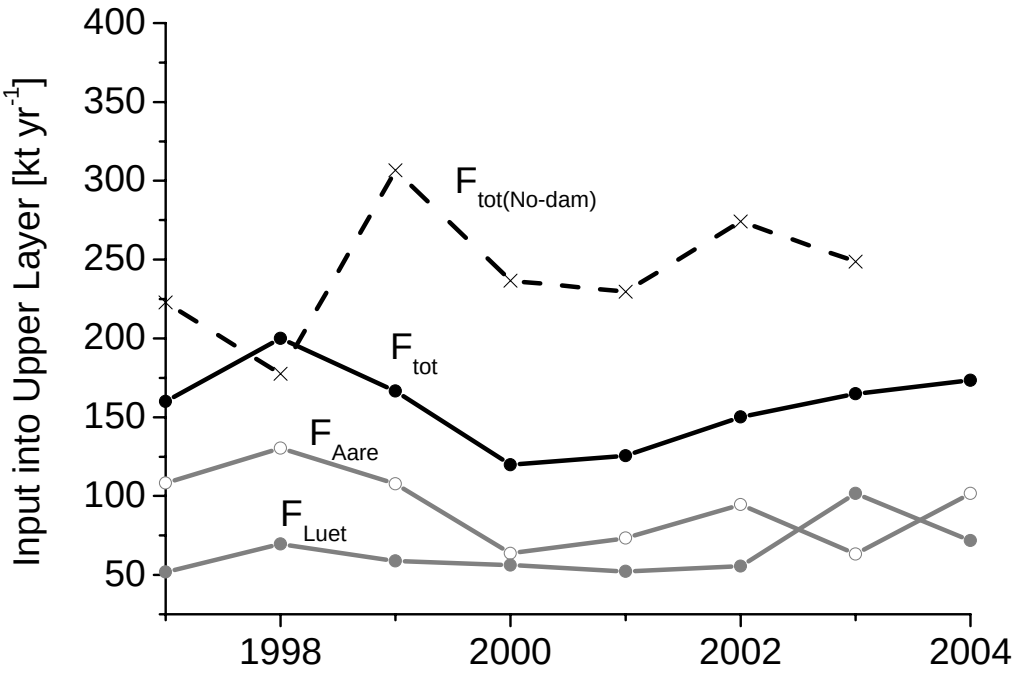

Figure 2.6: Particle input to the upper layer (depth < 50 m) based on estimated intrusion depths and loads in the two rivers; F_{Aare} : load from Aare; F_{Luet} : load from Lütschine; F_{tot} : total load entering the upper layer; $F_{tot(No-dam)}$: simulated no-dam load entering the upper layer.

2.4.4 Vertical Distribution of Suspended Particles

As ~99% of the particles collected in the two sets of sediment traps (section 2.3.4) are of inorganic nature (Müller et al., 2007a) we assume in the following that Lake Brienz particles are entirely allochthonous. The general dynamics of the vertical distribution of CL in the lake are illustrated in Figure 2.7 (longitudinal cross-sections) and Figure 2.8 (time series) for the years 2003/4 and 1997 to 2004, respectively. In addition, Figure 2.8 furthermore illustrates the influence of suspended particles on Secchi recordings. The integrated mass of suspended particles in the upper layer (MCL_{upper}; top 50 m) is illustrated in Figure 2.9. The turbidity dynamics reveal a temporal pattern which can best be described in terms of the four seasons.

(1) During winter the entire water column clears up and CL drops below 1.5 g m^{-3} leading to Secchi depths of up to 10 m. Elevated CL is only observed along the thalweg close to the Aare entrance (Figure 2.7a). Winter convection and upwelling driven by the river intrusions prevent MCL_{upper} dipping below 2 kt (Figure 2.9). Small particle sizes and low CL

lead to minimal sedimentation rates in 50 m depth of $S_{50} \approx 0.8$ g m^{-2} d^{-1} (Table 2.7). Consequently the particles residence time in the upper layer ($\tau_{upper} = MCL_{upper} / S_{50}$) can exceed 40 days. Integrated mass of suspended particles varies between 6 and 8 kt in the entire lake (MCL_{lake}) with residence times in the entire lake (τ_{lake}) of over 30 days.

(2) In spring, with the onset of snow melting (usually April) turbidity currents occur either into the thermocline or along the thalweg. Hence, the intensity of spring turbidity is especially sensitive to meteorological conditions and varies much from year to year. Typically CL stays below 3 g m^{-3} in the open water and increased CL can be noticed in density-driven deep intrusions. As long as no major suspended particle input occurs, τ_{upper} remains above 20 days. τ_{lake} varies significantly because of the dynamics of particle input which can surpass 20 kt d^{-1} during high discharge events.

(3) In summer, usually MCL_{lake} reaches its maximum between July and September. Then, two distinct turbidity layers can be observed. One is located in the upper layer in which maximum CL is recorded at a depth of ~20 m (22 g m^{-3} in 2003; 10 g m^{-3} in 2004). As a result, the Secchi depths are reduced to less than 2 m. MCL_{upper} varies significantly from year to year (1997 to 2004: 6 kt to 10.5 kt). Suspended particles are generally larger than during winter (Chanudet and Filella, 2007) leading to higher settling velocities. Consequently sedimentation rates reach a maximum between June and August 2003: 24.8 g m^{-2} d^{-1}; 2004: 20.2 g m^{-2} d^{-1}) and τ_{upper} drops to a few days. The second turbidity layer occurs in the deepest reaches, where CL > 20 g m^{-3} was observed. Generally the south western part of the lake (closer to Lütschine entrance) is more affected by such layers, indicating more frequent deep water intrusions from Lütschine. Sedimentation at 255 m depth reaches maxima of up to 21 g m^{-2} d^{-1}, indicating a shorter τ_{lake} of ~12 days.

(4) In fall, low particle input from both rivers lead to a gradual clear-up of the entire water body until the initial winter status is reached.

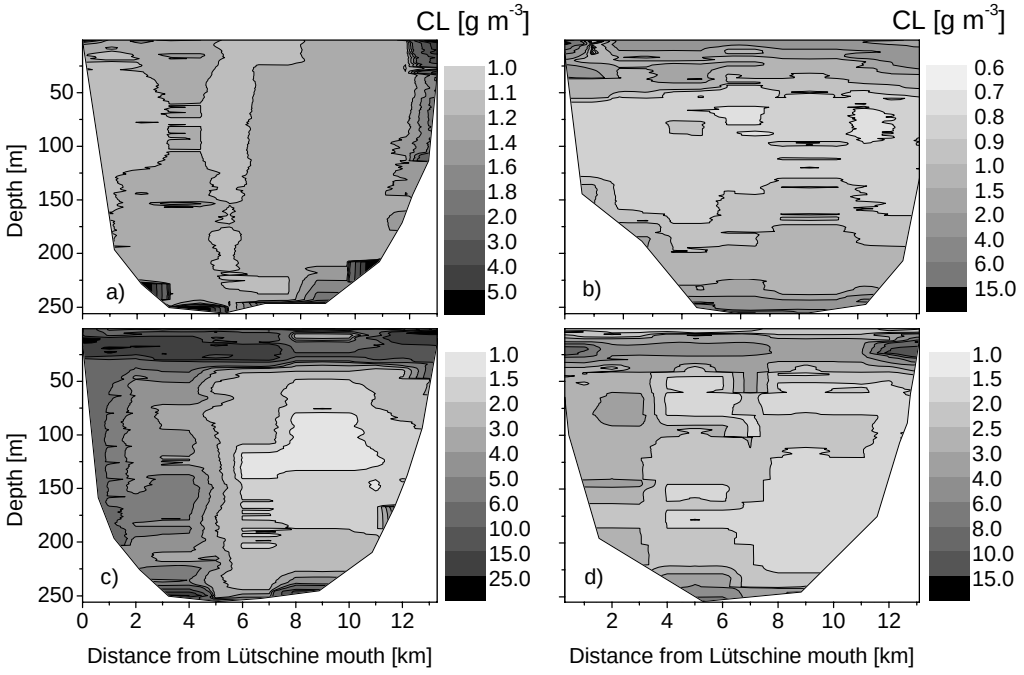

Figure 2.7: Longitudinal cross-section of the suspended particle concentrations (CL) in Lake Brienz; a) 25 February 2003; b) 12 May 2003; c) 22 August 2003 and d) 11 October 2004; Note: Graph d) displays the situation in 2004, as no turbidity currents occurred in fall 2003.

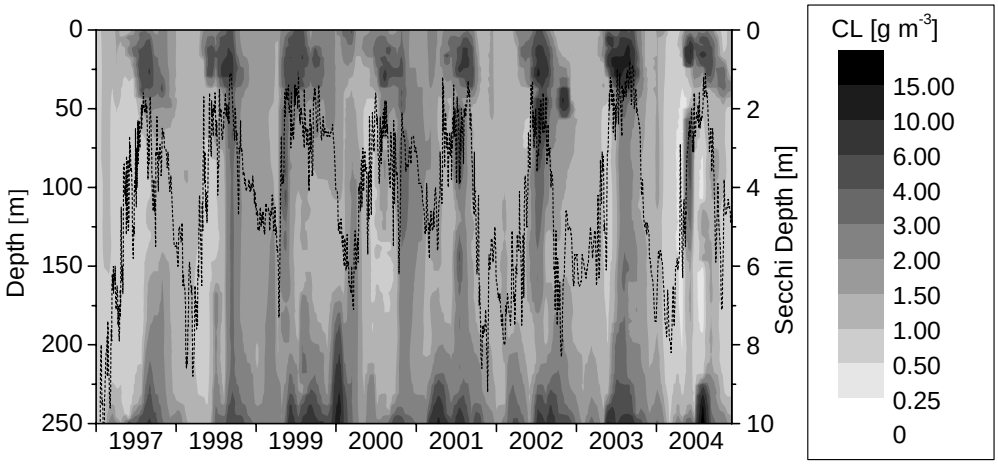

Figure 2.8: Time series of vertical distribution of particle concentrations CL (contour plot) and Secchi depth recordings (dashed line) in the center of Lake Brienz from January 1997 until December 2004.

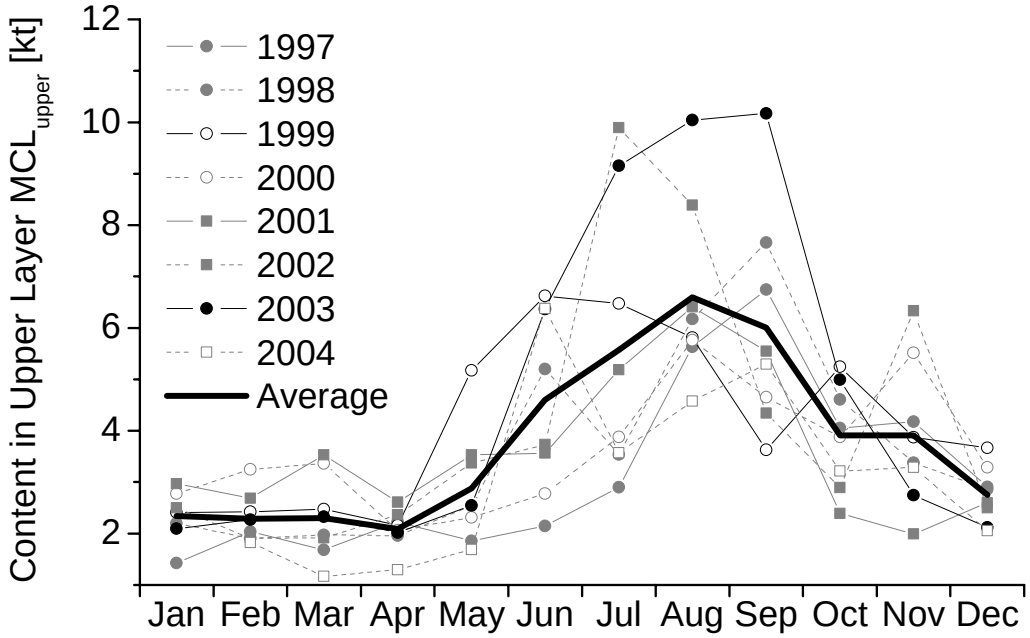

Figure 2.9: Integrated particle mass in the upper layer (< 50 m depth) of Lake Brienz.

Table 2.7: Lake internal content, sedimentation rates and residence times

Month	**MCL$_{upper}$** [kt]	**S$_{50}$-flux**[(a)] [g m^{-2} d^{-1}]	**S$_{50}$** [kt d^{-1}]	τ_{upper} [d]	σ_{upper} [(a)] [d^{-1}]
Feb 04	1.8	2.9	0.09	21.4	0.047
Mar 04	1.2	0.8	0.03	46.3	0.022
Apr 04	1.3	2.1	0.06	20.4	0.049
May 04	1.7	1.6	0.05	36.4	0.027
Jun 04	6.4	20.2	0.60	10.6	0.095
Jul 04	3.6	10.4	0.31	11.6	0.086
Aug 04	4.6	33.9	1.01	4.5	0.221
Sep 04	5.3	13.1	0.39	13.6	0.073
Oct 04	3.2	6.0	0.18	18.0	0.056
Nov 04	3.3	4.6	0.14	23.8	0.042
Dec 04	2.1	2.6	0.08	26.3	0.038

(Table continues on next page)

Table 2.7: Lake internal content, sedimentation rates and residence times (continued)

Month	MCL_{lake} [kt]	S_{255}-flux[(a)] [g m^{-2} d^{-1}]	S_{255} [kt d^{-1}]	τ_{lake} [d]	σ_{lake} [(a)] [d^{-1}]
Jan 04			0.23		
Feb 04	6.0	9.6	0.29	21.0	0.048
Mar 04	4.4	4.9	0.15	30.2	0.033
Apr 04	4.9	10.1	0.30	16.2	0.062
May 04	4.4	7.3	0.22	20.2	0.050
Jun 04	19.9	20.8	0.62	32.1	0.031
Jul 04	7.5	20.8	0.62	12.2	0.082
Sep 03[(b)]	20.7	39.3	1.17	17.6	0.057
Oct 04	9.5	21.5	0.64	14.8	0.067
Nov 04	8.0	11.4	0.34	23.6	0.042
Dec 04	5.8	5.4	0.16	36.5	0.027

[(a)] S_{50}-flux: Sedimentation rate in 50 m depth; τ_{upper} = Content of upper layer/ S_{50} ; σ_{upper} = 1/ τ_{upper} ; S_{255}-flux: Sedimentation rate in 255 m depth; τ_{lake} = Content of lake/ S_{255}; σ_{lake} = 1/ τ_{lake} ; in 2004 monthly fluxes were calculated by averaging fluxes from S traps.

[(b)] Value of September 2003 because of hang slides in 2004.

Based on this turbidity dynamic and discharge recording at the outlet, the annual particle load leaving Lake Brienz amounts up to ~9 kt yr^{-1}, accounting for about 3% of the annual input.

In the following sections, we focus on turbidity in the upper layer, where the ecological consequences are primarily expected. Spatial analysis of the longitudinal CTD transects (Figure 2.7) imply that CTD profiles from the lake center (location C) adequately represent the vertical CL distribution in the upper layer, slightly overestimating them in fall, and underestimating them during maximal turbidity in summer in both instances by less than 15%. First, we want to point out particularities of the years 1999 and 2003.

The winter 1998/1999 saw extreme snowfalls in the *Bernese Oberland*. Intense snowmelt and above average precipitation caused flooding during the following spring. Hence, river flow and erosion rates were elevated and led to the eight years (1997 - 2004) maxima of 400 kt yr^{-1} of suspended particle input (compared to the 302 kt yr^{-1}average; Table 2.3). Particularly during May, the spring floods flushed 136 kt of particle into the lake - 4.1 times the average load in May (1997-2004) of 33 kt mo^{-1}. Although MCL_{upper} never exceeded 6.3 kt, the onset of higher particle content was clearly earlier and lasted for longer in 1999 (compared to other years when 4 kt is only exceeded between June and October).

During summer 2003 a record-breaking heat wave hit the European continent (Schär et al., 2004) leading to hot-dry weather which induced intense glacier melting in the watershed.

As a direct consequence ablation was enhanced and particle loads were 39% above average (242 kt yr^{-1}) in non-dammed Lütschine and 49% below average in dammed Aare (65 kt yr^{-1}). The low load in Aare is a consequence of the glacial particle retention in the reservoirs and low erosion downstream of the reservoirs due to the unusual dry summer. The absence of heavy rains further reduced plunging of the two rivers. Consequently MCL_{upper} (top 50 m) surpassed in summer 2003 the eight-year average maximum by over 60%.

The two unusual years 1999 and 2003 impressively demonstrate the sensitivity of the particle budget dynamics to local meteorological conditions.

2.4.5 *Simulated Present Particle Budget of Lake Brienz*

As autochthonous particles are negligible in Lake Brienz, the estimated riverine particle input governs directly its content and sedimentation. In Figure 2.10 continuous riverine loads are compared to sedimentation fluxes in 50 and 255 m depth at the lake center. Disregarding peak sedimentations between 27 July 2004 and 15 September 2004 (with S_{255} exceeding 21 kt d^{-1}) which are caused by underwater slides (a frequent phenomenon in lakes with steep morphology and high sedimentation rates), mean sedimentation rates at 255 m depth between 25 March 2003 and 18 October 2004 (average S_{255}: 0.75 kt d^{-1}) match almost perfectly the estimated riverine loads (mean input: 0.85 kt d^{-1}). The missing 12% can easily be attributed to sedimentation closer to the river entrances. Furthermore a time lag between particle input and sedimentation of about two weeks can be observed. Siegenthaler et al. (1996) determined a similar time lag, concluding that particles entering the lake need about 15 days to reach the lake center. In fact, horizontal mixing determined with tracers in several comparable lakes (Peeters et al., 1996) correspond well to such velocities of ~0.5 km d^{-1}.

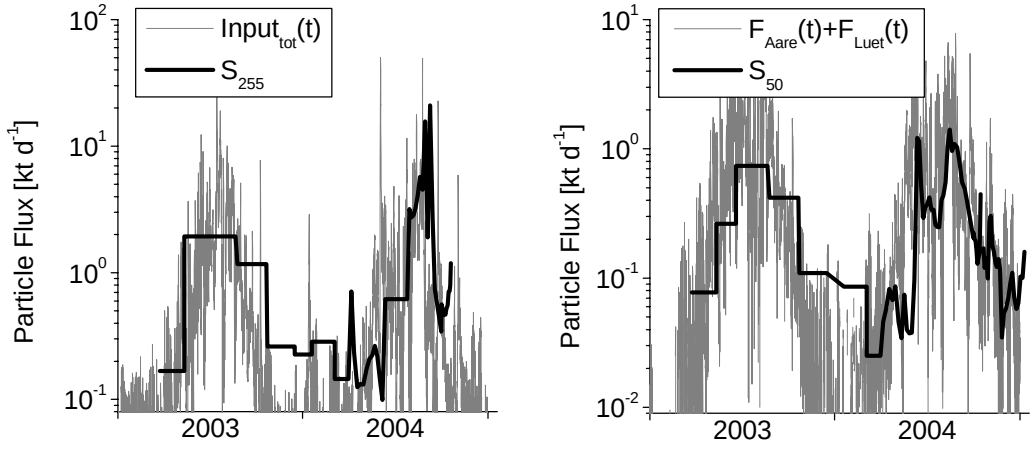

Figure 2.10: left: sedimentation at location C at 255 m depth (S_{255}) and total riverine particle input ($Input_{tot}(t)$); right: sedimentation at location C at 50 m depth (S_{50}) and riverine particle input into the upper layer ($F_{Aare}(t) + F_{Luet}(t)$).

More than half of the annual particle input enters the upper layer (< 50 m depth). In Figure 2.10 (right plot) the estimated particle input into the upper layer is compared to sedimentation measured in 50 m depth at the lake center. Between 25 March 2003 and 30 December 2004 mean input (0.52 kt d^{-1}) was almost double the time-averaged sedimentation (S_{50} = 0.30 kt d^{-1}). This is primarily explained by sinking of coarse particles below 50 m depth before reaching the sediment trap at the center. Fine matter however stays suspended for several weeks and distributes more evenly across the upper layer.

Particle size distribution measured at the reservoir outlets depict a fraction of fine matter (diameter < 4 μm) in the suspended load of 82% ($X^{l}_{reservoir}$) in February and 56% ($X^{h}_{reservoir}$) in August. At the lake entrance of Aare (where reservoir particles constitute less than 31%), particle size distributions indicate a fraction of fine matter similar to Lütschine of ~27% (X_{river}). Considering these ratios the suspended load of fine matters in the rivers (Aare: 43 kt yr^{-1}; Lütschine: 47 kt yr^{-1}) and the load of fine matter entering the upper layer (32 kt yr^{-1} in Aare (represents ~38% of riverine load) and 18 kt yr^{-1} in Lütschine (represents ~27% of riverine load) were determined with equation (2.10).

Figure 2.11 illustrates the simulated and measured MCL_{upper} between 1997 and 2004. The good agreement strengthens our confidence in the input estimates to the upper layer. Fine

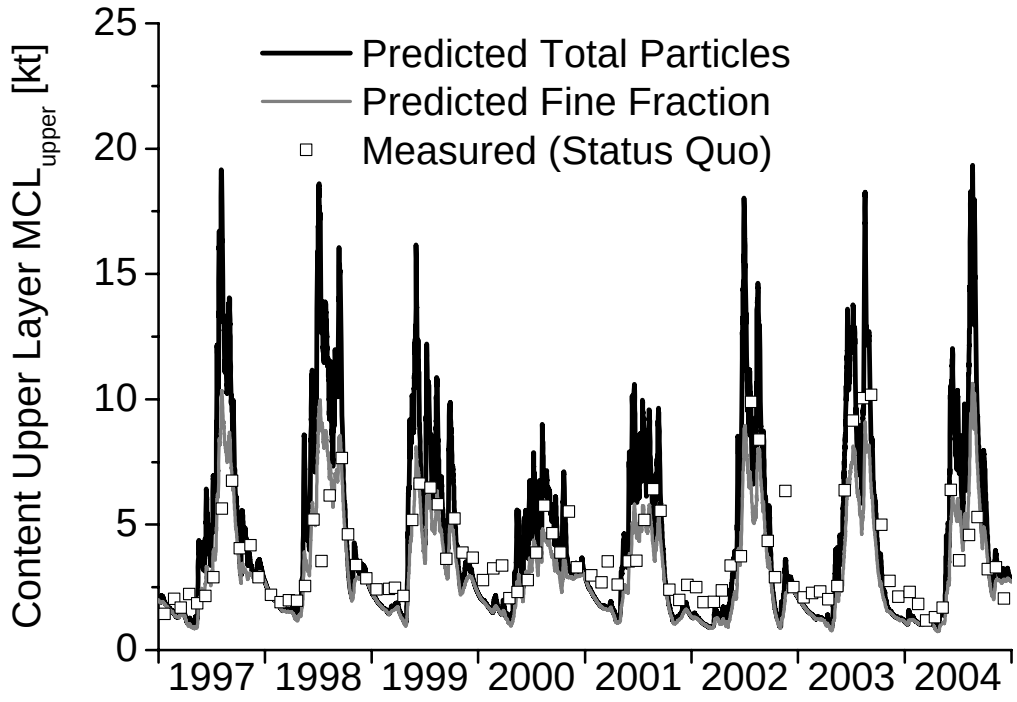

Figure 2.11: Predicted and measured mass of particles in the upper layer of Lake Brienz from 1997 to 2004.

matter with long residence times constitute most of the content throughout the year, while coarse particles contribute to peak contents but settle out within days. Consistency of simulations and observations imply that the model can be used to perform calculations for hypothetical scenarios, such as without hydropower dams.

2.4.6 Particle Budget of Lake Brienz without Dams

As explained in section 2.3.6 reconstructed particle loads in non-dammed Aare were scaled to match present loads plus the retention in the reservoirs (128 kt yr^{-1} + 232 kt yr^{-1} = 360 kt yr^{-1}; Table 2.3). River intrusion simulations of the reconstructed no-dam situation indicate that 67% (or 242 kt yr^{-1}) of the annual load would enter Lake Brienz above 50 m water depth (compared to 73% of today (93 kt yr^{-1})). Together with the Lütschine load the estimated particle input to the upper layer ($F_{tot(No\text{-}dam)}$) would amount up to 307 kt yr^{-1}, almost twice the present input (Figure 2.6).

Based on particle size distributions measured in the sediment at locations H, I and J in Grimselsee (Figure 2.1) the fraction of fine matter (diameter < 4 μm) can be estimated to 3%.

Hence, the one box model defined in equation (2.12) was applied to the no-dam Aare, assuming the same particle sedimentation constants (σ_{coarse} and σ_{fine}). Based on these assumptions, the load of fine matter amounts up to 54 kt yr^{-1} (15% of total load). It is remarkable, that the annual input of fine matter for the no-dam Aare is only 11 kt yr^{-1} higher than today (43 kt yr^{-1}).

Simulated content in the upper layer is illustrated in Figure 2.12. The maximum values during summer are three times as large as today. However, the high fraction of coarse particles leads to rapid sedimentation in fall and the low particle input during winter causes an almost entire clear-up of the lake during winter (Figure 2.12).

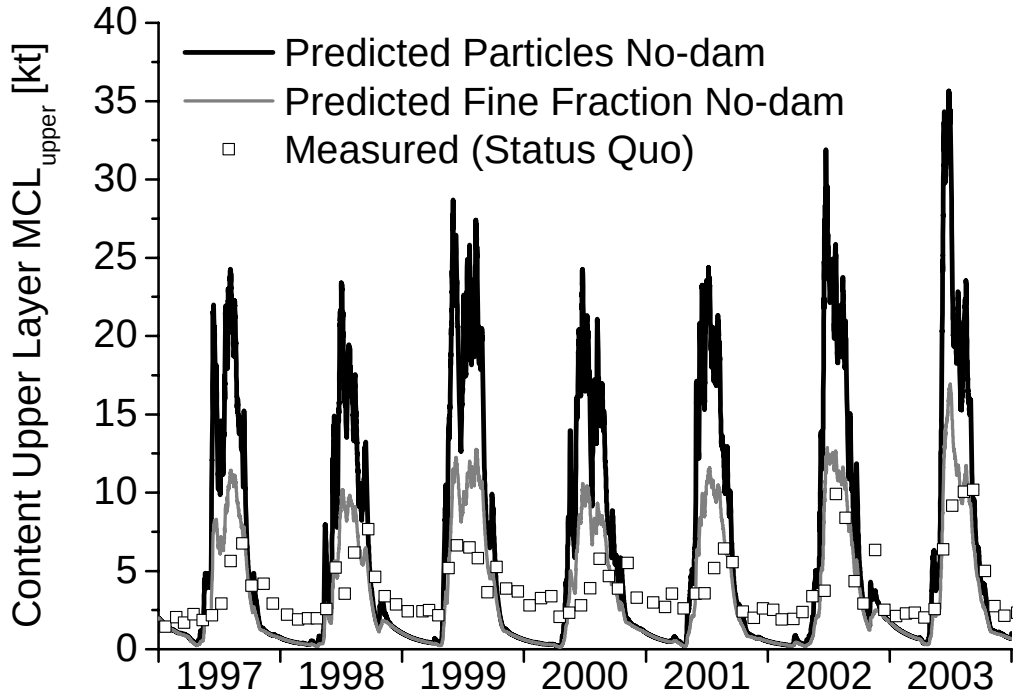

Figure 2.12: Simulated mass of particles in the upper layer for no-dam scenario, assuming same sedimentation constants (σ_{coarse} and σ_{fine}) as today.

Based on the similarity of the two river catchments and their hydrological regime, it could have been expected that the no-dam Aare would reach a similarly high percentage of deep-water intrusions as the Lütschine today. However, this is not the case because of the following two factors: (1) Due to its crystalline catchment average salinity lies at 0.069 g kg^{-1} (compared to 0.189 g kg^{-1} in Lütschine). Therefore, it needs higher particle concentrations in

Aare for deep water intrusions to occur. (2) For no-dam conditions Moosmann (2005) estimated ~1 °C warmer water temperatures than today. These simulated no-dam summer temperatures are potentially an upper limit, as they approach the highest values observed in other rivers at this altitude (Meier et al., 2003). When ignoring this temperature effect, no-dam test runs show that deep water intrusions would occur three times more frequently as today (Table 2.8). However, an overestimation in the simulated no-dam temperature would have caused only a slight over prediction of the summer surface turbidity.

Table 2.8: Summary of intrusion dynamics

	Aare	No-dam Aare	No-dam Aare[(a)]	Lütschine
Entire year (1997 – 2004)[(b)]				
Discharge [km^3 yr^{-1}][(c)]	1.195	1.138	1.138	0.620
Load [kt yr^{-1}]	128	360	360	174
Temperature [°C]	5.9	6.7	5.9	5.7
Deep water intrusion duration [h yr^{-1}]	1276	1343	1337	3030
Discharge entering upper layer [km^3 yr^{-1}]	1.073	1.023	0.951	0.499
Load integrated entering upper layer [kt yr^{-1}]	93	242	194	65
Fraction of load entering upper layer [-]	0.72	0.67	0.54	0.37
April-October (1997 – 2004) [(d)]				
Discharge integrated [km^3]	0.943	1.023	1.023	0.543
Load integrated [kt]	115	357	357	171
Temperature [°C]	7.1	8.7	7.1	7.0
Deep water intrusion duration [h]	119	183	371	447
Discharge entering upper layer [km^3]	0.908	0.931	0.855	0.473
Load integrated entering upper layer [kt]	86	240	192	64
Fraction of load entering upper layer [-]	0.75	0.67	0.54	0.37
April-October 1999				
Discharge integrated [km^3]	1.135	1.210	1.210	0.629
Load integrated [kt]	162	497	497	224
Temperature [°C]	6.7	8.6	6.7	6.9
Deep water intrusion duration [h]	211	353	694	725
Discharge entering upper layer [km^3]	1.042	1.032	0.897	0.511
Load integrated entering upper layer [kt]	99	306	227	59
Fraction of load entering upper layer [-]	0.61	0.62	0.46	0.26
April-October 2003				
Discharge integrated [km^3]	0.915	0.985	0.985	0.534
Load integrated [kt]	62	317	317	241
Temperature [°C]	7.3	8.2	7.3	6.8
Deep water intrusion duration [h]	0	142	353	612
Discharge entering upper layer [km^3]	0.915	0.916	0.828	0.440
Load integrated entering upper layer [kt]	62	248	187	101
Fraction of load entering upper layer [-]	1.00	0.78	0.59	0.42

[(a)] Test run for pre-dam situation disregarding any temperature changes.

[(b)] Averages for the given time periods (Note: all no-dam simulations were performed for the time periods 1997-2003).

[(c)] Annual differences between status quo discharge and no-dam discharge must be attributed to numerical errors.

[(d)] Averages of the noted summer for the time period between 1997 and 2004.

2.5 Discussion

Considering the eight years (1997-2004), Aare transports today 26% less particles into Lake Brienz than Lütschine (Table 2.8). However, due to the infrequent plunging of Aare (58% less frequent than Lütschine), 59% of the annual load entering the upper layer can be attributed to Aare. For the reconstructed no-dam Aare, the frequency of deep water intrusions increases during summer by 54% primarily driven by particle concentrations. Nevertheless due to lower salinity and ~1 °C warmer river water the plunging frequency would however remain significantly below the frequency observed in Lütschine. In regard to the surface turbidity, the additional particles, currently trapped in the upstream reservoirs (232 kt yr^{-1}), would dwarf the effect of increased plunging. In fact the annual load entering the upper layer from no-dam Aare would be 2.6 times higher compared to the present situation.

However the simulations predict a significant temporal shift of particle input. Today about 10% and 2% of the annual particle loads from Aare and Lütschine, respectively, enter the lake in winter. The larger winter load in Aare stems from reservoirs release (in 2003/4: 87% from reservoirs). Although river waters are subjected to cabbeling and plunge to greater depths during winter, convective mixing and upwelling in the lake lead to a continuous supply of particles to the upper layer. Consequently, today concentrations remain throughout the winter at a standing crop of about 1 to 2 g m^{-3} (corresponding to mean MCL_{upper} of ~2.2 kt; Figure 2.9). No-dam simulations show that the winter load of Aare would be ~0.51 kt mo^{-1} (comparable with the Lütschine load of ~0.58 kt mo^{-1}). Consequently in a no-dam situation the particle supply to the upper layer drops to almost zero, engendering a clear-up of the entire water column. The higher winter turbidity today has subsequently an adverse effect on primary production, especially during spring when plankton communities need to regenerate from the harsh winter season (Finger et al., 2007a).

Aare particle transport in summer would be 3.1 times higher under no-dam conditions compared to present. Despite an increase of Aare plunging events, total particle supply (both inflows) to the upper layer would double during summer (today: 21 kt mo^{-1}; no-dam: 43 kt mo^{-1}). Even extreme years such as 1999 (snowfall, followed by flooding) and 2003 (extreme heat wave; intense glacier melting) did not cause such large particle inputs to the upper layers.

Besides the temporal shift, another important factor for the lakes surface turbidity is the particle size distribution. While today the load originating from the reservoir is composed primarily of fine matter, the no-dam load has a higher coarse fraction (Grimselsee sediment contains only ~ 3% of fine matter). The reservoirs primarily trap coarse particles, while the fine matter remains suspended and is discharged throughout the year to downstream Lake

Brienz (annual load of fine matter: 43 kt yr^{-1} today and 54 kt yr^{-1} no-dam). Consequently today the load entering in winter is dominated by fine matter with accordingly small settling velocities and long residence times in the lake of over 40 days. The effects on the mean particle concentrations in the upper layer are illustrated in Figure 2.13. For no-dam, the rather coarse particles settled out faster in fall, leading to a clear-up of the entire water column. During summer, however, the intense particle supply to the upper layer would cause almost three times higher maximal concentrations. These findings consistently explain differences between recent Secchi depths (Jaun et al., 2007) and historical Secchi depths recordings performed by Flück (1926). Analysis of the data sets indicate, that today's Secchi readings during summer (> 2 m) reach about three times deeper compared to pre-dam recordings (< 1 m) from the 1920's (Siegenthaler, 2003). Contrary to the winter, lower summer turbidity led to enhanced primary production (Finger et al., 2007a).

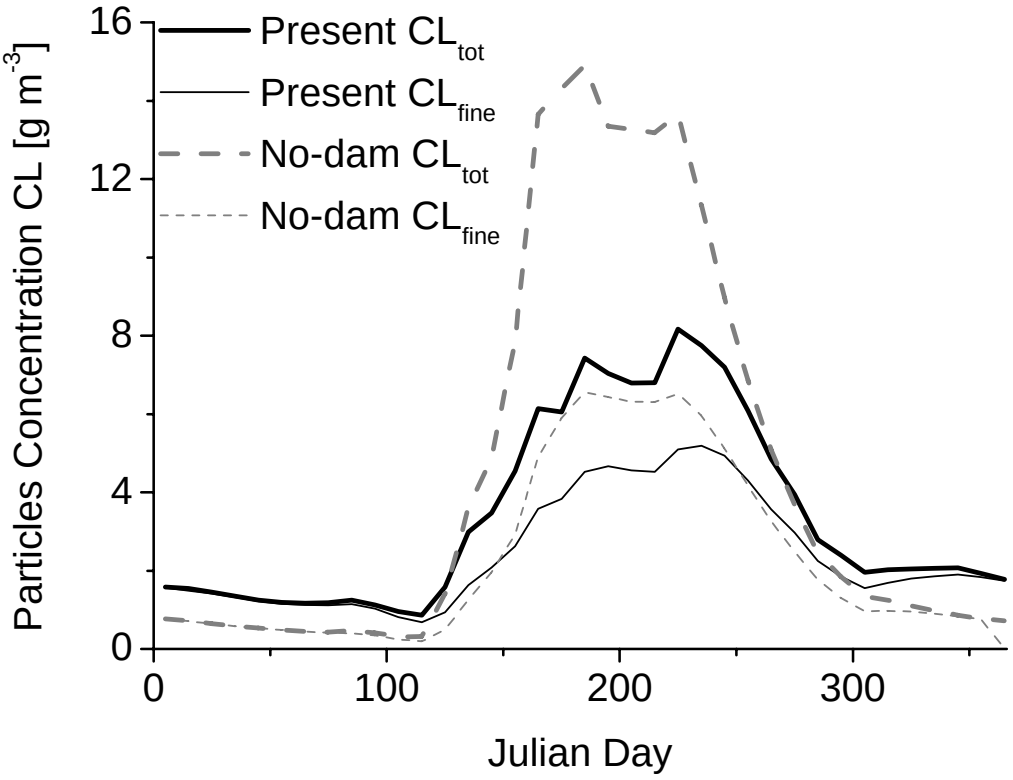

Figure 2.13: Average particle concentrations today (black line) and for no-dam conditions (dashed gray line) in the upper layer of Lake Brienz. The bold lines represent the total particle concentration and the fine line represents the concentration of fine matter (smaller than 4 μm).

2.6 Conclusions

The effects of damming on downstream riverine particle transport and density intrusions into a peri-alpine lake were determined by assessing the particle balance of Lake Brienz throughout eight years. The procedure used is applicable to other similar settings in peri-mountainous regions. In a first step suspended particle loads in the two major tributaries, Aare (heavily dammed) and Lütschine (no dams), were estimated. A river intrusion model for both rivers was evaluated using thermistor moorings and CTD data in order to estimate particle input to the surface layer of the lake. Estimated input was crosschecked with sedimentation in a one box model of the upper layer of the lake (< 50 m depth). This model then allowed estimating riverine particle transport and balancing suspended matter in Lake Brienz for no-dam conditions. Based on this analysis, we draw the following conclusions:

1. Although Aare discharge is almost twice that of Lütschine, the annual sediment loads are almost the same in both rivers. This contrast stems from the 232 kt yr^{-1} of sediment trapped in the upstream reservoirs of the Aare catchment (Anselmetti et al., 2007).

2. Due to water retention, sediment loads are shifted from summer to winter. While the average suspended load in Lütschine drops to 0.6 kt mo^{-1} during winter, the Aare carries at least 2 kt mo^{-1} throughout the year. Visa versa, during summer the average suspended loads in Lütschine (24.4 kt mo^{-1}) lie ~50% above Aare loads (16.4 kt mo^{-1}).

3. The water retention in the reservoirs reduces the frequency of high flow and elevated particle concentrations in Aare. Combined with the lower salinity, this leads to lower densities of Aare water compared to Lütschine. Consequently, Aare intrudes into the upper layer for 86% of the time compared to only 65% for Lütschine (Table 2.8). The difference of plunging frequencies (below 50 m depth) is even more distinct in summer: Lütschine plunges about 3.8 times more frequently (8.7% of the time) than Aare (2.3%).

4. As a direct consequence of the intrusion dynamics, the annual particle input to the upper layer of the lake is dominated by Aare (92.8 kt yr^{-1} compared to 64.7 kt yr^{-1} from Lütschine). 75% of the annual load from Aare but only 37% from Lütschine enter the upper layer of the lake.

5. The annual variability of the load entering the upper layer is substantial and a direct consequence of meteorological conditions. While Aare discharge is leveled out by the reservoirs, the particle loads in Lütschine are more sensitive to precipitation and glacier melting. During heat waves, such as in summer 2003, the suspended load entering the upper layer can be dominated by Lütschine.

6. Particle residence times vary with the size fractions. The maximum of over 40 days is reached during winter (dominated by fine matter input), whereas in summer they drop below 10 days (primarily coarse particles).

7. Under a hypothetical situation without hydropower dams the mean annual suspended load in Aare would be ~2.8 times higher (today: 128 kt yr^{-1}; no-dam: 360 kt yr^{-1}) and water temperature would be about 0.8 °C warmer (Moosmann, 2005). Although high discharge is more frequent under natural conditions, low salinity and warmer Aare temperature limit frequent deepwater intrusions. Consequently the no-dam particle load entering the upper layer would double (today: 158 kt yr^{-1}; no-dam: 307 kt yr^{-1}).

8. Only about 3% of the sediment trapped in the reservoirs is fine matter (< 4 μm diameter). Consequently the load of fine matter to the downstream lake does not change a lot due to damming (today: 43 kt yr^{-1}; no-dam: 54 kt yr^{-1}).

9. Regarding ecological aspects, the light availability for primary production is clearly improved by damming during summer. However, increased winter turbidity might lead to enhanced light attenuation and subsequently hamper primary production during winter and early spring.

2.7 Acknowledgements

The present study is part of a collaborative research project on ecological changes in Lake Brienz. Funding was provided by (1) the Regional Government Canton of Bern, (2) Kraftwerke Oberhasli AG (KWO), (3) Federal Office for the Environment (FOEN), (4) Lake Brienz shoreline communities and (5) Eawag. The presented data relies on the contributions from a large number of people we would like to express our sincere thanks: Dr. A. Jakob (LHG-BWG) and Dr. M. Zeh (GSA) provided river and lake data presented in Figure 2.2 and Figure 2.8 respectively; R. Clausen and R. Wiegenbröker (both KWO) provided water flow data from the hydropower scheme; Dr. M. Sturm and Dr. F. Anselmetti provided supportive discussions on sedimentation; B. Bommer and Dr. T. Graule provided technical advice on particle size measurements. Furthermore our cordially thanks for joint efforts in the field to M. Schurter and the following persons who were a great help: A. Zwyssig, L. Jaun, C. Hoyle, C. Rellstab, T. Diem, P. Kumar, Dr. D. McGinnis, Dr. A. Lorke, D. Richter, A. Wagenhoff, M. Alp and C. Meukow.

CHAPTER 3

EFFECTS OF UPSTREAM HYDROPOWER OPERATION AND OLIGOTROPHICATION ON THE LIGHT REGIME OF A TURBID PERI-ALPINE LAKE

Lorenz Jaun, David Finger, Markus Zeh, Michael Schurter and Alfred Wüest

(Aquatic Sciences, accepted)

Abstract

Anthropogenic activities in catchments may alter the light regimes in downstream natural waters, affecting light attenuation and the perceived optical properties of the waters. We analyzed the effects of upstream hydropower operation and oligotrophication on light attenuation and reflectance in Lake Brienz (Switzerland). For this purpose, we reconstructed its light regime for the pre-dam condition and for periods of 4-fold increased primary productivity, based on direct observations of light and beam attenuations as well as concentrations of optically active compounds, especially observed and simulated mineral particle concentrations. Based on our assessment, light attenuation before the construction of upstream dams was double the current value during summer and nearly half in winter. This result is consistent with pre-dam measurements of Secchi depths in the early 1920s. Using a simple optical model, a significant increase in reflectance since the 1970s was estimated, assuming a 4-fold decrease of optical active organic compounds within the lake. As reflectance is perceived by human eyes as turbidity, this may explain subjective reports by local residents of increasing turbidity in recent years.

3.1 Introduction

Sunlight is the primary energy source for biological production providing the basis for aquatic life. Therefore, light availability is a critical boundary condition affected by both autochthonous (*in situ* produced) constituents and allochthonous substances from catchments. In the open ocean, phytoplankton and associated substances may determine the optical properties (Gordon and Morel, 1983; Morel, 1988). In contrast, inland and coastal waters are influenced by various optically active constituents defining the "multicomponental" water (Arst, 2003).

Light attenuation and the appearance of lake waters are sensitive to anthropogenic activities in their catchments (Swift et al., 2006), such as particle input due to erosion (Effler et al., 2001) or mining (Davies-Colley et al., 1993; Guenther and Bozelli, 2004). These changes may lead to ecological effects including reduced primary production due to light limitation (Jewson and Taylor, 1978; Krause-Jensen and Sand-Jensen, 1998) and lower visibility, affecting predator-prey interactions (Aksnes and Utne, 1997; Beauchamp et al., 1999; Davies-Colley and Smith, 2001). However, enhanced nutrient input due to erosion, untreated wastewater or agricultural runoff leads to higher production and subsequently increased concentrations of particulate and dissolved organic substances in downstream lakes.

Thus, lake eutrophication is often associated with reduced water clarity and stronger light attenuation (Goldman, 1988; Sanden and Hakansson, 1996), whereas oligotrophication is usually related to an increase of water clarity (Schanz, 1994; Jeppesen et al., 2005).

Some lakes have experienced significant changes in their riverine particle input (Biggs and Davies-Colley, 1990; Davies-Colley et al., 1993; Finger et al., 2006), especially in mountainous regions with high ablation rates (Hinderer, 2001) and glaciated catchments (Bezinge, 1987). For example, extensive damming for hydroelectric power in the European Alps during the last decades has led to significant particle retention (Schleiss and Oehy, 2002; Anselmetti et al., 2007), and alteration of the seasonal particle flux, thereby affecting the physical boundary conditions in downstream lakes (Loizeau and Dominik, 2000; Finger et al., 2006). Lake Brienz, which is located in the foothills of the Swiss Alps, contains a volume of 5.15 km^3, covers a surface area of 30 km^2 and is 260 m deep, provides an excellent example of this phenomenon. About 20% of the 933 km^2 large alpine watershed is covered by glaciers. Today, ~300 kt yr^{-1} of inorganic particles are delivered by the two main tributaries, the Aare and Lütschine Rivers (Figure 3.1), leading to a turbid, turquoise appearance of the lake during glacier melting in summer (Finger et al., 2006). During the last 70 years seven hydropower reservoirs with an operable storage volume of 0.197 km^3 have been constructed in the headwaters of the Aare. These reservoirs retain ~232 kt yr^{-1} of coarse particles (Anselmetti et al., 2007) and shift ~14% of the annual Aare discharge from summer to winter, thereby increasing the particle flux during winter by ~5 times (Finger et al., 2006). In the following we will refer to the period before the construction of the first dam as the **pre-dam scenario** and the period since the completion of the last dam as the **status quo scenario**. Beside changes in light attenuation due to the altered particle input, the soluble reactive phosphorus supply to the lake has continuously declined since the 1970s due to the construction of sewage treatment plants (Müller et al., 2007a), limiting the biological productivity in Lake Brienz (Finger et al., 2007a).

The goal of this paper is to examine the role of upstream hydropower operation and oligotrophication on the light attenuation and reflectance in Lake Brienz by addressing three questions: (1) How is the light attenuation affected by hydropower operation? (2) What are the main causes for the inter-annual and short-term variability of attenuation? and (3) What are the potential causes for the subjective changes in turbidity observed by locals in the last few decades?

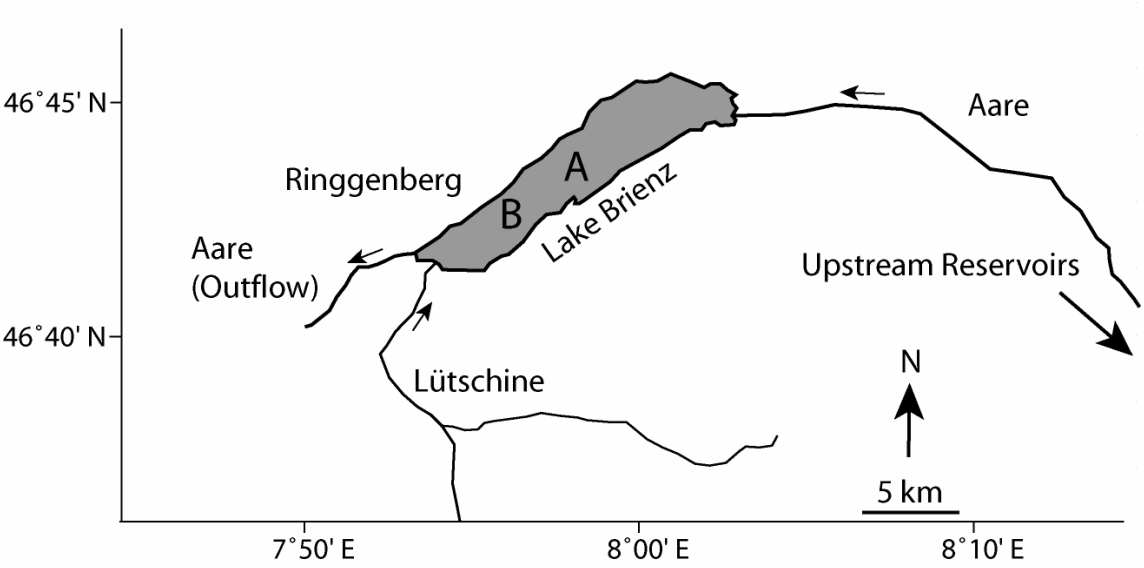

Figure 3.1: Map of Lake Brienz and inflows Lütschine and Aare. Hydropower reservoirs are located ~30 km upstream of Aare inlet. A denotes the deepest location, where most sampling took place (CH coordinates: 640.235 / 175.139). B indicates site near Ringgenberg, where Secchi depths were measured before 1954.

3.2 Concepts of light regimes in natural waters

The simplest method to determine water clarity consists of lowering a Secchi disk into the water and measuring the depth at which it is no longer visible. The Secchi depth is governed by light attenuation and thus is based on the decrease of irradiance with depth in a water body (Tyler, 1968; Preisendorf, 1986; Davies-Colley and Smith, 2001). Conversely, beam attenuation defines the weakening of a light ray sent through a water sample. Two processes are responsible for the attenuation: (1) scattering, mainly by inorganic particles and (2) absorption by pure water, organic tripton (inanimate particulate organic matter), gilvin (dissolved colored organic matter, mainly humic substances) and phytoplankton (Kirk, 1994). In oligotrophic lakes attenuation due to phytoplankton, organic tripton and gilvin is very low (Kirk, 1994; Krause-Jensen and Sand-Jensen, 1998), and the scattering of light by inorganic particles becomes dominant. The intensity of scattering depends mainly on the mineralogical composition, as well as particle size and concentration (Baker and Lavelle, 1984; Spinrad, 1986). Whereas scattering can lead to effective beam attenuation (any scattering of the original light beam is attributed to attenuation), light attenuation is much less affected. Only backward scattering (backscattering) leads directly to attenuation, whereas forward scattering merely prolongs the light path and only thereby increases absorption (Kirk, 1985).

The ratio between backscattering and absorption defines the reflectance as the proportion of upward to downward irradiance (Kirk, 1994). High reflectance is associated with

a cloudy turquoise appearance of the water, colloquially called turbidity. Scientifically, turbidity denotes the scattering of light at a specific angle (mostly 90 °) relative to an arbitrary standard; therefore turbidity is a relative quantity (Davies-Colley and Smith, 2001). The key factor to resolve with respect to lake productivity is in-situ vertical light attenuation, as it governs the ambient light availability.

3.3 Materials and Methods

In order to assess the impact of hydropower operation on the seasonal pattern of light attenuation, we correlated measured attenuations with observed and modeled particle concentrations as well as Secchi depths. These empirical relationships allow us to reconstruct the light attenuation prior to the construction of hydropower dams based on pre-dam Secchi depths and simulated no-dam particle concentrations (Finger et al., 2006). By quantifying reflectance based on measurements of optical properties, the analysis of optically active constituents and published data, we can estimate, semi-quantitatively, the perceived turbidity during the course of oligotrophication in the last 30 years. All measurements and data sets used within this study are summarized in Table 3.1.

3.3.1 Beam attenuation and optically active constituents

To determine the beam attenuation, water samples at different depths in Lake Brienz were collected at five occasions between August 2004 and March 2005 at location A (Figure 3.1). Spectral beam attenuation was measured in the samples at 400 to 700 nm wavelengths using a U2000 spectrophotometer (Hitachi, Japan). In order to distinguish between attenuation due to suspended and dissolved substances, spectra were determined in unfiltered and filtered samples, using 11 µm mesh size nylon filter (Milipore, USA) and 0.2 µm pore size cellulose acetate membrane filters (Schleicher und Schuell, Germany), consecutively. Based on the measured radiant flux Φ in the water sample beam attenuation coefficients, $c_\Phi(\lambda)$, of the optically active water compounds were determined according to Kirk (1994):

$$c_\Phi(\lambda) = 2.303 \cdot \log\left[\Phi_0(\lambda)/\Phi(\lambda)\right]/r = \ln\left[\Phi_0(\lambda)/\Phi(\lambda)\right]/r \qquad [m^{-1}] \qquad (3.1)$$

where Φ is measured relative to a nanopure water reference (Φ_o) after passing a cell length r of 0.10 m. Wheras beam attenuation in the unfiltered water samples is due to all optically

Table 3.1: Overview of measurements and available data

Parameter	Symbol	Unit	Period	Sampling	N[(a)]	Source
LIGHT MEASUREMENTS						
Scalar irradiance PAR	E_0	$\mu E\ m^{-2}\ s^{-1}$	1999-2005	monthly	84	GSA, unpublished
			1987	monthly	13	Kirchhofer, 1990
			1994	monthly	6	Pfunder, 1995
Downward irradiance	$E_d(\lambda,z)$	$W\ m^{-2}$	2004-2005	Aug - Mar[(b)]	5	Authors
Upward radiance	$L_u(\lambda,z)$	$W\ m^{-2}\ sr^{-1}$	2004-2005	Aug - Mar[(b)]	5	Authors
Beam attenuation	$c_\theta(\lambda)$	m^{-1}	2004-2005	Aug - Mar[(b)]	49	Authors
OPTICALLY ACTIVE CONSTITUENTS						
Particulate matter	C	$mg\ L^{-1}$	2004-2005	Aug - Mar[(b)]	49	Finger et al., 2006
Dissolved organic carbon	DOC	$mg\ L^{-1}$	2004-2005	Aug - Mar[(b)]	30	Authors
Particulate organic carbon	POC	$mg\ L^{-1}$	2004-2005	Aug - Mar[(b)]	49	Rellstab et al., 2007
SECCHI DEPTH						
Secchi depth	z_{SD}	m	1921-1923	biweekly	37	Flück, 1926 [(c)]
			1945-1949	weekly	140	Hofer, 1952 [(c)]
			1953-1954	bimonthly	9	Nydegger, 1957
			1985-1989	monthly	33	Kirchhofer, 1990
			1993-2005	biweekly	2964	GSA, unpublished [(d)]
			1999-2005	monthly	71	GSA, unpublished [(e)]

[(a)] N denotes the number of profiles or samples

[(b)] 25 August 2004, 11 October 2004, 9 November 2004, 21 December 2004, 22 March 2005.

[(c)] Measurements performed in the western part of the lake (Figure 3.1)

[(d)] Measurements performed by a fisherman on behalf of GSA

[(e)] Data was used for correlation with attenuation and particle concentration, determined simultaneously

active compounds, beam attenuation in the filtered water can be attributed to the absorption of gilvin (Kirk, 1994).

All samples were analyzed for total suspended particles (C), particulate organic carbon (POC) and dissolved organic carbon (DOC). C was determined gravimetrically on glass microfibre filters (GF/F, Whatman, UK) (APHA, 1998; Finger et al., 2006). POC was measured by Rellstab et al. (2007), applying combustion at 880 °C with a Rok 3/30 furnace (Heraeus, Germany) and subsequent IR-detection of the produced CO_2. DOC was quantified in the filtered samples after acidification with 1% of 2 M HCl, combustion and subsequent detection of the generated CO_2 in a TOC-5000 (Shimadzu, Japan).

3.3.2 *In situ attenuation measurements*

The Office of Water Protection and Waste Management of Canton Bern (GSA) has measured profiles of photosynthetically active radiation (PAR, denoted as E_0 ; $\mu E\ m^{-2}\ s^{-1}$; 400

< λ < 700 nm) in the lake since 1999 using a spherical underwater LI-193SA sensor (LI-COR Inc, USA) and a corresponding LI-190SA radiometer above the surface. Additional PAR measurements are available from previous studies (Kirchhofer, 1990; Pfunder, 1994) (Table 3.1). Underwater E_0 was corrected for short-term variations of incoming light (due to clouds) by multiplying it with the quotient of the simultaneously measured irradiance above the surface and to the reference surface irradiance determined at the beginning of the measurement. Attenuation coefficient K_0 was determined by fitting an exponential function to the corrected E_0 profile from the surface (z_0) to the euphotic depth z_{eu}.

$$E_0(z) = E_0(z_0) \cdot e^{-K_0 \cdot z} \qquad [\mu E\ m^{-2}\ s^{-1}] \qquad (3.2)$$

z_{eu} denotes the depth in a homogenous water column where quantum fluxes have decreased to 1% of the subsurface value. It can also be expressed as a function of K_0:

$$z_{eu} = \ln(100) / K_0 = 4.61 / K_0 \qquad [m]. \qquad (3.3)$$

3.3.3 Secchi recordings

The Secchi depth z_{SD} has been systematically recorded about four times per week since 1993 by a local resident, wheras prior to 1993 z_{SD} was recorded on a biweekly to monthly basis (Flück, 1926; Hofer, 1952; Nydegger, 1957; Kirchhofer, 1990) (Table 3.1). Before 1954 Secchi depths were measured in the western part of the lake (~500 m off shore; B in Figure 3.1) due to lack of motorized transportation. Although this location might be more affected by particles from the Lütschine, Flück (1926) demonstrated empirically that his sampling site were representative for the open water of the lake in the summer.

3.3.4 Reflectance measurements

To estimate reflectance in Lake Brienz, *in situ* downward irradiance $E_d(\lambda, z)$ (W m^{-2}; 180° opening angle) and upward radiance $L_u(\lambda, z)$ (W m^{-2} sr^{-1}; 15 ° opening angle) were measured from 1 to 20 m depth at each sampling date (August 2004 to March 2005; Table 3.1). This was achieved using two GER 1500 radiometers (Geophysical and Environmental Research, USA) that were assembled into one dual-radiometer instrument by the Remote Sensing Laboratory of the University of Zürich (Keller, 2001), which enabled simultaneous measurements of *in situ* $E_d(\lambda, z)$ and $L_u(\lambda,z)$. Spectral irradiance reflectance $R(\lambda,z)$ is defined according to Kirk (1994) by

$$R(\lambda,z)=\frac{E_u(\lambda,z)}{E_d(\lambda,z)}=\frac{Q\cdot L_u(\lambda,z)}{E_d(\lambda,z)} \qquad [-] \qquad (3.4)$$

where Q (sr) denotes an experimentally defined factor to convert upward radiance to upward irradiance E_u (W m^{-2}). Q was estimated experimentally by flipping the dual-radiometer upside down to measure $E_u(\lambda, z)$ and dividing $E_u(\lambda, z)$ by $L_u(\lambda,z)$. For wavelengths of 450, 550 and 650 nm, $Q \approx 2.0$ sr was found in March 2005. We assume constant Q for all five observations, as R is in the same range for all five instances (Jaun, 2005).

3.3.5 Parameterization of reflectance for past conditions

Human perception of lake conditions depend on the intensity and spectral distribution of the reflectance. To assess the perceived increase in turbidity, reflectance (i.e. equation 3.4) was parameterized for summer conditions using present levels of optically active compounds and then compared to the hypothetical scenario of a 4-fold increase in productivity, expected during late 1970s. For this purpose, reflectance was calculated from the total backscattering coefficient b_b (m^{-1}) and the total absorption coefficient a (m^{-1}) as widely used in the literature (Pierson and Strömbeck, 2001; Frauendorf, 2002; Wozniak and Stramski, 2004; Kallio, 2006):

$$R(\lambda)=\Omega\cdot\frac{b_b(\lambda)}{b_b(\lambda)+a(\lambda)} \qquad [-] \qquad (3.5)$$

where Ω denotes a dimensionless factor dependent on the angle of the incoming sunlight. As we consider relative changes of R, the value of Ω needs not to be exact and Ω = 0.35 was chosen as a typical clear sky value (Morel and Prieur, 1977; Kirk, 1994; Frauendorf, 2002). The total absorption coefficient a(λ) is the sum of absorption by the different optically active compounds:

$$a(\lambda)=a_w(\lambda)+a_p(\lambda)+a_{Chl\,a}(\lambda)+a_g(\lambda) \qquad [m^{-1}] \qquad (3.6)$$

where the subscripts w, p, *Chl a* and g denote pure water, particles, Chlorophyll a and gilvin (represented throughout this study by DOC), respectively. The spectral absorption coefficient of water is taken from Pope and Fry (1997). The dependency of absorption by particulate or dissolved matter on the concentration of the specific compounds (C, *Chl a*, DOC) was determined by means of concentration-normalized absorption coefficients a* taken from various studies as follows:

$$a_p(\lambda)=a_p^*(\lambda_0)\cdot[C]\cdot\exp^{-S_p(\lambda_0-\lambda)} \qquad [m^{-1}] \qquad (3.7)$$

$$a_{Chl\text{-}a}(\lambda) = A(\lambda) \cdot [\text{Chl a}]^{(1 - B(\lambda))} \quad [m^{-1}] \quad (3.8)$$

$$a_g(\lambda) = a^*_g(\lambda_0) \cdot [DOC] \cdot \exp^{-S_g(\lambda_0 - \lambda)} \quad [m^{-1}] \quad (3.9)$$

The values of a* at reference wavelength λ_o and of the exponent S in equations (3.7) and (3.9) are specified in Table 3.2. Equation (3.8) and the parameters A and B have been derived from numerous observations by Bricaud et al. (1995). B is a dimensionless number, A and *Chl a* have units of m^{-1} and mg m^{-3}, respectively.

Similar to equation (3.6), the scattering coefficient b is defined as the sum of scattering by pure water, particles and *Chl a*, whereas scattering by gilvin is negligible (Bricaud et al., 1981):

$$b(\lambda) = b_w(\lambda) + b_p(\lambda) + b_{Chl\text{-}a}(\lambda) \quad [m^{-1}] \quad (3.10)$$

The backscattering coefficient of water $b_{b,w}$ is half of the scattering coefficient b_w, since water molecules scatter light isotropically (Morel, 1974). For the spectral backscattering of particles and *Chl a* we used the following parameterizations:

$$b_{b,p}(\lambda) = 0.033 \cdot \left[b^*_p(\lambda_0) \cdot [C] \cdot (\lambda/\lambda_0)^{-T_p} \right] \quad [m^{-1}] \quad (3.11)$$

$$b_{b,Chl\,a}(\lambda) = 0.004 \cdot \left[b^*_{Chl\,a}(\lambda_0) \cdot [\text{Chl a}] \cdot (\lambda/\lambda_0)^{-T_{Chl\,a}} \right] \quad [m^{-1}] \quad (3.12)$$

For particles, the ratio of backscattering to scattering is typically 0.019 (Kirk, 1994) with values up to 0.07 to 0.08 (Whitlock et al., 1981; Tassan and Ferrari, 1995), whereas for phytoplankton this ratio is only ~0.001 to 0.004 (Frauendorf, 2002). The two factors (0.033 and 0.004) were chosen to match the measured R(λ) (Equation 3.5). A wide rang of values have been reported for the specific scattering coefficients b* and the exponents T (Table 3.2). Whereas T_p and b^*_p were estimated by Jaun (2005), $b^*_{Chl\,a}$ was chosen according to Kirk (1994), and $T_{Chl\,a}$ was taken from (Wozniak and Stramski, 2004).

Table 3.2: Parameterization of reflectance

	Wavelength λ_0 (nm)	Value	Unit	Equation	Range	References
$a_p^*(\lambda_0)^{(a)}$	450	0.02	$m^2\ g^{-1}$	(3.7)	0.01 - 0.067	(Babin et al., 2003; Doxaran et al., 2006)
S_p		0.02	nm^{-1}	(3.7)	0.005 - 0.021	(Doxaran et al., 2006)
$a_g^*(\lambda)^{(a)}$	440	0.048	$m^2\ g^{-1}$	(3.9)	-	(Keller, 2001)
S_g		0.015	nm^{-1}	(3.9)	0.01 - 0.02	(Kirk, 1994)
$b_p^{*(a)}$	550	0.58	$m^2\ g^{-1}$	(3.11)	0.3 - 0.9	(Tassan and Ferrari, 1995; Wozniak and Stramski, 2004; Doxaran et al., 2006)
T_p		0.9	-	(3.11)	0 - 1	(Doxaran et al., 2006)
$b_{Chl\ a}^{(a)}$	550	0.1	$m^2\ mg^{-1}$	(3.12)	0.044 - 0.139	(Kirk, 1994)
$T_{Chl\ a}$		0.8	-	(3.12)	0 - 1	(Frauendorf, 2002)

[(a)] The numerical values of the specific absorption and scattering coefficients a* and b* at wavelength λ_o are indicated for particles (p), gilvin (g) and *Chl a* with the corresponding exponents S and T. The typical ranges are documented with literature references.

3.3.6 Reconstruction of attenuation by Secchi depth and particles

Based on our data from 1999 to 2004 (Table 3.1) K_0 relates to the inverse of the Secchi depth, z_{SD}, as follows:

$$K_0 = \beta_1 + \alpha_1 \cdot z_{SD}\text{-}1 \qquad [m^{-1}] \qquad (3.13)$$

Using this relation K_0 can be reconstructed with Secchi depths for periods previous to our sampling and compared to the radiometric measurements performed by Kirchhofer (1990) and Pfunder (1994). Furthermore, K_0 was correlated with simultaneously determined particle concentration C (Finger et al., 2006) according to the following relation:

$$K_0 = \beta_2 + \alpha_2 \cdot C \qquad [m^{-1}] \qquad (3.14)$$

For C we used average particle concentrations from the euphotic zone $\overline{C}(z_{eu})$ and from the top 50 m water column $\overline{C}(z_{50})$. Since there are no K_0 and only scarce z_{SD} recordings available for the first half of the last century, $\overline{C}(z_{50})$ was simulated from 1995 to 2004, using water discharge, particle loads and intrusion dynamics according to Finger et al. (2006). The same model was also used to reconstruct $\overline{C}(z_{50})$ for the hypothetical scenario without hydropower dams in the headwaters of the Aare (Finger et al., 2006).

This procedure provides two independent estimates on how attenuation in Lake Brienz has changed by upstream damming: firstly, via particle concentrations (Finger et al., 2006), and secondly via pre-dam Secchi depth records (Flück, 1926).

3.4 Results

3.4.1 Present light regime in Lake Brienz

The inorganic particle loads (Finger et al., 2006) in the two major inflows (~300 kt yr^{-1}) dominate the light attenuation in Lake Brienz. Consequently, the particle dynamics in the top 50 m of Lake Brienz are governed by snow/glacial melting and heavy precipitation events during summer (leading to high particle loads) and low discharge, since most precipitation occurs as snow in winter (implying minimal particle loads; Finger et al., 2006). During summer the vertically-averaged concentrations $\overline{C}(z_{50})$ in the uppermost 50 m of the water column reach $\overline{C}(z_{50})$ > 5 mg L^{-1}, whereas in winter $\overline{C}(z_{50})$ drops back to 1 to 2 mg L^{-1} throughout the entire volume (Figure 3.2). The Secchi depth, light attenuation K_0 and euphotic depth z_{eu} determined from measured PAR profiles (equation 3.3) follow the temporal dynamics of C (Figure 3.2a). While during summer, when C reaches a maximum, light is limited to the top 10 m, z_{eu} in winter can reach down to 25 m depth.

The low concentrations of POC (0.05 to 0.25 mg L^{-1}; Rellstab et al., 2007) and *Chl a* (0.1 to 2 µg L^{-1}; Finger et al., 2006) reinforce the assumption that attenuation is mainly due to scattering caused by small inorganic particles. In fact, calculations of the scattering contributions reveal that particles with diameters smaller than 4 µm account for ~70 to 80% of the scattering (Jaun, 2005; Swift et al., 2006). The beam attenuation of gilvin (a_g), measured in filtered water samples, was mostly below the sensitivity limit of the spectrophotometer of 0.1 m^{-1}. This is reasonable, since typical concentrations of dissolved organic carbon (DOC) are 0.5 mg L^{-1}. Using the specific DOC attenuation values of 0.0539 m^2 g^{-1} for 400 to 700 nm (Jaquet et al., 1994) and ~0.015 m^2 mg^{-1} for *Chl a* (Morel and Prieur, 1977), it was estimated that *Chl a* and gilvin account for only ~5% of the beam attenuation.

3.4.2 Temporal development of Secchi depth during the 20th century

Secchi depth z_{SD} recordings of various temporal resolutions exist since 1921 (Table 3.1). Concerning the role of the upstream hydropower development, the following periods of z_{SD} recordings (Figure 3.3) are of interest: (i) pre-dam: 1921 to 1923 (natural flow), (ii) inter-dam: 1945 to 1949 (completion of half of the dams) and (iii) present (completion and operation of all dams). We separate the present period (iii) into: 1985 to 1989 (high productivity) and 1993 to 2005 (oligotrophication; status quo scenario). The recordings in 1953 and 1954 (Nydegger,

1957) consist of only nine data points and should be interpreted with caution (Siegenthaler, 2003).

Present z_{SD} follow the same seasonal structure as $\overline{C}(z_{50})$ (Figure 3.2): In summer z_{SD} reaches a minimum of 2 to 3 m while reaching a maximum of 5 to 7 m in winter. Spring is characterized by strong fluctuations (Figure 3.3).

Pre-dam z_{SD} recordings (Table 3.1) - available in 1921 / 1922 (bi-weekly) and 1923 (one z_{SD} recording only) - show a strong variation in spring with $z_{SD} \sim 8$ to 9 m and 5 to 6 m, respectively (Figure 3.3). The shallowest pre-dam z_{SD} was observed in summer 1923 (0.45 m). In summer Secchi depths reached deeper during the inter-dam period of the 1940s and were deepest under present conditions, although the inter-annual fluctuations were large.

Exceptionally clear water was observed from 1995 to 1997: z_{SD} reached an extraordinary maximum of 16.9 m in fall 1995, when no rain fell for more than four weeks (data: MeteoSwiss). Conversely, especially low clarity was measured after the flood in August 2005 ($z_{SD} = 0.7$ m).

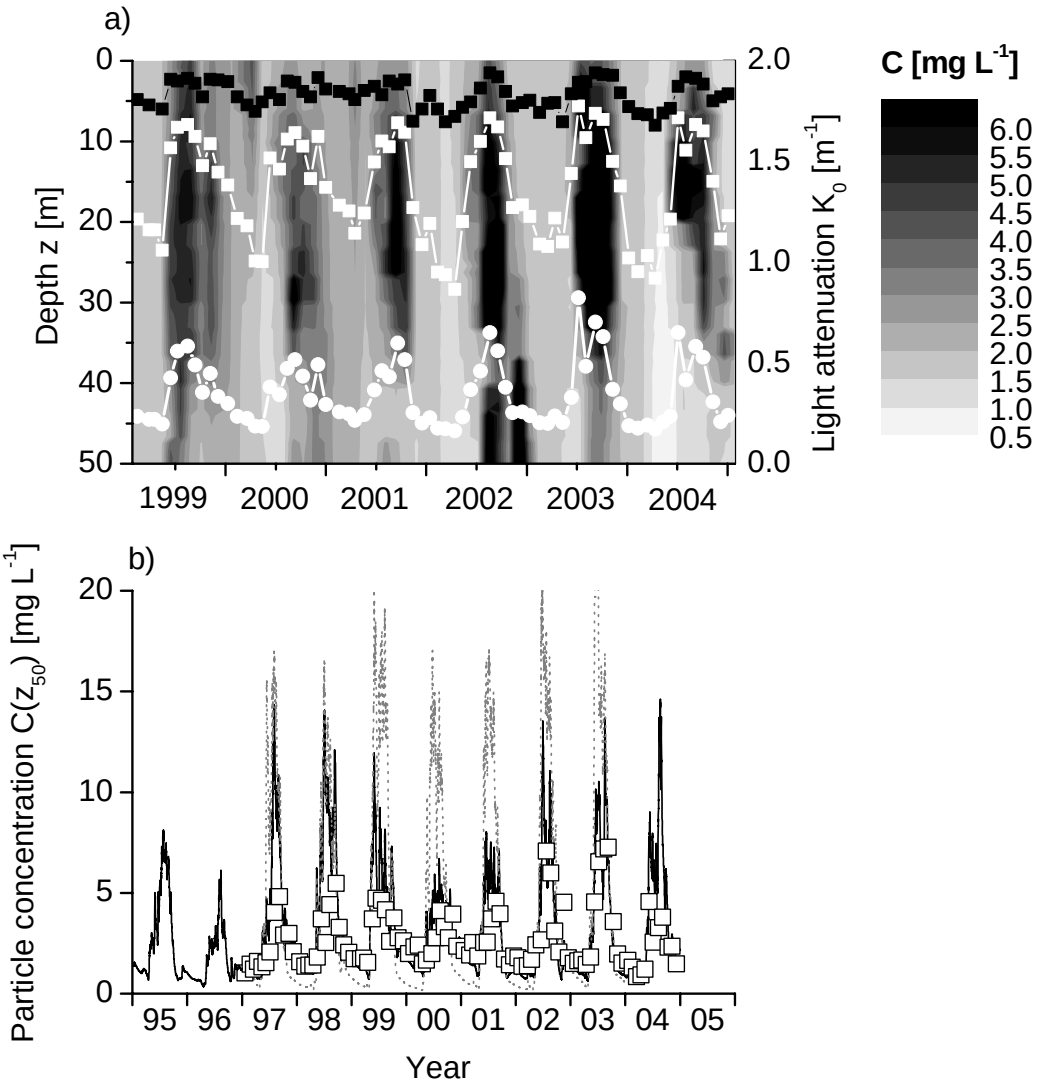

Figure 3.2: Status quo particle concentrations in the top 50 m water column of Lake Brienz from 1995 to 2005 as (a) contour plot and (b) average in the top 50 m. (a) also presents Secchi depth (black squares), euphotic depth (white squares) and light attenuation (white circles; right scale). (b) illustrates average particle concentrations in the top 50 m determined in water samples (open squares), simulated (black line) for status quo scenario and simulated for no-dam scenario (dotted grey line). The Figure was adopted from Finger et al. (2006).

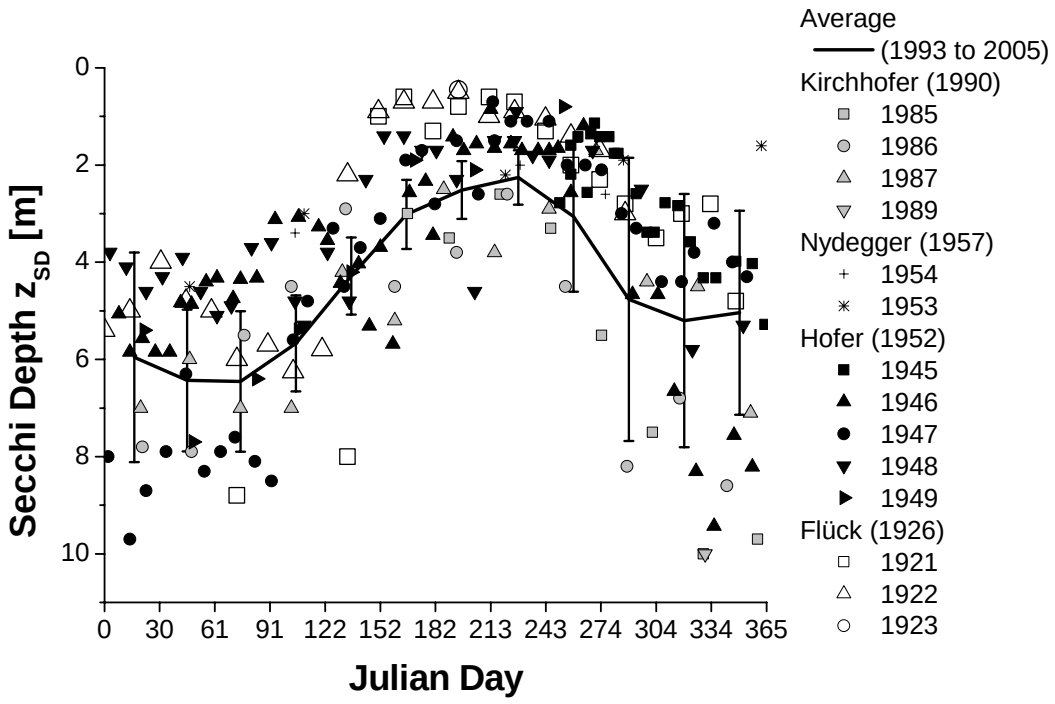

Figure 3.3: Secchi depth in Lake Brienz from 1921 to 2005. Recordings are grouped according to different episodes of hydropower exploitation: pre-dam (open symbols), inter-dam (black symbols) and present situation (since the late 1980s: grey symbols). For orientation the average and standard deviations for the period 1993 to 2005 is illustrated as a solid line.

3.4.3 Correlation of attenuation with Secchi depth and particles

As we lack attenuation measurements from the past, we use the Secchi depth z_{SD} and particle concentrations $\overline{C}(z_{50})$ as surrogates for reconstructing light attenuation prior to 1999. The variables are moderately to highly correlated, with R^2 between 0.55 and 0.85 (Figure 3.4). The regressions were calculated separately for summer (May to September) and winter (October to April) for two reasons: (1) In summer there is a significant vertical particle gradient in the top 50 m (Figure 3.2), which is not present during the times of deep convective mixing in winter. Therefore K_0 and $\overline{C}(z_{50})$ do not pertain to the same layers. (2) During winter (low input), the particles are smaller on average (Finger et al., 2006), leading to different K_0 per unit mass.

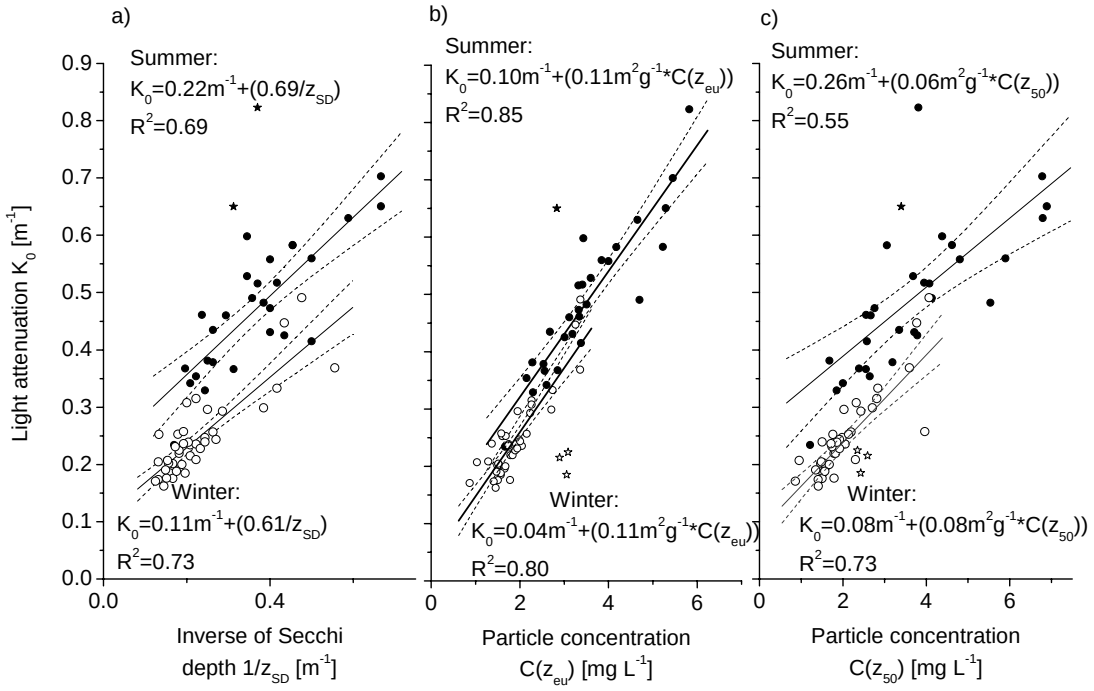

Figure 3.4: Correlation of light attenuation K_0 with a) Secchi depth, b) mean particle concentration in the euphotic layer and c) mean particle concentrations in the top 50 m. Black circles indicate data points during summer (May to September) and open circles during winter (October to April) of monthly measurements from 1999 to 2004 (N_W = 39, N_S = 30; $p < 0.001$). The solid line represents the respective linear regressions, dotted line illustrates the upper and lower 95% confidence limits and star symbols represent outliers not considered for regression (criteria for outliers were determined in b).

As K_0 is estimated within the euphotic zone, the correlation of K_0 with particles is stronger for $\overline{C}(z_{eu})$ than for $\overline{C}(z_{50})$ (Figure 3.4). However, due to the complexity of the processes involved and the vertical resolution of the simulated particle distributions (Finger et al., 2006), we chose $\overline{C}(z_{50})$ as the proxy for the concentrations in the past. From 1999 to 2004, the two independent K_0 estimates can be compared to the status quo scenario (Figure 3.5). Predictions based on Secchi depth and simulated particle concentrations have a higher temporal resolution (1 day and 0.1 day, respectively), also depicting short term turbidity events.

This reconstruction allows a comparison of the attenuations of the status quo scenario with scenarios without dams based on no-dam $\overline{C}(z_{50})$ and on pre-dam Secchi depths z_{SD} (Figure 3.6). Although the inter-annual and short-term variations of attenuation are very large (Figure 3.5), the overall outcome is clear; attenuation without dams would be about twice compared to

present in summer, whereas in winter K_0 would be about half of the status quo level. Although the uncertainty of the reconstructed no-dam K_0 is high, both particles and Secchi depth levels indicate an enhanced attenuation in summer compared to the status quo conditions.

3.4.4 Natural variability of attenuation

To evaluate the reconstructed attenuation, we compared K_0 estimates based on the Secchi depth and simulated particle concentrations with K_0 determined from measured PAR profiles. Independent radiometric measurements in 1987 and 1994 by Kirchhofer (1990) and Pfunder (1994) show convincing agreement with K_0 derived from z_{SD} (Figure 3.5). Exceptions are the data from 7 July 1987, when heavy rainfall occurred immediately before sampling (Kirchhofer, 1990).

The z_{SD}-based attenuation in 1985 and 1986 was clearly below the 1987 estimates. This is consistent with the observation that particle inputs were well below average in 1985 and well above average in 1987. Extremely low attenuation was observed from fall 1995 to spring 1997. As discussed below, this variability can be explained by discharge and load patterns in the two river inflows.

In winter and spring 1999 exceptional snow- and rainfall caused unusually high discharge in May 1999 along with particle loads 4-fold higher than average (Finger et al., 2006). During this period, Secchi depths and attenuation showed decreased and increased values, respectively.

During the heat wave in summer 2003 enhanced glacial melting increased the particle load of the Lütschine to ~35% above average, whereas it was reduced to half in the Aare because there was almost no precipitation, while glacial particles were largely retained in the upstream reservoirs (Finger et al., 2006). Since both rivers intruded mostly into the surface layer during this period, K_0 was higher than usual. Extreme conditions occurred in August 2005 as a result of flooding. Exceptional particle input increased K_0 to 0.9 to 1.2 m^{-1}.

We conclude that inter-annual and short-term fluctuations due to exceptional weather conditions can reach as much as a factor of 2. The fluctuations in Secchi depth and attenuation are mainly explained by variations in natural discharge and not so much by hydropower operations, since there were no significant inter-annual changes of the ratio of reservoir discharge per total discharge (KWO, unpublished data).

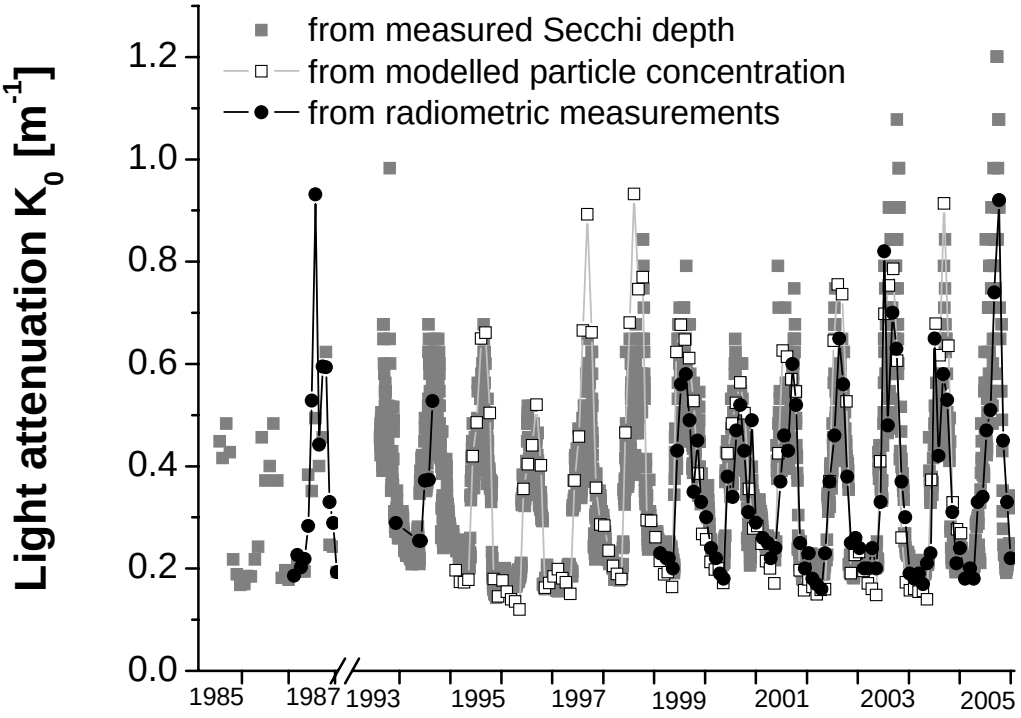

Figure 3.5: Light attenuation K_0 from 1985 to 2005 from radiometric profiles (black circles: determined with equation 3.2), from continuous z_{SD} recordings (grey squares: predicted with correlations (Winter and Summer) from Figure 3.4) and from modeled $C(z_{50})$ (white squares: predicted with correlations from Figure 3.4).

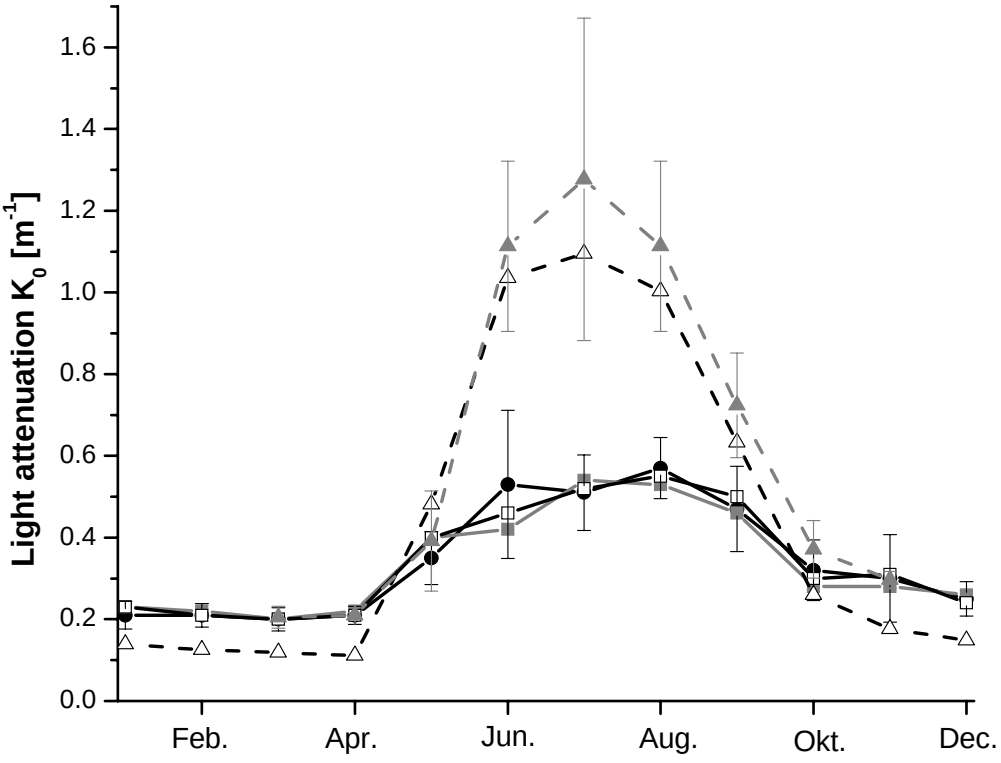

Figure 3.6: Comparison of current light attenuation K_0 (solid lines) and under conditions without upstream hydropower operation (dashed lines). Values depict monthly averages of attenuation for 1999 to 2004 and are compared to K_0 derived from light measurements (black circles), measured Secchi depth (grey squares) and particle concentrations (white squares). Corresponding attenuation without dams is derived from measured pre-dam Secchi depths (grey triangles) and modeled no-dam particle concentrations (open triangles). The error bars represent the standard deviations (SD) of monthly-averages.

3.4.5 Changes in reflectance due to oligotrophication

Local residents claim that turbidity has increased during the last decades. Reflectance, the ratio of backscattering per total attenuation (scattering plus absorption; Equation 3.5), quantifies best the visual perception of turbidity in natural waters. Measurements revealed that the reflectance in the upper 8 m of Lake Brienz varied from 12 to 24% in the spectral range of 500 to 550 nm (Figure 3.7). At longer wavelengths reflectance is low because of high absorption by water, whereas the increased absorption by organic compounds towards shorter wavelengths also causes lower reflectance.

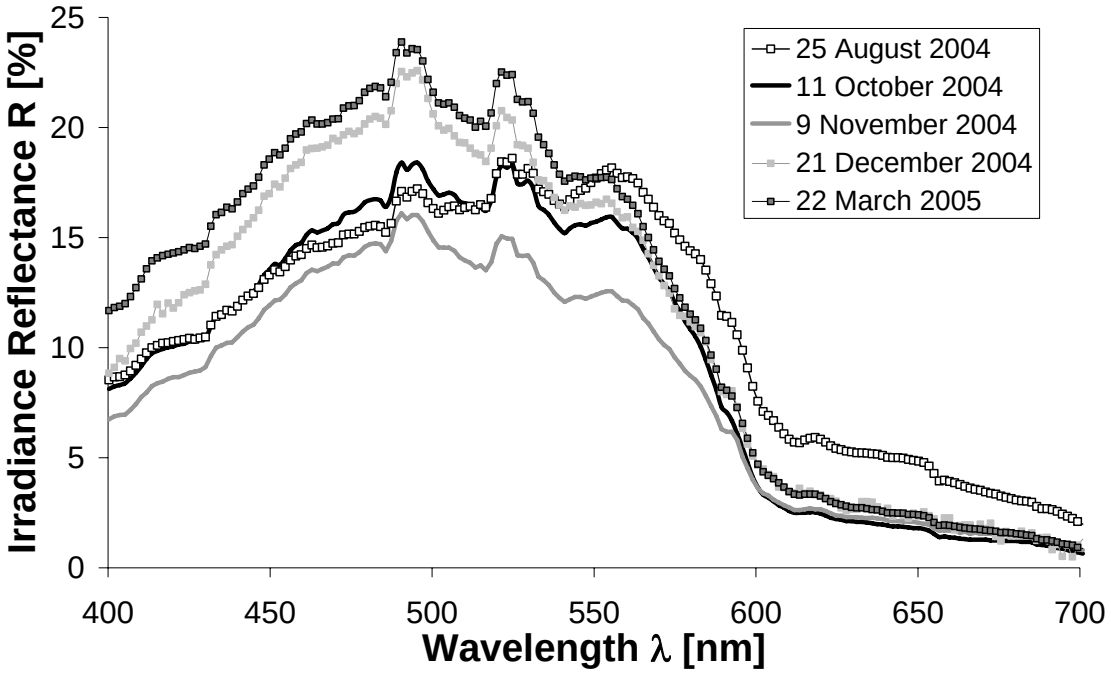

Figure 3.7: Average reflectance R in the top 8 m of Lake Brienz, measured on five occasions from August 2004 to March 2005.

During winter and spring (profiles from December and March) the reflectance is highest, since there are only low levels of light-absorbing organic compounds but backscattering is pronounced due to the small particles (Finger et al., 2006). In summer (profiles from August and October) reflectance is lower than in winter, since absorption at enhanced levels of organic matter increases more than the particle-induced backscattering. This effect was strongest in November 2004, when the organic fraction of particulate matter was highest and consequently reflectance was at a minimum. The vertical variation of reflectance in the upper 8 m water column is ~10% of its value, with the largest fluctuations in August (~25%) and October (40%) due to vertical particle gradients (Figure 3.2).

Lake Brienz has been subjected to a continuous decline of bio-available phosphorus input from ~33 t yr^{-1} in the late 1970s to ~8 t yr^{-1} in recent years (Müller et al., 2007a). As primary production in Lake Brienz is strongly phosphorus limited (Finger et al., 2007a), it can be assumed that optically active organic substances have been decreasing proportionally to the phosphorus input. Using equation (3.5) the reflectance is calculated for a status quo summer situation, using concentrations of optically active constituents as measured on 25 August 2004 (Table 3.3) and for 4-fold higher concentrations of optically active organic substances, expected in the late 1970s (Müller et al., 2007a). The most pronounced differences due to

Table 3.3: Typical concentration values for particles, *Chl a* and DOC in summer.

	Unit	Present [(a)]	Productive Period [(b)]	Equation
Particles, C	g m^{-3}	4 ± 1	4 ± 1	(3.7), (3.11)
Chl a	mg m^{-3}	2	8	(3.8), (3.12)
DOC	g m^{-3}	0.5	2	(3.9)

[(a)] For the present situation mean concentrations from 25 August 2004 are listed.

[(b)] For the productive period (late 1970s), according to equation (3.6), a 4-fold increase of *Chl a* and DOC is assumed.

oligotrophication are expected during the productive season. Higher productivity in Lake Brienz is expected to have two effects: (1) enhanced concentrations of *Chl a* and DOC and (2) increased sedimentation of inorganic particles due to biological and chemical coagulation (Gliwicz, 1986; Chanudet and Filella, 2007).

In order to assess the effects of oligotrophication on the perceived turbidity, we predicted reflectance for a 4-fold higher concentration of organic compounds using the parameterization of equations 3.5 to 3.12. The reflectance at the wavelength of ~550 nm, which is the maximum sensitivity of human eyes (Kirk, 1985), yields ~16% for the status quo scenario in summer (Figure 3.8). A typical variation in particle concentration of ±1 mg L^{-1} in summer causes a range of ~14% to 18% reflectance under present levels of optically active compounds. For a hypothetical summer during a productive decade (4-fold levels of *Chl a* and DOC) one could expect a reflectance of 11 to 14%. Assuming that the particle concentration and characteristics were the same in the past, the calculations indicate an increase in reflectance by ~20 to 25% as a result of oligotrophication. In addition, assuming further a realistic increase in particle concentration of 1 mg L^{-1} due to weakened bio-enhanced sedimentation (Chanudet and Filella, 2007), reflectance could have increased by 40 to 45% during the last 25 years. Moreover, in the last few years the summer maxima of fine particles were enhanced due to strong glacial melting (Finger et al., 2006), also causing enhanced backscattering and reflectance in Lake Brienz.

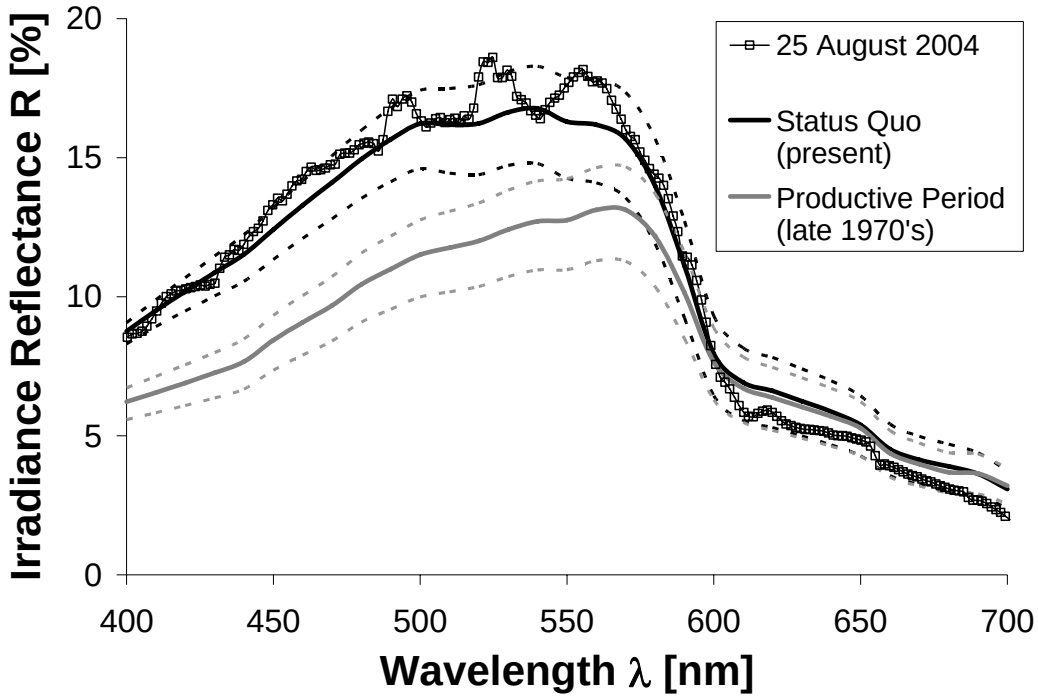

Figure 3.8: Comparison of current reflectance R (black lines) and under conditions in the late 1970s with presumed 4-fold *Chl a* and DOC levels (grey lines). Black squares illustrate measured reflectance in Lake Brienz on 25 August 2004, bold black line stands for modeled status quo reflectance in summer. The dashed lines indicate the range of modeled variations for altered C of ±1 mg L^{-1}.

3.5 Discussion

3.5.1 Present light conditions in Lake Brienz

The present light regime in Lake Brienz is defined predominantly by fine inorganic particles originating from its glaciated catchment. These small particles induce attenuation mainly by scattering and less by absorption, causing the turbid appearance of the water. Since productivity is low, organic substances like *Chl a* and gilvin are of minor relevance for the optical properties. Consequently, absorption contributes only ~5% to beam attenuation. The remaining ~95% of attenuation is by scattering and causes a high reflectance. Accordingly, water clarity is low with Secchi depths of ~2 m in summer and ~6 m in winter.

Secchi depths are often used as a surrogate for attenuation, as they are easy to measure. For Lake Brienz, we found a correlation between attenuation and Secchi depth similar to the relation in Koenings and Edmundson (1991) derived for turbid waters. In contrast, other studies

(Cristofor et al., 1994; Armengol et al., 2003; Reinart et al., 2003) reported steeper slopes, α_1, in equation (3.13). The reason for this is most probably due to lower scattering, as variations in α_1 reflect changes in the proportions of absorption to scattering (Effler, 1996). The intercept, β_1, of 0.22 m^{-1} (summer) and 0.11 m^{-1} (winter) is an empirical correction, accounting for the heterogeneity of the vertical particle distribution (Figure 3.4). Although, the use of $\overline{C}(z_{50})$ is not an ideal proxy for the surface particle content, it is the best possible compromise for the reconstruction of the particle concentration, given the limitations of modeling.

Despite these shortcomings it was possible to reconstruct attenuation from the Secchi depth and particle concentrations. Average attenuations for the status quo scenario - i.e. 0.5 to 0.6 m^{-1} in summer and ~0.2 m^{-1} in winter – were predicted. Furthermore the seasonal short-term variations with maxima of ~0.9 to 1.2 m^{-1} after heavy floods in summer and minima of ~0.1 m^{-1} during exceptional low discharge in the two tributaries were predicted.

Periods of unusual water clarity can be explained by discharge patterns and riverine particle transport. The high attenuation in 1987 (Figure 3.5) is explained by the combined particle load of the Aare and Lütschine (450 kt yr^{-1}), which was 1.5-times the average (Finger et al., 2006) in this particular year. Moreover, the extremely low attenuation from fall 1995 to spring 1997 (Figure 3.5) corresponds well with the natural discharge during this period, which was 10 to 40% below the long-term average (1983 to 2001). In 1996 the annual particle load to the lake was ~100 kt yr^{-1}, a factor 3 below the long-term average (Finger et al., 2006). During the period of maximum clarity in fall 1995 no rain fell for more than four weeks.

3.5.2 Effect of hydropower on light attenuation

We reconstructed the expected attenuations based on modeled particle concentrations for hypothetical no-dam conditions and on measured Secchi records prior to dam construction to evaluate the effect of upstream hydropower operation on attenuation in downstream Lake Brienz. Since pre-dam Secchi recordings are sparse (data only from 1921, 1922 and 1923) and cover a complete annual cycle only in 1922, a large uncertainty remains. Winter and spring Secchi depths vary significantly, with values of 8 to 9 m (1921) and 5 to 6 m (1922). These variations can, however, be explained by 25% above-average discharge in 1922 and 25% below-average discharge in the first half of 1921.

Compared to the status quo scenario, attenuation in Lake Brienz would double during summer without dams, since particles would not be retained in the upstream reservoirs. This result is supported by Secchi recordings in the 1940s (inter-dam period), when Secchi depths in

summer show values between no-dam conditions and status quo. Without dams, attenuation in winter would drop to half the present values due to low and almost particle-free natural discharge. These effects can even be observed when the Secchi depth from recent years, characterized by extraordinary climatic conditions (e.g. flood in 1999, heat wave 2003 and flood in 2005), are considered in the assessment. Although such short-term climatic conditions can overrule the effects of hydropower operations, the impacts of hydropower operations prevail over the long term.

3.5.3 *Effect of oligotrophication on reflectance*

We infer that the relative contribution of absorption and scattering remained approximately the same from pre-dam to the status quo conditions. Since we expect that the phosphorus level prior to eutrophication is about the same as after oligotrophication (Müller et al., 2007a), productivity and subsequently the concentration of organic substances are thought to be similar for pre-dam and present conditions. However, for the productive decade (late 1970s) - when more organic material was available - we lack an optical model for the multicomponental waters of that period. Optical data is only available for 1985 to 1987 (Kirchhofer, 1990), and therefore only semi-quantitative estimations of the attenuation and the light regime are possible for the productive late 1970s. However, we do not expect a large effect by the higher content of organic compounds, as presently the organic material contributes only 5% to attenuation. Although this contribution was surely larger in the late 1970s, it was still low and partly compensated by lower particle concentrations due to enhanced bio-induced sedimentation (Chanudet and Filella, 2007).

To quantify the change in perceived turbidity, we parameterized reflectance for summer as a function of particle concentration, *Chl a*, DOC and their optical properties found in the literature. Due to the natural variability of the governing concentrations, the calculated reflectance has a large uncertainty but matches with the measured reflectance on 24 August 2004 (Figure 3.8). Therefore the relative changes in reflectance due to oligotrophication are expected to be reasonable.

Kallio (2006) presents a decrease of reflectance and shift of maximum values to shorter wavelength for the transformation from eutrophic to oligotrophic conditions, due to the decrease of optically active constituents. However, it is likely that reflectance in Lake Brienz was lower during the productive decade, since both higher concentrations of light-absorbing organic constituents and lower concentrations of light-scattering particles reduced reflectance. In the last few summers increased glacial melting elevated the fraction of the finest particles,

also causing higher reflectance (Wozniak and Stramski, 2004). Therefore, the increase in turbidity in the last decades, as perceived by fishermen and residents, can well be explained by higher reflectance caused by less absorption per attenuation as a result of oligotrophication.

3.6 Conclusions

Based on the presented simulations and measurements of light attenuation and reflectance under present conditions, during the eutrophication phase in the late 1970s and under hypothetical conditions without hydropower in the catchment of the Aare the following conclusions can be drawn:

(1) Damming in the upstream catchment has significantly changed the seasonal particle flux to downstream Lake Brienz by reducing input during summer and enhancing input during winter. As a result, the present attenuation in summer (0.5 to 0.6 m^{-1}) is about half the attenuation without dams (1 to 1.2 m^{-1}). In contrast, during winter the present attenuation (~0.2 m^{-1}) is approximately twice its value for 'no-dam' conditions (~0.1 m^{-1}). These results are supported by the agreement of the simulated particle concentrations with Secchi depths measured since the 1920s.

(2) Strong inter-annual and short-term fluctuation of attenuation, especially in spring and fall, is a direct consequence of variability in a natural discharge regime. Extremely low attenuation, such as in fall 1995 (~0.15 m^{-1}) was caused by exceptionally low discharge. Conversely, maximum attenuation was measured after heavy floods such as in August 2005 (0.9 to 1.2 m^{-1}). As a result, the light attenuation can temporarily reach minimal and maximal values similar to those of no-dam conditions.

(3) During summer the present reflectance at wavelengths of 550 nm is ~14 to 18%. We estimate current reflectance to be ~20 to 25% higher than three decades ago during the productive late 1970s when organic compounds were assumed to be 4-fold levels higher. In addition to reduced absorption by less autochthonous organic substances, the biological and chemical sedimentation of fine particles is now also reduced (Chanudet and Filella, 2007). Higher levels of fine particles would enhance scattering and could increase reflectance by another ~20%. These findings are consistent with the subjective observations of increasing turbidity in the last decades by local residents.

3.7 Acknowledgements

This publication is part of an interdisciplinary research project to investigate the effects of catchment alterations on the ecosystem of Lake Brienz. Funding of the study was provided by the Regional Government of Canton Bern, KWO Grimselstrom, Swiss Federal Office for the Environment (FOEN), communities on the shoreline of Lake Brienz and Eawag. Local fishermen have collected Secchi depths on behalf of GBL several times per week since 1993. R. Illi and his crew measured particle concentrations, POC and DOC. S. Robele measured part of the beam attenuation spectra. Furthermore, M. Filella, V. Chanudet and C. Rellstab collaborated in the field and contributed with interesting discussions. Valuable input to an earlier version of this manuscript was provided by Prof. J. Ackerman, Prof. B. Wehrli and two anonymous reviewers.

CHAPTER 4

EFFECTS OF ALPINE HYDROPOWER OPERATION ON PRIMARY PRODUCTION IN A DOWNSTREAM LAKE

David Finger, Peter Bossard, Martin Schmid, Lorenz Jaun, Beat Müller, Daniel Steiner, Erwin Schäffer, Markus Zeh and Alfred Wüest

(Aquatic Science, accepted)

Abstract

Water storage in alpine hydropower reservoirs substantially alters particle loads in effluent rivers and, therefore, the turbidity in downstream lakes. In oligotrophic lakes, phytoplankton growth usually extends to great depths and thus is sensitive to changes in light conditions. In oligotrophic Lake Brienz (Switzerland), primary production is especially precarious in summer, when high particle loads from the glaciated catchment limit light penetration. During the past century, the construction of hydropower dams in the watershed has significantly altered the dynamics of turbidity. To assess these effects, we measured the *in situ* carbon assimilation rates and ambient light intensities during 18 months. Based on the experimental data, a numerical model was established to assess gross primary production under present light conditions and under the hypothetical case without upstream dams. Light conditions for the hypothetical 'no-dam' situation were estimated from pre-dam Secchi depths and simulated 'no-dam' particle concentrations. Current gross primary production is low (~66 gC m^{-2} yr^{-1}), and would not increase by more than ~44% if the lake was free of turbidity. Disregarding nutrient retention in the dams, we estimate that gross primary production would be ~35% lower in summer but up to ~23% higher in winter in the absence of reservoirs. The annual primary production (~58 gC m^{-2} yr^{-1}) would decrease not more than ~12% compared to the current primary production with dams. According to our model calculations, hydropower operations can significantly alter the seasonal dynamics, but they have only a limited effect on the annual primary production.

4.1 Introduction

Lacustrine ecosystems are strongly influenced by their catchment characteristics (Duarte and Kalff, 1989; Kratz et al., 1997; Dixit et al., 2000). Particularly, the construction of more than 500,000 reservoirs during the second half of the 20th century has altered the hydrology in downstream rivers and lakes (McCully, 1996; Vörösmarty et al., 1997; Vörösmarty et al., 2003). The ecological and social effects of water storage on downstream regions have been well studied (Rosenberg et al., 1995; Rosenberg et al., 1997; Rosenberg et al., 2000), especially with regard to the biological impacts in rivers (Ward and Stanford, 1995; Nilsson et al., 1997; Hart and Poff, 2002) and occasionally in downstream lakes (Ashley et al., 1997; Stockner et al., 2000; Friedl and Wüest, 2002). In the case of glaciated catchments, reservoirs retain much of the glacial till (Anselmetti et al., 2007) and thus alter the allochthonous particle input to downstream lakes, which in turn affects the dynamics of their turbidity

(Finger et al., 2006) and nutrient input (Humborg et al., 2000; Friedl et al., 2004). Moreover, the suspended particles can significantly reduce light penetration, thus limiting primary production (Jewson and Taylor, 1978; Krause-Jensen and Sand-Jensen, 1998) and reducing the visual range of aquatic animals (Aksnes and Utne, 1997).

The general relation between light intensity (photosynthetically active radiation; PAR) and photosynthesis, measured using the ^{14}C method (Steemann Nielsen, 1952), provides the basis for modelling the primary production of a water body as a function of light availability (Jassby and Platt, 1976; Platt and Jassby, 1976; Platt et al., 1980). In simple cases, such models can be used to estimate primary production under varying light conditions (Sakshaug and Slagstad, 1991), neglecting the effects of internal mixing (Diehl, 2002), sediment resuspension (Schallenberg and Burns, 2004), plankton competition for nutrients (Litchman et al., 2004) or changes in nutrients availability (Müller et al., 2007a), which all affect primary production.

Lake Brienz, situated at the foothills of the Alps in the *Bernese Oberland*, Switzerland, provides an ideal example to study the effects of turbidity on primary production. Over 20% of the catchment is covered by glaciers, leading to the highest particle input per catchment area (324 t km^{-2} yr^{-1}) in Swiss lowland lakes. As a result, Lake Brienz becomes turbid during the summer, when snow and glacier melting reaches a maximum. The construction of several hydropower facilities in its catchment has significantly altered the hydrological regime of the water and particle inflow.

The purpose of this study is to assess the effects of altered turbidity regimes on the primary productivity of Lake Brienz using monthly profiles of *in situ* carbon (C) assimilation rates and numerical relationships between *in situ* primary production and *in situ* light intensity. These data were used to develop a mathematical model to estimate carbon assimilation rates between 1999 and 2005. To evaluate the effects of suspended particles, this calibrated procedure was used to estimate primary production in neighbouring Lake Thun, which is almost identical in an eco-geographical sense, but practically free of inorganic turbidity. Finally, the model is used to explore the conditions prior to dam construction and to quantify the effects of hydropower dams on primary production in Lake Brienz.

4.2 Study site - Lake Brienz

Lake Brienz is situated about 70 km southeast of Bern (7° 58’ E, 46° 43’ N), with a surface of 29.8 km^2, a volume of 5.17 km^3, and a maximum depth of 259 m, which is typical

of the peri-alpine lakes (Table 4.1). The two major inflows, the Aare and Lütschine, enter the lake at opposite ends (Figure 4.1). These two tributaries drain a catchment area of 933 km^2 and carry average particle concentrations of ~160 g m^{-3}, resulting in an annual suspended particle input of ~300 kt yr^{-1} (Finger et al., 2006). Over half of this mass enters into the surface layer, leading to average particle concentrations in the top 50 m of up to 25 g m^{-3} (Finger et al., 2006). Only about 9 kt yr^{-1} (or 3%) of the particles are discharged downstream into Lake Thun (Figure 4.1).

Unlike the Lütschine, whose hydrological regime has remained almost natural, the Aare is characterized by a complex damming system, operated by the *Kraftwerke Oberhasli AG*. Over 60% of the annual discharge in the Aare is stored in reservoirs and released when electricity demand is high. According to seismic measurements, ~232 kt yr^{-1} of sediments are retained annually in these hydropower reservoirs (Anselmetti et al., 2007), which indicates that the particle load to Lake Brienz has been reduced by 45% since 1932 (Finger et al., 2006). Moreover, the operation of the hydropower reservoirs have decreased turbidity in Lake Brienz in the summer through particle retention, and increased turbidity during winter through hydropower production. Based on these findings, Jaun et al. (2007) concluded that the altered particle dynamics led to a doubling of light attenuation during winter and a reduction of ~50% during summer.

In addition to the aforementioned changes in hydrology and particle input, there have been some recent changes noted in the biology of the system. Specifically, time series of phytoplankton and zooplankton indicate a continuous decline of biological activity in the lake since 1994 (Rellstab et al., 2007). Investigations of whitefish growth rates indicate that the whitefish (*Coregonus fatioi*), feeding mainly on *Daphnia* (Cladocera), were suffering from under-nourishment (Müller et al., 2007b). Moreover, there was a drastic collapse (of over 90%) of the fishing yield in 1999, which coincided with the quasi disappearance of *Daphnia* (primarily *Daphnia hyalina*) (Wüest and Zeh, 2007). These observations suggest that the loss of *Daphnia* was due to reduced algal production through bottom-up control, which may have been caused by: (1) a decrease of particulate and dissolved bio-available phosphorus (bio-P) as a consequence of sewage treatment and trapping of nutrients in the upstream reservoirs (Müller et al., 2007a); or (2) the reduction of *in situ* irradiance due to changes in turbidity dynamics caused by hydropower activities. Whereas the first hypothesis is evaluated in (Müller et al., 2007a), we focus on the latter hypothesis – namely the effect of turbidity on primary production.

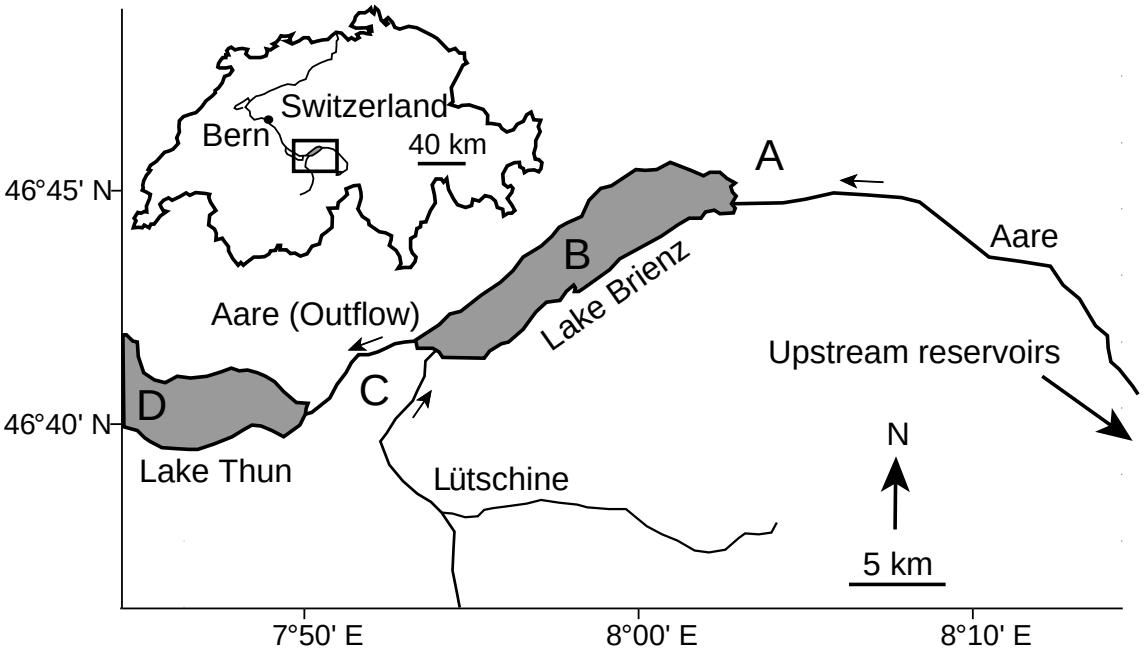

Figure 4.1: Overview of the study area including the sampling sites within and around Lake Brienz. Site A (only surface), B and D depict locations of photosynthetically active radiation (PAR) measurements. Site B marks the lake water sampling position. Site C localizes the continuous global radiation monitoring site operated by MeteoSwiss. Small arrows show river flow directions. Hydropower reservoirs are situated 15 km upstream on Aare (large arrow indicates direction).

Table 4.1: Characteristics of Lake Brienz and Lake Thun

Property	Unit	Lake Brienz	Lake Thun	Reference
Surface area	km^2	29.8	48.4	(Finger et al., 2006)
Volume	km^3	5.17	6.44	(Finger et al., 2006)
Maximum depth	m	259	217	
Average depth	m	173	135	
Altitude of lake level	m asl	564	558	(LHG-BWG, 2005)
Average discharge at outflow in 2004[(1)]	$m^3 s^{-1}$	59.7	108	(LHG-BWG, 2005)
Average residence time	yr	2.7	1.9	
Average water temperature[(2)]	°C	9.5	10.9	
Average euphotic depth[(3)]	m	15.2	21.7	

[(1)] Data publicly available at: http://www.bwg.admin.ch/service/hydrolog/d/

[(2)] Average water temperature in the top 10 m of the lake based on monthly CTD-profiles between 1999 and 2005.

[(3)] Average euphotic depth based on monthly PAR-profiles between 1999 and 2005.

4.3 Material and Methods

A number of different physical and biological parameters (Table 4.2) were measured in order to assess the primary production in Lake Brienz. In this section we review the experimental procedures and techniques used.

Table 4.2: Overview of sampling program

Parameters	Symbol	Location[(1)]	Sampling period	Unit	Frequency of sampling	Performed by/reference
^{14}C Assimilation[(2,3)]	P^B	B	2004/5	mgC m^{-3} h^{-1}	monthly	authors
Chlorophyll a[(2,3)]	$Chla$	B	2004/5	mg m^{-3}	monthly	authors
Chlorophyll a[(4)]	$Chla_{mean}$	B	1999-2005	mg m^{-3}	monthly	GBL
In situ PAR[(3,5)]	$I_{in-situ}$	B	1999-2005	µE m^{-2} s^{-1}	monthly	authors/GBL[(5)]
In situ PAR (Lake Thun)	$I_{in-situ}$	D	1999-2005	µE m^{-2} s^{-1}	monthly	GBL
PAR at surface[(3)]	I_s	A	2004/5	µE m^{-2} s^{-1}	monthly	authors
Global radiation	$I_s^{MeteoSwiss}$	C	1999-2005	W m^{-2}	hourly	MeteoSwiss
CTD[(6)]	T; Tr	B	1999-2005	°C; %	monthly	GBL/authors
CTD (Lake Thun)	T	D	1999-2005	°C	monthly	GBL
Secchi depth[(7)]	s_d	B	1921-1922 1993-2005	m	varying	diverse
Reactive phosphorus	SRP	B	2003-2004	mgP m^{-3}	~monthly	authors

(1) Locations marked in Figure 4.1.

(2) Chlorophyll a and ^{14}C assimilations were determined at the following depths (m): 0, 0.5, 1, 1.5, 2.5, 3.75, 5, 7.5, 10, 12.5, 15, 20, 25, 30, and 35 (note: before 30 March 2004 samples were only collected to a depth of 25 m).

(3) Sampling dates: 18 December 2003; in 2004: 3 March, 30 March, 4 May, 8 June, 6 July, 27 July, 25 August, 21 September, 20 October, 23 November, 15 December; in 2005: 9 March, 5 April, and 3 May.

(4) Chlorophyll a determined by GBL on a monthly basis for integrated water samples (0 to 20 m depth).

(5) *In situ* PAR-profiling has been conducted by GBL on a monthly basis since 1999 and by the authors during each P^B-sampling.

(6) CTD profiling comprises profiles of temperature, conductivity and light transmission (Tr: percentage of light transmitted over a path length of 0.1 m). *CTD* profiling is conducted since 1997 by GBL in the framework of a regional monitoring; additional CTD profiling was conducted during P^B-sampling.

(7) Secchi recordings are conducted by GBL since 1993; historic data from 1921 and 1922 were performed by *Flück* (1926). Since 1993 recordings exist twice a week; before 1993 recording resolution is varying.

4.3.1 Lake in situ primary production measurements

Water was sampled from 0 to 35 m depth in the centre of Lake Brienz (location B; Figure 4.1) on 15 occasions between 18 December 2003 and 3 May 2005. Each sample was subdivided to determine C assimilation rates P^B (mgC m^{-3} h^{-1}) with the ^{14}C technique (Steemann Nielsen, 1952) and chlorophyll *a* concentration *Chla* (mg m^{-3}). Two 120 ml sub-samples were inoculated with 15 µCi $NaH^{14}CO_3$ in Duran bottles (one dark sample and one with transmission properties of 22% absorption at 325 nm and 4% at 350 nm) and incubated in their corresponding depths for 4 hours between 10:00 and 14:00 local time (CET). After incubation all samples were processed by the acidic bubbling method, according to Gächter and Mares (1979). 7 ml of each sample were blended with 10 ml of Instagel™ (Packard, USA). Subsequently, the radioactivity of the sample was measured with a liquid scintillation spectrometer (TRICARB, Packard, USA) at room temperature. P^B was determined by comparing the activity in the scintillation vial before and after acid bubbling and expressed as a %-fraction of added radioactive C assimilated into the algal cells during incubation. The fractional amount of ^{14}C taken up by the algae multiplied by the total dissolved inorganic carbon (DIC) in the incubated water sample corresponds to the instantaneous P^B. DIC was determined from alkalinity and *pH* following Rodhe (1958). All P^B values were corrected for non-photosynthetic C uptake, as determined in the dark sample.

Chla was determined in the second sub-sample according to DEV (1972-1989). After filtering through Whatman GF/F filters, samples were placed into Sovirel tubes filled with 8 ml of 90% ethanol. Chlorophyll was extracted by heating the samples for 10 min in a water bath at 75 ^oC and subsequent sonification (for 5 min) at room temperature. Afterwards the *Chla* extracts were filtered through Millipore Millex FG 0.2 µm membrane filters. The *Chla* content was determined through two independent procedures: (a) spectrophotometrically following DEV (1972-1989) using a U2000 dual path spectrophotometer (Hitachi, Japan) and (b) with high performance liquid chromatography (HPLC). HPLC-analysis was performed according to Meyns et al. (1994) and Murray et al. (1986) by separating *Chla* isocratically at a flux rate of 1.0 ml min^{-1} in a mixture of 49.5% methanol, 45% ethyl acetate and 5.5% water. Throughout this study photometrically determined *Chla* values are presented, while the results of the HPLC analysis were used to verify the photometric results.

Additional water sampling for soluble reactive phosphorus (SRP) was performed from 19 February 2003 to 7 July 2004 at various depths in the center of the lake. Samples were filtered through cellulose acetate membrane filters and SRP was determined photometrically with the ammonium molybdate method (DEV, 1972-1989).

In situ photosynthetically active radiation (PAR denoted as $I_{in-situ}$ (µE m^{-2} s^{-1})) was measured with a scalar quantum sensor (LI 190 SB) connected to an integrating quantum meter (LI 188;LI-COR Inc). A cosine corrected PAR sensor (LI 190) served as a reference, measuring PAR above the water surface (I_s) at location A.

Monthly CTD profiles of conductivity, temperature, pH, light transmission and dissolved oxygen (SBE 19; Seabird USA) and PAR profiles (with a spherical underwater sensor from LI-COR Inc, USA) at locations B (Lake Brienz) and D (Lake Thun) have been taken by the Laboratory for Water and Soil Protection of the Canton of Bern (GBL) since 1999. In addition samples, integrating from 0 to 20 m depth, were collected monthly with a Schröder (1969) bottle, and analyzed for phytoplankton (including *Cyanophyceae* and *Bacillariophyceae*) and $Chla_{mean}$ (mg m^{-2}). Zooplankton was sampled with a 95-µm mesh size net (Rellstab et al., 2007).

4.3.2 Model approach

The specific C assimilation rate P^B per unit $Chla$, i.e. the ratio $P^{chla} = P^B / Chla$ (mgC h^{-1} $(mgChla)^{-1}$), was determined for all samples in order to interpolate P^B in time and space between sampling. All P^{chla} were normalized to a reference temperature (T_{norm} = 10 °C) assuming exponential temperature-dependent growth rates:

$$P_{norm}^{chla} = P^{chla} e^{\left(\ln(Q_{10})\frac{(T_{norm}-T)}{10}\right)} \qquad (4.1)$$

where $Q_{10} = 2$ denotes the typical factor of logarithmic growth rate increase for 10 °C warming, as determined experimentally in natural waters (Eppley and Sloan, 1966; Williams and Murdoch, 1966; Eppley, 1972). Accordingly, P_{norm}^{chla} (mgC h^{-1} $(mgChla)^{-1}$) denotes the C assimilation rate at T_{norm}. The value of Q_{10} in the studies cited above varies between 1.88 and 2.5, but in our case model results are not sensitive to such changes in Q_{10} (see discussion).

This temperature- and *Chla* -normalized C assimilation rate (P_{norm}^{chla}) is primarily a function of ambient light intensity ($I_{in-situ}$). We used the mathematical approach proposed by Platt et al. (1980) to interpolate P_{norm}^{chla} vertically between measured samples:

$$P_{norm}^{chla}(z) = P_S^B \left(1 - e^{-\left(\frac{\alpha \cdot I_{in-situ}}{P_S^B}\right)} \right) \cdot e^{-\left(\frac{\beta \cdot I_{in-situ}}{P_S^B}\right)} \quad (4.2)$$

where P_S^B denotes the hypothetical maximum photosynthetic output without photoinhibition (i.e., the decline of photosynthesis due to strong light fields (Powles, 1984)). The empirical coefficient α denotes the increase of P_{norm}^{chla} with increasing $I_{in-situ}$ and β accounts for the decrease of P_{norm}^{chla} caused by photoinhibition. The three empirical coefficients (P_S^B, α and β) were determined through a least-square fit of equation (4.2) to the measured P_{norm}^{chla} (Figure 4.2a) and cross checked for plausibility for each sampling profile. SRP levels (Figure 4.2b) limit P_S^B and were considered implicitly in the fits. Whereas convective mixing and low productivity leads to slightly higher SRP in winter, stratification and high productivity induces SRP depletion in summer. Accordingly, P_S^B varies between ~5 mgC h^{-1} $(mgChla)^{-1}$ in winter and 1.6 mgC h^{-1} $(mgChla)^{-1}$ in summer (Figure 4.2a). As SRP values above 2 mg m^{-3} are rapidly depleted in summer, elevated SRP values can usually be attributed to recent river intrusions. Therefore, monthly sampling adequately describes seasonal evolution of SRP limitation. The light limitation factor α ranged between 0.04 and 0.25 (mgC m^2 s (h µE $mgChla)^{-1}$), and the photoinhibition factor β varied between 0.002 to 0.03 (same units as α).

In order to interpolate depth-dependent $P_{norm}^{chla}(z)$ between profiles with high temporal resolution throughout the sampling period, ambient light $I_{in-situ}(z,t)$ for the photic layer was used. We defined the *in-situ* relative light $I_{rel}(z)$ (-) by the quotient of $I_{rel}(z) = I_{in-situ}(z) / I_s$. As $I_{rel}(z)$ is governed by suspended and dissolved substances in the water and hence not subject to short-term variation, we obtained time series of $I_{rel}(z,t)$ by linear interpolation between the monthly profiles. Assuming that $I_s(t)$ is linearly proportional to the global radiation of $I_s^{MeteoSwiss}(t)$ (W m^{-2}) recorded at the MeteoSwiss monitoring site C (Figure 4.1), we determined $I_{in-situ}(z,t)$ with one-hour resolution according to:

$$I_{in-situ}(z,t) = I_{rel}(z,t) \cdot I_s(t) = I_{rel}(z,t) \cdot c \cdot I_s^{MeteoSwiss}(t) \quad (4.3)$$

where $c = \frac{\overline{I_s}}{\overline{I_s^{MeteoSwiss}}}$ and $\overline{I_s}$ denotes the average reference PAR (µE m^{-2} s^{-1}) measured with our sensor (at location A). The empirical coefficient $c = 1.54$ µE s^{-1} W^{-1} accounts for the conversion of units and different sunlight exposures of the two sites due to shadowing from the high mountains surrounding Lake Brienz.

The time series of gross primary productivity in Lake Brienz can then be estimated by linearly interpolating the coefficients P_S^B , α and β in equation (4.2). The back transformation of $P_{norm}^{chla}(z,t)$ from T_{norm} to ambient water temperature ($T(z,t)$) is given by:

$$P^{chla}(z,t) = P_{norm}^{chla}(z,t) \cdot e^{\left(\ln(Q_{10})\frac{(T(z,t)-T_{norm})}{10}\right)} \qquad (4.4)$$

By multiplying $P^{chla}(z,t)$ with instant $Chla(z,t)$ - also obtained by linear interpolation - the actual $P^B(z,t)$ can be determined. Using this approach, $P^B(z,t)$ profiles are obtained with hourly resolution. The corresponding areal primary production is obtained by vertically integrating the $P^B(z,t)$ profile.

For periods beyond P^B sampling only temperature, light attenuation and global radiation (data: MeteoSwiss) are known. Extrapolations were made by assuming α, β, P_S^B and $Chla(z,t)$ as determined in 2004. Nevertheless, algal standing crop and bio-P input vary and can significantly affect P^B. In order to evaluate the potential effects of these parameters on the model results and to be able to judge the reliability of the estimated effects of turbidity, the following additional model calculations were performed:

To account for varying algae standing crop, a model run was performed in which we predicted *in situ* $Chla(z,t)$ for 1999 to 2005 by assuming a proportional relation between *in situ* $Chla(z,t)$ and areal $Chla_{mean}$ determined monthly by GBL:

$$Chla(z,t_y) = \frac{Chla_{mean}(t_y)}{Chla_{2004,mean}(t_y)} Chla_{2004}(z,t_y) \qquad (4.5)$$

where t_y denotes the time elapsed in the specific year, and $Chla_{mean}(t_y)$ and $Chla_{2004,mean}(t_y)$ stand for the vertically integrated *Chla* concentrations (values between sampling: linearly interpolated). We justify this approach by the fairly good correlation (R^2 = 0.56) between phytoplankton (wet biomass) and $Chla_{mean}$.

To estimate the effect of the varying bio-P input, we assumed P_S^B linearly proportional to bio-P input of the specified year:

$$P_{S,norm}^B = \frac{P_{year}}{P_{2004}} P_S^B \qquad (4.6)$$

where P_{2004} = 7.8 t yr^{-1} denotes the bio-P input during 2004 according to (Müller et al., 2007a)

and P_{year} stands for the annual bio-P input as estimated by Finger et al. (2007b). We justify the simple approach of equation (4.6) by the strong bio-P limitation.

Finally, the simulated results were compared to those from a biogeochemical model, presented in detail by Finger et al. (2007b), which considers phosphorus cycling, phytoplankton, zooplankton, physical mixing processes, nutrient loadings, water discharge and turbidity.

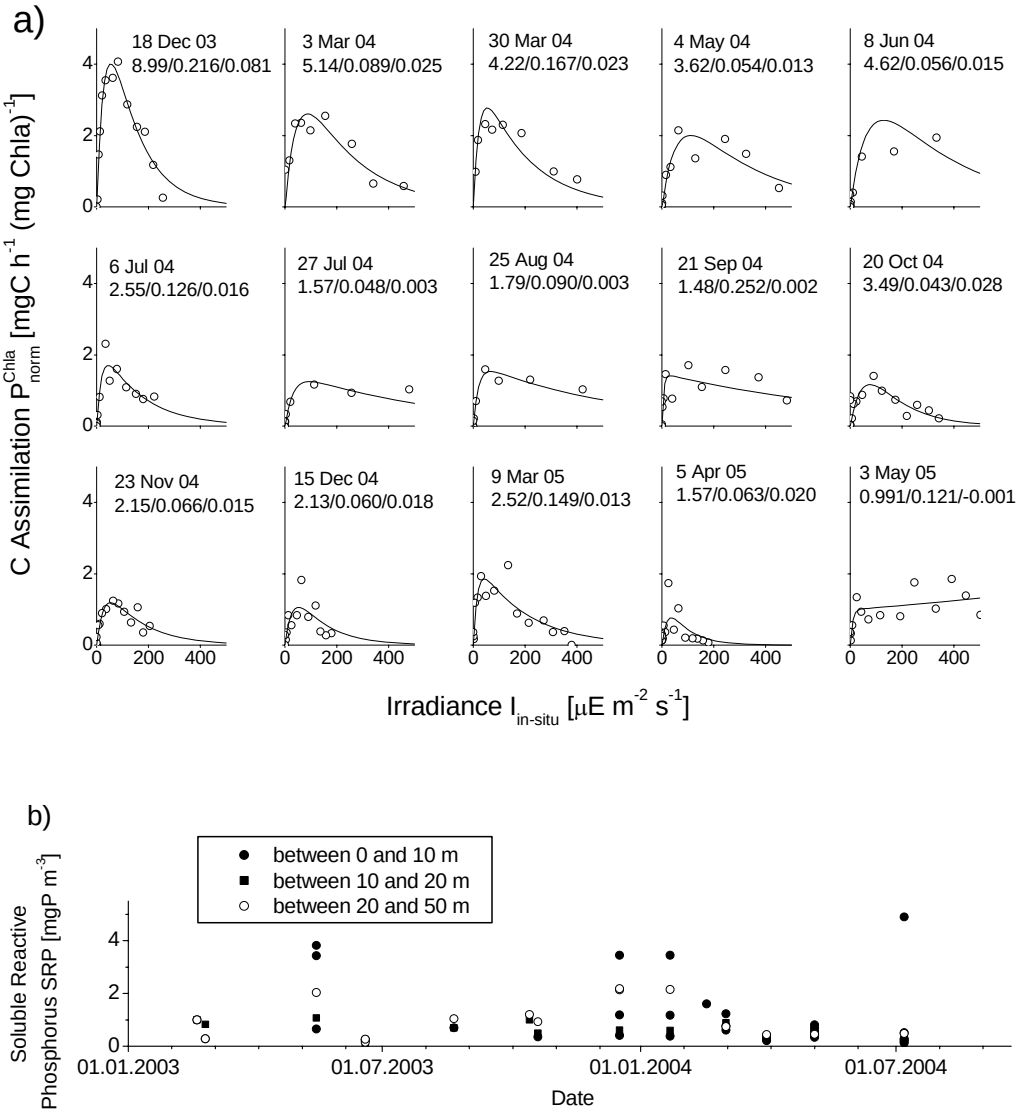

Figure 4.2: a) Fits of equation (4.2) to monthly measured *in situ* carbon assimilation profiles between 18 December 2003 and 3 May 2005. Numbers on graphs indicate date of sampling and the three fit values ($P_S^B / \alpha / \beta$). b) SRP concentrations from three depth ranges between 19 February 2003 and 7 July 2004.

4.3.3 Estimation of production in clear water

The drastic collapse of fishing yield after the flood of 1999 was limited to Lake Brienz, whereas the fishery in downstream lakes (affected also by flooding but not turbidity; e.g. Lake Thun, Lake Biel) was unaffected. Hence, we compared the modeled primary productions in Lake Brienz with those of turbidity-free Lake Thun. We used equations (4.1) to (4.4) for Lake Brienz as well as temperature and *in situ* light data from Lake Thun (location D; Figure 4.1) to calculate the hypothetical P^B rates from 1999 to 2005 in turbidity-free water. As these simulations rely on the algorithm calibrated for Lake Brienz, the results provide a relative - not an absolute - comparison for the effects of turbidity.

4.3.4 Estimation of production under pre-dam conditions

To assess the effects of hydropower damming, we estimated the primary production for the hypothetical situation with light conditions as in the 1920s (pre-dam) but nutrient conditions similar to today (Müller et al., 2007a). We used recorded Secchi depths (s_d) from Flück (1926) to reconstruct 'no-dam' light conditions. Light attenuation coefficients (K_0) and s_d can be correlated according to Jaun et al. (2007):

$$K_0 = \frac{\ln\left(I_{z_0} / I_{z_{eu}}\right)}{z_{eu} - z_0} = k_1 + \frac{k_2}{s_d} \qquad (4.7)$$

where z_0 and z_{eu} correspond to the surface level (water-side) and euphotic depths, respectively. The right side of equation (4.7) describes the empirical relation between measured K_0 and s_d. Jaun et al. (2007) determined $k_1 = 0.22$ m^{-1} and $k_2 = 0.69$ for intense turbidity periods (May to September) and $k_1 = 0.11$ m^{-1} and $k_2 = 0.61$ for reduced turbidity periods (October to April). For a given K_0, the corresponding light profile in the lake for the instant global radiation is given by:

$$I_{in-situ}(z) = I_s e^{-K_0 z} \qquad (4.8)$$

In order to estimate $P^B(z,t)$ for light conditions in 1921 and 1922, we used the light attenuation determined from equations (4.7) and (4.8) and the fits of equation (4.2) during 2004. Given K_0, the euphotic depth z_{eu} (= $\ln(100)/K_0$) is calculated as the depth where *in situ* light reaches 1% of surface light (Kirk, 1994). As the Secchi recordings in 1921 and 1922 may not represent typical pre-dam conditions, a model calculation for an average 'no-dam'

scenario was also undertaken. For this purpose, simulated suspended particle concentrations for a hypothetical 'no-dam' situation (i.e., without any hydropower operation affecting the hydrological input to Lake Brienz) were adopted from Finger et al. (2006). K_0 for this 'no-dam' scenario was determined according to the following regression:

$$K_0 = k_3 + k_4 \cdot PC \qquad (4.9)$$

with k_3 = 0.06 m^{-1} and k_4 = 0.26 $m^2\ g^{-1}$ during periods of intense surface turbidity, k_3 = 0.08 m^{-1} and k_4 = 0.08 $m^2\ g^{-1}$ during periods of reduced surface turbidity and PC (g m^{-3}) denoting suspended particle concentration in the upper 50 m of the water column in Lake Brienz (Jaun et al., 2007). Hence, primary production under typical 'no-dam' light conditions was estimated using predicted K_0 (equation (4.9)) and the fits of equation (4.2) during 2004.

4.4 Results and observations

4.4.1 Boundary conditions for primary production during sampling period

The dynamics of the five parameters that affect primary production in Lake Brienz (SRP, T, $I_s^{MeteoSwiss}(t)$, $I_{rel}(z)$ and $Chla$) are evaluated below. The SRP concentration was very low both in the lake (usually below 1 mg m^{-3}) and in the Aare and Lütschine tributaries (Müller et al., 2007a). SRP was depleted by algae growth as soon as it entered the lake in summer, whereas in winter SRP reached slightly higher levels due to deep convective mixing (Figure 4.2b). This seasonal pattern has to be considered with caution, as SRP levels (i) vary with discharge and (ii) are close to the detection limit.

The time-averaged temperature in both inflows of Lake Brienz lies at ~5.9 °C due to glaciers (~20% of the catchment) (Finger et al., 2006). Thus the surface temperature in Lake Brienz rarely exceeded 20 °C (Figure 4.3a). Although global radiation during winter was somewhat limited by the high mountains to the south of the lake, the mean sunshine duration of 1929 h yr^{-1} (1997 to 2004; location C) was slightly above the typical Swiss average (1600 to 1900 h yr^{-1}). The rather harsh winters led to convective mixing, which frequently reached the maximum depth of the lake.

The allochthonous inorganic particle input of over 300 kt yr^{-1} (Finger et al., 2006) led to a mean light attenuation of ~0.5 to ~0.6 m^{-1} during the summer (Jaun et al., 2007). Consequently, *in situ* relative light (I_{rel}) was governed primarily by suspended particle concentrations, as illustrated in Figure 4.3b. Thus, the euphotic depth reached 27 m in early

spring, whereas during summer, when particle concentrations were highest, the euphotic depth dropped to less than 7 m. Secchi depths were over 7 m deep during winter and less than 2 m during summer.

The *in situ* light conditions appeared to govern the distribution of *Chla*, phytoplankton and zooplankton (Figure 4.4a). During winter, plankton and *Chla* were at a seasonal minimum, mainly due to short daytime (~5 h) and deep convective mixing. In spring when light penetration was elevated, increased *Chla* of ~1.5 mg m^{-3} was observed between 0 and 20 m depth. On 8 June 2004 a maximum of 4.8 mg m^{-3} was reached at 12.5 m depth (confirmed by HPLC). Since measured P^B was enhanced as well, the sample did not create artefacts in the model calculations. This high value of *Chla* may be explained by short-term dynamics in plankton biomass (algae spring bloom and subsequent grazing by zooplankton), which cannot be resolved in profiles at monthly intervals (Finger et al., 2007b). During the turbid summer *Chla* reached values above 2 mg m^{-3} at ~3 m depth, whereas below 10 m depth *Chla* did not exceed 0.25 mg m^{-3}. Zooplankton concentrations reached their maximum in June, just after the spring algal bloom.

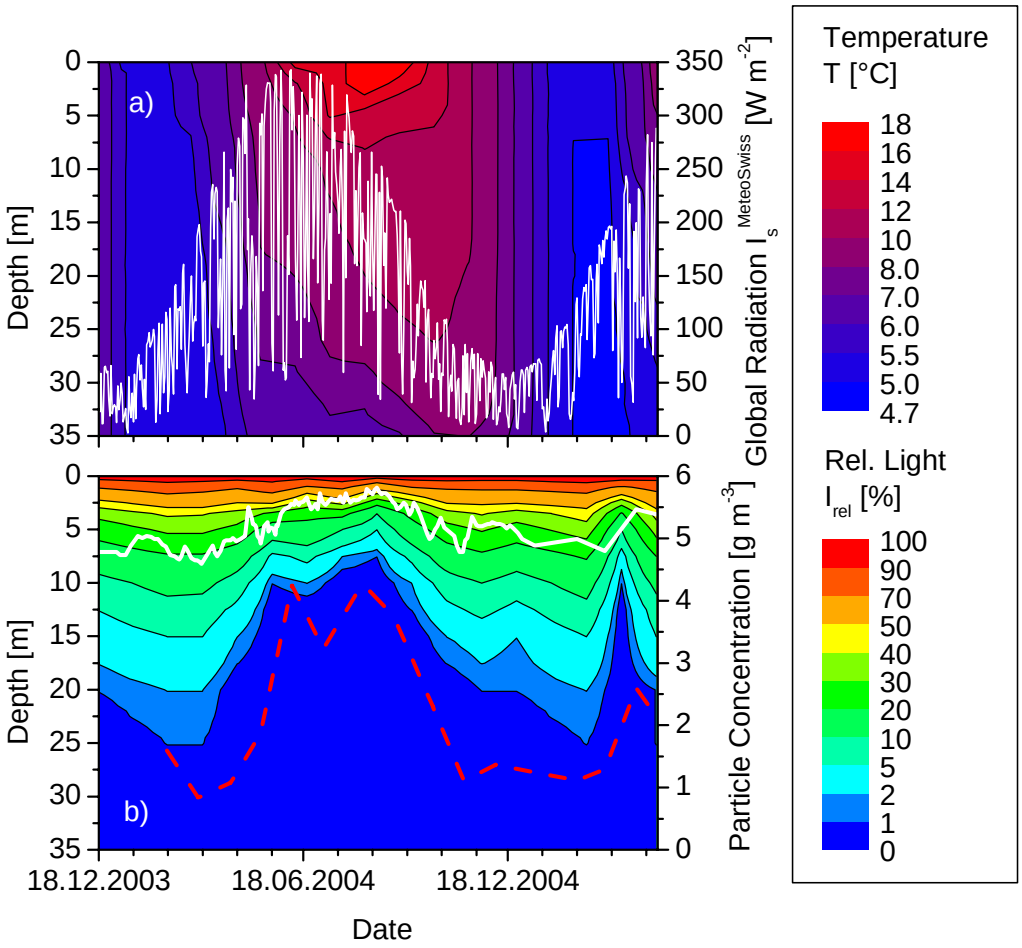

Figure 4.3: Physical conditions from 18 December 2003 to 3 May 2005 in Lake Brienz: a) *In situ* water temperature (contour plot) and mean daily global radiation (solid line; right scale). b) *In situ* PAR relative to surface PAR ($I_{rel} = I_{in\text{-}situ} / I_s$; contour plot). The solid white line represents Secchi depth recordings (left scale) and the red dashed line illustrates average particle concentration (right scale) in the uppermost 50 m, determined with monthly light transmission profiles according to Finger et al. (2006).

4.4.2 Primary production during the sampling period

The seasonal evolution of productivity can be described in four phases:

(1) Winter (December – March): in the winter phase deep convective mixing occurred (Finger et al., 2006) and daylight was reduced (~5 h d^{-1}). Consequently algae were continuously mixed beneath the euphotic depth, limiting algae biomass in the top 20 m to 3 g m^{-2} (Figure 4.4a). Although euphotic depth reached up to 27 m productivity remained at a minimum, with an average *in situ* areal primary production of 78 mgC m^{-2} d^{-1} (Figure 4.4b).

Even at the surface, primary production was usually below 10 mgC m^{-3} d^{-1} , but nevertheless, the productive zone reached below 25 m, where P^B was still significant.

(2) Spring (usually April and May; but varying for specific years): the spring phase started as soon as thermal stratification built up and lasted until the first major turbidity input limited productivity. As warmer water and available nutrients improved conditions for algal growth, stratification allowed a build-up of phytoplankton in the top 20 m. Consequently, relatively intense P^B of up to 20 mgC m^{-3} d^{-1} were observed at depths between the surface and ~17 m, but P^B was negligible below 28 m. The areal primary production reached its yearly maximum of up to 400 mgC m^{-2} d^{-1} just before the summer phase (Figure 4.4b).

(3) Summer (June – August): Allochthonous particle input from the two major inflows resulted in a turbid layer across the entire lake, causing enhanced light attenuation. The euphotic depth was reduced to a seasonal minimum of ~8 m, limiting primary production to the uppermost layer. In the euphotic zone, P^B reached a maximum of up to 60 mgC m^{-3} d^{-1} at about 2 m depth, as photoinhibition hampered P^B closer to the surface. Despite long daylight hours (~11 h d^{-1}) and maximal phytoplankton densities, the areal primary production was less than 260 mgC m^{-2} d^{-1} (less than in spring).

(4) Autumn (September – December): During fall, allochthonous particle input dropped and, therefore, the lake cleared up. The euphotic depth increased and P^B exceeded the detection limit down to a depth of 20 m. Short daytime hours and convective mixing reduced P^B to less than 10 mgC m^{-3} d^{-1} in the entire euphotic zone, and consequently areal primary production dropped below 100 mgC m^{-2} d^{-1} (Figure 4.4b).

The temporal integral over 2004 resulted in an annual gross primary production of 70 gC m^{-2} yr^{-1}. This value reflects the ultra-oligothropic state of Lake Brienz, as it lies way below the mean primary production of all the other oligotrophic peri-alpine lakes, such as Lake Lucerne (~160 gC m^{-2} yr^{-1}) or Walensee (180 gC m^{-2} yr^{-1}) (Gammeter et al., 1996).

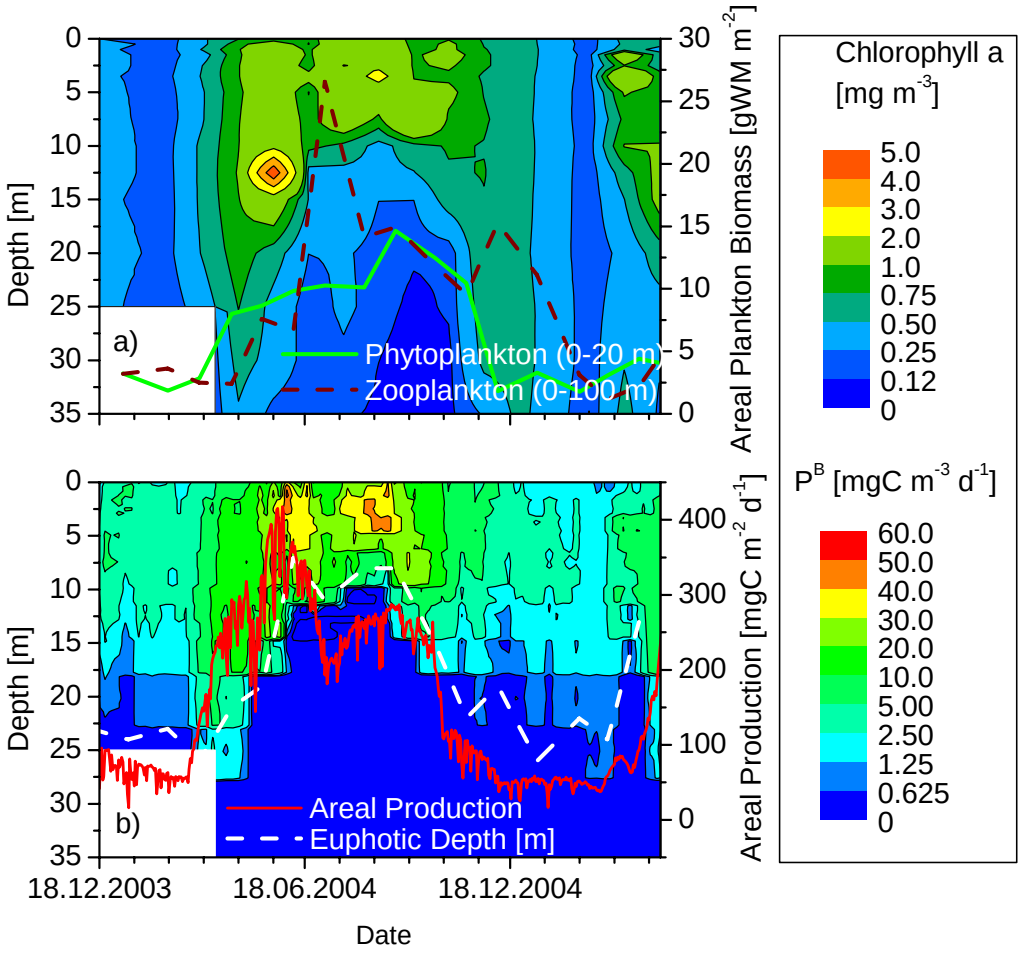

Figure 4.4: Primary production indicators in Lake Brienz from 18 December 2003 to 3 May 2005: a) measured *in situ* chlorophyll a is shown as contour plot, based on monthly profiles. The solid green line illustrates phytoplankton (wet mass) in the top 20 m and the dashed brown line denotes zooplankton (wet mass) in the top 100 m (data: net hauls by GBL). b) Calculated daily primary production (contour plot) based on 18 monthly C assimilation profiles. The solid red line illustrates the areal primary production (right scale) and the dashed white line indicates the euphotic depth (left scale; definition in text).

4.4.3 Physical boundary conditions during recent years

The average global radiation measured at location C (Figure 4.1) was 132 W m^{-2} (Figure 4.5a). In March and April 2001 global radiation was about 18% below average, and during the heat wave in August 2003 (Schär et al., 2004) it was about 20% above average. Although the extremely hot weather caused maximum temperatures in most Swiss lakes (LHG-BWG, 2005), significantly warmer water was recorded in Lake Brienz only in July 2003 (Figure 4.5b). Two factors explain this anomaly: (1) the warm air temperatures led to intense glacial

melting and subsequent cold inflows and (2) intense turbidity - due to the high load of glacial particles - reduced the light penetration and therefore limited warming at greater depths. This interesting mechanism protects the lake from extreme temperatures but also limits temperature-dependent primary production.

There were three periods when exceptional particle concentrations affected the light availability (Figure 4.5c): (1) the flood in spring 1999 led to high particle concentrations uncommonly early in the season, which reduced light availability; (2) in 2003 exceptionally high particle concentrations were observed between July and September due to severe glacier melting as a result of the heat wave (Finger et al., 2006); and (3) after the extreme flood of 22 August 2005 (Beniston, 2006) record particle concentrations were observed.

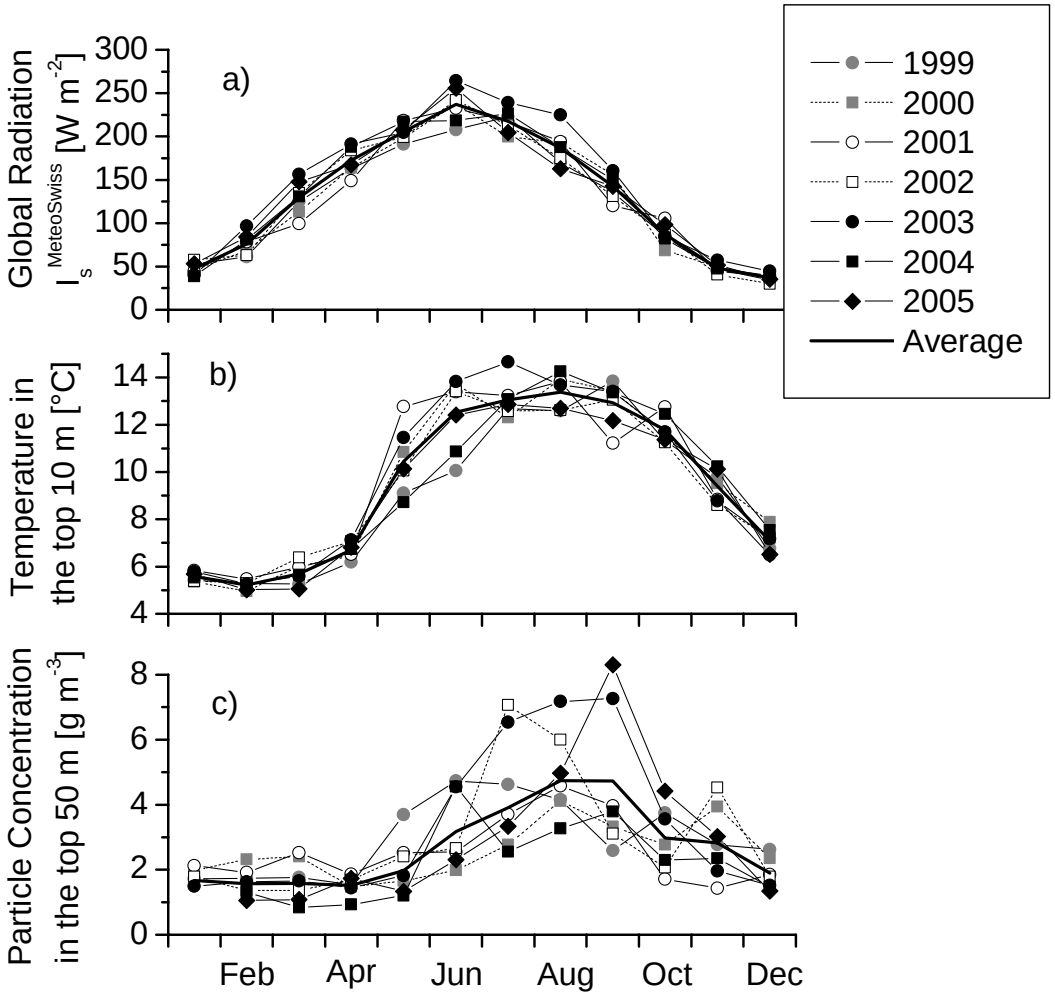

Figure 4.5: Physical conditions in Lake Brienz from 1999 to 2005: a) Monthly-averaged global radiation at Interlaken (location C; Figure 4.1); b) Monthly average water temperature in top 10 m; c) Average particle concentration in the top 50 m. Modified from Finger et al. (2006).

4.4.4 Estimated primary production during recent years

As only temperature and light availability are considered in the model approach, differences among predictions for specific years may be directly attributed to the physical boundary conditions presented in Figure 4.5. The average annual gross primary production from 1999 to 2005 was estimated at ~66 gC m^{-2} yr^{-1} (Figure 4.6a). Elevated particle concentrations during May and June 1999 led to ~10% lower primary production (60 gC m^{-2} yr^{-1}). Conversely, below average particle concentration and above average water temperatures led to ~9% higher primary production (72 gC m^{-2} yr^{-1}) in 2000. High particle concentrations and reduced light availability during the heat wave in 2003 led to ~3% below average primary production (64 gC m^{-2} yr^{-1}).

The effects of the physical boundary conditions (Figure 4.5) were even more pronounced when monthly averages were considered (Figure 4.7). Excellent conditions in June 2000 with high radiation and low turbidity led to ~37% above average primary production. Low radiation and high turbidity led to ~22% below average primary production in May and June 1999. This minimum is important evidence for the collapse of the *Daphnia* population in 1999 (Rellstab et al., 2007). Finally, ~28% below average primary production was predicted just after the 'flood of the century' in August 2005 (Beniston, 2006).

The simulated time series of primary production was compared to the results of the biogeochemical model by Finger et al. (2007b) and the test runs with year specific $Chla(z,t_y)$ and bio-P input (Figure 4.6a). Although the biogeochemical model has been calibrated with the primary production measured in 2004, it is an independent approach which considers bio-P input, temperature, light attenuation, vertical mixing, phyto- and zooplankton. The inter-annual primary production deviated by less than 7% for specific years and showed an underestimation of only 4% for 2004.

The model test run with year specific $Chla(z,t_y)$ (equation 4.5) resulted in 16% higher average primary production, because the observed *Chla* concentrations were relatively low in the reference year 2004 (Figure 4.6b). Gross primary production in 2002 was predicted to be ~49% higher, primarily because of the up to ~60% above average $Chla_{mean}$ in May and June. However, there was no complementary evidence for increased production during this period, such as uncommon phyto- and zooplankton densities (Finger et al., 2007b; Müller et al., 2007b; Rellstab et al., 2007), low turbidity, high bio-P input or high global radiation (Figures 4.5 and 4.6c). Thus, the higher value of $Chla_{mean}$ for 2002 may simply represent the natural

variability within Lake Brienz. Furthermore, the *Chla* scaling degraded the agreement with the biogeochemical model, indicating that light and nutrient limitation were more important driving variables for primary production than algal standing crop.

A test run with P_S^B scaled to annual bio-P input (equation 4.6) revealed 7% higher average primary production (Figure 4.6a). This discrepancy can be attributed to the floods (e.g. 1999 and 2005), since bio-P input (P_{year}) was assumed proportional to water discharge (Finger et al., 2007b). Disregarding the flood year and 2002 (unexplainable high $Chla_{mean}$) differences remain below 5%.

Our primary goal was to assess the effects of light and turbidity on productivity. For this reason we relied on the simulations which do not consider $Chla_{mean}$ or P_{year}. The additional test runs were performed in order to estimate the potential effects of these variables on productivity. Based on the results of the test runs we estimate the error of average annual primary production to less than 16% (Figure 4.6a).

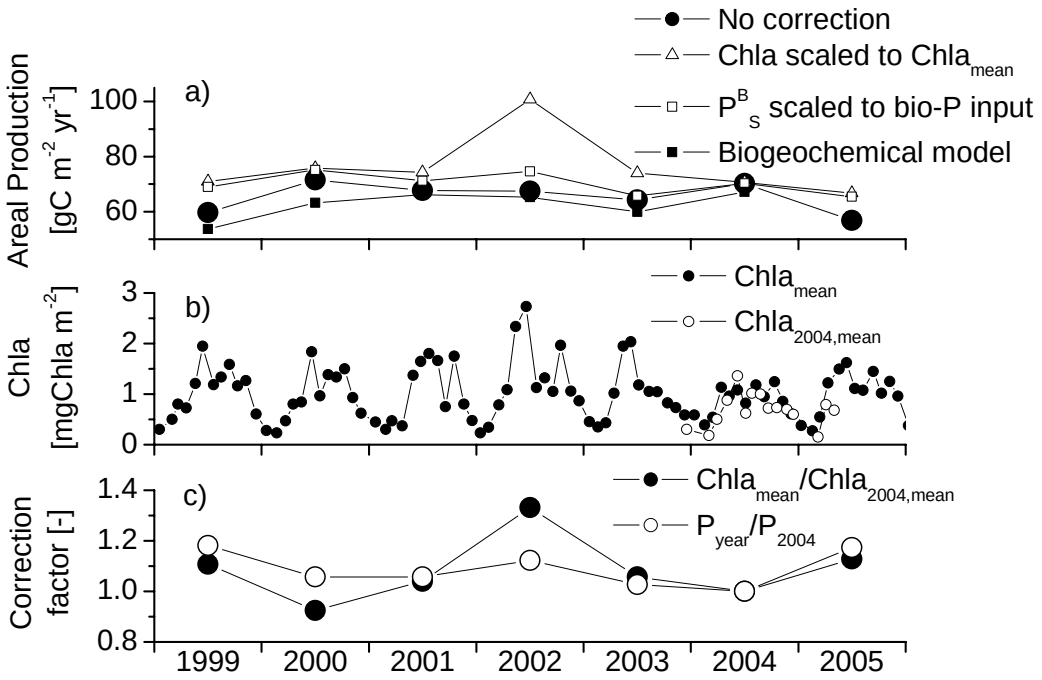

Figure 4.6: a) Predicted annual gross primary production from 1999 to 2005 compared to two test runs (see text) and a biogeochemical model described in Finger et al. (2007b); b) areal chlorophyll a concentration (GSA data) and mean concentrations during our sampling; c) mean correction-factors $Chla_{mean}/Chla_{2004,mean}$ (equation 4.5) and P_{year}/P_{2004} (equation 4.6).

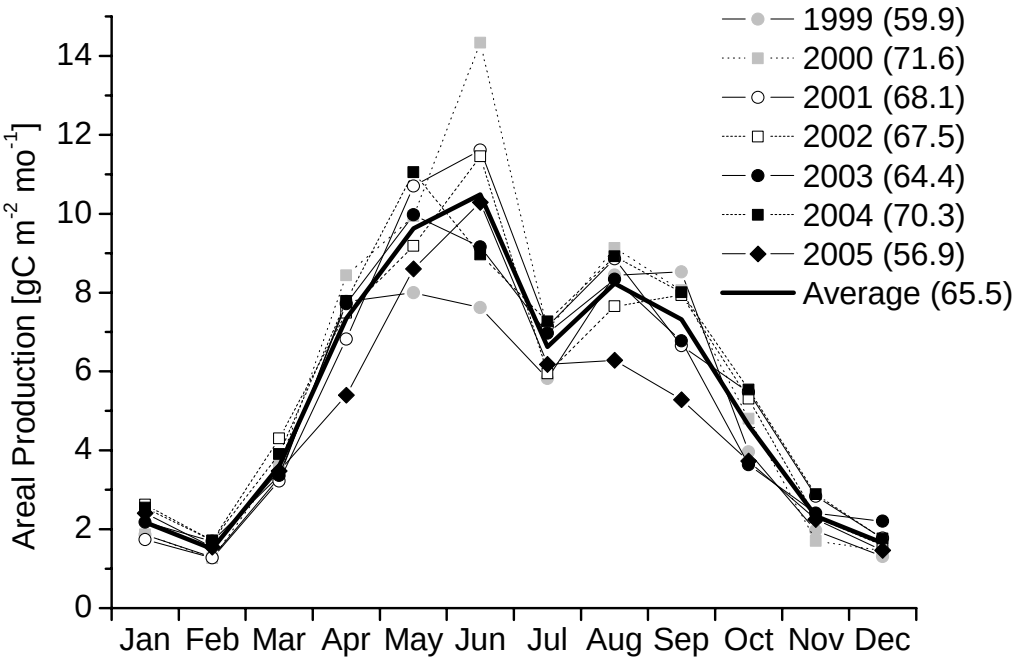

Figure 4.7: Predicted monthly gross primary production from 1999 to 2005 based on global radiation, PAR-profiles, water temperature, chlorophyll a and the monthly fits in 2004 (Figure 4.2). Values in parentheses denote annual gross primary production (gC m^{-2} yr^{-1}) integrated for the year specified.

4.4.5 Effects of turbidity on primary production

About 97% of the suspended particles entering Lake Brienz settle, and only 9 kt yr^{-1} are transported downstream to Lake Thun (Finger et al., 2006). Nevertheless, Lake Thun has a similar trophic status as Lake Brienz (SRP < 1 mg m^{-3} in spring). In recent years, the fishing yield in Lake Thun has been about twice as high as in Lake Brienz, indicating that turbidity might limit algal production and cause the difference in biomass output. To assess this hypothesis, we performed simulations of P^B for the light and temperature conditions of Lake Thun. *In situ* light availability was significantly higher (Figure 4.8a); the euphotic depth reached ~34 m in winter (~24 m in Lake Brienz) and dropped to ~15 m in summer (~7 m in Lake Brienz). The lower turbidity and warmer inflows (> 60% stems from Lake Brienz with average temperature of ~10 °C) during summer led to almost 3 °C higher water temperatures (Figure 4.8b). Both higher euphotic depth and water temperatures enhance primary production.

Estimated areal primary production under the hypothetical turbidity-free conditions of Lake Thun would be ~44% higher (~95.3 gC m^{-2} yr^{-1}; Figure 4.9) than in Lake Brienz. This increase is in line with a recent investigation of effects of glacial sediments on primary production in arctic lakes (Whalen et al., 2006), which indicated that primary production would be about two thirds higher without glacial sediments, especially during times of high turbidity (June – August). The minimum primary production in winter (January - May) would remain ~25% above the rates of Lake Brienz. The highest primary production (~23 gC m^{-2} mo^{-1}) for Lake Thun conditions would have been reached in June 2003 and June 2005, and minimal primary production (~11% below average; ~85 gC m^{-2} yr^{-1}) would have occurred during the flood of 1999.

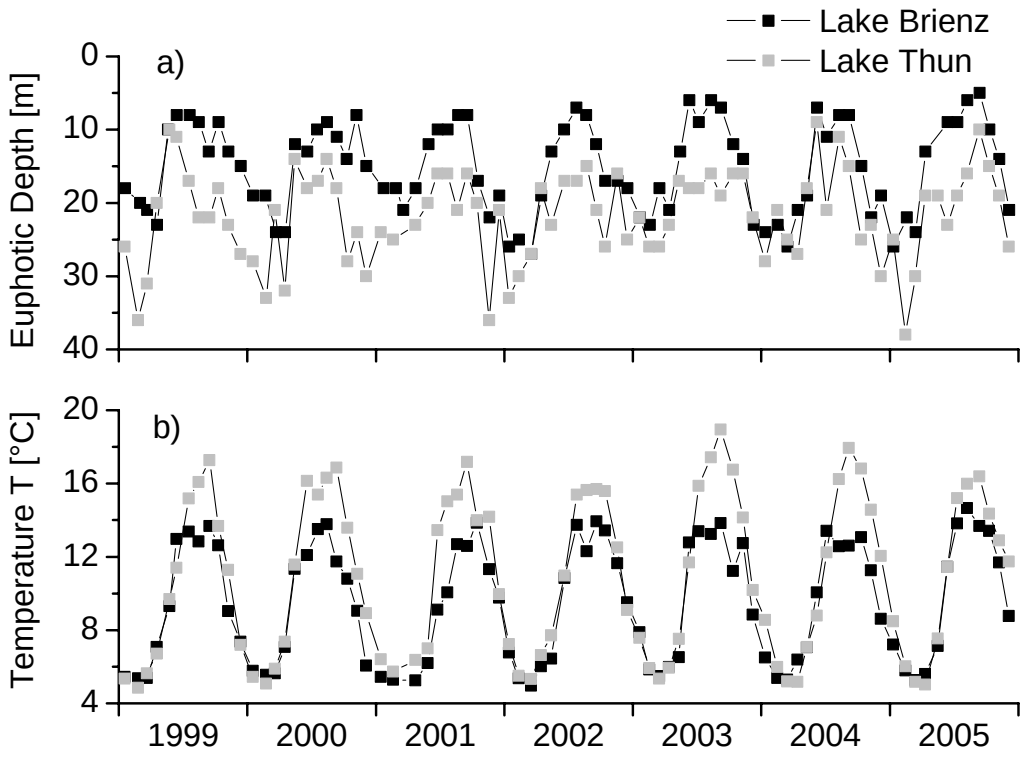

Figure 4.8: Euphotic depth (a) and average (top 10 m) water temperatures (b) in Lakes Brienz and Thun.

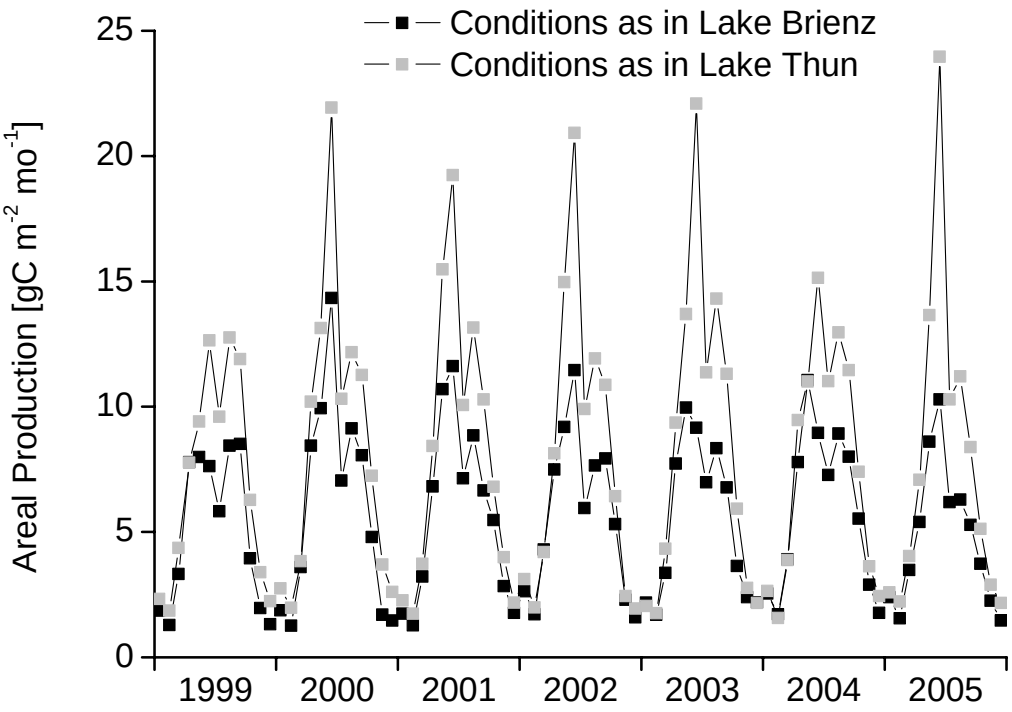

Figure 4.9: Predicted primary production under light and temperature conditions as in Lakes Brienz and Thun using the model based on the *in situ* primary production measurements in Lake Brienz.

4.4.6 Effects of hydropower operations on primary production

Hydropower production decreased particle concentrations in the surface layer of Lake Brienz by almost ~50% during summer but increased them by ~100% during winter and spring (Finger et al., 2006). These findings are supported by time series of Secchi depths from 1921 and 1922 (Figure 4.10), before the construction of the dams (Flück, 1926; Jaun et al., 2007). Using the correlations between Secchi readings (s_d), particle concentrations (PC) and light attenuation (Jaun et al., 2007), we reconstructed the pre-dam light regime and estimated the corresponding primary production using T, *Chla* and $I_s^{MeteoSwiss}$ for the year 2004.

We compared primary production between 1999 and 2005 with primary production for 1921 and 1922 and the hypothetical 'no-dam' conditions (Figure 4.11), assuming that bio-P input was similar (Müller et al., 2007a). The annual primary production under 'no-dam' conditions averaged ~12% (58 gC m^{-2} yr^{-1}) below present conditions. Pronounced differences were noted from June to August, where pre-dam primary production estimates were ~35% lower (~5.4 gC m^{-2} mo^{-1}; more particles) than today (~8.4 gC m^{-2} mo^{-1}; less particles). In

contrast, lower light attenuation without dams increased primary production to ~4.5 gC m^{-2} mo^{-1} from January to May, which is about ~23% higher compared to present (~3.6 gC m^{-2} mo^{-1}). In comparison to the increase of primary production during summer the decrease during winter was 1.5 times weaker.

The most significant changes were observed in spring, when snowmelt and precipitation events led to the first turbidity intrusions in the lake. As is the case today, the Secchi readings of 1921 and 1922 showed high inter-annual fluctuations (Figure 4.10). The estimated primary production in May 1921 was ~50% higher than average primary production in May today, whereas the estimated primary production in May 1922 remained ~28% below the contemporary level. It is likely that previous to damming fluctuations in turbidity were stronger than today, as the reservoir retention smoothes heavy rain runoff.

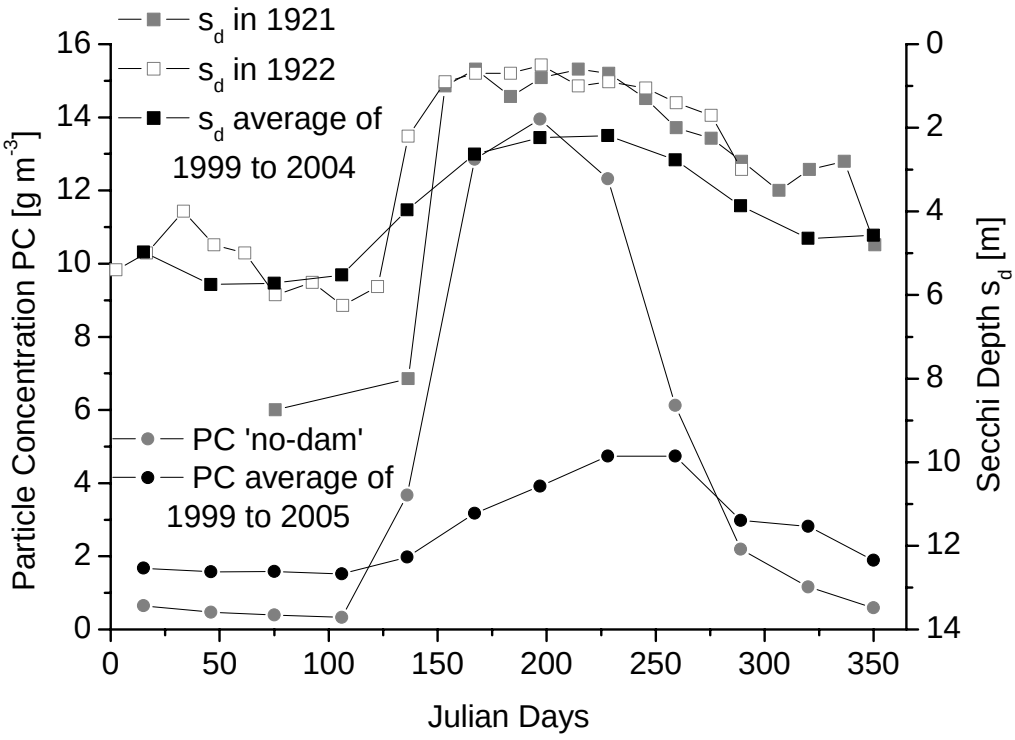

Figure 4.10: Secchi depth recordings (squares) for 1921 and 1922, as well as the average for the period 1999 to 2004 (right scale). Modeled average particle concentrations (circles) for today (1999 to 2005) and for 'no-dam' conditions (left scale) modified from Finger et al. (2006).

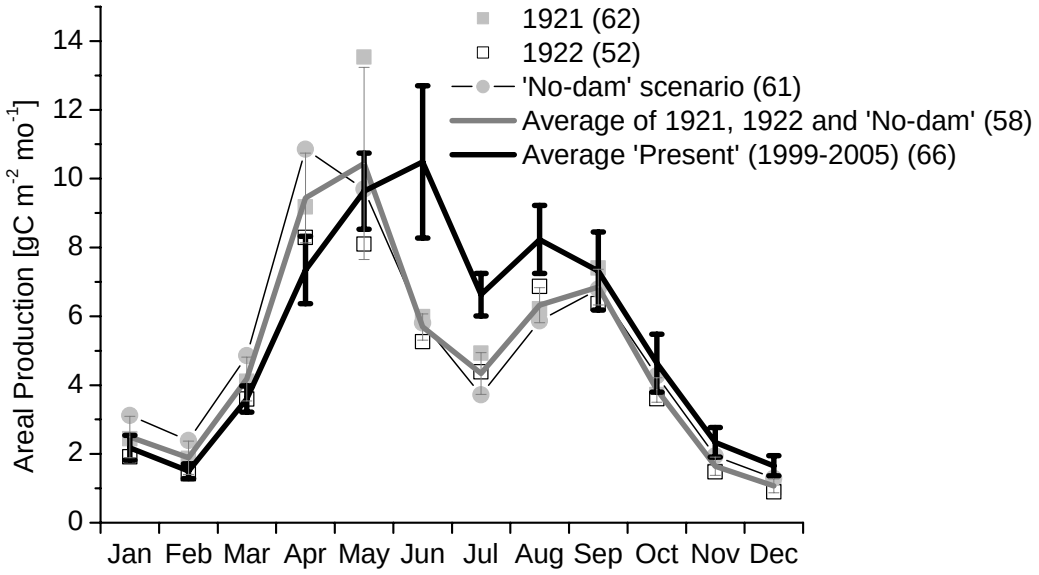

Figure 4.11: Predicted monthly gross primary production rates under present (1999 to 2005) and 'no-dam' light conditions (1921 and 1922 is based on Secchi recordings before the construction of the dams). Error bars on the averages for present and 'no-dam' primary production indicate the standard deviations. Values in parentheses denote annual gross primary production (gC m^{-2} yr^{-1}).

4.5 Discussion

Primary production depends on numerous biotic and abiotic factors, leading to uncertainties in model simulations. Temperature has little effect (equation 4.1) on model results because temperature-independent simulations (Q_{10} = 1) deviate less than 5%. This falls in line with a recent study by Staehr and Sand-Jensen (2006) and reveals the low sensitivity of model results to Q_{10}. The low SRP levels suggest a strong dependence of primary production on varying bio-P input and algae standing crop. During ordinary years, without flood events (e.g. 1999, 2005) or unexplainable algae bloom (e.g. 2002), results of an additional simulation with year specific algal standing crop or P_S^B scaled by bio-P input indicate that the effects of bio-P input or standing crop is less than 15%. However, in regard to the impacts of hydropower dams, the effects of light and turbidity on primary production are most relevant and we therefore rely on the simulation which does not consider bio-P input or algal standing crop.

The simulated gross primary production in Lake Brienz amounted up to ~70 gC m^{-2} yr^{-1} in 2004, whereas primary production for 1999 to 2005 averaged at ~66 gC m^{-2} yr^{-1}. Müller et

al. (2007a) estimated the net organic carbon mineralization rate at the deepest point of the lake at ~15.7 gC m^{-2} yr^{-1}. This implies that organic carbon is recycled about four times per year, which lies within the range of typical values determined for oligotrophic lakes (Wetzel, 2001). The low gross primary production (about half of other peri-alpine lakes) is a consequence of low bio-P input, limiting the intensity of primary production, and high turbidity, restricting primary production to the top layer of the lake.

Model simulations with light and temperature data from Lake Thun indicate ~44% higher primary production if Lake Brienz was not affected by allochthonous particle input. Although primary production would still be very low, fishing yield and plankton time series of Lake Thun indicate that such a primary production rate could compensate for harsh conditions, such as the flood of 1999.

Increased turbidity during May and June 1999 decreased the simulated annual primary production in 1999 by ~10%. High temperatures during the heat wave in summer 2003 stimulated primary production but also led to enhanced glacier melting and subsequently to an increase in particle input and light attenuation. Thus, these two opposing effects led to a ~3% below average primary production in 2003. While these estimations seem realistic, primary production in 2005 was probably underestimated, as bio-P input must have been over 20% above the 2004 level (Figure 4.6b).

The reduced primary production in spring 1999, low water temperatures and high discharge provide a plausible explanation for the collapse of the *Daphnia* population (and subsequently fishing yield) in 1999. Rellstab et al. (2007) determined the mean intrinsic rate of growth of the *Daphnia* population in Lake Brienz to vary around 0.04 d^{-1} in spring. Model calculations by Rellstab et al. (2007) indicate that reduced growth and increased flushing (due to higher throughflow) could lead to orders of magnitude lower *Daphnia* concentrations at the end of June. Nevertheless, no significant declines were observed in zoo- (i.e. *Daphnia*) and phytoplankton populations during the flood in August 2005. Test runs with P_S^B scaled to bio-P input indicate that the negative impacts of the flood 2005 were partially reversed by enhanced bio-P input. Furthermore, the *Daphnia* population in Lake Brienz is especially sensitive to reduced primary production at the beginning of summer when regeneration is necessary after the extremely low population density during the winter.

Although severe meteorological conditions may have led to the *Daphnia* collapse in 1999, the long-term decline in phyto- and zooplankton were not caused by short-term meteorological events. As the annual bio-P input today is comparable to the bio-P input prior to damming (Müller et al., 2007a), the changes in turbidity (Figure 4.10) present the most

significant effect of hydropower production. The model runs for 1921, 1922 and the modeled 'no-dam' scenario illustrate the effects of hydropower operation (Figure 4.11). The annual primary production without hydropower dams is estimated to be ~12% lower than today. Primary production in summer under pre-dam conditions is predicted to be ~35% lower than today. Yet, average primary production under 'no-dam' conditions between January and May is estimated ~23% (~5.7 gC m^{-2} mo^{-1}) above present primary production (~4.9 gC m^{-2} mo^{-1}), at the time when regeneration of zooplankton is important. However, standard deviations of primary production rates in spring today and under 'no-dam' conditions overlap, making it difficult to determine consistent trends. Moreover, May and June 1922 can be identified as a high water event (discharge rates were 32% above the average of 1910 to 1929), presumably with a particle load substantially above average. Consequently, Secchi readings from spring 1921 may be more representative for a typical pre-dam situation than those from 1922, suggesting that average 'no-dam' primary production in spring is rather underestimated. Thus, hydropower operations led to a temporal displacement of maximal areal primary production (Figure 4.11) from May (during pre-dam conditions) to June (today). This time shift might be critical for the spring regeneration of zooplankton.

4.6 Conclusions

The effects of hydropower operations on primary production in downstream lakes were quantified by modelling primary production under the present light regime (1999 to 2005) and under 'no-dam' conditions. Furthermore, the model was used to estimate primary production in a hypothetical turbidity-free scenario, using temperature and light data from neighbouring downstream Lake Thun. From the *in situ* measurements and the numerical simulations the following conclusions can be drawn:

(1) Average annual gross primary production for 1999 to 2005 in Lake Brienz amounted to 66 ± 11 gC m^{-2} yr^{-1} (error was estimated with additional test runs). The low primary production can be explained by the exceptionally low SRP level (< 1 mg m^{-3}) and strong light attenuation caused by allochthonous particles especially during summer. The maximum areal primary production of up to 400 mgC m^{-2} d^{-1} is reached between May and June, when SRP is slightly higher and light availability is favorable. During summer, primary production is high (up to 60 mgC m^{-3} d^{-1}), but limited to the top 10 m of the water column by high turbidity. Consequently, areal primary production in summer (~270 mgC m^{-2} d^{-1}) is substantially lower than during spring (~400 mgC m^{-2} d^{-1}) but much higher than in winter (~50 mgC m^{-2} d^{-1}).

(2) Upstream hydropower reservoirs have halved light attenuation during summer and doubled attenuation during winter (Jaun et al., 2007) and, as a consequence, the estimated primary production under 'no-dam' conditions was about ~35% lower in summer and up to ~23% higher in winter compared to present conditions. Annual gross primary production is estimated at ~12% below present. As shown by Finger et al. (2007b), these alterations are small compared to the effects of nutrient reductions due to sewage treatment in the last 30 years.

(3) The largest inter-annual variability in primary production were estimated in May and June (standard deviation: up to ~20%), representing a critical period for zooplankton communities, based on their need to regenerate from the harsh winter. This became evident when a collapse of the *Daphnia* population and fishing yield occurred just after the flood in spring 1999 (Müller et al., 2007b). Low temperatures and elevated particle loads in the rivers reduced primary production in spring (May and June) to ~22% below long-term average, probably jeopardizing the regeneration of zooplankton (Rellstab et al., 2007). Contrary, the modeled primary production was reduced only ~10% below average following the 'flood of the century' with exceptionally high particle concentrations in August 2005 (Beniston, 2006). As no decline in zooplankton was observed after this flood, it can be assumed that this period in summer is less critical for sustaining the zooplankton population.

(4) Simulations with light and temperature data from turbidity-free Lake Thun indicate that primary production would be ~44% higher if Lake Brienz had a similar level of clarity as Lake Thun. Nevertheless, primary production would still remain at an extremely low level compared to other Swiss peri-alpine lakes.

4.7 Acknowledgments

The present study is part of the interdisciplinary research project investigating the ecological effects of anthropogenic changes in the watershed of Lake Brienz. The study was funded by (1) Regional Government of Canton Bern, (2) *Kraftwerke Oberhasli AG* (KWO), (3) Swiss Federal Office of Environment (FOEN), (4) communities on the shoreline of Lake Brienz and (5) Swiss Federal Institute of Aquatic Science and Technology (Eawag). Most phosphorus analyses were performed by C. Hoyle within the framework of her M.S. thesis. Global radiation data was made available by MeteoSwiss. J. Ackerman, P. Reichert and an anonymous reviewer provided valuable input on the earlier version of this manuscript.

CHAPTER 5

EFFECTS OF OLIGOTROPHICATION AND UPSTREAM HYDROPOWER DAMS ON PLANKTON AND PRODUCTIVITY IN PERI-ALPINE LAKES

David Finger, Martin Schmid and Alfred Wüest

(Water Resources Research, submitted)

Abstract

In recent decades, many peri-alpine lakes have been affected by oligotrophication due to efficient sewage treatment and by altered water turbidity due to upstream hydropower operations. Such simultaneous environmental changes often lead to public debate on the actual causes of observed productivity reductions. We evaluate the effects of those two changes by a combined approach of modeling and data interpretation for a case study on Lake Brienz (Switzerland), a typical oligotrophic peri-alpine lake, located downstream of several hydropower reservoirs. A physical k-ε scheme and a biogeochemical advection-diffusion-reaction model have been implemented. These models are applied for several hypothetical scenarios with different nutrient loads and different particle input dynamics and the simulation results are compared to long-term biotic data collected from 1999 to 2004. The analysis suggests that enhanced nutrients supply increases the nutritious value of algae, stimulating zooplankton growth, but phytoplankton growth is then limited by stronger top-down control. Surprisingly, annually integrated productivity is only slightly influenced by altered turbidity, as phosphorus limitation prevails. Simulations indicate that the spring production peak is delayed due to increased turbidity in winter caused by hydropower production. As a consequence, the entire nutritious cycle is seasonally delayed, creating an additional stress for fish production.

5.1 Introduction

In the 1960's eutrophication was recognized as the major water quality problem, progressively affecting valuable lakes, rivers, and costal areas (Sawyer, 1966; Vollenweider, 1968). Anthropogenic inputs of nitrogen (N) and phosphorus (P), often from non-point sources, were identified as the primary causes for increasing algal biomass in temperate lakes (Vollenweider, 1968; Vallentyne, 1973; Dillon and Rigler, 1974). In order to mitigate eutrophication, waste water treatment plants - including Fe-induced P precipitation - were constructed throughout the industrialized world (Schindler, 1974; Forsberg, 1987). Subsequently algal proliferation was prevented and water quality restored (Anderson et al., 2005; Jeppesen et al., 2005). The successful reduction of algal biomass resulted in many cases in a unintended decline of freshwater fisheries (Ashley et al., 1997; Larkin and Slaney, 1997; Stockner et al., 2000).

In many peri-alpine streams and lakes long-term fishing yields indicate a persistent decline since the 1970's (Burkhardt-Holm et al., 2002; Borsuk et al., 2006; Müller et al.,

2007b). Besides the evident nutrient reduction mentioned, numerous potential causes have been identified (Burkhardt-Holm et al., 2002; Borsuk et al., 2006). One of the important anthropogenic impacts is the alteration of water turbidity caused by land use change (Swift et al., 2006), altered erosion (Effler et al., 2001), mining (Guenther and Bozelli, 2004) or upstream damming (Finger et al., 2006). A reduction of in situ light radiation limits primary production (Jewson and Taylor, 1978; Krause-Jensen and Sand-Jensen, 1998) which subsequently affects the entire ecosystem.

Peri-alpine regions of the European Alps and the Rocky Mountains are specifically affected by mineral riverine particle loads, due to the high ablation rates of 0.1 to 0.65 mm yr^{-1} (Hinderer, 2001). Consequently, alpine and peri-alpine rivers transport enormous masses of suspended solids to lowland lakes. Sediment retention in upstream reservoirs leads to reduced particle concentrations in downstream rivers lowering the water density, often overriding thermal effects, and changing their plunging and intrusion in downstream lakes (Finger et al., 2006). Consequently deep water renewal may be reduced (Loizeau and Dominik, 2000) and allochthonous particle supply to the epilimnion may become more frequent (Finger et al., 2006). In addition, damming often leads to a seasonal shift of particle fluxes and downstream lake turbidity. An alteration of lake turbidity subsequently affects in situ primary production disturbing the entire food web of the lake (Finger et al., 2007a).

In summary, cultural eutrophication and man-made alterations in the upstream catchment, such as water diversion, damming and reservoir construction have been the two most prominent anthropogenic impacts on water quality of peri-alpine lake ecosystems during the last century. It is therefore essential to assess the effects of oligotrophication and upstream hydropower operations on plankton and productivity in peri-alpine lakes to improve water resources management and preserve near-natural lake ecosystems.

In the present study we asses the effects of changing P input and altered turbidity on plankton growth in peri-alpine Lake Brienz. To estimate these anthropogenic impacts, a one-dimensional physical and biogeochemical model was calibrated to present conditions. This model was then used to simulate hypothetical scenarios with increased P supply (as during the 1980's) and natural surface turbidity (as prior to damming). For plausibility, the simulation results of the scenarios were compared to long-term data sets of phytoplankton biomass. The study concludes by comparing fishing yields to other peri-alpine lakes and assessing the main reasons for the exceptionally low yields in Lake Brienz.

5.2 Study site: Lake Brienz

Lake Brienz, located in the foothills of the *Bernese Oberland* (Figure 5.1), is characterized by a 260 m deep basin (Table 5.1) eroded of the Mesozoic rocks by fluvial and glacial forces (Sturm and Matter, 1978). Over 80% of the 1127 km^2 large catchment is drained by the two major inflows, Aare and Lütschine, which enter the lake at the eastern and western longitudinal ends (Figure 5.1). While Aare drains a 554 km^2 large crystalline watershed, Lütschine is supplied by a 379 km^2 large sedimentary catchment (Sturm, 1976). About 20% of both watersheds are covered by glaciers (LHG-BWG, 2005) causing a large suspended particle transport of about 128 kt yr^{-1} in Aare and 174 kt yr^{-1} in Lütschine (Finger et al., 2006). These tremendous loads lead to particles concentrations within Lake Brienz of up to ~25 g m^{-3} during the peak of snow and glacier melting in summer (Finger et al., 2006).

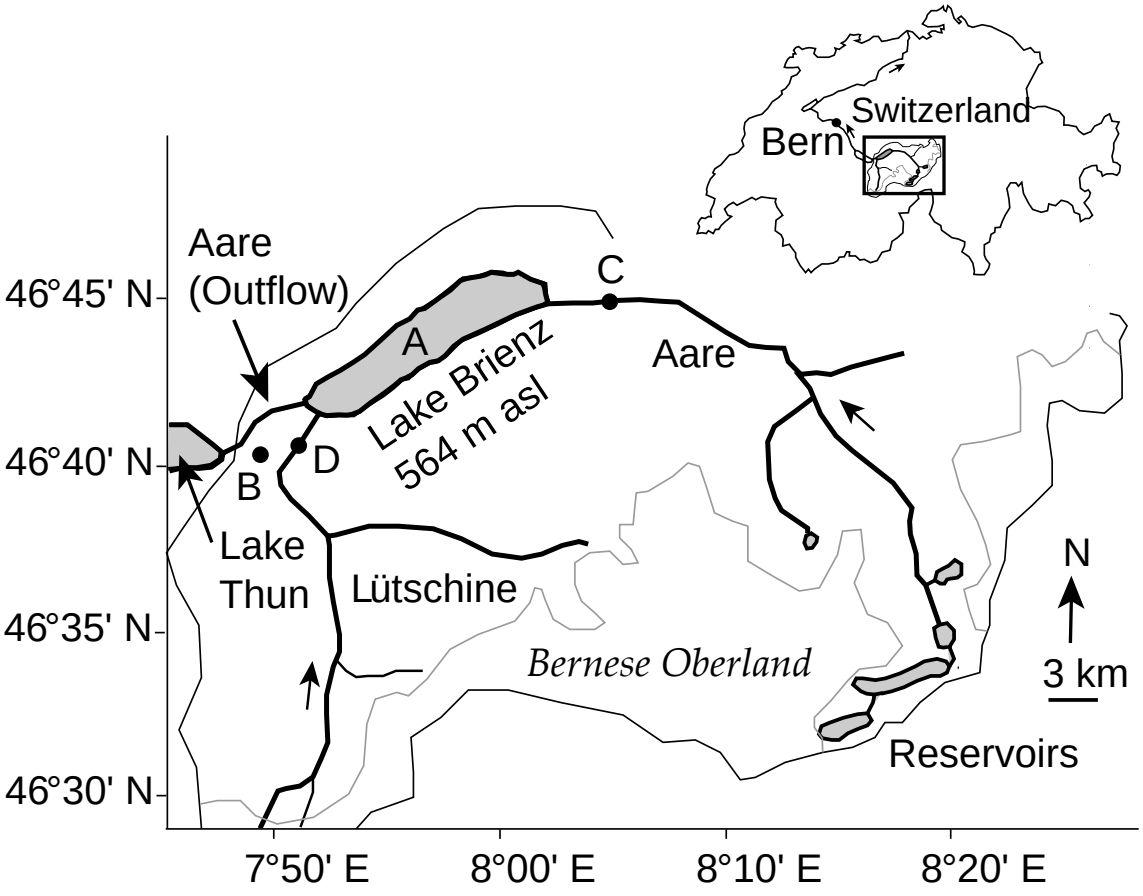

Figure 5.1: Geographical overview of study area and sampling sites. Upper right map locates Lake Brienz within Switzerland. Rivers are illustrated as bold lines, the border of the alpine water shed is indicated with a light line and glaciated areas are delimited by a grey line. Arrows indicate flow directions of rivers.

Table 5.1: Characteristics of Lake Brienz

Property	Unit	Value
Location		46° 43' 13.6'' N
(deepest point)		7° 57' 14.4'' E
Altitude	m asl	564
Catchment area	km^2	1127
Population density	Pers. km^{-2}	29
Average (highest) altitude of catchment [(1)]	m asl	1950 (4274)
Surface	km^2	29.8
Volume	km^3	5.17
Maximal (average) depth	m	260 (173)
Average discharge in Aare[(2)]	$m^3 s^{-1}$	37.9
Average discharge in Lütschine[(2)]	$m^3 s^{-1}$	19.7
Annual outflow[(3)]	$m^3 s^{-1}$	63.3
Water residence time	yr	2.7

[(1)] Highest peak in catchment is Finsteraarhorn at 4274 m asl.

[(2)] Average total discharge in Aare and Lütschine (1997 – 2004).

[(3)] Average discharge at the outflow (1997 – 2004); the difference between inflow and outflow is due to (1) precipitation minus evaporation and (2) minor inflows.

In response to eutrophication, effective sewage treatment plants with Fe-induced P precipitation have been constructed since the 1970's. In the weakly populated catchment of Lake Brienz these measures, along with a prohibition of P-containing detergent, have drastically reduced P loads to a fifth of the loads during the 1970's (Figure 5.2a). Consequently Lake Brienz is today an ultra-oligotrophic lake ($P < 1$ mg m^{-3}), as it was before the eutrophication phase at the beginning of the twentieth century (Müller et al., 2007a). Simultaneously to the declining P input fishing yield has dropped to almost a quarter since the late 1970's (Figure 5.2a), while plankton densities have been halved (Figure 5.2b).

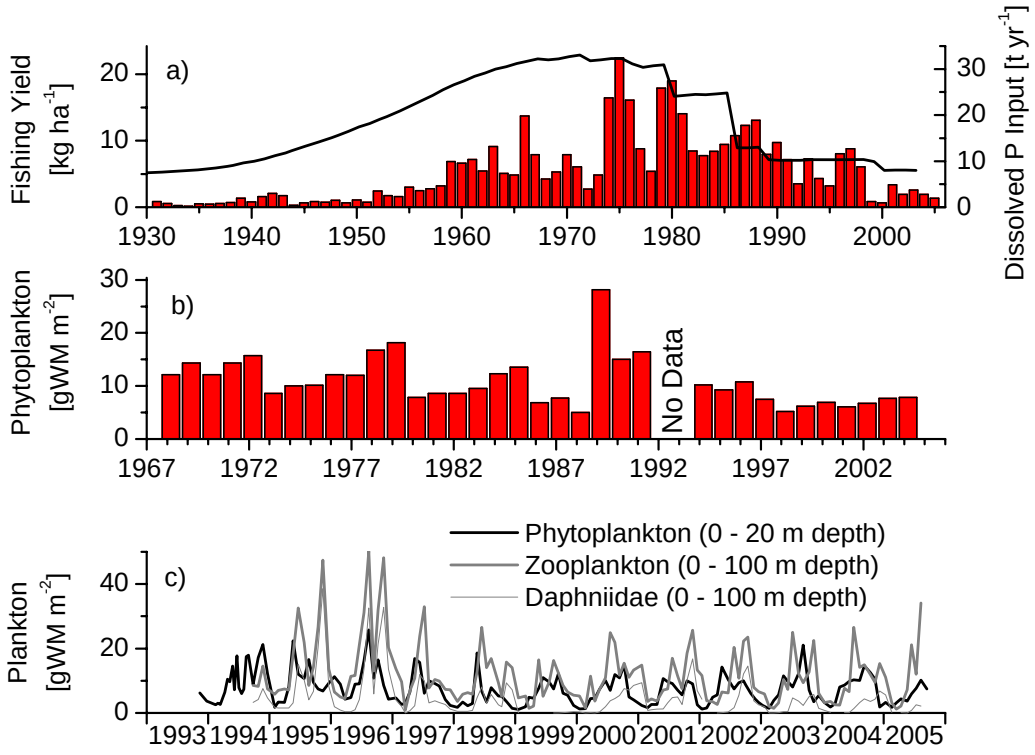

Figure 5.2: Biological data of Lake Brienz (note different scales): a) Fishing yield (red bars; left scale) (Müller et al., 2007b) and dissolved P input (solid line; right scale) to Lake Brienz since 1930 (Müller et al., 2007a); b) average annual phytoplankton wet mass between 1967 and 2004 (Nef, 1992); c) plankton dynamics between 1993 and 2005 (GBL data).

Following the flood of 1999, fishing yield collapsed almost completely, coinciding with the disappearance of *Daphnia* – Cladocera (Wüest and Zeh, 2007). Low algae production due to high turbidity and low temperatures (Finger et al., 2007a) and high discharge flushing *Daphnia* out of the lake (Rellstab et al., 2007) are hypothesized causes for the collapse.

Besides the anthropogenically altered P input, during the last century seven hydropower reservoirs have been built in the headwaters of Aare (Figure 5.1). The effects of hydropower-induced water retention on the downstream riverine thermal regime, particle transport and on the turbidity dynamics in Lake Brienz have been assessed in a recent study (Finger et al., 2006). While thermal effects are negligible in the downstream lake, particle retention in the reservoirs amounts up to 232 kt yr^{-1} (Anselmetti et al., 2007), decreasing the annual suspended load by over 50%. Contrary, hydropower production has doubled the particle load

during winter. As a consequence, today, Lake Brienz is more turbid during winter and less turbid during summer than prior to the construction of the dams (Jaun et al., 2007). Besides the mineral particles, hydropower reservoirs retain annually about two tons of bio-available P (Müller et al., 2007a) or ~25% of the annual P supply to Lake Brienz.

In summary Lake Brienz has been affected by two anthropogenic impacts during the last century: (i) cultural eutrophication up to the late 1970's and subsequent re-oligotrophication due to effective waste water treatment and (ii) modified turbidity due to the construction and operation of dams in the Aare headwaters.

5.3 Modeling Approach and Data

For assessing potential biotic changes within Lake Brienz, various data of past investigations have been analyzed (Table 5.2) and are used in the present modeling study. In the following we present relevant data and the modeling approach used to interpret these data.

Table 5.2: Overview of data set

Parameters	Symbol	Location[1]	Sampling period	Typical Value	Unit	Frequency of sampling	Performed by/reference
CTD[2]	T; S; S_{O_2}; Tr, pH	A	1999-2005	see reference	°C; ‰; g m^{-3}; -; -	monthly	(Finger et al., 2006)
Suspended solids	SSC	A	1997-2004	1 - 25	g m^{-3}	monthly	(Finger et al., 2006)
Light attenuation	K_0	A[3]	1999-2005	0.2 – 0.8	m^{-1}	monthly	GBL
Meteorological data[4]	I; v; Φ; p_g; T_a	B	1999-2005	~130; 2.6; 76; 9.8; 9.2	W m^{-2}; m s^{-1}; %; mb; °C	hourly	MeteoSwiss
Phytoplankton[5]	X_{ALG}	A	1994-2005	6.9	gWM m^{-2}	monthly	GBL
Zooplankton[5]	X_{ZOO}	A	1994-2005	10.1	gWM m^{-2}	monthly	GBL
Phosphate	S_{HPO_4}	A	2003-2005	<1.2	mg m^{-3}	monthly	(Wüest et al., 2007)
C assimilation rate[6]	P^B	A	2004	67	gC m^{-2} d^{-1}	monthly	(Finger et al., 2007a)
Hydrological data of Aare[7]	Q_A, T_A, S_A	C	1905-2005	37.9 5.9 0.069	m^3 s^{-1} °C g kg^{-1}		(Finger et al., 2006); (LHG-BWG, 2005)
Hydrological data of Lütschine[7]	Q_L, T_L, S_L	D	1908-2005	19.7 5.7 0.189	m^3 s^{-1} °C g kg^{-1}		(Finger et al., 2006); (LHG-BWG, 2005)
Phosphate in Inflows[8]	$S_{HPO_4,in}$	C, D	2004	3.5 2.1	mg m^{-3}		(Müller et al., 2007a)

[1] Locations A: deepest location of the lake; B: near west end of the lake; C: about 2 km upstream of Aare inlet; D: about 2 km upstream of Lütschine inflow (Figure 5.1).

[2] CTD profiling comprises profiles of temperature (T), salinity (S) (calculated by the means of electrical conductivity after Wüest et. al. (1996)), light transmission (Tr) dissolved oxygen (S_{O2}) and pH.

[3] Light attenuation was additionally monitored at the center of Lake Thun (Figure 5.1).

[4] Global radiation (I), wind speed (v), relative humidity (Φ), vapor pressure (p_g) and air temperature (T_a). Data publicly available at www.meteoschweiz.ch; values given represent average from 1999 to 2004.

[5] Phyto- and zooplankton monitoring was performed in the framework of the continuous monitoring (GBL), using net hauls (phytoplankton: 0 to 20 m depth; zooplankton: 0 to 100 m depth). Values represent average densities between 1999 and 2004.

[6] C assimilation integrated over the entire photic zone (0-35 m depth)

[7] Q denotes discharge, T denotes temperature and S denotes salinity (T and S have only been monitored since 1974); values represent averages between 1997 and 2004.

[8] Values represent the load averaged concentrations in Aare and Lütschine, respectively.

5.3.1 Model input data

As part of the lakes monitoring, the Water and Soil Protection Laboratory of the canton Berne (GBL) performs sampling at the deepest location on Lake Brienz. Since 1994, the survey includes monthly CTD profiles using a SBE-19 (Seabird, USA) equipped with conductivity, temperature, depth, pH and dissolved oxygen sensors (as well as, since 1997, a 10 cm SeaTech transmissometer). Light transmission casts have been converted into suspended solid concentration profiles according to Finger et al. (2006). Since 1995, GBL additionally performs monthly phyto- and zooplankton net hauls, and since 1999 also monthly photosynthetic active radiation (PAR) profiles measured with an underwater LI-COR sensor (Bioscience, USA). Such profiles are also available from downstream Lake Thun (Figure 5.1), which is much less affected by glacial particle input. Furthermore, between 25 February 2003 and 7 July 2004 water samples have been collected also at the deepest location and analyzed by sequential extraction (Hoyle, 2004) and standard methods for soluble reactive P (Wüest et al., 2007).

In the tributaries Aare and Lütschine discharge (Q), temperature (T) and electrical conductivity, converted to salinity (S) according to Wüest et al. (1996), are monitored by the Swiss Hydrological Survey (LHG-BWG). While Q has been recorded since 1905 (in Lütschine since 1908), T monitoring started in 1974 and S has been occasionally determined since 1991. The mean riverine P loads have been estimated by establishing a consistent P balance (Müller et al., 2007a; Wüest et al., 2007), which is based on river water samples, ablation rates estimated from land use data, and lake internal net sedimentation measured in sediment traps and cores (Table 5.2).

Meteorological data (global radiation (I), wind speed (v), relative humidity (Φ), vapor pressure (p_g) and air temperature (T_a)) have been continuously measured since 1999 at a weather station of MeteoSwiss near the west end of Lake Brienz (position B in Figure 5.1).

5.3.2 Modeling approach

Numerical simulations were performed with a physical lake model developed by Goudsmit et al. (2002) combined with a modified biogeochemical advection-diffusion-reaction model implemented in several earlier studies (Omlin et al., 2001; Mieleitner and Reichert, 2006; Matzinger et al., 2007) based on the simulation software AQUASIM developed by Reichert (1994).

In a first step vertical turbulent diffusivity $K_z(z)$ was estimated for the years 1999 to 2004. The stratification in Lake Brienz is dominated by temperature, while the effects of salinity and suspended solids (apart from short-term turbidity events) are negligible. Three model-specific parameters were fitted by the least-square method to reproduce the monthly measured temperature profiles. These three parameters are (Table 5.3): (i) the scaling factor for the infrared heat flux (p_1), (ii) the scaling factor for the wind energy transfer to the internal seiches (α), and (iii) a coefficient defining the vertical distribution of seiche energy dissipation (q) (Goudsmit et al., 2002). As input we used hydrological data from both inflows (Q, T, S), intrusion depth dynamics as determined by Finger et al. (2006), meteorological data (I, v, Φ, p_g, T_a) measured by MeteoSwiss (Table 5.2), and light attenuation coefficients determined from the PAR profiles collected by GBL (Table 5.2).

Table 5.3: Overview of major changes relative to Omlin's (2001) work

Process/Equation	Symbols/Values/Units	Explanation
River Intrusion [(1)]: $Q_{epi} = Q \cdot (1 - k_{hyp})$ $Q_{hyp} = Q \cdot k_{hyp}$	Aare: $k_{hyp,\,wint} = 0.34$ Aare: $k_{hyp,\,sum} = 0.04$ Lütschine: $k_{hyp,\,wint} = 0.65$ Lütschine: $k_{hyp,\,sum} = 0.13$ $S_{HPO_4,in,Aare}$ = 3.5 mg m^{-3} $S_{HPO_4,in,Luet}$ = 2.1 mg m^{-3} T (°C)	Splitting of inflows into input to epilimnion and hypolimnion was parameterized according to Finger et al. (2006); $S_{HPO_4,in}$ is the load-averaged P concentration according to Müller et al. (2007a); T is recorded continuously by LHG.
Non-point P sources : $S_{HPO_4,add}$	$S_{HPO_4,add}$ = 6 kgP d^{-1}	According to Müller et al. (2007a).
$I_{Surface} = 134.6 - 100.3 \times \cos\left(\frac{2\pi \cdot t_{year}}{365.25}\right)$	t_{year} : Day of year	Coefficients of $I_{Surface}$ (W m^{-2}) were fitted to mean global radiation (MeteoSwiss) for 1999 to 2004.
Additional photoinhibition term in growth of algae process $\exp\left(\frac{-E(z)}{E_{photo}}\right)$	E_{photo} = 330 W m^{-2}	To account for photoinhibition an additional term was added to the algae growth process; E_{photo} was determined from typical productivity profiles (Finger et al., 2007a).
C Assimilation: $P^B = \frac{M_C}{M_{Bio}} r_{gro,ALG}$	M_C = 12 g mol^{-1} M_{bio} = 30 g mol^{-1}	Experimental observations of C assimilation are presented in Finger et al. (2007a).
Vertical turbulent diffusion: K_z	$p_1 = 1.138$ [(2)] $\alpha = 0.029$ [(2)] $q = 0.464$ [(2)]	A detailed description of the physical lake model is given in Goudsmit et al. (2002).

Furthermore:

- Components concerning the nitrogen cycle were removed, as it can be neglected for our purposes.
- Sediment compartment was removed. As sedimentation rates exceed 0.64 cm yr^{-1} (Finger et al., 2006), interaction (e.g. mineralization) with sediment can be neglected (Müller et al., 2007a).
- 'Planktothrix rubescens' was removed as it is irrelevant for Lake Brienz.

[(1)] Each river input was split up into surface intrusion Q_{epi} and deep water intrusion Q_{hyp} in order to avoid numerical problems. Intrusion depth of Q_{epi} was set between 10 and 60 m depth; Intrusion depth of Q_{hyp} was set between 205 m and 155 m depth; $k_{hyp,wint}$ is valid for days 315 - 81; $k_{hyp,sum}$ is valid for days 101 - 295 (between these time periods, the values were linearly interpolated); S_{HPO_4} was obtained by dividing annual P load (Müller et al., 2007a) by average discharge.

[(2)] Coefficients for the physical lake model to simulate K_z

In a second step the biogeochemical model established by Omlin et al. (2001) was adapted for our purposes. The changes relative to Omlin et al. (2001) are listed in Table 5.3, while the complete model is summarized in the Appendix (section 5.7). The following dynamic variables were simulated for the period 1999 to 2004 (starting conditions for all simulations were obtained by an initialization run using year 2002): temperature (T), bio-available phosphate (S_{HPO_4}), dissolved oxygen (S_{O_2}), phytoplankton biomass (X_{ALG}), P incorporated in phytoplankton ($X_{P,ALG}$), dead organic matter (X), P incorporated in dead organic material (X_P), P adsorbed to dead organic material ($X_{P,I}$), and zooplankton biomass (X_{ZOO}). The interactions between these variables are described by eight processes: (1) growth of algae, (2) respiration of algae, (3) death of algae, (4) growth of zooplankton, (5) respiration of zooplankton, (6) death of zooplankton, (7) adsorption of phosphate to organic particles and (8) aerobic mineralization within the water column.

Riverine P inputs were divided up between the productive epilimnion and the deep water, as summarized in Figure 5.3. During thunderstorms, intrusion depths may vary between 20 and 255 m depth within one hour (Finger et al., 2006). Since such high variability could cause numerical problems, river inputs were seasonally averaged and split up into deep water input Q_{hyp} and surface intrusion Q_{epi} (Table 5.3).

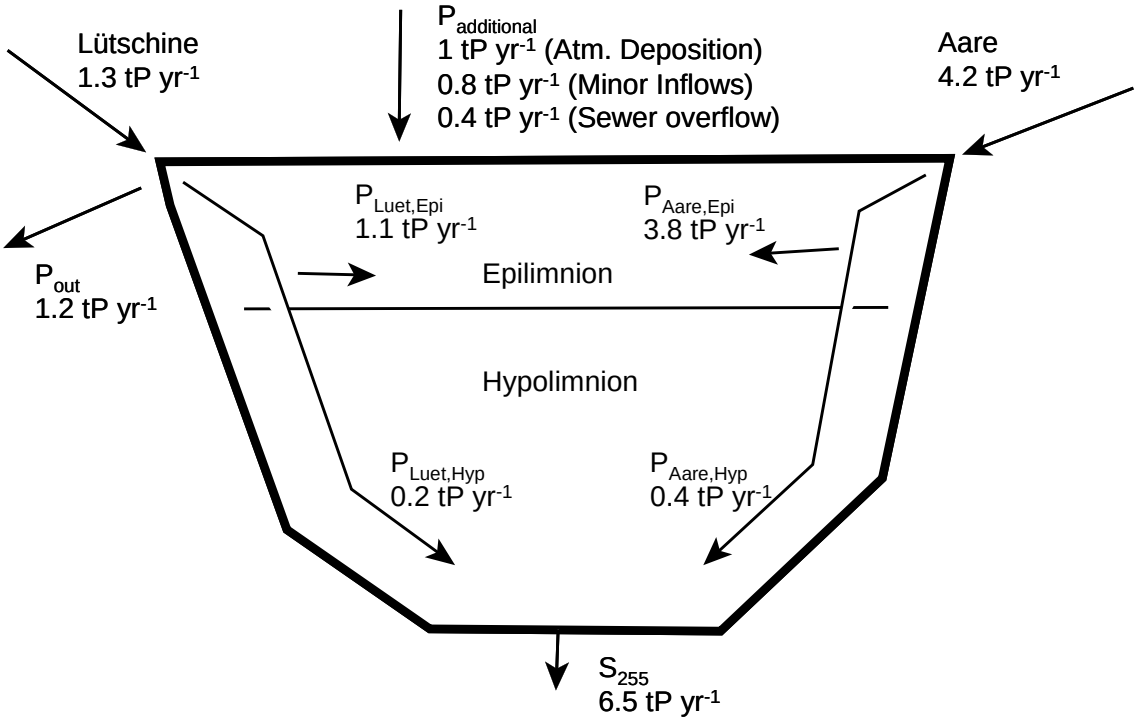

Figure 5.3: Schematic bio-available P balance in Lake Brienz according to Müller et al. (2007a). Input load of bio-available P is composed mainly of phosphate. Sedimentation fluxes are primarily particulate P.

For algae growth in oligotrophic systems P incorporation into algae becomes of major importance. It is often assumed that S_{HPO_4} in algae (b_P) follows a constant molar P:C ratio of 1:106, the so-called Redfield ratio (Redfield, 1958). However, observations in oligotrophic freshwaters indicate that P:C shifts dramatically towards C at S_{HPO_4} lower than ~7 mg m^{-3} reaching values of up to 1:700 (Guildford and Hecky, 2000). Observations in other lakes indicate furthermore, that P:C in algae alters seasonally (Hupfer et al., 1995). Based on these insights and numerical simulations, Omlin et al. (2001) demonstrated, that b_P can be expressed as a steady function of S_{HPO_4}, as defined in equation (5.1).

$$b_P = \frac{\left(b_{P,\min} + b_{P,\max}\right)}{2} + \frac{\left(b_{P,\max} - b_{P,\min}\right)}{2} \times \tanh\left(\frac{S_{HPO_4} - S_{HPO_4,crit}}{\Delta S_{HPO_4}}\right) \qquad (5.1)$$

$S_{HPO_4,crit}$ defines the critical value and ΔS_{HPO_4} defines the range within which production switches to reduced P content. In contrast, C:P ratios within natural freshwater zooplankton populations show little variation, even in starvation and food enrichment experiments (Andersen and Hessen, 1991). Consequently, the food requirement per zooplankton mass

(F_{ZOO}), under varying P incorporation in algae, must be equal to the ratio of P content in algae under Redfield conditions ($a_{P,red}$) and P content in newly built algae ($F_{ZOO} = a_{P,red} / b_P$). In ultra-oligotrophic waters, such as Lake Brienz, low P incorporation in algae is of major importance, as discussed below.

In accordance with the findings of Mieleitner et al. (2006) the following parameters were calibrated iteratively with the following 'sensitive' subsets of the available data (Table 5.4): maximal growth rate of algae ($k_{gro,ALG,20}$) and maximal specific death rate of algae ($k_{death,ALG,20}$) were adapted to observed phytoplankton density; maximal growth rate of zooplankton ($k_{gro,ZOO,20}$) and maximal specific death rate of zooplankton ($k_{death,ZOO,20}$) were adapted to zooplankton density; half-saturation concentration for algal growth with respect to phosphate ($K_{HPO_4,ALG}$) and half-saturation light intensity for algal growth ($K_{I,ALG}$) were adapted to measured productivity and observed phyto- and zooplankton density; the coefficient ΔS_{HPO_4} in equation (5.1) was adapted to in situ phosphate and annual P fluxes; and maximal uptake rate of phosphate on sinking particles (k_{up}) was fitted to the P flux at the lake bottom.

As test runs indicate, simulations of the biogeochemical cycling are very sensitive to b_P (Equation 5.1). In order to conserve conformity with data presented by Guildford and Hecky (2000) $S_{HPO_4,crit}$ was not altered during model calibration. As the entire lake is usually almost saturated with dissolved oxygen (section 5.4.1), we renounced using dissolved oxygen profiles (CTD data) for parameter estimation.

Table 5.4: Adapted and fitted parameters compared to other published applications

Parameter	Unit	Lake Brienz (this work)	Lake Zurich (Omlin et al., 2001)	Lake Zurich (Mieleitner and Reichert, 2006)	Lake Ohrid (Matzinger et al., 2007)
$k_{gro,ALG,20}$	d^{-1}	3	1.1	1.6	1.88
$k_{gro,ZOO,20}$	$gDM^{-1}\ m^3\ d^{-1}$	5	0.3	0.4	3.47
$k_{death,ZOO,20}$	d^{-1}	0.04	0.029	0.01/0.035/0.11	0.029
$k_{death,ALG,20}$	d^{-1}	0.06	0.03	0.03	0.03
k_{upt}	$m^4\ gP^{-1}\ d^{-1}$	3000	1200		1200
$K_{HPO_4,ALG}$	$gP\ m^{-3}$	0.0008	0.0019	0.0005	0.0019
$K_{I,ALG}$	$W\ m^{-2}$	11	34	10	
$S_{HPO_4,crit}$	$gP\ m^{-3}$	0.0042	0.0042	0.004	0.004
ΔS_{HPO_4}	$gP\ m^{-3}$	0.0025	0.0013	0.0013	0.00125
E_{photo}	$W\ m^{-2}$	330	-	-	-
$a_{P,\max}$	-	0.007	0.009	0.007	0.0052
w_{zoo}	-	12.5	5	10	5
w_{alg}	-	5	5	5	5
v_{alg}	$m\ d^{-1}$	0.4	0.2	0.2	0.2
v_{org}	$m\ d^{-1}$	10	10	10	0.46
v_{zoo}	$m\ d^{-1}$	v_{up} [(1)]	0	0	0
$k_{miner,aero,20}$	d^{-1}	0.02	0.01	0.01	0.008
β_{BAC}	$°C^{-1}$	0.046	0.046	0.046	0.09
β_{ALG}	$°C^{-1}$	0.069	0.048	0.048	0.048

(1) $v_{up}(z) = Q(z) / A(z)$ where Q(z) stands for discharge and A(z) for cross-sectional area at depth z.

5.3.3 Model scenarios

In order to understand the effects of hydropower operations (altering light attenuation) in relation to reduced P input (oligotrophication) on the ecosystem of Lake Brienz and to evaluate the sensitivity of individual parameters, a set of hypothetical scenarios was developed with (i) increased phosphate input and (ii) altered light attenuation dynamics

Table 5.5: Scenarios with altered P input and altered light attenuation.

Scenario	Description	Modified Parameters
'Present'[(1)]	Present situation (1999-2004)	$S_{HPO_4,in,Aare}$ = 3.5 mg m^{-3} $S_{HPO_4,in,Luet}$ = 2.1 mg m^{-3}
'P1'	'Present' scenario with additional 2 tP yr^{-1}	$S_{HPO_4,in,Aare}$ = 5.16 mg m^{-3} $S_{HPO_4,in,Luet}$ = 2.1 mg m^{-3}
'P2'	'Present' scenario with doubled P input	$S_{HPO_4,in,Aare}$ = 7.0 mg m^{-3} $S_{HPO_4,in,Luet}$ = 4.2 mg m^{-3}
'P3'	'Present' scenario with triple P input	$S_{HPO_4,in,Aare}$ = 10.5 mg m^{-3} $S_{HPO_4,in,Luet}$ = 6.3 mg m^{-3}
'P4'	'Present' scenario with fourfold P input	$S_{HPO_4,in,Aare}$ = 14 mg m^{-3} $S_{HPO_4,in,Luet}$ = 8.4 mg m^{-3}
'P5'	'Present' scenario with fivefold P input	$S_{HPO_4,in,Aare}$ = 17.5 mg m^{-3} $S_{HPO_4,in,Luet}$ = 10.5 mg m^{-3}
'No-dam 1'	'Present' scenario with 'No-dam' light attenuation and 'No-dam' discharge pattern	K_0^{No-dam} (Figure 5.4) Q^{No-dam} (average of 1910-1930)
'No-dam 2'	'Present' scenario with 'No-dam' light attenuation, additional 2 tP yr^{-1}, 'No-dam' discharge pattern, and altered intrusion depth	K_0^{No-dam}, Q^{No-dam}, Aare: $k_{hyp,\ wint}$ = 0.2 Aare: $k_{hyp,\ sum}$ = 0.09 $S_{HPO_4,in,Aare}$ = 5.16 mg m^{-3}
'Lake Thun'	'Present' scenario using light attenuation from PAR profiles of Lake Thun	$K_0^{LakeThun}$

(1) Further details to scenario 'Present' are given in Table 5.3.

(Table 5.5). These are then compared to the simulation results of the calibrated model for the years 1999 to 2004, in the following referred to as the 'Present' scenario.

In the first six scenarios, only the inflow S_{HPO_4} is varied ranging from present input (~7.8 tP yr^{-1}) to enhanced input (~30 tP yr^{-1}), as assumed during the 1970's (Figure 5.2a; *Müller et al.,* 2007a). In scenario 'P1' the P load in river Aare is enhanced by 2 tP yr^{-1}, representing a hypothetical situation without P retention in the upstream reservoirs. This scenario is essential in order to address impacts of hydropower installations on the

biogeochemical cycling within Lake Brienz. The remaining scenarios ('P2' to 'P5') represent a gradual increase of P loads in both rivers, representing the continuous decline of P loads since the 1970's.

As illustrated in Figure 5.4, hydropower-related upstream water retention reduces turbidity during summer, but increases turbidity during winter when the stored particle-laden water is released for hydropower production (Finger et al., 2006; Jaun et al., 2007). Besides water flow, particle content and turbidity, the hydropower operations alter river water density and thereby river intrusion depths (Finger et al., 2006), affecting the vertical distribution of riverine P inputs. To assess the sensitivity on each of these impacts two hypothetical scenarios were established: (1) 'No-dam 1': 'Present' scenario using light attenuation as predicted for a hypothetical situation without upstream hydropower dams (Figure 5.4; Jaun et al. 2007) and mean discharge from 1910 to 1930, representing the epoch previous to damming; (2) 'No-dam 2': in addition to changes adapted in scenario 'No-dam 1', river intrusion dynamics were altered as predicted by Finger et al. (2006) and riverine P load in Aare was increased by 2 tP yr^{-1} (accounting for P retention in the reservoirs; Müller et al. 2007a) to reflect conditions previous to damming (Table 5.5).

Since the severe collapse in fishing yield occurred only in Lake Brienz, while downstream Lake Thun (Figure 5.1) remained almost unaffected, we are specifically interested to evaluate the effects of glacial inorganic particles on the biogeochemical cycling within Lake Brienz. For this purpose we implemented the 'Lake Thun' scenario, equal to the 'Present' scenario but using light attenuation measured in Lake Thun (Table 5.5).

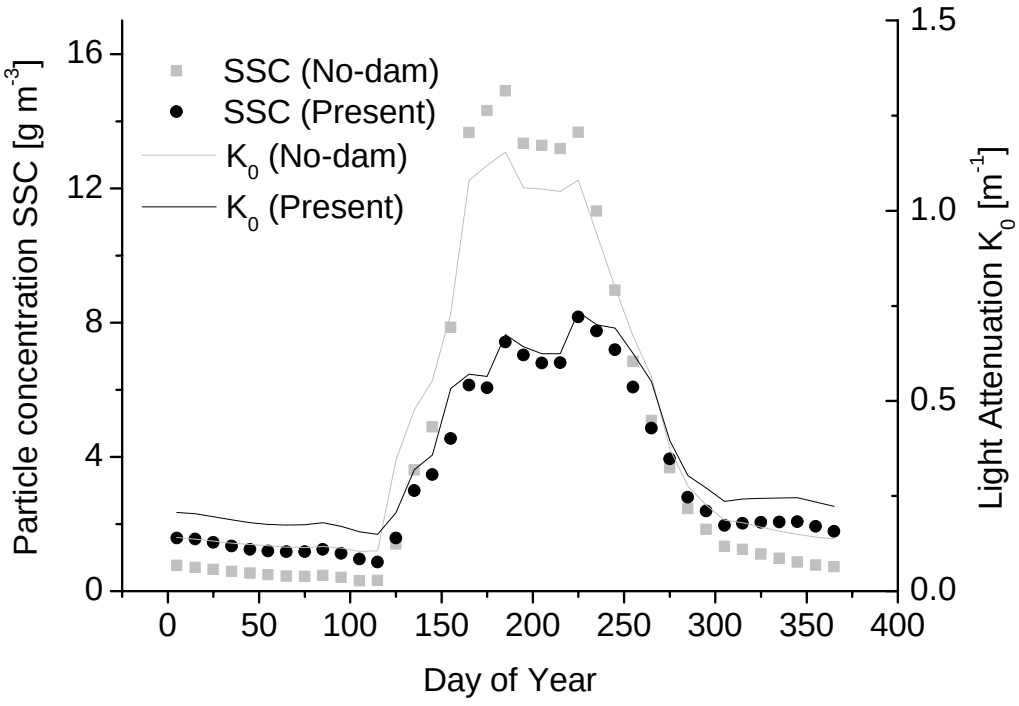

Figure 5.4: Mean surface turbidity in Lake Brienz for present conditions (average 1997 to 2004) and under conditions without hydropower dams in the headwaters of Aare. Figure adapted from Finger et al. (2006) and Jaun et al. (2007).

5.4 Observations and Model Results

In the following sections the results of simulations are presented and the anthropogenic effects are evaluated. First the 'Present' scenario is discussed in order to demonstrate the plausibility of the simulations.

5.4.1 Vertical mixing

A unique characteristic of Lake Brienz is its steep and 260 m deep basin. Nevertheless, temperature profiles reveal frequent convective mixing supplying the deep water with dissolved oxygen, which remain most of the time above 8 g m^{-3} (Figure 5.5). The exceptionally low values observed in 1996 can be attributed to subaquatic slumps (Girardclos et al., 2006), which released large amounts of anoxic sediments. Yet, oxygen supply to the deepwater is maintained by particle-driven deep water intrusion of the main tributaries (Finger et al., 2006) and deep convective mixing in winter. These processes can be observed in time series of temperature profiles illustrated in Figure 5.5a. Particle-driven intrusions

caused abrupt warming (e.g. flood of August 2005) and winter circulation led to cooling of the deep water (e.g. March 1999, 2003, 2004, 2005).

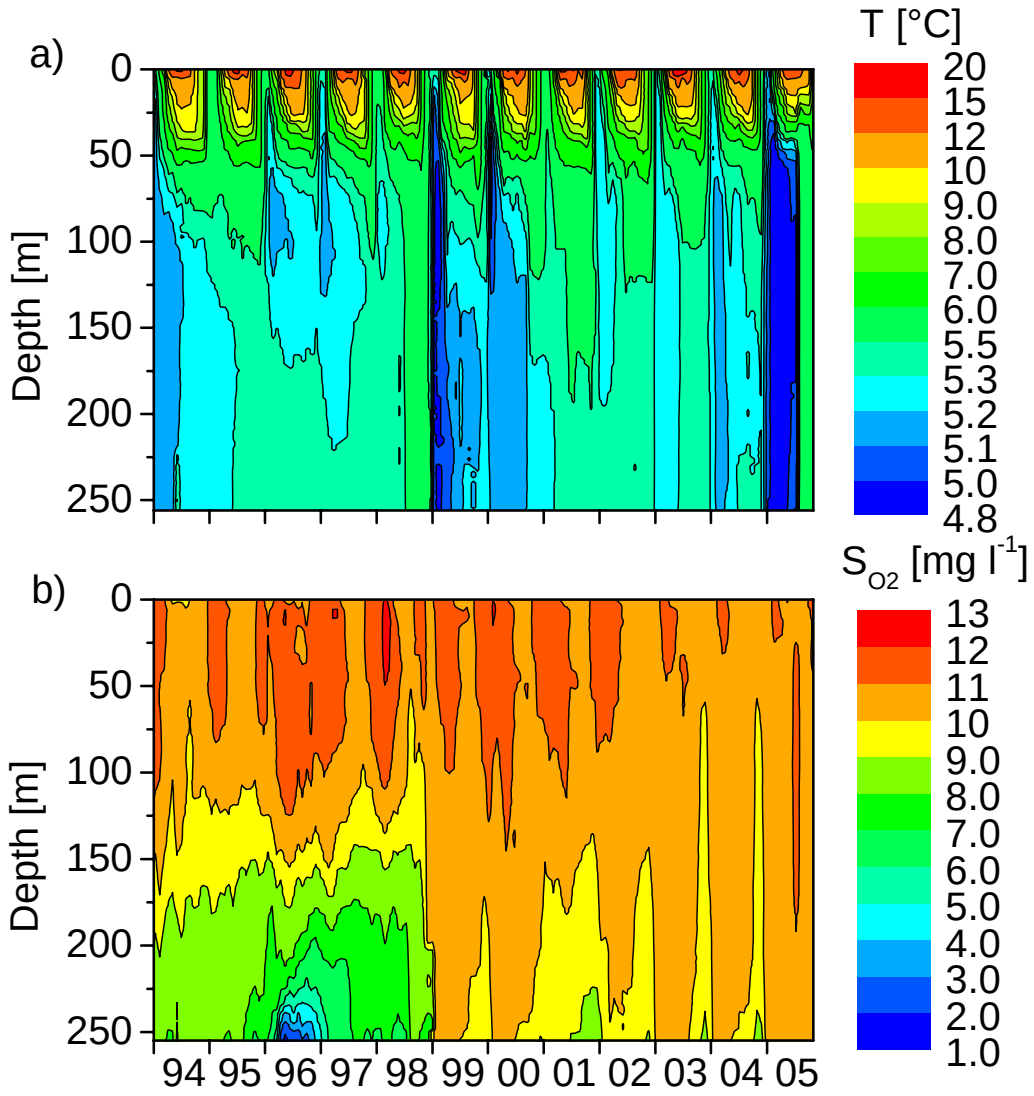

Figure 5.5: Observed temperature (contours a) and dissolved oxygen concentrations (contours b) in Lake Brienz from 1994 to 2005.

As outlined in section 5.3.2 vertical turbulent diffusivity was estimated from 1999 to 2004 with the buoyancy-extended k-ε model of Goudsmit et al. (2002). Simulated and measured temperature at 25, 50, 100 and 250 m depth are illustrated in Figure 5.6. Simulated temperatures correspond in value and in seasonal dynamics well to the measured temperatures at all depths, which indicates that vertical mixing was well reproduced by the model.

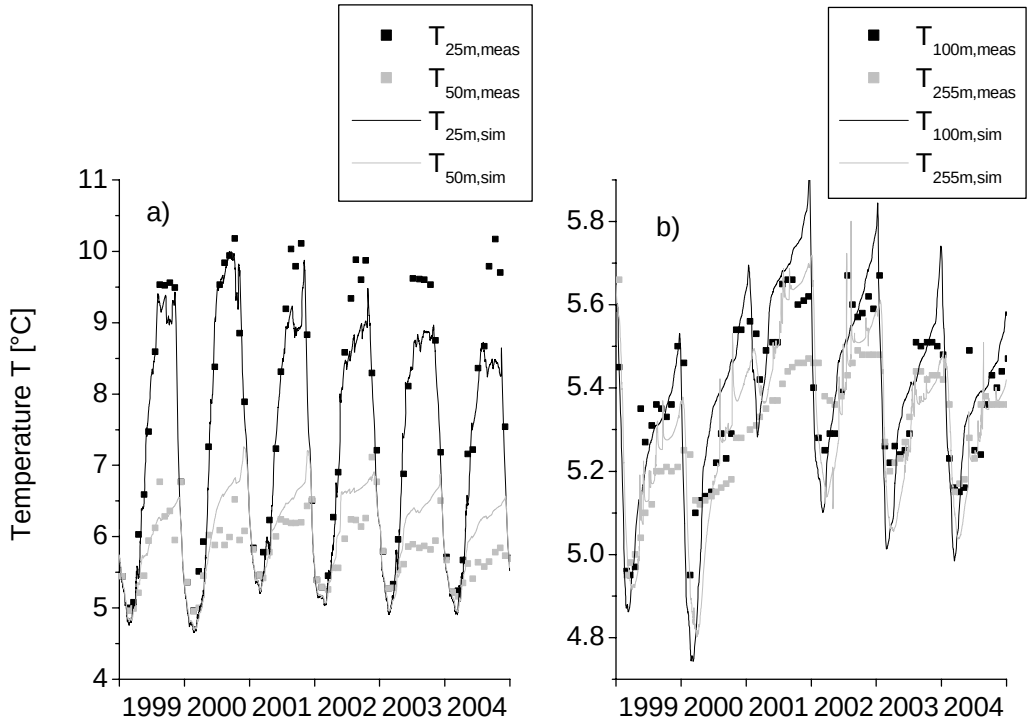

Figure 5.6: Time series of measured (symbol) and simulated (line) temperature at 25 and 50 m (a) and 100 and 255 m depth (b).

Although Lake Brienz is thermally stratified, mean average water temperature in the upper 10 m reaches only ~13.4 °C in August (average 1995 to 2005). This temperature is ~3.5 °C below that of Lake Thun, situated 5 km downstream of Lake Brienz (Finger et al., 2007a). The lower temperature in Lake Brienz is explained by the low temperatures in Lütschine and Aare (annual average 5.8 °C compared to ~10 °C at the inflow of Lake Thun) and intense surface turbidity which increases the albedo and reduces the penetration of solar radiation.

Over 70% of S_{HPO_4} is imported by Aare and Lütschine. While in summer river intrusions govern the vertical distribution of S_{HPO_4}, during winter convective mixing distributes S_{HPO_4} in the entire water column. Observed S_{HPO_4} between 25 February 2003 and 7 July 2004 at different depths in the lake are presented in Figure 5.7. Most values are < 1 mg m^{-3} indicating the extremely oligotrophic status of Lake Brienz. While elevated S_{HPO_4} during summer season is attributed to recent river intrusions, the general increase during winter is

attributed to convective mixing, transporting S_{HPO_4} from the deep water into the productive epilimnion.

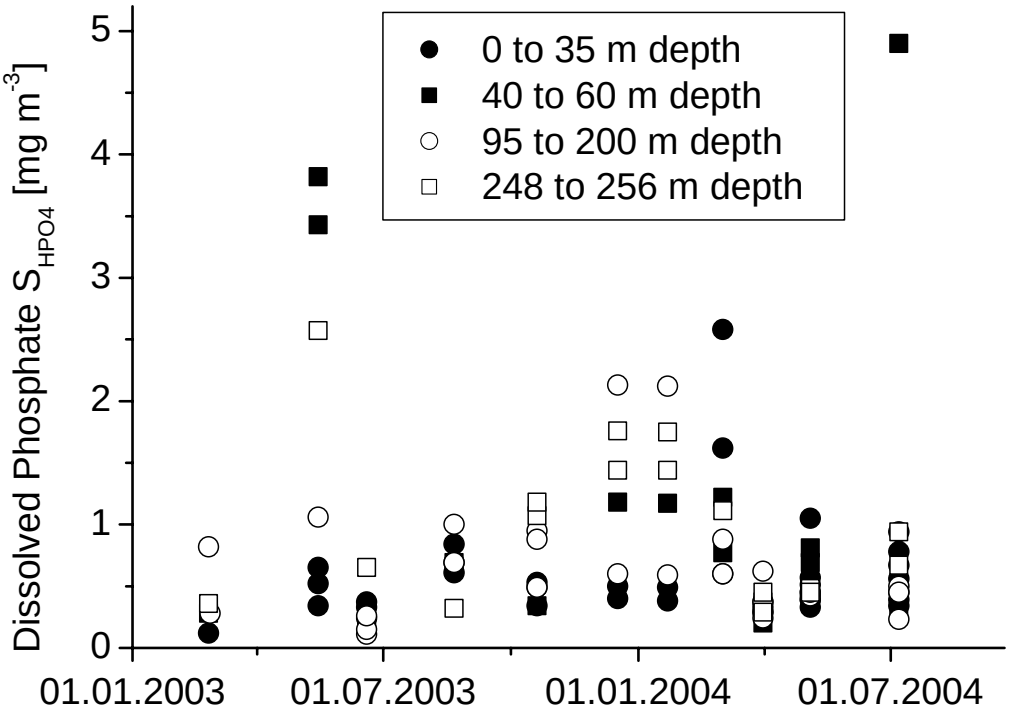

Figure 5.7: Measured dissolved reactive P concentration from different depths within Lake Brienz. Filled (open) symbols represent values from epilimnion (hypolimnion).

5.4.2 Simulations for 1999 to 2004

In Table 5.4 all parameters, which were adapted in order to perform the simulations presented below, are summarized and compared to recent studies on similar lakes. The most significant changes concern the parameters $k_{gro,ALG,20}$, $k_{gro,ZOO,20}$, $k_{death,ZOO,20}$, $k_{death,ALG,20}$ and $K_{HPO_4,ALG}$. As numerous test runs indicate, $k_{gro,ZOO,20}$ has to be considerably higher than in other lakes, because growth is reduced by the small phosphate content in algae ($a_{P,ALG}$). Likewise, $k_{gro,ALG,20}$ has to be elevated, as low S_{HPO_4} and T deteriorate growth conditions for phytoplankton. In order to obtain reasonable $a_{P,ALG}$ and P sedimentation rates, ΔS_{HPO_4} had to be adjusted slightly, while $S_{HPO_4,crit}$ was kept in accordance with experimental C:P ratios observed in numerous natural waters with different trophic status (Guildford and Hecky,

2000). Test runs revealed that X_{ALG} is very sensitive to ΔS_{HPO_4}, but qualitative differences between scenarios were consistent for different values of ΔS_{HPO_4}. The important differences of some parameters compared to other studies is a direct consequence of the extremely oligotrophic status of Lake Brienz, where S_{HPO_4} rarely exceeds 1 mg m^{-3}. The values seem reasonable, given that all other lakes listed in Table 5.4 present a much higher trophic status than Lake Brienz.

In Table 5.6 simulated P fluxes, algae growth and plankton densities are compared with observations presented in companion studies. Simulated P fluxes to the sediment match almost perfectly estimations made by Müller et al. (2007a). As input flows are defined by constant S_{HPO_4} concentrations in the rivers (Table 5.3), they are directly proportional to water discharge, leading to slightly higher input during the flood of 1999. Then the outflow P_{out} of P was ~23% above average, while sedimentation of particulate P (S_{255}) was only ~5% above average, indicating an enforced upwelling and washout. With an average input of ~7.8 tP yr^{-1} simulated mean phosphate concentration in Lake Brienz vary around 1 mg m^{-3}, which falls in line with observed phosphate concentration presented in Figure 5.7. Simulated annual gross algae production lies about 6% below the estimated C assimilation (Finger et al., 2007a).

Table 5.6: Simulated annual P fluxes, algae growth and plankton densities

	Unit	1999	2000	2001	2002	2003	2004	Average	Observed
$P_{additional}$	tP yr^{-1}	2.2	2.2	2.2	2.2	2.2	2.2	2.2	2.2
$P_{Aare,epi}$	tP yr^{-1}	4.4	3.7	3.7	4.0	3.6	3.4	3.8	3.8
$P_{Luet,epi}$	tP yr^{-1}	1.2	1.0	1.0	1.1	1.0	1.0	1.1	1.1
$P_{Aare,hyp}$	tP yr^{-1}	0.5	0.4	0.4	0.5	0.4	0.4	0.4	0.4
$P_{Luet,hyp}$	tP yr^{-1}	0.3	0.3	0.3	0.3	0.2	0.2	0.3	0.2
P_{out} [(1)]	tP yr^{-1}	2.3	1.9	1.8	2.0	1.7	1.5	1.8	1.2
S_{255} [(2)]	tP yr^{-1}	6.3	5.8	5.9	6.2	5.7	5.8	5.9	6.0
Mean S_{HPO_4} in 5 m	mg m^{-3}	1.0	1.0	1.0	0.9	1.0	0.8	1.0	< 1
Mean S_{HPO_4} in 200 m	mg m^{-3}	1.1	1.1	1.1	1.0	1.1	1.0	1.1	< 1
Annual P^B	gC m^{-2} yr^{-1}	53.8	63.2	66.2	65.3	59.9	67.2	62.6	67
Average phytoplankton (upper 20 m)	gDM m^{-3}	0.079	0.079	0.086	0.081	0.078	0.081	0.081	0.083
Average zooplankton (upper 100 m)	gDM m^{-3}	0.009	0.009	0.010	0.012	0.010	0.012	0.010	0.010

(1) P_{out} represents outflow of P given by the product of the sum of $X_{P,ALG}$, X_P, $X_{P,I}$, and S_{HPO_4} at 0 m depth and instant Q.

(2) S_{255} represents P flux to sediment: For the simulations this was set equal to total P Input - P_{out}.

Regarding the biological processes within Lake Brienz the seasonal evolution is of greater importance. Simulated and observed light attenuation, irradiance (5 m depth), temperature (5 m depth), phosphate concentration (5 and 200 m depth), phytoplankton densities (average of top 20 m) and zooplankton densities (average of top 100 m) between 1999 and 2004 are illustrated in Figure 5.8. The seasonal dynamics can be described in four seasons:

(1) Winter: Convective mixing as well as plunging inflows lead to water exchange between hypo- and epilimnion. Accordingly S_{HPO_4} is homogenized in the entire water column. Although turbidity is low (K_0 = ~0.2 m^{-1}), short days and weak radiation during winter lead to low E_z at 5 m depth. Together with low T, algae growth is limited (< 0.05 gC m^{-2} d^{-1}) and subsequently phyto- and zooplankton densities reach a minimum (~0.015 gDM m^{-3}, 0.002 gDM m^{-3}, respectively). During this season simulated plankton densities correspond well to measurements.

(2) Spring: Just before the onset of snow melt and subsequent elevated surface turbidity, conditions are excellent for algal growth: S_{HPO_4} > 1 mg m^{-3}, average irradiance increases due to longer days, turbidity is still low, water temperatures are rising and the zooplankton population is not yet fully developed. Consequently P^B reaches a maximum (measured maximum: 0.36 gC m^{-2} d^{-1}) leading to an important build-up of X_{ALG}. As illustrated in Figure 5.9, simulations overestimate algal growth during this period. Numerous test runs with different growth rates indicate, however, that such a growth rate is necessary in order to adequately simulate zooplankton biomass, annual P fluxes and annual production. Mieleitner et al. (2005) demonstrated that modeling different functional groups of algae improves predictions of seasonal biomass by broadening the spring peak. Nevertheless we renounced incorporating multiple functional classes in order to avoid over-parameterization and to preserve sensitivity to light and nutrients. Furthermore, heterogeneity of S_{HPO_4} observations (Figure 5.9) and local and short-term algal blooms observed during early spring (Finger et al., 2007a) also cause a broadening of the spring productivity peak, which is not considered in the model. Nevertheless, as simulations underestimate algal production just after the spring bloom, the temporally integrated production matches the observations almost perfectly.

(3) Summer: As a result of the intense algae growth in spring S_{HPO_4} drops below 0.5 mg m^{-3}. Simultaneously X_{ZOO} feeds on X_{ALG}, leading to typical phyto- and zooplankton densities

of ~0.12 gDM m^{-3} and ~0.015 gDM m^{-3}, respectively. Moreover, irradiance is reduced due to enhanced particle input (K_0 = ~0.6 m^{-1}). All these factors lead to low P^B of ~0.25 gC m^{-2} d^{-1} during the warmest months of the year. Overall, the summer is well predicted by the simulations.

(4) Fall: Upwelling, convective mixing and remineralization lead to an increase of S_{HPO_4} above 1 mg m^{-3}. Simultaneously surface turbidity decreases and light availability is increased. Therefore, algae growth experiences a second peak, which, however, is heavily smoothened due to elevated X_{ZOO} feeding immediately on X_{ALG}. Consequently the production peak in fall is more expressed by X_{ZOO} than by X_{ALG}.

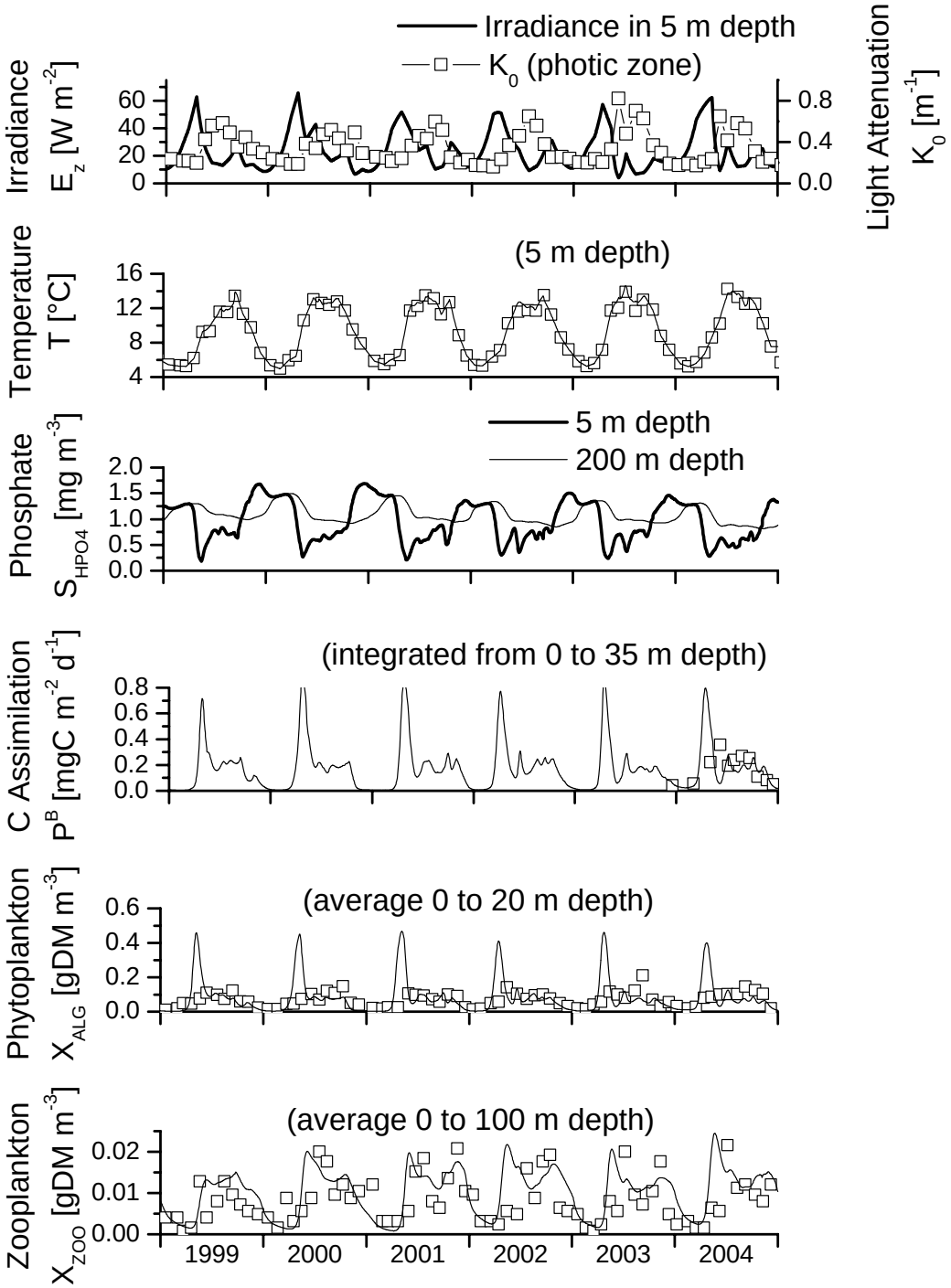

Figure 5.8: Simulated and observed productivity-related parameters in the epilimnion of Lake Brienz between 1999 and 2004: open squares represent measurements presented in companion studies (references in Table 5.4). Solid lines illustrate simulations.

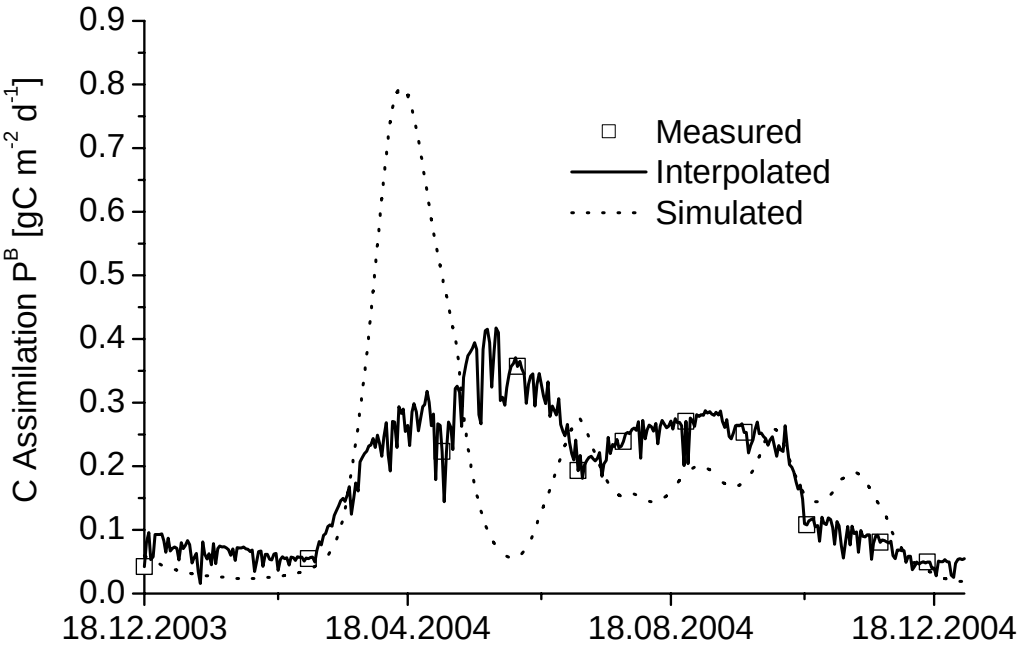

Figure 5.9: Estimated C Assimilation in the photic layer of Lake Brienz: open squares illustrate measured in situ assimilation, black line shows interpolations according to Finger et al. (2007a) and dotted line represents simulated C assimilation.

Despite the fact that these simulations include only one class of phytoplankton, they predict present observations reasonably well. As our objective is the assessment of the effects of anthropogenic influences, the annually integrated predictions are of greater relevance than the details of the short-term temporal dynamics.

5.4.3 The flood of 1999

In May 1999 discharge from Lake Brienz was 63% above the seasonal mean. As discussed by Finger et al. (2006; 2007a) intense snow fall during the preceding winter and heavy precipitation led to flooding and subsequent enhanced surface turbidity, reducing gross algae production in Lake Brienz. Nevertheless, besides *Daphnia* densities, no significant reduction in plankton densities (Figure 5.2) or composition was observed after the flood. Simulations predict zooplankton densities significantly below average in spring 1999 (Figure 5.10). Although the simulations probably overestimate algae production during spring, they demonstrate the relative effect of the 1999 flood on plankton biomass. Lower temperatures and enhanced surface turbidity delayed the algae production by about half a month, which

however was compensated later on due to S_{HPO_4} availability. Subsequently, X_{ZOO} remained significantly below typical values in spring, as growth was limited by low temperatures and X_{ALG} . It could therefore not compensate the increased washout due to unusually high discharge. Considering that these simulations include only one functional zooplankton group, we can conclude that plankton with lower growth rates are even less capable of compensating washout. As simulated growth is overestimated in spring it can be assumed that the effect of plankton washout in 1999 is rather underestimated. Taking into account the relatively low growth rates of *Daphnia*, a selective washout as postulated by Rellstab et al. (2007) seems realistic.

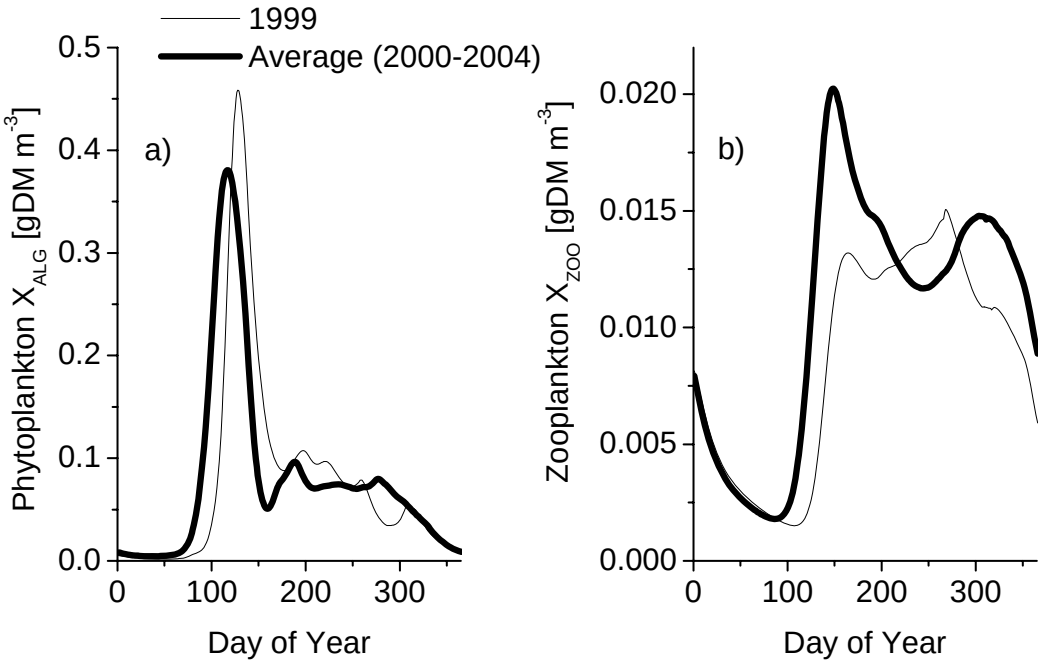

Figure 5.10: Simulated concentrations of phytoplankton (average 0 to 20 m depth; a) and zooplankton (average 0 to 100 m depth; b) for the year 1999 and the average for the years 2000 to 2004.

5.4.4 Scenarios with increased phosphate input

For assessing the effects of changing P input (Figure 5.2), simulations of the hypothetical scenarios with altered P input were performed as summarized in Table 5.5. Since the model has been calibrated for present conditions, the following predictions do not account for different plankton composition and adapted growth rates which may occur under changing

trophic conditions (Anneville et al., 2005). Nevertheless, the simulations indicate general alterations within the ecosystem of Lake Brienz.

Annual P fluxes, average in situ S_{HPO_4}, annual gross production, average P content in algae and average plankton density for altered P input (scenarios 'P1' to 'P5') are summarized in Table 5.7. Average S_{HPO_4} increases almost proportionally with increasing P input both in the epilimnion and in the hypolimnion (e.g. for a 5-fold of present S_{HPO_4} input, the simulation predicts 6.8 times higher average S_{HPO_4} concentrations). Yet, P^B increases only slightly with P input and drops below present values for 4- and 5-times present P input, and X_{ALG} shows a similar behavior. On the other hand, algal P content and average X_{ZOO} increase proportionally to P input (Table 5.7). Test runs without X_{ZOO} predict much higher X_{ALG} indicating the strong top-down limitation. This top-down effect appears to become stronger with increasing P input. Simulations for doubled P input (scenario 'P2') fall in line with observations of plankton biomass and production during 1987 (Kirchhofer, 1990), when P input amounted up to ~13 tP yr^{-1} (Table 5.7; Figure 5.2a).

Algae growth is modeled with a variable C:P ratio with respect to phosphate (Equation 5.1). In contrast, zooplankton is modeled with constant Redfield composition. In order to maintain a fixed C:P ratio under varying P content in algae biomass (b_P), the feeding requirement of zooplankton must be inversely proportional to the P content in algae (Figure 5.11). In the 'Present' scenario the ultra-oligotrophic status of the lake leads to extremely low b_P and subsequently the feeding requirement of zooplankton is accordingly high. With increasing S_{HPO_4} the nutritional value of algae increases and the top-down limitation by zooplankton becomes more important.

Table 5.7: Simulated P fluxes, production, phosphate and plankton concentrations for the different P scenarios [1]

	Unit	**'Present'**	**'P1'**	**'P2'**	**'P3'**	**'P4'**	**'P5'**	**1987**[2]
$P_{additional}$	tP yr^{-1}	2.2	2.2	2.2	2.2	2.2	2.2	
$P_{Aare,epi}$	tP yr^{-1}	3.8	5.6	7.6	11.4	15.2	19.1	
$P_{Luet,epi}$	tP yr^{-1}	1.1	1.1	2.1	3.2	4.3	5.3	
$P_{Aare,hyp}$	tP yr^{-1}	0.4	0.7	0.9	1.3	1.8	2.2	
$P_{Luet,hyp}$	tP yr^{-1}	0.3	0.3	0.5	0.8	1.1	1.3	
P_{TOT}	tP yr^{-1}	7.8	9.8	13.4	18.9	24.5	30.1	12.9
P_{out}	tP yr^{-1}	1.8	2.3	3.2	5.1	8.1	12.0	
S_{255}[3]	tP yr^{-1}	5.9	7.5	10.2	13.9	16.4	18.1	
Average S_{HPO_4} in 5 m	mg m^{-3}	1.0	1.2	1.7	2.9	4.6	6.8	1.7 to 4.2
Average S_{HPO_4} in 200 m	mg m^{-3}	1.1	1.3	1.7	2.6	4.4	6.5	1.7 to 4.2
C Assimilation	gC m^{-2} yr^{-1}	62.6	71.8	82.2	81.8	61.8	46.0	103
$a_{P,ALG} = \frac{X_{P,ALG}}{X_{ALG}}$ [4]	gP gDM^{-1}	0.0019	0.0021	0.0024	0.0035	0.0056	0.0074	
Phytoplankton density	gDM m^{-3}	0.080	0.080	0.076	0.061	0.040	0.028	0.077
Zooplankton density	gDM m^{-3}	0.010	0.013	0.019	0.025	0.031	0.034	

[1] All values present averages for 1999 to 2004

[2] Observations in 1987: total P Input (P_{TOT}) according to Müller et al. (2007a), other values according to Kirchhofer (1990).

[3] S_{255} represents P flux to sediment: $P_{TOT} - P_{out}$.

[4] Average algal P content.

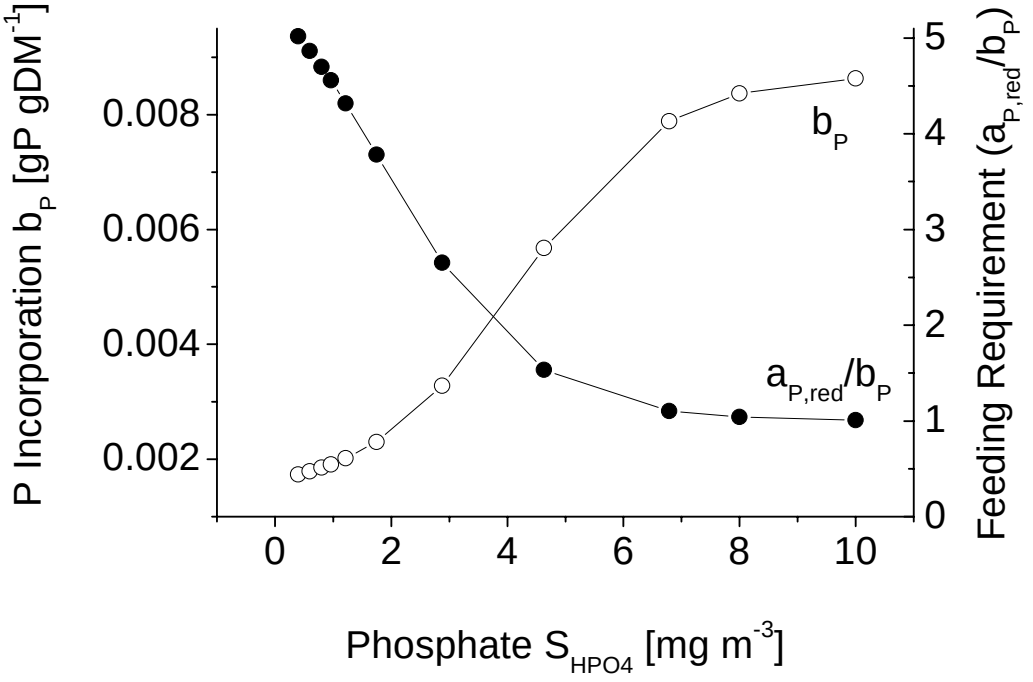

Figure 5.11: P incorporation (b_P) in algae and feeding requirement per mass zooplankton on phytoplankton ($a_{P,red} / b_P$) as a function of phosphate concentration.

The partial insensitivity of X_{ALG} is supported by long-term phytoplankton observations since 1968 (Nef, 1992), which show little to no trends, even though P supply to the lake has varied considerably throughout the same time period (Figure 5.2). Similar nutrient-limited zooplankton growth has been observed in numerous other studies (Hessen, 1992; Urabe and Watanabe, 1992; Elser and Hassett, 1994).

The temporal dynamics of simulated S_{HPO_4}, P^B, and plankton densities for four scenarios listed in Table 5.5 are illustrated in Figure 5.12: 'Present' scenario with present S_{HPO_4} loads, 'P1' scenario with two tons of additional S_{HPO_4} input - corresponding to the amount of P presently trapped in the upstream reservoirs (Müller et al., 2007a) - and ('P2', 'P3' and 'P5' scenarios) with successively increasing S_{HPO_4} up to 5-times present loads. A temporal shift can be observed in the simulations of plankton dynamics. Phytoplankton, as well as zooplankton populations regenerate earlier in the year with increasing P supply. The simulations indicate that the zooplankton spring peak might have developed up to two months earlier during the eutrophication phase compared to the present situation. This insight falls in

line with observations of *Daphnia* populations, which appear to reach today maximal densities later in the year than ten years ago (Rellstab et al., 2007). Furthermore, a clear-water phase following the spring peak, where X_{ALG} drops to very low levels, can be observed in the scenarios with increased P input. This clear-water phase has been rudimentarily observed in 1987 (Kirchhofer, 1990) when annual P input is estimated to ~13 tP yr^{-1}, as discussed in section 5.5.

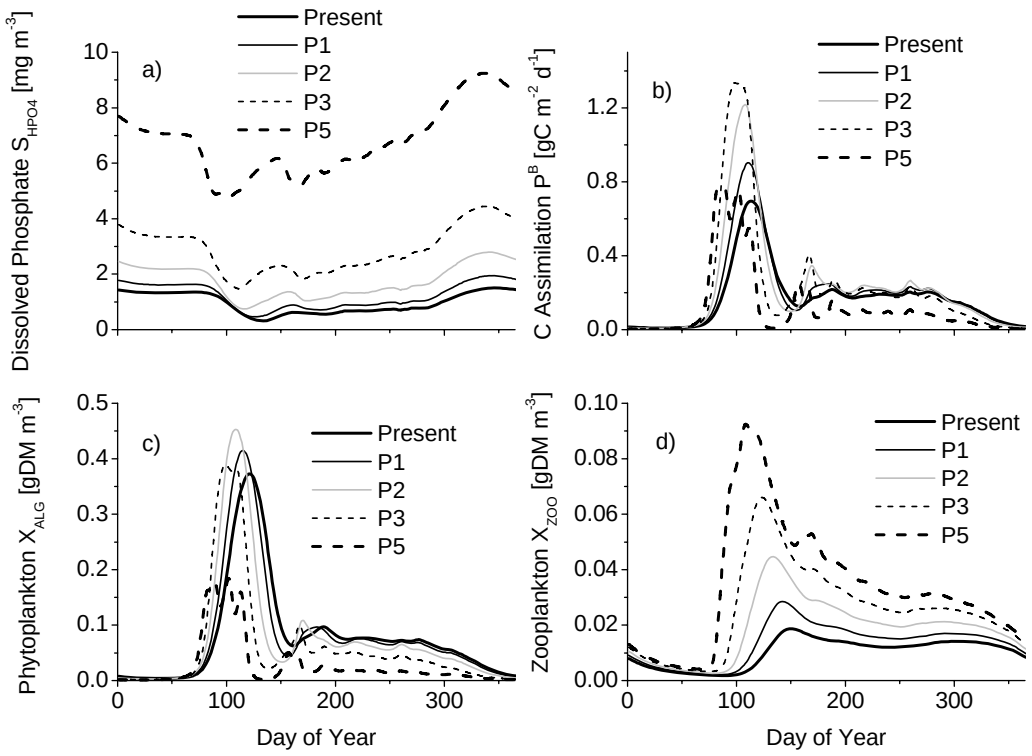

Figure 5.12: Simulated phosphate concentration (a), C assimilation (b), as well as phytoplankton (average 0 to 20 m depth; c) and zooplankton (average 0 to 100 m depth; d) for different P loads. Definition of scenarios is given in Table 5.5.

5.4.5 Scenarios without upstream hydropower

Regarding the effects of hydropower operations on the biogeochemical cycling in Lake Brienz, four altered boundary conditions have to be considered: (1) the altered seasonal dynamics of riverine P input to Lake Brienz as a result of water retention during summer and its release during winter, (2) the modified light attenuations as summarized in Figure 5.4, (3) retention of up to 2 tP yr^{-1} of phosphate in the hydropower reservoirs (Müller et al., 2007a),

and (4) altered river intrusion depth as parameterized by Finger et al. (2006). Model runs indicate that simulated plankton density reacts most sensitive to altered light attenuation and P retention, whereas the effects of altered intrusion or seasonal discharge dynamics alone are negligible.

In Table 5.8 annual P fluxes, average S_{HPO_4} in the epilimnion and hypolimnion, annual gross production, average P content in phytoplankton and average phyto- and zooplankton density are summarized for the following scenarios: 'No-dam 1' scenario with 'no-dam' light attenuation and discharge patterns, 'No-dam 2' as 'No-dam 1' but with an additional input of 2 tP yr^{-1} (upstream P retention) and 'no-dam' river intrusion dynamics, and 'Lake Thun' scenario representing the hypothetical situation in Lake Brienz without the impact of allochthonous particles (using light attenuation from Lake Thun).

Table 5.8: Simulated P fluxes, production, phosphate and plankton concentrations in the 'Present', the 'no-dam' and the 'Lake Thun' scenarios [1]

	Unit	**'Present'**	**'No-dam 1'**	**'No-dam 2'**	**'Lake Thun'[2]**	**Lake Thun measured**
$P_{additional}$	tP yr^{-1}	2.2	2.2	2.2	2.2	
$P_{Aare,epi}$	tP yr^{-1}	3.8	3.6	5.1	3.8	
$P_{Luet,epi}$	tP yr^{-1}	1.1	1.1	1.1	1.1	
$P_{Aare,hyp}$	tP yr^{-1}	0.4	0.3	0.6	0.4	
$P_{Luet,hyp}$	tP yr^{-1}	0.3	0.3	0.3	0.3	
P_{TOT}[3]	tP yr^{-1}	7.8	7.4	9.2	7.8	
P_{out}	tP yr^{-1}	1.8	1.8	2.2	1.3	
S_{255}[4]	tP yr^{-1}	5.9	5.6	7.0	6.4	
Average S_{HPO_4} in 5 m	mg m^{-3}	1.0	0.9	1.1	0.7	< 3[5]
Average S_{HPO_4} in 200 m	mg m^{-3}	1.1	0.8	1.0	0.8	< 3[5]
C Assimilation	gC m^{-2} yr^{-1}	62.6	63.1	71.1	74.5	95.0[6]
$a_{P,ALG} = \frac{X_{P,ALG}}{X_{ALG}}$ [7]	gP gDM^{-1}	0.0019	0.0019	0.0020	0.0018	
Phytoplankton density	gDM m^{-3}	0.081	0.080	0.079	0.087	0.112
Zooplankton density	gDM m^{-3}	0.010	0.011	0.015	0.013	0.016

[1] All values present averages for 1999 to 2004

[2] 'Lake Thun' scenario represents the scenario of Lake Brienz with light conditions as observed in Lake Thun.

[3] Discharge previous to damming (1910 to 1930) was about 5% below present discharge (probably due to global warming), explaining the lower P input in 'No-dam1' scenario.

[4] S_{255} represents P flux to sediment: P_{TOT} - P_{out}.

[5] Total P during winter circulation (Ochsenbein and Mattmann, 2003).

[6] Estimations for Lake Brienz with light conditions of Lake Thun according to Finger et al. (2007a).

[7] Average algal P content.

The annual production and average plankton biomass are only weakly influenced by the different light conditions in the 'No-dam 1' scenario. Significant differences can only be noted in scenarios 'No-dam 2' where the P input is increased by 2 tP yr^{-1}. In 'No-dam 2' scenario the annual production increases by ~15%, average P content in algae by ~5% and subsequently zooplankton density increases by ~40%. In the 'Lake Thun' scenario, implying a clear lake, annual production increases by ~19%, while average P content in algae decreases by ~5%. As a consequence, both, phyto- and zooplankton density increase by ~7% and ~28%, respectively. Long-term observations in Lake Thun indicate indeed about ~30% more phytoplankton than in Lake Brienz (Nef, 1992).

The temporal dynamics of S_{HPO_4}, P^B, X_{ALG} and X_{ZOO} in the 'Present' scenario and the two 'No-dam' scenarios are compared in Figure 5.13. The lower light attenuation in the 'No-dam' scenarios favors algae growth during winter and spring. Subsequently S_{HPO_4} is earlier depleted, and the phyto- and zooplankton peaks occur almost two months earlier in the year. During summer intense turbidity and low S_{HPO_4} reduce algae production. Consequently zooplankton is diminished as well, while S_{HPO_4} increases due to low production. As a result, a second, less intense algae peak and a distinct second zooplankton maximum occur in fall. This temporal behavior was qualitatively observed in the year 1922 before the construction of the dams (Flück, 1926).

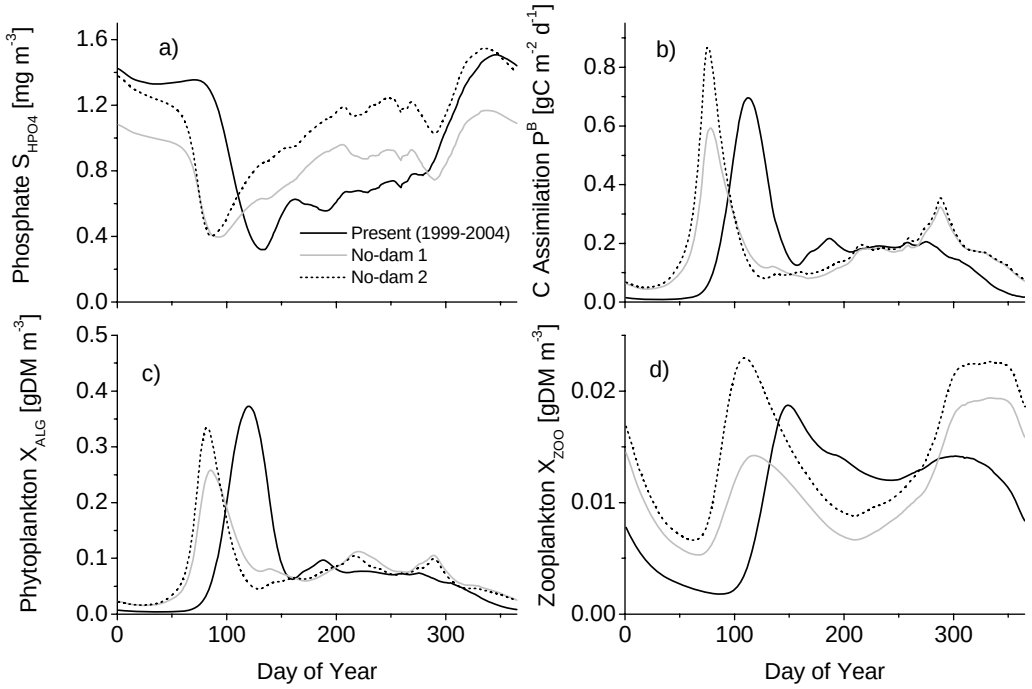

Figure 5.13: Simulated phosphate concentration (a), C assimilation (b), as well as phytoplankton (average 0 to 20 m depth; c) and zooplankton (average 0 to 100 m depth; d) for the 'present situation' scenario and under hypothetical 'no-dam' conditions. Definition of scenarios is given in Table 5.5.

5.5 Discussion

Although numerical simulations remain a partial description of reality, they are a powerful tool to interpret experimental observations. In this case study on Lake Brienz, the sensitivity of the biological functioning was assessed in regard to two recent anthropogenic influences: (i) oligotrophication and (ii) altered surface turbidity due to upstream damming.

Attention was drawn to Lake Brienz because of declining fishing yields, which indicate that the ecosystem is drastically affected by one or both of those interferences. While the fishing yield declined between 1975 and 2005 almost proportionally to decreasing P supply, average phytoplankton mass appears to be less sensitive to P decline (Figure 5.2). Experimental data show that phytoplankton adapts to the trophic status of natural waters (Guildford and Hecky, 2000), incorporating less P per unit biomass at low P levels, whereas zooplankton reveals an almost constant C:P ratio (Andersen and Hessen, 1991) and consequently adapts its feeding requirement to P content in algae. By applying this concept in

our model, we could show that phytoplankton density is not very sensitive to increasing P input, falling in line with the long-term phytoplankton observations (Figure 5.2). In contrast, zooplankton grows much more efficiently on the same amount of algal mass, as the nutritious value of algae becomes higher with increasing P content. Consequently, simulated zooplankton density increases almost linearly with the P input, while algal dry mass remains almost at present levels.

Simulations for more than 4-fold present P input produced unrealistic results, indicating a drastic change in the composition of phyto- and zooplankton that would require a different calibration of the model. Such a change in composition was also observed by Kirchhofer (1990), when he compared plankton composition in 1987 (higher P input than today; Figure 5.2) with observations from the year 1922 prior to cultural eutrophication (Flück, 1926).

Comparison of present algae dynamics and observations of phytoplankton wet mass in 1987 (Kirchhofer, 1990) confirm the temporal differences observed in simulations with different P inputs (Figure 5.14): Considering that in 1987, P input must have been ~13 t yr^{-1} (Figure 5.2a), the observations from 1987 can be compared to scenario 'P2' (Figure 5.12). Both simulated and observed phytoplankton depict a stronger and earlier spring peak for higher P input. Yet, on an annual basis only zooplankton increases with higher P inputs, indicating that zooplankton is nutrient-limited. Especially *Daphnia* have been found to be affected by such nutrient limited growth (Sommer, 1992; Urabe et al., 1997).

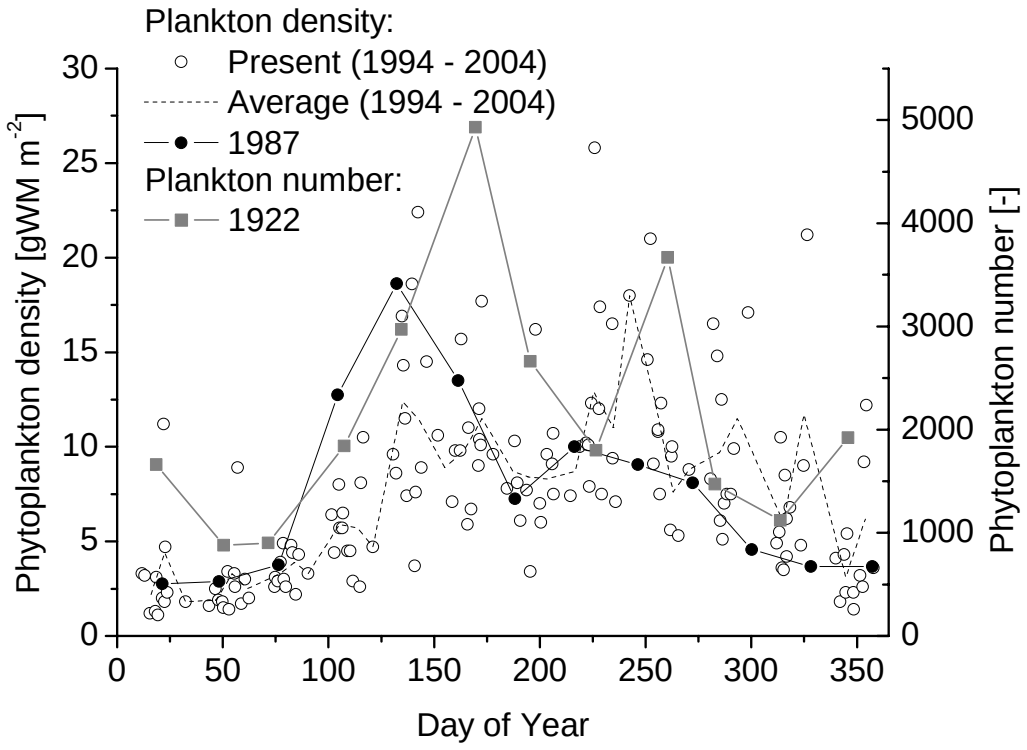

Figure 5.14: Observed phytoplankton densities (left scale) in Lake Brienz (0-20 m depth) during different epochs: open circles represent recent (1994 - 2004) plankton densities, filled circles indicate observations during enhanced P input in 1987 (Kirchhofer, 1990) and grey squares illustrate phytoplankton counts (right scale) observed in 1922 before the construction of hydropower dams (Flück, 1926).

While fishing yields in Lake Brienz were comparable to other peri alpine Swiss lakes during eutrophication, they declined to less than half of other lakes for P concentrations below 3 mg m^{-3} (Figure 5.15). This indicates that low P input alone cannot explain the declines in fishing yields. Besides low P the increased light attenuation due to allochthonous particles is the main cause for the low productivity of Lake Brienz (Finger et al., 2007a).

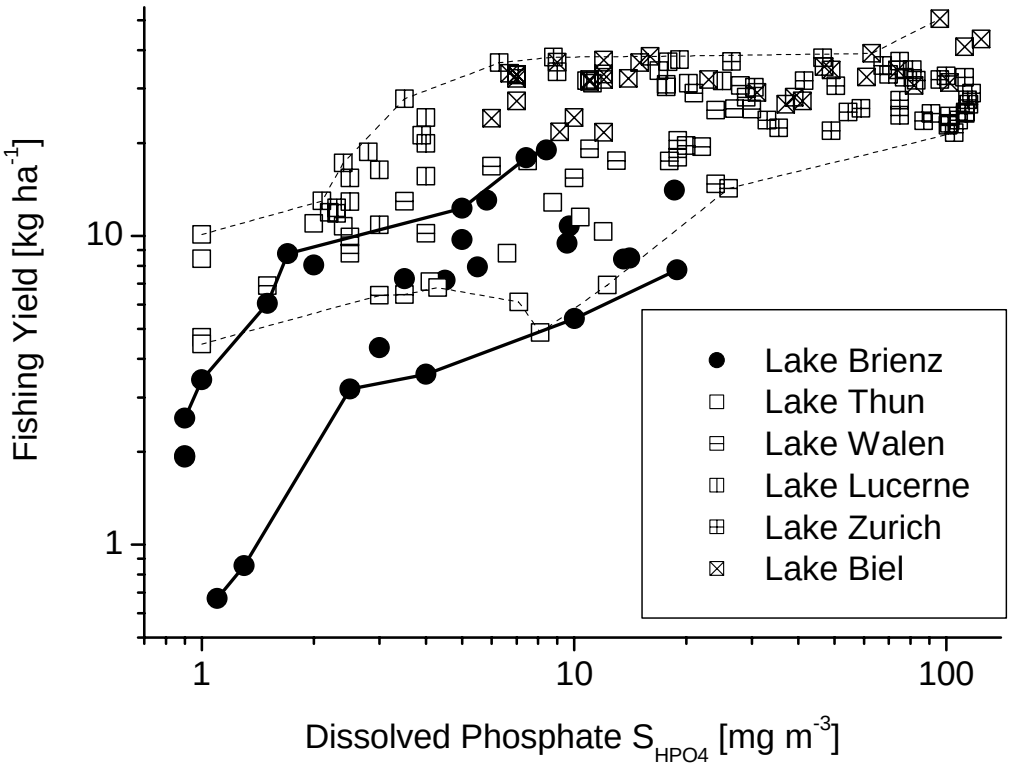

Figure 5.15: Comparison of fishing yields in the largest peri-alpine Swiss lakes. Circles indicate yields in Lake Brienz, squares indicate yields in other lakes, solid and dashed lines illustrate extreme yields in Lake Brienz and other lakes respectively. Figure adopted from Müller et al. (2007b).

Especially during winter when algae are randomly distributed by convective mixing, high turbidity reduces algal growth. Predictions of a hypothetical situation with no glacial particles (using PAR profiles from Lake Thun) indicate a 19% higher algal growth, while densities of phyto- and zooplankton increase by 7% and 28%, respectively. In contrary to increased P input, algal density reacts sensitively to increased irradiance. Due to unchanged P content in algae, the top-down limitation does not increase. Accordingly, phyto- and zooplankton profit both from enhanced light availability. These insights and the low fishing yields in Lake Brienz compared to Lake Thun indicate that turbidity especially affects production (and herewith fishing yields) under oligotrophic conditions (Figure 5.15). Furthermore it suggests that production and the entire food chains react sensitive to alterations in turbidity.

The main effect of altered surface turbidity due to upstream damming is a temporal shift of algae production. The 'No-dam' scenarios indicate that higher light availability during winter and spring would lead to higher production during this season, depleting P in the lake. Consequently, P concentrations would be lower at the end of spring, when water temperatures increase. During summer algae production would be primarily limited due to higher light attenuation (Figure 5.4), allowing an accumulation of P but causing a minimum in zooplankton biomass. Better light conditions in fall lead to a second algae growth peak, strongly top-down limited by zooplankton. This dynamics is confirmed by historical plankton counts from the year 1922 (Flück, 1926) illustrated in Figure 5.14. However, as discharge in spring 1922 was above average in both inflows, the lake may have been atypically turbid due to increased particle input (Finger et al., 2006). As a consequence, the algae bloom in spring might have occurred in 1922 later than under typical pre-dam conditions.

In summary, based on our simulations and long-term plankton density observations it can be concluded that in ultra-oligotrophic lakes algal biomass may not necessarily increase with increasing P input. However, the nutritious value of the algae increases proportionally to P availability. Thus, zooplankton becomes nutrient-limited at low P concentrations, as its feeding requirement per zooplankton mass is inversely proportional to the nutritious value of algae. In comparison to oligotrophication, temporal shifts of plankton dynamics due to hydropower production appear to have a minor effect on average zooplankton densities. However, these effects of light limitation become more important with ongoing oligotrophication. While the results of the present study do not indicate that the upstream dams were the main cause for the recent decline in fishing yields, they suggest that the damming induced changes must probably have amplified the effects of oligotrophication.

5.6 Acknowledgments

Time series of plankton densities and CTD profiles from 1994 to 2005 were kindly provided by Dr. M. Zeh of the Water and Soil Protection Laboratory of the Canton Berne (GBL). Phosphorus analyses were performed by C. Hoyle in the framework of her M.S. thesis. L. Jaun provided light attenuation data and P. Bossard, D. Steiner and E. Schäffer conducted primary production measurements. The manuscript profited from discussions with B. Müller, I. Ostrovsky, B. Wehrli, P. Reichert and J. Mieleitner. The research was funded by (1) Regional Government of Canton Bern, (2) KWO Grimselstrom, (3) Swiss Federal Office of Environment (FOEN), (4) communities on the shoreline of Lake Brienz and (5) Swiss Federal Institute of Aquatic Science and Technology (Eawag).

5.7 Appendix

All simulations were performed using the bio-geochemical model for mesotrophic Lake Zurich by Omlin et al. (2001). All changes from the original model are indicated in ***italics***.

Compartments: Lake

Mineral sedimentation in Lake Brienz exceeds 0.64 cm yr^{-1} (Finger et al., 2006) covering organic material at a high rate. Accordingly interactions with sediment can be neglected (Müller et al., 2007a). We therefore removed the two sediment layers in the original mode.

State variables (in alphabetical order):

State variable	Unit	Description
S_{HPO_4}	gP m^{-3}	Bio-available P (phosphate)
S_{O_2}	g m^{-3}	Dissolved oxygen
T	°C	Temperature
X	gDM m^{-3}	(Degradable) dead organic material
X_{ALG}	gDM m^{-3}	Algal biomass (dry mass)
X_P	gP m^{-3}	P incorporated in dead organic material
$X_{P,ALG}$	gP m^{-3}	P incorporated in algae
X_{PI}	gP m^{-3}	Phosphates adsorbed to dead organic material
X_{ZOO}	gDM m^{-3}	Zooplankton biomass (dry mass)

Variables concerning the nitrogen cycle have been removed from the original model, as nitrogen can be neglected for our purposes. Furthermore algal species were modeled as one class ('Planktothrix rubescens' was removed as it is irrelevant for Lake Brienz).

Process rates of biogeochemical conversion (in order of appearance):

	Process rate	Unit	Description
1	$r_{gro,ALG}$	gDM m^{-3} d^{-1}	Growth of algae
2	$r_{resp,ALG}$	gDM m^{-3} d^{-1}	Respiration of algae
3	$r_{death,ALG}$	gDM m^{-3} d^{-1}	Death of algae
4	$r_{gro,ZOO}$	gDM m^{-3} d^{-1}	Growth of zooplankton
5	$r_{resp,ZOO}$	gDM m^{-3} d^{-1}	Respiration of zooplankton
6	$r_{death,ZOO}$	gDM m^{-3} d^{-1}	Death of zooplankton
7	P_{up}	gP m^{-3} d^{-1}	Adsorption of phosphates to organic particles
8	$r_{miner,aero}$	gDM m^{-3} d^{-1}	Aerobic mineralization in water column
9	T_{relax}	°C d^{-1}	Adaptation of T to measured temperature in the surface layer to mimic heat budget

Processes of nitrification and anoxic mineralization were omitted compared to Omlin et al. (2001).

Inputs: River Aare ($S_{HPO_4,in,Aare}$, T_A), River Lütschine ($S_{HPO_4,in,Luet}$, T_L), and non-point sources ($S_{HPO_4,add}$)

Outputs: Outflow of River Aare

Other fluxes: S_{O_2} -gas exchange at surface

The following tables describe each of the processes mentioned above. The top cell indicates the respective process rate. Contribution of a process to the transformation rate of state variables is given by the product of the rate and the corresponding stoichiometric coefficient. Formulas for stoichiometric coefficients and appertaining constants are listed in sub tables below.

Process 1: Growth of algae

$$r_{gro,ALG} = k_{gro,ALG,20} \cdot \exp\left(\beta_{ALG} \cdot (T-20)\right) \cdot \frac{E(z)}{K_{I,ALG} + E(z)} \cdot \exp\left(\frac{-E(z)}{E_{photo}}\right) \cdot \frac{S_{HPO_4}}{K_{HPO_4,ALG} + S_{HPO_4}} \cdot X_{ALG}$$

Bio-geochemical conversion processes

State Variables	Stoichiometric coefficients	Description
X_{ALG}	1	Algal growth
$X_{P,ALG}$	b_P	Algal uptake of phosphate (Stoichiometry dependent on S_{HPO4})
S_{O_2}	***1.24***	According to the Redfield-ratio
S_{HPO_4}	$-b_P$	Reduction of phosphate in water

Equations	Description
$I_{Surface} = 134.6 - 100.3 \cdot \cos\left(t_{year} \cdot 2\pi / 365.25\right)$	*Average global radiation [W m^{-2}] for Lake Brienz; parameterized with measured data of MeteoSwiss*
K_0	Light attenuation coefficient [m^{-1}]
$E(z) = I_{Surface} \cdot e^{-K_0 z}$	In situ irradiance [W m^{-2}]
$b_P = \frac{\left(b_{P,\min} + b_{P,\max}\right)}{2} + \frac{\left(b_{P,\max} - b_{P,\min}\right)}{2} \cdot \tanh\left(\frac{S_{HPO_4} - S_{HPO_4,crit}}{\Delta S_{HPO_4}}\right)$	Dependence of P incorporation as a function of phosphate concentration [gP gDM^{-1}]

Constant variables	Unit	Value	Description
$k_{gro,ALG,20}$	[d^{-1}]	***3.0***	Max. specific growth rate at 20°C; fitted parameter
β_{ALG}	[°C^{-1}]	***0.069***	Temperature dependency coefficient for algae
E_{photo}	[W m^{-2}]	***330***	
$K_{HPO_4,ALG}$	[gP m^{-3}]	***0.0008***	Concentration at half saturation rate with respect to phosphate
$K_{I,ALG}$	[W m^{-2}]	***11***	Light intensity at half saturation rate for algal growth
$b_{P,\min}$	[gP gDM^{-1}]	0.0014	Minimum and maximum P content of newly produced algae
$b_{P,\max}$		0.0087	
w_{ALG}	[gWM gDM^{-1}]	5	factor for converting phytoplankton dry mass to wet mass
$S_{HPO_4,crit}$	[gP m^{-3}]	0.0042	Phosphate concentration at which algal growth switches to reduced P content
ΔS_{HPO_4}	[gP m^{-3}]	***0.0025***	Range within which production switches to reduced P

Process: Respiration of algae

$$r_{resp,ALG} = k_{resp,ALG,20} \cdot \exp\left(\beta_{ALG} \cdot (T-20)\right) \cdot \frac{S_{O_2}}{K_{O_2,resp} + S_{O_2}} \cdot X_{ALG}$$

Bio-geochemical conversion processes

State Variables	Stoichiometric coefficients	Description
X_{ALG}	-1	'Feeding' of algae on their biomass
$X_{P,ALG}$	$-a_{P,ALG}$	P release to water column
S_{O_2}	***-1.24***	S_{O_2} consumption; according to Redfield ratio; differs from Omlin et al. (2001) as we do not consider nitrogen cycle.
S_{HPO_4}	$a_{P,ALG}$	P release to water column

Equations	Description
$a_{P,ALG} = \frac{X_{P,ALG}}{X_{ALG}}$	Average algal P content [gP gDM^{-1}]

Constant variables	Unit	Value	Description
$k_{resp,ALG,20}$	[d^{-1}]	0.05	Maximum specific respiration rate at 20 °C
β_{ALG}	[°C^{-1}]	***0.069***	Temperature dependency coefficient for algae
$K_{0_2,resp}$	[g m^{-3}]	0.5	Concentration at half saturation rate

Process: Death of algae

$$r_{death,ALG} = k_{death,ALG,20} \cdot \exp\left(\beta_{ALG} \cdot (T-20)\right) \cdot X_{ALG}$$

Bio-geochemical conversion processes

State Variables	Stoichiometric coefficients	Description
X_{ALG}	-1	Algal death
$X_{P,ALG}$	$-a_{P,ALG}$	P transfer to dead organic matter
X	1	Increase in dead organic matter
X_P	$a_{P,ALG}$	P transfer to dead organic matter

Equations	Description
$a_{P,ALG} = \frac{X_{P,ALG}}{X_{ALG}}$	Average algal P content [gP gDM^{-1}]

Constant variables	Unit	Value	Description
$k_{death,ALG,20}$	[d^{-1}]	***0.06***	Specific death rate at 20 °C
β_{ALG}	[°C^{-1}]	0.046	Temperature dependency coefficient for algae

Process: Growth of zooplankton

$$r_{gro,ZOO} = k_{gro,ZOO,20} \cdot \exp\left(\beta_{ZOO} \cdot (T-20)\right) \cdot X_{ALG} \cdot X_{ZOO} \cdot \left(\min\left(1, \frac{a_{P,ALG}}{a_{P,red}}\right)\right)$$

Bio-geochemical conversion processes

State Variables	Stoichiometric coefficients	Description
X_{ZOO}	1	Zooplankton growth
X_{ALG}	-1 / Y_{ZOO}	Zooplankton feeding on algae
$X_{P,ALG}$	- $a_{P,ALG}$ / Y_{ZOO}	P transfer from phytoplankton to zooplankton
X	c_e × (1- Y_{ZOO}) / Y_{ZOO}	Increase of dead organic material due to fecal pellets
X_P	0	Fecal pellets contain no P
S_{O_2}	*-1.24* × (1- c_e) × (1 - Y_{ZOO}) / Y_{ZOO}	Oxidation of food, which is not excreted and not used for zooplankton biomass. Factor according to Redfield ratio; differs from Omlin et al. (2001) as we do not consider nitrogen cycle.
S_{HPO_4}	$a_{P,ALG}$ / Y_{ZOO} - $a_{P,red}$	P release due to inefficient zooplankton feeding

Equations

$a_{P,ALG} = \frac{X_{P,ALG}}{X_{ALG}}$	Average algal P content [gP gDM^{-1}]
$Y_{ZOO} = Y_{ZOO,\max} \cdot \left(\min\left(1, a_{P,ALG} / a_{P,red}\right)\right)$	Yield for zooplankton growth; the smaller the algal P content, the more algae must be eaten for zooplankton growth. [-]

Constant variables	Unit	Value	Description
$k_{gro,ZOO,20}$	[(gDM m^{-3})$^{-1}$d^{-1}]	***5.0***	Max. specific growth rate at 20 °C; fitted parameter
β_{ZOO}	[°C^{-1}]	0.08	Temperature dependency coefficient for zooplankton
c_e	[-]	0.7	Fraction of food excreted as fecal pellets (not used for zooplankton biomass)
$a_{P,red}$	[gP gDM^{-1}]	0.0087	P content of organic material according to Redfield
w_{ZOO}	[gWM gDM^{-1}]	***12.5***	factor for converting zooplankton dry mass to wet mass
$Y_{ZOO,\max}$	[-]	0.5	Maximum yield for zooplankton growth

Process: Respiration of zooplankton

$$r_{resp,ZOO} = k_{resp,ZOO,20} \cdot \exp\left(\beta_{ZOO} \cdot (T-20)\right) \cdot \frac{S_{O_2}}{K_{O_2,resp} + S_{O_2}} \cdot X_{ZOO}$$

Bio-geochemical conversion processes

State Variables	Stoichiometric coefficients	Description
X_{ZOO}	-1	"Feeding" on own biomass
S_{O_2}	***-1.24***	S_{O_2} consumption; according to Redfield ratio; differs from Omlin et al. (2001) as we do not consider nitrogen cycle.
S_{HPO_4}	$a_{P,red}$	P release to water column

Constant variables	Unit	Value	Description
$k_{resp,ZOO,20}$	[d^{-1}]	0.003	Maximum specific respiration rate
β_{ZOO}	[$°C^{-1}$]	0.08	Temperature dependency coefficient zooplankton
$a_{P,red}$	[gP gDM^{-1}]	0.0087	P content of organic material according to Redfield
$K_{O_2,resp}$	[g m^{-3}]	0.5	Concentration at half saturation rate

Process: Death of zooplankton

$r_{death,ZOO} = k_{death,ZOO,20} \cdot \exp(\beta_{ZOO} \cdot (T - 20)) \cdot X_{ZOO}$

Bio-geochemical conversion processes

State Variables	Stoichiometric coefficients	Description
X_{ZOO}	-1	Zooplankton death
X	1	Increase in dead organic matter
X_P	$a_{P,red}$	P transfer to dead organic matter

Constant variables	Unit	Value	Description
$k_{death,ZOO,20}$	[d^{-1}]	***0.04***	Specific death rate at 20 °C
β_{ZOO}	[$°C^{-1}$]	0.08	Temperature dependency coefficient zooplankton
$a_{P,red}$	[gP gDM^{-1}]	0.0087	P content of organic material according to Redfield

Process: Adsorption of phosphates to organic particles

$$P_{up} = abs\left(\frac{AreaGradient}{Area}\right) \cdot k_{upt} \cdot \left(a_{P,\max} - a_{PI}\right) \cdot \frac{S_{O_2}}{K_{O_2,ads} + S_{O_2}} \cdot S_{HPO4} \cdot X$$

Bio-geochemical conversion processes

State Variables	Stoichiometric coefficients	Description
X_{PI}	1	Adsorption of P to organic matter
S_{HPO_4}	-1	Reduction in phosphates

Equations

$a_{PI} = X_{PI} / X$	Mass of adsorbed phosphate per mass of X [gP gDM^{-1}]

Constant variables	Unit	Value	Description
$abs\left(\frac{AreaGradient}{Area}\right)$	[m^{-1}]		Sediment area per lake volume
k_{upt}	[m^4 gP^{-1} d^{-1}]	***3000***	Phosphate uptake rate constant
$a_{P,\max}$	[gP gDM^{-1}]	0.007	Maximum mass fraction of phosphate adsorbed to org. matter
$K_{O_2,ads}$	[g m^{-3}]	0.5	Concentration at half saturation rate

Process: Aerobic mineralization of organic material in open water

$$r_{miner,aero} = k_{miner,aero,20} \cdot \exp\left(\beta_{BAC} \cdot (T-20)\right) \cdot \frac{S_{O_2}}{K_{O_2,aero} + S_{O_2}} \cdot X$$

Bio-geochemical conversion processes			
State Variables	**Stoichiometric coefficients**		**Description**
X	-1		Mineralization of organic matter
X_P	$-a_P$		Release to water of incorporated P
X_{PI}	$-a_{PI}$		Release to water of adsorbed P
S_{O_2}	***-1.24***		Consumption of S_{O_2} ; according to Redfield ratio; differs from Omlin et al. (2001) as we do not consider nitrogen cycle.
S_{HPO_4}	$a_P + a_{PI}$		P release to water column
Equations			
$a_P = X_P / X$			Average P content in organic matter [gP gDM^{-1}]
$a_{PI} = X_{PI} / X$			Average P adsorbed to organic matter [gP gDM^{-1}]
Constant variables	**Unit**	**Value**	**Description**
$k_{miner,aero,20}$	[d^{-1}]	***0.02***	Aerobic specific mineralization rate at 20 °C in open water; fitted parameter
β_{BAC}	[°C^{-1}]	0.046	Temperature dependency coefficient bacteria
$K_{O_2,aero}$	[g m^{-3}]	0.2	Concentration at half saturation rate

Process: Heat exchange at surface (measured temperatures as boundary conditions)

T_{relax} = if z < $z_{epi,meta,\min}$ then k_{relax} × (T_{meas} - T) else 0 end if

Bio-geochemical conversion processes

State Variables	Stoichiometric coefficients	Description
T	1	Adaptation of T to measured surface temperature to mimic heat budget (except for short-wave solar radiation)

Constant variables	Unit	Value	Description
$z_{epi,meta,\min}$	[m]	***20***	Depth adapted to CTD measurements
k_{relax}	[d^{-1}]	20	Rate of temperature adaptation
T_{meas}	[°C]		Measured or interpolated temperatures from CTD profiles (as used in k-ε simulations)

Other processes:

Sedimentation [(1)]

Constant variables	Unit	Value	Description
$v_{sed,ZOO}$	[m d^{-1}]	$v_{up}(z) = Q(z) / A(z)$	Zooplankton does not sediment
$v_{sed,ALG}$	[m d^{-1}]	***0.4***	Settling velocity of algae X_{ALG}
$v_{sed,ORG}$	[m d^{-1}]	10	Settling velocity of organic material

[(1)] the incorporated sedimentation process effects the settling of particulate variables, as well as their removal, when reaching the sediment surface.
[(2)] Q stands for discharge and A for cross-sectional area at depth z.

Vertical mixing

Monthly diffusivity-profiles were determined with the physical lake model presented in Goudsmit et al. (2002).

CHAPTER 6

Conclusions and outlook

6.1 Approach

In many Swiss lakes and streams long-term fishing yields indicate a persistent decline since the late 1970's. The causes, however, remain largely unknown (Burkhardt-Holm et al., 2002). A typical example is peri-alpine Lake Brienz and its two major tributaries, which are affected by allochthonous glacial particles, rendering them turbid during summer. There the fishing yield has dropped from over 15 kg ha^{-1} during the 1970's to less than 5 kg ha^{-1} in recent years. During the same period, build-up of efficient water treatment plants have reduced the bio-available phosphorus input from 30 tP yr^{-1} to about 8 tP yr^{-1}. Furthermore, since the 1930's several hydropower installations have been constructed in the headwaters of the main inflow, altering the turbidity dynamics.

The present thesis assesses the effects of damming and the impacts of reduced nutrient load on plankton biomass in Lake Brienz. For this purpose the particle balance of Lake Brienz was assessed throughout eight years (1997 to 2004). Based on numerical simulations the riverine particle transport and suspended matter concentrations in Lake Brienz were estimated for hypothetical conditions without upstream hydropower dams. These estimations allowed an assessment of the in-situ light attenuation for present and for no-dam conditions. Algae production, determined with the ^{14}C method, was measured throughout 18 months and related to in-situ light conditions. This relation was then used to estimate production under no-dam conditions. Finally, the assembled insights allowed the establishment and calibration of a one-dimensional biogeochemical model of Lake Brienz. The calibrated model was then used to estimate plankton densities for various scenarios with altered turbidity and increased P input.

Based on these measurements, simulations, and data analysis the following conclusions were drawn regarding anthropogenic impacts on (1) suspended particle loads and intrusion dynamics of the inflows, (2) light attenuation in the surface waters of Lake Brienz, (3) primary production in the photic layer of the lake, and (4) biomass development.

6.2 Suspended particle loads and intrusion dynamics

The annual allochthonous particle input to Lake Brienz amounts up to 300 kt yr^{-1}. Based on seismic measurements, Anselmetti et al. (2007) estimate that about 232 kt yr^{-1} of sediment is trapped in the upstream reservoirs of the Aare catchment. Consequently, the annual sediment loads are about 26% lower in Aare (128 kt yr^{-1}) than in Lütschine (174 kt yr^{-1}), although Aare discharge is twice that of Lütschine. The water retention in the reservoirs shifts sediment loads from summer to winter, increasing the suspended load during winter by ~2 kt mo^{-1}. During summer the suspended load is reduced by two thirds compared to the load without upstream reservoirs. The lower particle concentrations in Aare, combined with the lower salinity, reduce the density of Aare water. Consequently, Aare today intrudes over 80% of the time into the upper layer of Lake Brienz (compared to only 65% for Lütschine). As a direct consequence of the intrusion dynamics, the annual particle input to the upper layer of the lake is dominated by Aare (93 kt yr^{-1} as compared to 65 kt yr^{-1} from Lütschine). Nevertheless meteorological conditions can lead to considerable annual variability. For example during the heat wave in summer 2003, intense glacier melting led to a suspended particle load in Lütschine of 39% (242 kt yr^{-1}) above average, while the Aare load remained far below the long-term average. Accordingly, in 2003 particle supply to the upper layer of Lake Brienz was dominated by Lütschine.

Relevant for the biological production in the lake is the particle supply to the epilimnion. The numerical simulations show that hydropower operations doubled particle supply during winter, but halved the supply over the entire year (today: 158 kt yr^{-1}; no-dam: 307 kt yr^{-1}).

6.3 Light attenuation in the productive layer

The tremendous particle input leads to suspended particle concentrations in the surface layer (<50 m) between 1 and 2 g m^{-3} in winter and over 8 g m^{-3} during summer. According to numerical simulations particle concentrations would be below 1 g m^{-3} during winter and over 15 g m^{-3} during summer without hydropower dams. Based on this estimation, present light attenuation in summer (0.5 to 0.6 m^{-1}) is about half the attenuation under conditions without dams (1 to 1.2 m^{-1}). In contrast, during winter the present attenuation (~0.2 m^{-1}) is approximately twice the value for no-dam conditions (~0.1 m^{-1}).

The natural discharge regime - not the hydropower operation - is responsible for the strong inter-annual and short-term variability of attenuation, especially in spring and fall.

Extremely low attenuation, such as in fall 1995 (~0.15 m^{-1}), was caused by exceptionally low discharge. Vice versa, maximum attenuation was measured after heavy floods such as in August 2005 (0.9 to 1.2 m^{-1}). As a result, the light attenuation nowadays can temporarily still reach similar minimal and maximal values as under no-dam conditions.

Human perception of turbidity in natural waters can be quantified by light reflectance in the surface layer. Compared to the conditions during the productive late 1970's we expect reflectance presently to be ~20 to 25% higher than three decades ago because of lower absorption by organic compounds. In addition the biological and chemical sedimentation of fine particles is now reduced (Filella and Chanudet, unpublished data). More fine particles would enhance scattering and could increase reflectance by another ~20%. These findings give a realistic explanation for the increase in turbidity in the last decades as observed by residents.

6.4 Effects of light conditions on algae production

The annual gross production in Lake Brienz in 2004 amounts to ~70 gC m^{-2} yr^{-1}, which is particularly low when compared to other peri-alpine Swiss lakes. The reasons for the low production are the exceptionally low phosphorus level (< 1 µg L^{-1}) and strong light attenuation caused by allochthonous particles especially during summer. Maximum areal production of up to 0.4 gC m^{-2} d^{-1} is reached between May and June when phosphate concentrations are highest and light availability is favorable, as suspended particle concentrations have not yet reached their summer maximum. While production in spring occurs down to 30 m depth, it is limited to the upper 10 m of the water column during summer season. Consequently areal production in summer (~0.27 gC m^{-2} d^{-1}) is substantially lower than during spring. During the cold winter season areal production reaches a minimum (~0.05 gC m^{-2} d^{-1}).

Simulations with light and temperature data from Lake Thun (downstream of Lake Brienz, not affected by surface turbidity) indicate that production would be ~45% higher (~95 gC m^{-2} yr^{-1}) if the water in Lake Brienz were as clear as in Lake Thun. Nevertheless, production would still remain lower than in any of the other Swiss peri-alpine lakes.

Regarding the ecology of Lake Brienz, the heavy flooding in spring 1999 is of special interest, as drastic collapses of *Daphnia* population and fishing yields occurred for several months following the flood. Intense snow melt in spring led to low temperatures and elevated particle loads in the rivers. As a result, gross production was 23% below long-term average in May and June. The 'flood of the century' in August 2005 (Beniston, 2006) engendered an

exceptionally high particle concentration for that season in Lake Brienz. Accordingly, simulations indicate 13% lower annual production than average (1999-2005). However, no zooplankton decline was observed after the flood.

6.5 Biomass development during the last century

The biogeochemical model provides an ideal tool to synthesize the results of the previous chapters and to assess the overall effects on Lake Brienz. In contrast to the estimations based only on light attenuation, the biogeochemical model takes the entire nutrient cycling into account, allowing an assessment of the nutritious value of algae. Simulations and long-term observations indicate that phytoplankton hardly changed during the last 40 years, while phosphate, zooplankton, and fishing yield indicate a strong decline. This can be explained by a decline of the nutritious value of phytoplankton. As bio-available phosphorus decreases, algae incorporate less P, revealing a lower nutritious value. Subsequently zooplankton grows slower on the same amount of algae. In the late 1970's algal biomass had a higher nutritious value, and accordingly zooplankton could grow on the same amount of algae more efficiently.

Disregarding potential bio-available phosphorus retention in the reservoirs, hydropower operations primarily alter the temporal dynamics of plankton growth. The higher turbidity during winter and spring slows down production, leaving more phosphate for the following summer season. Consequently, the spring production peak is delayed by about two months. The higher production during summer consumes phosphate continuously, preventing a second production peak in fall. Without hydropower production, algae growth during summer would be severely hampered due to intense surface turbidity. This would allow an accumulation of phosphate and provoke a second production peak in fall.

6.6 Oligotrophication versus hydropower – synthesis and future challenges

The results of the presented model calculations allow a quantification of the effects of hydropower operations and reduced nutrients supply on algae production within Lake Brienz. Although hydropower operations significantly affect the temporal dynamics of surface turbidity and algae production, annual zooplankton biomass is primarily affected by the efficient sewage water treatment, which reduces nutrient supply to the lake. Hence, in regard

to the continuous decline of fishing yields since the late 1970's, the primarily responsible factor is re-oligotrophication, not upstream hydropower operations. The most eminent impact caused by hydropower operations appears to be the bio-available phosphorus retention (~25% of the total annual load) in the upstream reservoirs. Nevertheless, present phosphorus input is still estimated to be higher today than at the beginning of the 20th century (Müller et al., 2007a).

Following the press conference of 4 July 2006, where, amongst other studies, the results of this thesis were presented, demands for artificial fertilization or less efficient sewage treatment have grown stronger. Such measures are not advisable for the following reason:

In 1953 the Swiss citizens decided to introduce water protection into the federal constitution, establishing the framework for a nation-wide conservation of natural waters. The ulterior motive of the law was to protect natural waters, preserve valuable drinking resources, establish lasting recreational areas for locals and provide living space for flora and fauna. Within this spirit it is not advisable to artificially fertilize a lake which depicts a naturally low trophic status.

The changes in surface turbidity due to hydropower operations do affect the temporal dynamics of biomass development in Lake Brienz. However, the results of the present study and companion studies indicate a minor or insignificant effect on fish populations (Müller et al., 2007a; Müller et al., 2007b; Rellstab et al., 2007; Wüest and Zeh, 2007). Nevertheless, with ongoing oligotrophication the effects of light limitation become more important for primary production. While oligotrophication is the primary cause for declining fishing yields, the results of the presented model calculations suggest that the effects of oligotrophication are amplified by damming induced changes in turbidity. This is especially important in regard to future dam projects upstream of Lake Brienz.

In order to boost hydropower production in winter, KWO plans to increase the dams of Grimselsee in the near future by 23 m (Figure 6.1). Such a reservoir extension would increase the hydropower production by less than 1% (additional energy production: ~20 GWh yr^{-1}; present production: ~2250 GWh yr^{-1}; KWO data). The financial incentive of such a project lies in the energy production during winter when energy prices are high. Winter energy production in turn increases the suspended particle load to Lake Brienz during this period and hence the effects of hydropower operation would be amplified. An increase of the dam would also imply a greater retention of bio-available phosphorus in the reservoirs. Hence, under conditions with an increased dam Lake Brienz would become still more oligotrophic and the effects of hydropower operations would be intensified. From a water management point of

view further clarifications should be undertaken to predict ecological consequences of such future hydropower projects. The presented numerical models are appropriate tools to perform such predictions and to assess the risk of potentially severe ecological consequences. Furthermore, model calculations of future scenarios could be used to elaborate adequate mitigation measures in order to minimize impacts of future dam projects.

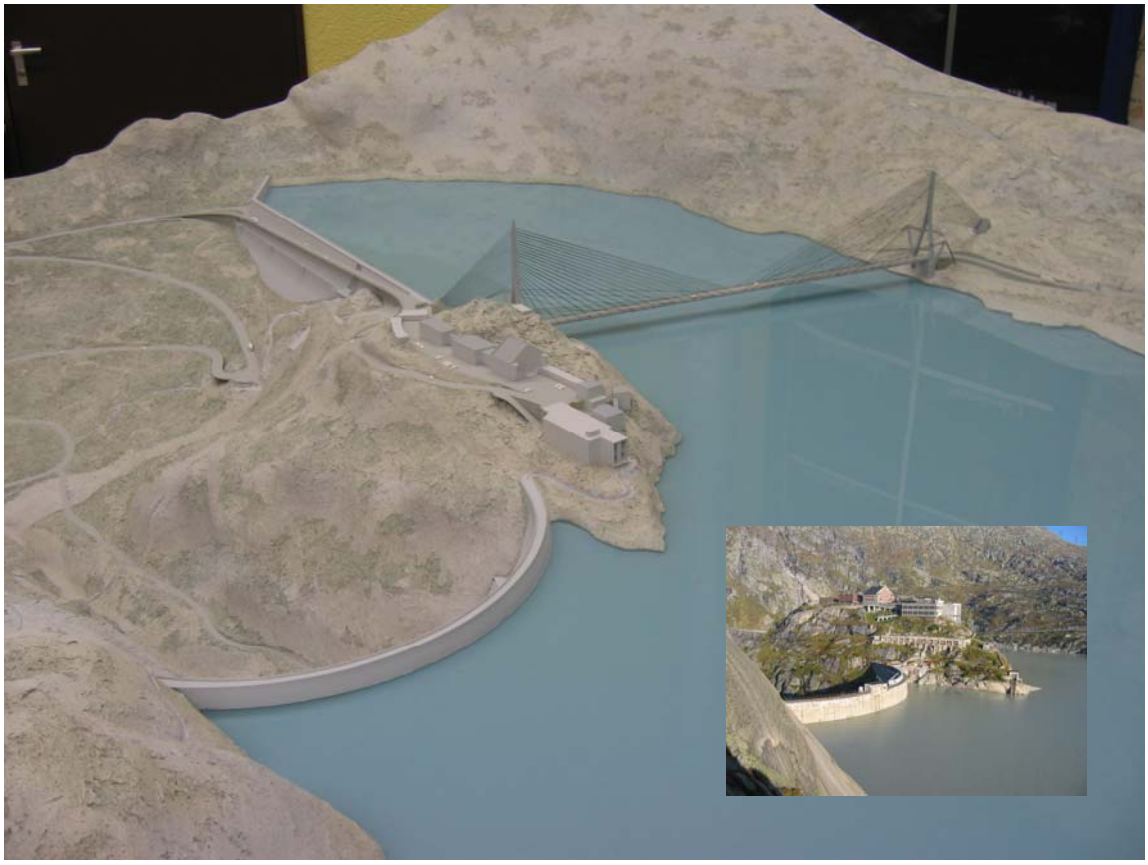

Figure 6.1: Model for a 23 m higher dam of Grimselsee (big picture) and present Grimselsee (small picture).

ACKNOWLEDGEMENTS

After four years of research on Lake Brienz I am just about to accomplish my Ph.D. To have made it so far I owe lots of thanks to many people for their help and encouragement throughout my thesis. I would like to take this opportunity to express my sincere thanks to some of the inspirers.

Alfred Wüest, alias 'Johny', was literally sparkling with new ideas as soon as I accomplished the old ones. 'Johny' has the remarkable talent to identify immediately which aspects of a scientific problem are essential and which are irrelevant. This is perhaps the most important competence in nowadays research. Thanks 'Johny' for all the inspiration and pointing out the little but important details in the world of science...

The one and only Michael Schurter! I guess every Ph.D. student from kb will agree with me that 'Michi' is just fabulous! I will really miss the long days with 'Michi' on Lake Brienz, by sun, rain, snow and hail... Thanks Michi for showing me all the helpful fieldwork tricks!

No arithmetic problem can puzzle Martin Schmid. Martin was of outstanding help for any logical or arithmetic problem. Besides his ingenuity, he is a talented writer and cross-read my manuscripts several times improving them significantly. Thanks Martin for all your help!

Everyone who ever worked with Catherine Hoyle will never ever forget her enthusiasm and endurance, whether it be for labelling samples, cutting sediment cores or sequentially extracting phosphorus... but most of all, her cheerfulness is unforgettable. Thanks Catherine for your collaboration and for all the happiness!

A mission has to be accomplished? It's a Lorenz Jaun job! Lorenz has the excellent quality to manage any situation well tempered and factually. When other people's blood pressure rises, Lorenz remains the calmness in person. Thanks Lorenz for your continuous and thorough support!

The success of this thesis was only possible due to excellent collaboration between various institutions. For this reason I would like to express my sincere thanks to the following persons who shared valuable data sets and important know how, which were essential for the success of the present study: Adrian Jakob (LHG) and Markus Zeh (GSA) provided river and lake data; Romeo Clausen and René Wiegenbröker (both KWO) provided water flow data from the hydropower scheme; Michael Sturm (Eawag), Flavio Anselmetti (ETH) and Stephanie Girardclos (ETH) provided supportive discussions on sedimentation. Bastian Bommer (EMPA) and Denis Mavrcordatis (Eawag) instructed me on particle size distribution analysis; Montserrat Filella and Vincent Chanudet (both University of Geneva) provided important input on colloids. Beat Müller and Ruth Stierli (both Eawag) performed numerous phosphorus analysis. Peter Bossard (Eawag) provided me with valuable ideas and information on modeling primary production.

Furthermore I would like to address my cordial thanks for joint efforts on the field to Alois Zwyssig, Christian Rellstab, Torsten Diem, Andreas Lorke, Daniel Steiner, Erwin Schäffer, Prashant Kumar, Lorenz Moosmann, Esther Keller, Daniela Richter, Annika Wagenhoff, Maria Alp and my sister Corinna Meukow.

Special thanks go also to my office mates Andreas Matzinger, Werner Göggel, Dan McGinnis, Claudia Lorrai and Emel Sahan for numerous every day advices and to Susanne Bauer who cross-read large parts of the thesis.

Last but not least, I express my sincere gratitude to my girlfriend Estellita. Estelle Bianchi encouraged me with her patience and tenderness and always had an open ear during tough times. Merci pour ta patience ☺!

Funding for the Ph.D. project was provided by (1) regional government Canton of Bern, (2) KWO Grimselstrom, (3) Swiss Federal Office of Environment, Forest and Landscape (BUWAL), (4) Lake Brienz shoreline communities and (5) Eawag.

REFERENCES

Aksnes, D. L., and A. C. W. Utne, 1997. A revised model of visual range in fish. Sarsia **82:** 137-147.

Andersen, T., and D. O. Hessen, 1991. Carbon, nitrogen, and phosphorus content of freshwater zooplankton. Limnology and Oceanography **36:** 807-814.

Anderson, N. J., E. Jeppesen, and M. Sondergaard, 2005. Ecological effects of reduced nutrient loading (oligotrophication) on lakes: an introduction. Freshwater Biology **50:** 1589-1593, doi:10.1111/j.1365-2427.2005.01433.x.

Anneville, O., S. Gammeter, and D. Straile, 2005. Phosphorus decrease and climate variability: mediators of synchrony in phytoplankton changes among European peri-alpine lakes. Freshwater Biology **50:** 1731-1746, doi:10.1111/j.1365-2427.2005.01429.x.

Anselmetti, F. S., R. Bühler, D. Finger, S. Girardclos, A. Lancini, C. Rellstab, and M. Sturm, 2007. Effects of Alpine hydropower dams on particle transport and lacustrine sedimentation. Aquatic Sciences **in press**.

APHA, 1998. Standard methods for the examination of water and wastewater, American Public Health Association, Washington, DC, 2-57 - 2-58 pp.

Armengol, J., L. Caputo, M. Comerma, C. Feijoo, J. C. Garcia, R. Marce, E. Navarro, and J. Ordonez, 2003. Sau reservoir's light climate: relationships between Secchi depth and light extinction coefficient. Limnetica **22:** 195-210.

Arst, H., 2003. Optical properties and remote sensing of multicomponental water bodies, Springer, Praxis-Publisher, Chichester, 231 pp.

Ashley, K., L. C. Thompson, D. C. Lasenby, L. McEachern, K. E. Smokorowski, and D. Sebastian, 1997. Restoration of interior lake ecosystem: the Kootenay Lake fertilization experiment. Water Quality Research Journal of Canada **32:** 295-323.

Babin, M., D. Stramski, G. M. Ferrari, H. Claustre, A. Bricaud, G. Obolensky, and N. Hoepffner, 2003. Variations in the light absorption coefficients of phytoplankton, nonalgal particles, and dissolved organic matter in coastal waters around Europe. Journal of Geophysical Research **108:** 3211, doi:10.1029/2001JC000882.

Baker, E. T., and J. W. Lavelle, 1984. The effect of particle-size on the light attenuation coefficient of natural suspensions. Journal of Geophysical Research-Oceans **89:** 4C0622, 8197-8203.

Bartholow, J. M., S. Campbell, and M. Flug, 2005. Predicting the thermal effects of dam removal on the Klamath River. Environmental Management **34:** 856-874, doi: 10.1007/s00267-004-0269-5.

Beauchamp, D. A., C. M. Baldwin, J. L. Vogel, and C. P. Gubala, 1999. Estimating diel, depth-specific foraging opportunities with a visual encounter rate model for pelagic piscivores. Canadian Journal of Fisheries and Aquatic Sciences **56:** 128-139.

Beniston, M., 2006. August 2005 intense rainfall event in Switzerland: Not necessarily an analog for strong convective events in a greenhouse climate. Geophysical Research Letters **33:** L05701, doi:10.1029/2005GL025573.

Bezinge, A. 1987. Glacial meltwater streams, hydrology and sediment transport: the case of the Grande Dixence hydroelectricity scheme, pp. 473-498. In A. M. Gurnell, and M. J. Clark (Eds): *Glacio-Fluvial Sediment Transfer*, John Wiley and Sons, Chichester.

Biggs, B. J. F., and R. J. Davies-Colley, 1990. Optical-properties of Lake Coleridge - the impacts of turbid inflows. New Zealand Journal of Marine and Freshwater Research **24:** 441-451.

Bodo, B., and T. E. Unny, 1983. Sampling strategies for mass-discharge estimation. Journal of Environmental Engineering-Asce **109:** 812-829.

Borsuk, M. E., P. Reichert, A. Peter, E. Schager, and P. Burkhardt-Holm, 2006. Assessing the decline of brown trout (Salmo trutta) in Swiss rivers using a Bayesian probability network. Ecological Modelling **192:** 224-244, doi:10.1016/j.ecolmodel.2005.07.006.

Boss, E., W. S. Pegau, W. D. Gardner, J. R. V. Zaneveld, A. H. Barnard, M. S. Twardowski, G. C. Chang, and T. D. Dickey, 2001. Spectral particulate attenuation and particle size distribution in the bottom boundary layer of a continental shelf. Journal of Geophysical Research-Oceans **106:** 9509-9516.

Bricaud, A., M. Babin, A. Morel, and H. Claustre, 1995. Variability in the chlorophyll-specific absorption coefficients of natural phytoplankton: Analysis and parameterization. Journal of Geophysical Research **100:** 95JC00463, 13321-13332.

Bühler, J., C. Siegenthaler, R. Simitovic, A. Wüest, and M. Zeh, 2004. Trübeströme im Grimselsee. Wasser Energie Luft **96:** 129-135.

Burkhardt-Holm, P., A. Peter, and H. Segner, 2002. Decline of fish catch in Switzerland - Project Fishnet: A balance between analysis and synthesis. Aquatic Sciences **64:** 36-54.

BUWAL, 1994. Der Zustand der Seen in der Schweiz, Bundesamt für Umwelt, Wald und Landschaft, Bern.

Carmack, E. C., C. B. J. Gray, C. H. Pharo, and R. J. Daley, 1979. Importance of lake-river interaction on seasonal patterns in the general-circulation of Kamloops Lake, British-Columbia. Limnology and Oceanography **24:** 634-644.

Chanudet, V., and M. Filella, 2007. The fate of inorganic colloidal particles in Lake Brienz. Aquatic Sciences **accepted**.

Chen, C. A., and F. Millero, 1986. Precise thermodynamic properties for natural waters covering only the limnological range. Limnology and Oceanography **31:** 657-662.

Cohn, T. A., 1995. Recent advances in statistical-methods for the estimation of sediment and nutrient transport in rivers. Reviews of Geophysics **33:** 1117-1123.

Cohn, T. A., L. L. Delong, E. J. Gilroy, R. M. Hirsch, and D. K. Wells, 1989. Estimating constituent loads. Water Resources Research **25:** 937-942.

Commoner, B., and D. Lipkin, 1949. The application of the Beer-Lambert Law to optically anisotropic systems. Science **110:** 41-43.

Crawford, C. G., 1991. Estimation of suspended-sediment rating curves and mean suspended-sediment loads. Journal of Hydrology **129:** 331-348.

Cristofor, S., A. Vadineanu, G. Ignat, and C. Ciubuc, 1994. Factors affecting light penetration in shallow lakes. Hydrobiologia **275/276:** 493-498.

Davies-Colley, R. J., and D. G. Smith, 2001. Turbidity, suspended sediment, and water clarity: A review. Journal of the American Water Resources Association **37:** 1085-1101.

Davies-Colley, R. J., W. N. Vant, and D. G. Smith, 1993. Colour and clarity of natural waters, Ellis Horwood, New York, 310 pp.

DEV, 1972-1989. Deutsche Einheitsverfahren zur Wasser- Abwasser und Schlammuntersuchung, VCH Verlagsgesellschaft, Weinheim.

Diehl, S., 2002. Phytoplankton, light, and nutrients in a gradient of mixing depths: Theory. Ecology **83:** 386-398.

Dillon, P. J., and F. H. Rigler, 1974. Test of a simple nutrient budget model predicting phosphorus concentration in lake water. Journal of the Fisheries Research Board of Canada **31:** 1771-1778.

Dixit, A. S., R. I. Hall, P. R. Leavitt, R. Quinlan, and J. P. Smol, 2000. Effects of sequential depositional basins on lake response to urban and agricultural pollution: a palaeoecological analysis of the Qu'Appelle Valley, Saskatchewan, Canada. Freshwater Biology **43:** 319-337.

Doxaran, D., N. Cherukuru, and L. S. J., 2006. Apparent and inherent optical properties of turbid estuarine waters: measurements, empirical quantification relationships, and modeling. Applied Optics **45:** 2310-2324.

Duarte, C. M., and J. Kalff, 1989. The influence of catchment geology and lake depth on phytoplankton biomass. Archiv für Hydrobiologie **115:** 27-40.

Duarte, P., 1995. A mechanistic model of the effects of light and temperature on algal primary productivity. Ecological Modelling **82:** 151-160.

Effler, S. W., 1996. Limnological and engineering analysis of a polluted urban lake, Springer Verlag, New York, 782 pp.

Effler, S. W., R. K. Gelda, J. A. Bloomfield, S. O. Quinn, and D. L. Johnson, 2001. Modeling the effects of tripton on water clarity: Lake Champlain. Journal of Water Resources Planning and Management **127:** 224-234, doi:10.1061/(ASCE)0733-9496(2001)127:4(224).

Elser, J. J., and R. P. Hassett, 1994. A stoichiometric analysis of the zooplankton-phytoplankton interaction in marine and fresh-water ecosystems. Nature **370:** 211-213.

Eppley, R. W., 1972. Temperature and phytoplankton growth in the sea. Fishery Bulletin **70:** 1063-1085.

Eppley, R. W., and P. R. Sloan, 1966. Growth rates of marine phytoplankton - correlation with light absorption by cell chlorophyll alpha. Physiologia Plantarum **19:** 47-59.

Fan, J. H., and G. L. Morris, 1992. Reservoir Sedimentation. 2. Reservoir desiltation and long-term storage capacity. Journal of Hydraulic Engineering-Asce **118:** 370-384.

Field, S. D., and S. W. Effler, 1988. Temperature and the productivity-light relationship. Water Resources Bulletin **24:** 325-328.

Finger, D., P. Bossard, M. Schmid, L. Jaun, B. Müller, D. Steiner, E. Schäffer, M. Zeh, and A. Wüest, 2007a. Effects of alpine hydropower operations on primary production in a downstream lake. Aquatic Sciences **accepted**.

Finger, D., M. Schmid, and A. Wüest, 2006. Effects of upstream hydropower operation on riverine particle transport and turbidity in downstream lakes. Water Resources Research **42:** W08429, doi:10.1029/2005WR004751.

Finger, D., M. Schmid, and A. Wüest, 2007b. Effects of oligotrophication and upstream hydropower operations on plankton and productivity in peri-alpine lakes. Water Resources Research **submitted**.

Flück, H., 1926. Beiträge zur Kenntnis des Phytoplanktons des Brienzersees. Ph.D. thesis, ETH, Zurich, http://www.eawag.ch/brienzersee/.

Forel, F.-A., 1885. Les ravins sous-lacustres des fleuves glaciaires. C.R. Acad. Sci. **101:** 725-728.

Forsberg, C., 1987. Evaluation of Lake Restoration in Sweden. Schweizerische Zeitschrift für Hydrologie-Swiss Journal of Hydrology **49:** 260-274.

Frauendorf, J., 2002. Entwicklung und Anwendung von Fernerkundungsmethoden zur Ableitung von Wasserqualitätsparametern verschiedener Restseen des Braunkohlentagebaus in Mitteldeutschland. Ph.D. thesis, Martin Luther University, Halle.

Friedl, G., C. Teodoru, and B. Wehrli, 2004. Is the Iron Gate I reservoir on the Danube River a sink for dissolved silica? Biogeochemistry **68:** 21-32.

Friedl, G., and A. Wüest, 2002. Disrupting biogeochemical cycles - consequences of damming. Aquatic Sciences **64:** 55-65.

Gächter, R., and A. Marès, 1979. Comments to the acidification and bubbling method for determining phytoplankton production. Oikos **33:** 69-73.

Gammeter, S., R. Forster, and U. Zimmermann, 1996. Limnologische Untersuchung des Walensees 1972-1995, Wasserversorgung Zürich, Zürich.

Gilbert, R., and J. Shaw, 1981. Sedimentation in proglacial Sunwapta Lake, Alberta. Canadian Journal of Earth Sciences **18:** 81-93.

Girardclos, S., O. Schmidt, M. Sturm, D. Ariztegui, A. Pugin, and F. Anselmetti, 2006. The 1996 AD megaturbidite in Lake Brienz: A non-catastrophic delta collapse. Marine Geology **submitted**.

Gliwicz, M. Z., 1986. Suspended clay concentration controlled by filter feeding zooplankton in a tropical reservoir. Nature **323:** 323-325.

Goldman, C. R., 1988. Primary productivity, nutrients, and transparency during the early onset of eutrophication in ultra-oligotrophic Lake Tahoe, California-Nevada. Limnology and Oceanography **33:** 1321-1333.

Gordon, H. R., and A. Morel, 1983. Remote assessment of ocean colour for interpretation of satellite visible imagery: A review, Springer Verlag, New York, 114 pp.

Gordon, H. R., R. C. Smith, and J. R. V. Zaneveld, 1984. Introduction to ocean optics. Proceedings of the Society of Photo-Optical Instrumentation Engineers **489:** 1-41.

Goudsmit, G.-H., H. Burchard, F. Peeters, and A. Wüest, 2002. Application of k-epsilon turbulence models to enclosed basins: The role of internal seiches. Journal of Geophysical Research **107:** 3230, doi:10.1029/2001JC000954.

Grasso, D., 2003. Charge de sédiments en suspension. Gas wasser abwasser **12:** 898-905.

GSA, 2003. Veränderungen im Ökosystem Brienzersee, Office of Water Protection and Waste Management of the Canton of Bern (GSA), Bern, http://www.eawag.ch/brienzersee/.

Guenther, M., and R. Bozelli, 2004. Effects of inorganic turbidity on the phytoplankton of an Amazonian Lake impacted by bauxite tailings. Hydrobiologia **511:** 151-159.

Guildford, S. J., and R. E. Hecky, 2000. Total nitrogen, total phosphorus, and nutrient limitation in lakes and oceans: Is there a common relationship? Limnology and Oceanography **45:** 1213-1223.

Hakanson, L., and M. Jansson, 1983. Principles of lake sedimentology, Springer-Verlag, Berlin, Germany.

Hart, D. D., T. E. Johnson, K. L. Bushaw-Newton, R. J. Horwitz, A. T. Bednarek, D. F. Charles, D. A. Kreeger, and D. J. Velinsky, 2002. Dam removal: Challenges and opportunities for ecological research and river restoration. Bioscience **52:** 669-681.

Hart, D. D., and N. L. Poff, 2002. A special section on dam removal and river restoration. Bioscience **52:** 653-655.

Hessen, D. O., 1992. Nutrient element limitation of zooplankton production. American Naturalist **140:** 799-814.

Hinderer, M., 2001. Late Quaternary denudation of the Alps, valley and lake fillings and modern river loads. Geodinamica Acta **14:** 231-263.

Hofer, F., 1952. Über die Energieverhältnisse des Brienzersees. Beitr. Geol. Schweiz **7:** 95.

Hofmann, A., and J. Dominik, 1995. Turbidity and mass concentration of suspended matter in Lake Water - A comparison of 2 calibration methods. Aquatic Sciences **57:** 54-69.

Hoyle, C., 2004. Phosphorus cycling in Lake Brienz, Switzerland. M.S. thesis, Eawag, Kastanienbaum.

Humborg, C., D. J. Conley, L. Rahm, F. Wulff, A. Cociasu, and V. Ittekkot, 2000. Silicon retention in river basins: Far-reaching effects on biogeochemistry and aquatic food webs in coastal marine environments. Ambio **29:** 45-50.

Hupfer, M., R. Gächter, and R. Giovanoli, 1995. Transformation of phosphorus species in settling seston and during early sediment diagenesis. Aquatic Sciences **57:** 305-324.

Jaquet, J.-M., F. Schanz, P. Bossard, K. Hanselmann, and F. Gender, 1994. Measurements and significance of bio-optical parameters for remote sensing in two subalpine lakes of different trophic state. Aquatic Sciences **56:** 263-302.

Jassby, A. D., and T. Platt, 1976. Mathematical formulation of relationship between photosynthesis and light for phytoplankton. Limnology and Oceanography **21:** 540-547.

Jaun, L., 2005. Lichtregime im Brienzersee. M.S. thesis, ETH Zurich, Zurich, http://www.eawag.ch/brienzersee/.

Jaun, L., D. Finger, M. Zeh, M. Schurter, and A. Wüest, 2007. Effects of upstream hydropower operation and oligotrophication on the light regime of a turbid peri-alpine lake. Aquatic Sciences **accepted**.

Jeppesen, E., M. Sondergaard, J. P. Jensen, K. E. Havens, O. Anneville, L. Carvalho, M. F. Coveney, R. Deneke, M. T. Dokulil, B. Foy, D. Gerdeaux, S. E. Hampton, S. Hilt, K. Kangur, J. Köhler, E. Lammens, T. L. Lauridsen, M. Manca, M. R. Miracle, B. Moss, P. Noges, G. Persson, G. Phillips, R. Portielje, C. L. Schelske, D. Straile, I. Tatrai, E. Willen, and M. Winder, 2005. Lake responses to reduced nutrient loading - an analysis of contemporary long-term data from 35 case studies. Freshwater Biology **50:** 1747-1771, doi:10.1111/j.1365-2427.2005.01415.x.

Jewson, D. H., and J. A. Taylor, 1978. The influence of turbidity on net phytoplankton photosynthesis in some Irish lakes. Freshwater Biology **8:** 573-584.

Kallio, K., 2006. Optical properties of Finnish lakes estimated with simple bio-optical models and water quality monitoring data. Nordic Hydrology **37:** 183-204.

Keller, P., 2001. Imaging spectroscopy of lake water quality parameters. Ph.D. thesis, University of Zurich, Zurich.

Kirchhofer, A., 1990. Limnologische und ichthyologische Untersuchungen im Brienzersee unter besonderer Berücksichtigung der Differenzierung der sympatrischen Felchenpopulationen. Ph.D. thesis, University Bern, Bern, http://www.eawag.ch/brienzersee/.

Kirk, J. T. O., 1985. Effects of suspensoids (turbidity) on penetration of solar radiation in aquatic ecosystems. Hydrobiologia **125:** 195-208.

Kirk, J. T. O., 1994. Light and photosynthesis in aquatic ecosystems, Cambridge University Press, New York, 481 pp.

Kirk, J. T. O., 2003. The vertical attenuation of irradiance as a function of the optical properties of the water. Limnology and Oceanography **48:** 9-17.

Koenings, J. P., and J. A. Edmundson, 1991. Secchi disk and photometer estimates of light regimes in Alaskan lakes: Effects of yellow color and turbidity. Limnology and Oceanography **36:** 91-105.

Kratz, T. K., K. E. Webster, C. J. Bowser, J. J. Magnuson, and B. J. Benson, 1997. The influence of landscape position on lakes in northern Wisconsin. Freshwater Biology **37:** 209-217.

Krause-Jensen, D., and K. Sand-Jensen, 1998. Light attenuation and photosynthesis of aquatic plant communities. Limnology and Oceanography **43:** 396-407.

KWO, 1999. Vermessungen der Aaregletscher, Flotron AG, Meiringen.

Lambert, A., and F. Giovanoli, 1988. Records of riverborne turbidity currents and indications of slope failures in the Rhone delta of Lake Geneva. Limnology and Oceanography **33:** 458-468.

Lambert, A., K. Kelts, and U. Zimmermann, 1984. Turbidity currents in lakes - Oxygen-input by underflowing river water. Schweizerische Zeitschrift für Hydrologie-Swiss Journal of Hydrology **46:** 41-50.

Lambert, A. M., K. R. Kelts, and N. F. Marshall, 1976. Measurements of density underflows from Walensee, Switzerland. Sedimentology **23:** 87-105.

Larkin, G. A., and P. A. Slaney, 1997. Implications of trends in marine-derived nutrient influx to south coastal British Columbia salmonid production. Fisheries **22:** 16-24.

LHG-BWG, 2005. Hydrological Yearbook of Switzerland, Federal Office for Water and Geology (FOWG), Bern, http://www.bwg.admin.ch/service/hydro/d/jahrbuch.htm.

Litchman, E., C. A. Klausmeier, and P. Bossard, 2004. Phytoplankton nutrient competition under dynamic light regimes. Limnology and Oceanography **49:** 1457-1462.

Loizeau, J. L., and J. Dominik, 2000. Evolution of the upper Rhone River discharge and suspended sediment load during the last 80 years and some implications for Lake Geneva. Aquatic Sciences **62:** 54-67.

Matzinger, A., M. Schmid, E. Veljanoska-Sarafiloska, S. Patceva, D. Guseska, B. Wagner, B. Müller, M. Sturm, and A. Wüest, 2007. Eutrophication of ancient Lake Ohrid: Global warming amplifies detrimental effects of increased nutrient inputs. Limnology and Oceanography **52:** 338-353.

McCully, P., 1996. Silenced Rivers; the ecology and politics of large dams, Zed Books, London.

McGinnis, D., S. Bocaniov, C. Teodoru, G. Friedl, A. Lorke, and A. Wüest, 2006. Silica retention in the Iron Gate I reservoir on the Dabube River: the role of side bays as nutrient sinks. River Research and Applications **22:** 441–456, doi: 10.1002/rra.916.

Meier, W., C. Bonjour, A. Wüest, and P. Reichert, 2003. Modeling the effect of water diversion on the temperature of mountain streams. Journal of Environmental Engineering-Asce **129:** 755-764, doi: 10.1061/(ASCE)0733-9372(2003)129:8(755).

Meyns, S., R. Illi, and B. Ribi, 1994. Comparison of chlorophyll-a analysis by HPLC and spectrophotometry - Where do the differences come from. Archiv für Hydrobiologie **132:** 129-139.

Mieleitner, J., and P. Reichert, 2005. Modelling functional groups of algae in Lake Zürich. Proceedings of the 2005 European Simulation and Modelling Conference (ESM 2005), pp. 256-261.

Mieleitner, J., and P. Reichert, 2006. Analysis of the transferability of a biogeochemical lake model to lakes of different trophic state. Ecological Modelling **194:** 49-61, doi:10.1016/j.ecolmodel.2005.10.039.

Millero, F., 2000. The equation of state of lakes. Aquatic Geochemistry **6:** 1-17.

Moosmann, L., 2005. Rekonstruktion des Temperaturregimes der Aare ohne Kraftwerkeinfluss, Eawag, Kastanienbaum, http://www.eawag.ch/brienzersee/.

Moosmann, L., B. Müller, R. Gächter, A. Wüest, E. Butscher, and P. Herzog, 2005. Trend-oriented sampling strategy and estimation of soluble reactive phosphorus loads in streams. Water Resources Research **41**, doi: 10.1029/2004WR003539.

Morel, A. 1974. Optical properties of pure water and pure sea water, pp. 1-24. In N. Steeman (Ed.): *Optical aspects of oceanography.*, Academic Press, London.

Morel, A., 1988. Optical modeling of the upper ocean in relation to its biogeneous matter content (Case 1 waters). Journal of Geophysical Research **93:** 10,749-10,768.

Morel, A., and L. Prieur, 1977. Analysis of variation in ocean color. Limnology and Oceanography **22:** 709-722.

Müller, B., D. Finger, M. Sturm, V. Prasuhn, T. Haltmeier, P. Bossard, C. Hoyle, and A. Wüest, 2007a. Present and past bio-available phosphorus budget in the ultra-oligotrophic Lake Brienz. Aquatic Sciences **in press**.

Müller, B., R. Stierli, and A. Wüest, 2006. Phosphate adsorption by mineral weathering particles in oligotrophic waters of high particle content. Water Resources Research **42:** W10414, doi: 10.1029/2005WR004778.

Müller, R., 2003. Populationsdynamische Untersuchungen an den Felchen des Brienzersees, EAWAG, Kastanienbaum, http://www.eawag.ch/brienzersee/.

Müller, R., M. Breitenstein, M. M. Bia, C. Rellstab, and A. Kirchhofer, 2007b. Fish-zooplankton interactions in ultra-oligotrophic Lake Brienz and its implications for the fishery. Aquatic Sciences **accepted**.

Murray, A. P., C. F. Gibbs, A. R. Longmore, and D. J. Flett, 1986. Determination of chlorophyll in marine waters - intercomparison of a rapid HPLC method with full hplc, spectrophotometric and fluorometric methods. Marine Chemistry **19:** 211-227.

Naturaqua, 1993. Trübung Brienzersee, Amt für Gewässerschutz und Abfallwirtschaft des Kantons Bern, Bern.

Nef, W., 1992. Das Phytoplankton der grossen Berner Seen (Brienzersee / Thunersee / Bielersee), Amt für Gewässerschutz und Abfallwirtschaft (GSA), Bern, http://www.eawag.ch/brienzersee/.

Nilsson, C., R. Jansson, and U. Zinko, 1997. Long-term responses of river-margin vegetation to water-level regulation. Science **276:** 798-800.

Nydegger, P., 1957. Vergleichende limnologische Untersuchungen an sieben Schweizerseen. Beitr. Geol. Schweiz **9:** 80.

Ochsenbein, U., and B. Mattmann, 2003. Gewässerbericht 1997-2000, Amt für Gewässerschutz und Abfallwirtschaft (GSA), Bern.

Omlin, M., P. Reichert, and R. Forster, 2001. Biogeochemical model of Lake Zurich: model equations and results. Ecological Modelling **141:** 77-103.

Peeters, F., A. Wüest, G. Piepke, and D. M. Imboden, 1996. Horizontal mixing in lakes. Journal of Geophysical Research-Oceans **101:** 18361-18375.

Pfunder, M., 1994. Artenzusammensetzung und trophische Struktur des Planktons in einem trübstoffbelasteten oligotrophen See. M.S. thesis, ETH, Dübendorf, http://www.eawag.ch/brienzersee/.

Pierson, D. C., and N. Strömbeck, 2001. Estimation of radiance reflectance and the concentrations of optically active substances in Lake Mälaren, Sweden, based on direct and inverse solutions of a simple model. The Science of the Total Environment **268:** 171-188.

Platt, T., C. L. Gallegos, and W. G. Harrison, 1980. Photoinhibition of photosynthesis in natural assemblages of marine-phytoplankton. Journal of Marine Research **38:** 687-701.

Platt, T., and A. D. Jassby, 1976. Relationship between photosynthesis and light for natural assemblages of coastal marine-phytoplankton. Journal of Phycology **12:** 421-430.

Pope, R. M., and E. S. Fry, 1997. Absorption spectrum (380-700 nm) of pure water. II. Integrating cavity measurements. Applied Optics **36:** 8710-8723.

Powles, S. B., 1984. Photoinhibition of photosynthesis induced by visible-light. Annual Review of Plant Physiology and Plant Molecular Biology **35:** 15-44.

Preece, R. M., and H. A. Jones, 2002. The effect of Keepit Dam on the temperature regime of the Namoi River, Australia. River Research and Applications **18:** 397-414, doi: 10.1002/rra.686.

Preisendorf, R. W., 1986. Secchi disk science: Visual optics of natural waters. Limnology and Oceanography **31:** 909-926.

Preston, S. D., V. J. Bierman, and S. E. Silliman, 1989. An evaluation of methods for the estimation of tributary mass loads. Water Resources Research **25:** 1379-1389.

Redfield, A. C., 1958. The biological control of chemical factors in the environment. American Scientist **46:** 205-221.

Reichert, P., 1994. Aquasim - a tool for simulation and data-analysis of aquatic systems. Water Science and Technology **30:** 21-30.

Reinart, A., A. Herlevi, H. Arst, and L. Sipelgas, 2003. Preliminary optical classification of lakes and coastal waters in Estonia and south Finland. Journal of Sea Research **49:** 357-366, doi:10.1016/S1385-1101(03)00019-4.

Rellstab, C., V. Maurer, M. Zeh, H. R. Bürgi, and P. Spaak, 2007. Temporary collapse of the Daphnia population in turbid and ultra-oligotrophic Lake Brienz. Aquatic Sciences **accepted**.

Richards, R. P., and J. Holloway, 1987. Monte-Carlo studies of sampling strategies for estimating tributary loads. Water Resources Research **23:** 1939-1948.

Rodhe, W., 1958. The primary production in lakes: some results and restrictions of the 14C methods. J. Cons. Perm. Int. Expl. **144:** 122-128.

Rosenberg, D. M., F. Berkes, R. A. Bodaly, R. E. Hecky, C. A. Kelly, and J. W. M. Rudd, 1997. Large-scale impacts of hydroelectric development. Environ. Rev. **5:** 27-52.

Rosenberg, D. M., R. A. Bodaly, and P. J. Usher, 1995. Environmental and social impacts of large-scale hydroelectric development - Who is listening. Global Environmental Change-Human and Policy Dimensions **5:** 127-148.

Rosenberg, D. M., P. McCully, and C. M. Pringle, 2000. Global-scale environmental effects of hydrological alterations: Introduction. Bioscience **50:** 746-751.

Sägesser, M., and R. Weingartner, 2005. Veränderung der Hydrologie der Aare, Institute of Geography - University of Bern, Bern, http://www.eawag.ch/brienzersee/.

Sakshaug, E., and D. Slagstad, 1991. Light and productivity of phytoplankton in polar marine ecosystems - a physiological view. Polar Research **10:** 69-85.

Sanden, P., and B. Hakansson, 1996. Long-term trends in Secchi depth in the Baltic Sea. Limnology and Oceanography **41:** 346-351.

Sawyer, C. N., 1966. Basic concepts of eutrophication. Water Pollution Control Federation **38:** 737-744.

Schallenberg, M., and C. W. Burns, 2004. Effects of sediment resuspension on phytoplankton production: teasing apart the influences of light, nutrients and algal entrainment. Freshwater Biology **49:** 143-159.

Schallenberg, M., M. James, I. Hawes, and C. Howard-Williams, 1999. External forcing by wind and turbid inflows on a deep glacial lake and implications for primary production. New Zealand Journal of Marine and Freshwater Research **33:** 311-331.

Schanz, F., 1994. Oligotrophication of Lake Zürich as reflected in Secchi depth measurements. Annales de Limnologie **30:** 57-65.

Schär, C., P. L. Vidale, D. Lüthi, C. Frei, C. Häberli, M. A. Liniger, and C. Appenzeller, 2004. The role of increasing temperature variability in European summer heatwaves. Nature **427:** 332-336, doi:10.1038/nature02300.

Schindler, D. W., 1974. Eutrophication and recovery in experimental lakes - implications for lake management. Science **184:** 897-899.

Schleiss, A., and C. Oehy, 2002. Verlandung von Stauseen und Nachhaltigkeit. Wasser Energie Luft **94:** 227-234.

Schröder, R., 1969. A summarizing water sampler. Archiv für Hydrobiologie **66:** 241-243.

Schudel, B., and U. Ochsenbein, 1995. Brienzersee - Weniger Schwebstoffe und trotzdem trüber?, Gewässer- und Bodenschutzlabor des Kanton Berns (GBL).

Shimaraev, M. N., N. G. Granin, and A. A. Zhdanov, 1993. Deep ventilation of Lake Baikal Waters due to spring thermal bars. Limnology and Oceanography **38:** 1068-1072.

Siegenthaler, C., 2003. Veränderungen im Ökosystem Brienzersee - Projekt 3.1, GSA - GBL, Bern, http://www.eawag.ch/brienzersee/.

Siegenthaler, C., M. Sturm, H. Suter, and A. Wüest, 1996. Das Verhalten von Schwebstoffen im Brienzersee, EAWAG, Dübendorf.

Sommer, U., 1992. Phosphorus-limited Daphnia: Intraspecific facilitation instead of competition. Limnology and Oceanography **37:** 966-973.

Spinrad, R. W., 1986. A calibration diagram of specific beam attenuation. Journal of Geophysical Research-Oceans **91:** 6C0185, 7761-7764.

Staehr, P. A., and K. Sand-Jensen, 2006. Seasonal changes in temperature and nutrient control of photosynthesis, respiration and growth of natural phytoplankton communities. Freshwater Biology **51:** 249-262, doi:10.1111/j.1365-2427.2005.01490.x.

Steemann Nielsen, E., 1952. The use of radioactive carbon (C-14) for measuring organic production in the Sea. J. Cons. Perm. Int. Expl. **18:** 117-140.

Stockner, J. G., E. Rydin, and P. Hyenstrand, 2000. Cultural oligotrophication: causes and consequences for fisheries resources. Fisheries **25:** 7-14, doi:10.1577/1548-8446(2000)025<0007:CO>2.0.CO;2.

Sturm, M., 1976. Die Oberflächensedimente des Brienzersees. Eclogae geol. Helv. **69:** 111-123.

Sturm, M., and A. Matter, 1978. Turbidites and varves in Lake Brienz (Switzerland): deposition of clastic detritus by density currents. Spec. Publs Int. Ass. Sediment **2:** 147 - 168.

Swift, T., J. Perez-Losada, S. G. Schladow, J. Reuter, D. Jassby, and C. Goldman, 2006. Water clarity modeling in Lake Tahoe: linking suspended matter characteristics to Secchi depth. Aquatic Sciences **68:** 1-15, doi:10.1007/s00027-005-0798-x.

Tassan, S., and G. M. Ferrari, 1995. Proposal for the measurement of backward and total scattering by mineral particles suspended in water. Applied Optics **34:** 8346-8353.

Teodoru, C., and B. Wehrli, 2005. Retention of sediments and nutrients in the Iron Gate I reservoir on the Danube River. Biogeochemistry **76:** 539-565, doi: 10.1007/s10533-005-0230-6.

Thomas, R. B., and J. Lewis, 1995. An evaluation of flow-stratified sampling for estimating suspended sediment loads. Journal of Hydrology **170:** 27-45.

Turner, J. S., 1986. Turbulent entrainment - the development of the entrainment assumption, and its application to geophysical flows. Journal of Fluid Mechanics **173:** 431-471.

Tyler, J. E., 1968. The Secchi disk. Limnology and Oceanography **13:** 1-6.

Urabe, J., J. Clasen, and R. W. Sterner, 1997. Phosphorus limitation of Daphnia growth: Is it real? Limnology and Oceanography **42:** 1436-1443.

Urabe, J., and Y. Watanabe, 1992. Possibility of N or P limitation for planktonic cladocerans: An experimental test. Limnology and Oceanography **37:** 244-251.

Vallentyne, J. R., 1973. The algal bowl - a Faustian view of eutrophication. Federation Proceedings **32:** 1754-1757.

Veit, H., 2002. Die Alpen - Geoökologie und Landschaftsentwicklung, UTB, Stuttgart.

Vollenweider, R. A., 1968. Scientific fundamentals of the eutrophication of lakes and flowing waters, with particular reference to nitrogen and phosphorus as factors in eutrophication, Organisation for Economic Cooperation and Development, Paris.

Vörösmarty, C. J., M. Meybeck, B. Fekete, K. Sharma, P. Green, and J. P. M. Syvitski, 2003. Anthropogenic sediment retention: major global impact from registered river impoundments. Global and Planetary Change **39:** 169-190, doi:10.1016/S0921-8181(03)00023-7.

Vörösmarty, C. J., K. P. Sharma, B. M. Fekete, A. H. Copeland, J. Holden, J. Marble, and J. A. Lough, 1997. The storage and aging of continental runoff in large reservoir systems of the world. Ambio **26:** 210-219.

Walling, D. E., 1977. Assessing accuracy of suspended sediment rating curves for a small basin. Water Resources Research **13:** 530-538.

Ward, J. V., and J. A. Stanford, 1995. Ecological connectivity in alluvial river ecosystems and its disruption by flow regulation. Regulated Rivers-Research & Management **11:** 105-119.

WCD, 2000. Dams and development - a new framework for decision-making, World Commission on Dams. Earthscan Publications Ltd, London.

Weirich, F., 1986. The record of density-induced underflows in a glacial lake. Sedimentology **33:** 261-277.

Wetzel, R. G., 2001. Limnology - Lake and river ecosystems, Academic Press, San Diego.

Whalen, S. C., B. B. Chalfant, E. N. Fischer, K. A. Fortino, and A. E. Hershey, 2006. Comparative influence of resuspended glacial sediment on physicochemical characteristics and primary production in two arctic lakes. Aquatic Sciences **68:** 65-77, doi:10.1007/s00027-005-0804-3.

Whitlock, C. H., L. R. Poole, J. W. Usry, W. M. Houghton, W. G. Witte, W. D. Morris, and E. A. Gurganus, 1981. Comparison of reflectance with backscatter and absorption parameters for turbid waters. Applied Optics **20:** 517-522.

Williams, R. B., and M. B. Murdoch, 1966. Phytoplankton production and chlorophyll concentration in Beaufort Channel North Carolina. Limnology and Oceanography **11:** 73-82.

Wozniak, S. B., and D. Stramski, 2004. Modeling the optical properties of mineral particles suspended in seawater and their influence on ocean reflectance and chlorophyll estimation from remote sensing algorithms. Applied Optics **43:** 3489-3503.

Wüest, A., C. Hoyle, D. Finger, and B. Müller, 2007. Balancing of non-inert phosphorus in particle-laden ultra-oligotrophic lakes. Water Resources Research **submitted**.

Wüest, A., D. M. Imboden, and M. Schurter, 1988. Origin and size of hypolimnic mixing in Urnersee, the southern basin of Vierwaldstattersee (Lake Lucerne). Schweizerische Zeitschrift für Hydrologie-Swiss Journal of Hydrology **50:** 41-70.

Wüest, A., G. Piepke, and J. D. Halfman 1996. Combined effects of dissolved solids and temperature on the density stratification of Lake Malawi, pp. 183-202. In C. T. Johnson, and E. O. Odada (Eds): *The Limnology, Climatology and Paleoclimatology of East African Lakes*, Gordon and Breach, Toronto.

Wüest, A., and M. Zeh, 2007. Editorial - Introduction to a fascinating interdisciplinary catchment-to-lake project. Aquatic Sciences **accepted**.

Zimmermann, I., 1996. Möglichkeiten und Grenzen von Streulichtmessverfahren. Chemie Ingenieur Technik **68:** 422-425.

Curriculum Vitae

David Christian Finger

fingerd@gmx.net

1974	Born on 22nd August in Klagenfurt (Austria)
1980 – 1988	Primary school in Zurich
1988 – 1991	High school in Boston (USA)
1991 – 1994	*Collège Calvin* in Geneva (Swiss Matura Typus C)
1994 – 1995	Studies at the Swiss Federal Institute of Technology (ETH) Zurich, Department Mechanical and Process Engineering
1995 – 2002	Studies at the Swiss Federal Institute of Technology (ETH) Zurich, Department of Environmental Sciences
1999 - 2000	Volunteer in a rainforest conservation project in Ecuador
2001	Intern at Simultec AG, Zurich, Simulation of air dispersion
2002	Diploma in Environmental Sciences (Dipl. Umwelt-Natw. ETH)
2002	Research Assistant at the Swiss ornithological station
2002 - 2006	Ph.D. thesis at the Swiss Federal Institute of Aquatic Science and Technology (Eawag)
2002 – 2006	Teaching Assistant, Department of Environmental Sciences, ETH Zurich

Cover pictures: steaming Lake Brienz during winter (front cover); areal view of Lake Brienz (back cover); small pictures on back cover: frozen Oberaarsee (upper left); melt water from Unteraarglacier (upper center); boat on Grimselsee (upper right); dam of Lake Grimsel (lower left); Are inflow into Lake Brienz (lower center); shore of Lake Brienz during the flood 2005 (lower right); all pictures by D. Finger except lower right (by O. Seehausen) and lower center (U. Ochsenbein, GBL).